

2011

Characterization of Triggerable Quinones for the Development of Enzyme-Responsive Liposomes

Maria Fabiana Mendoza

Louisiana State University and Agricultural and Mechanical College, mmendo1@tigers.lsu.edu

Follow this and additional works at: https://digitalcommons.lsu.edu/gradschool_dissertations



Part of the [Chemistry Commons](#)

Recommended Citation

Mendoza, Maria Fabiana, "Characterization of Triggerable Quinones for the Development of Enzyme-Responsive Liposomes" (2011). *LSU Doctoral Dissertations*. 1173.
https://digitalcommons.lsu.edu/gradschool_dissertations/1173

This Dissertation is brought to you for free and open access by the Graduate School at LSU Digital Commons. It has been accepted for inclusion in LSU Doctoral Dissertations by an authorized graduate school editor of LSU Digital Commons. For more information, please contact gradetd@lsu.edu.

**CHARACTERIZATION OF TRIGGERABLE QUINONES
FOR THE DEVELOPMENT OF ENZYME-RESPONSIVE LIPOSOMES**

A Dissertation

**Submitted to the Graduate Faculty of the
Louisiana State University and
Agricultural and Mechanical College
in partial fulfillment of the
Requirements for the degree of
Doctor of Philosophy**

In

The Department of Chemistry

**by
Maria Fabiana Mendoza
B.S., Missouri Baptist University, 2005
May 2012**

DEDICATION

This dissertation is dedicated to my loving grandmother:

Mabel Cerri Burgantis de Mendoza

And to

My Mom, Ibis Elizabeth Paris Bargas

My Dad, Hector Eduardo Mendoza Cerri

My Brother, Facundo Horacio Jesus Mendoza Paris

My Brother, Jose Hector Mendoza Paris

My Partner, Dayna Tatiana Pastorino Martinez

ACKNOWLEDGMENTS

I would like to thank my advisor, Dr. Robin L. McCarley, for his extraordinarily guidance and support through all these years in graduate school. I still remember my visit to LSU and how from the moment I interacted with his graduate students and met him I knew that I would like to be a part of his group. I feel so lucky in having an advisor who I admired as a scientist and as a person. He will be definitely missed and I will always be grateful to God for putting him in my life.

To the McCarley research group, thank you for your support and friendship. It was the collection of people from different background and cultures that made this group very special. It has been a pleasure to work with each of you and I wish you all the best in life.

To my committee members, Dr. Doug Gilman, Dr. Carol Taylor, and Dr. Grover Waldrop, I would like to thank you all for always having your door open for me. To my Dean's representative, Dr. Jin-Woo Choi and his substitute Dr. Dorel Moldovan, thank you for being in my general exam and final examination, respectively.

I would also like to give special thanks to my colleagues Nicole Carrier, Jennifer De Guzman, Jeremiah Forsythe, and Elisabeta Mitran and to the Post-doctoral fellows in the McCarley group, Sreelatha Balamurugan, Winston Ong, and Martin Loew for their scientific discussions and proofreading of my documents. Nikki, Jenny, Eli and Sreelatha thanks for your friendship and I hope that we can continue to remain in touch for the rest of our lives.

I appreciate my dear friends, Nadya Braidă, Leila Juan, Florencia Belo, Victoria Garcia, Andres Vidal-Gadea and Santiago Claramunt for being there when I needed someone to cheer me up or just to listen. As a foreign person in the United State it has not always been easy and having friends willing to share some time and a word of encouragement has been of great help.

To my family, and to those that have known me since I was a little girl, thank you for helping me to mature and giving me strength to continue on this journey. Mom, dad, Facundo

and Jose thank you for helping me become into the person that I am today. I want to give a very special thanks to the most wonderful person in this world, my grandmother Mabel Cerri, whose unconditional love is greater than my words can express. She is definitely my heart and soul.

I would also especially like to thank my partner Taty, for being there for me at all times. You provided the peace that allowed me to focus on writing and to complete this process in a timely manner. You have taken care of me and everything else around me, I am so grateful to have you in my life.

Lastly, I would like to give thanks to all of the other the people that helped me through my graduate career here at LSU and especially those in the Department of Chemistry.

TABLE OF CONTENTS

DEDICATION	ii
ACKNOWLEDGMENTS	iii
LIST OF TABLES	viii
LIST OF FIGURES	ix
LIST OF SCHEMES.....	xiv
LIST OF ABBREVIATIONS AND SYMBOLS	xv
ABSTRACT.....	xx
CHAPTER 1. INTRODUCTION	1
1.1 Research Goals and Aims	1
1.2 Prodrugs Activated by Endogenous Oxidoreductase Enzymes Other Than NQO1	4
1.2.1 Aldehyde Oxidase.....	5
1.2.2 Amino Acid Oxidases	5
1.2.3 NADPH-Cytochrome P450 Reductase	6
1.2.4 Cytochrome P450s	8
1.2.5 Tyrosinase	10
1.3 Enzyme-Activated Liposomes	12
1.3.1 Elastase	12
1.3.2 Alkaline Phosphatase	13
1.3.3 Phospholipase C.....	14
1.3.4 Phospholipase A ₂ (PLA ₂).....	15
1.3.5 Matrix Metalloproteinase (MMP).....	18
1.4 NAD(P)H:Quinone Oxidoreductase Type-1 (NQO1)	21
1.4.1 Origin, Types, Structure, Mechanism, Location and Over Expression	21
1.4.2 Inhibitors of Human NQO1	24
1.4.3 Bioreductive Drugs Activated by Human NQO1	27
1.4.4 Prodrugs Presenting the Trimethyl-lock System Activated by Human NQO1	31
1.5 References.....	32
CHAPTER 2. ELECTROCHEMICAL BEHAVIOR OF QUINONE DERIVATIVES POTENTIALLY USABLE FOR DRUG DELIVERY APPLICATIONS	53
2.1 Introduction.....	53
2.2 Experimental Section	55
2.2.1 Materials and Methods.....	55
2.3 Results and Discussion	56
2.3.1 Thermodynamic Parameters of Naked Quinones	56
2.3.2 Thermodynamic Parameters of Propionic Acid Quinones and Q _{Me} -ETA.....	59

2.3.3	Propionic Acid Quinones and Their Cyclization Behavior	65
2.4	Conclusions.....	67
2.5	References.....	68
CHAPTER 3. TRIGGERABLE QUINONES ACTIVATED BY NAD(P)H:QUINONE OXIDOREDUCTASE TYPE-1 (HNQO1) FOR POTENTIAL DRUG DELIVERY APPLICATIONS		
		72
3.1	Introduction.....	72
3.2	Experimental Section	74
3.2.1	Materials	74
3.2.2	Enzyme Kinetic Assay.....	74
3.2.3	Molecular Docking	75
3.3	Results and Discussion	77
3.3.1	Kinetic Studies on Triggerable Quinones.....	77
3.3.2	Docking Studies on Triggerable Quinones.....	82
3.4	Conclusions.....	90
3.5	References.....	91
CHAPTER 4. QUINONE TRIGGER-BASED LIPIDS FOR FORMING ENZYME- RESPONSIVE LIPOSOMES AND THEIR RESPONSE TOWARD HNQO1 ASSAY CONDITIONS		
		100
4.1	Introduction.....	100
4.2	Experimental Section	101
4.2.1	Materials	101
4.2.2	Calcein-loaded Liposome Preparation.....	102
4.2.3	Characterization of Calcein-loaded Liposomes.....	103
4.2.4	Stability and Calcein Release Experiments	103
4.2.4.1	Bovine Serum Albumin	104
4.2.4.2	Reduced Nicotine Adenine Dinucleotide.....	104
4.2.4.3	Human NAD(P)H:Quinone Oxidoreductase Type-1 (hNQO1) and Type- 2 (hNQO2).....	105
4.2.4.4	Sodium Dithionite.....	105
4.3	Results and Discussion	106
4.3.1	Stability and Calcein Release for Q-DOPE Liposome Systems.....	106
4.3.1.1	Liposomes Composed of 100% Q _{Me} -DOPE	106
4.3.1.2	Liposomes Composed of 97% Q _{Me} -DOPE/3% PEG ₂₀₀₀ -DOPE.....	108
4.3.1.3	DOPC Liposomes	113
4.3.1.4	Liposomes Composed of 90% Q _{Me} -DOPE/10% DOPC and 80% Q _{Me} - DOPE/20% DOPC.....	116
4.3.1.5	Liposomes Composed of 70% Q _{Me} -DOPE/30% Cholesterol (CHO)....	119
4.3.2	DLS and Zeta Potential of Q-DOPE Liposome Systems	126
4.4	Conclusions.....	127
4.5	References.....	128

CHAPTER 5. CONCLUSIONS AND OUTLOOK	133
5.1 Summary	133
5.2 Conclusions.....	136
5.3 Outlook	136
5.4 References.....	137
APPENDIX A: SUPPLEMENTAL INFORMATION.....	139
APPENDIX B: PERMISSIONS	149
VITA.....	156

LIST OF TABLES

Table 2.1	Thermodynamic results for naked quinones. Potential scans were conducted at a rate of $V s^{-1}$ at 22 ± 2 °C in a pH 7.1 0.1 M PB/0.1 M KCl buffer solution. A three-electrode cell was used containing a glassy carbon electrode, a platinum counter electrode, and an Ag/AgCl (3M KCl) reference electrode. Potentials were converted to values versus the standard hydrogen electrode (SHE) by adding 0.210 V. Results are reported as the mean of 4 replicates \pm one standard deviation57
Table 2.2	Thermodynamic results for propionic acid quinones. Potential scans were conducted at a rate of $0.1 V s^{-1}$ at 22 ± 2 °C in a pH 7.1 0.1 M PB/0.1 M KCl buffer solution. A three-electrode cell was used containing a glassy carbon electrode, a platinum counter electrode, and an Ag/AgCl (3M KCl) reference electrode. Potentials were converted to standard hydrogen electrode (SHE) by adding 210 mV. Results are reported as the mean of 4 replicates \pm one standard deviation. The anodic peak potential of lactone oxidation, $E_{p,1}$, is reported for those propionic acid quinones that exhibit this voltammetric feature61
Table 2.3	Rate constant for the disappearance of propionic acid hydroquinones. Ratio measured between peaks current where the potential scan was conducted at a rate of $0.1 V s^{-1}$ at 22 ± 2 °C in a pH 7.1 0.1 M PB/0.1 M KCl buffer solution. Ratio measured between peaks current where the potential scan was conducted at a rate of $1 V s^{-1}$ 22 ± 2 °C in a 0.1 M PBS / 0.1 M KCl pH 7.1 buffer solution. A three-electrode cell was used containing a glassy carbon electrode, a platinum counter electrode, and an Ag/AgCl (3M KCl) reference electrode66
Table 3.1	Kinetic parameters for the reduction of quinone derivatives by hNQO1. Values are the mean \pm one standard deviation for three independent determinations.....78
Table 3.2	Energy score and distance from N5 of FAD to the possible hydride transfer atoms. Atoms closer in distance to N5 are highlighted in red.88
Table 4.1	Average diameters and zeta potentials of Q_{Me} -DOPE liposome systems. Experiments performed at 25 °C in pH 7.1 0.1M PB/0.1M KCl. Results are the average of 3 determinations \pm one standard deviation. Polydispersity indexes ≤ 0.3 are considered acceptable. Reference 2; pH 7.4 0.05 M PB/0.075 M KCl. Measurement done by Dr. Martin Loew126
Table 4.2	Summarized results from calcein release, DLS, and zeta potential experiments performed on Q_{Me} -DOPE liposome systems at 25 °C in pH 7.1 0.1 M PB/0.1 M KCl. Reference 2; pH 7.4 0.05 M PB/0.075 M KCl. Measurement done by Dr. Martin Loew129

LIST OF FIGURES

Figure 1.1	Illustration of quinone derivatives investigated in this dissertation.....	2
Figure 1.2	Mechanism of action of D-amino acid oxidase. Adapted from Pollegioni (2007).....	6
Figure 1.3	Reductive activation of TPZ. Adapted from Chen (2009).....	8
Figure 1.4	Reductive activation of AQ4N. Adapted from Chen (2009).....	10
Figure 1.5	Catalytic mechanism of tyrosinase. Adapted from Matoba (2006).....	11
Figure 1.6	Cleavage of peptide-DOPE structure by elastase. Adapted from Pak (1998).....	13
Figure 1.7	Mode of action of PLA ₂ versus other phospholipases. AA = arachidonic acid. Adapted from Kaiser (1999).....	15
Figure 1.8	ProAELs structures and mechanism of AELs release in the presence of PLA ₂ . Adapted from Andresen (2005).....	18
Figure 1.9	Schematic representation of FAD interactions with rat NQO1 (A) and human NQO1 (B). A) Shows hydrogen bonds of FAD with residues. W means water. B) Shows hydrogen bonds and van der Waals interactions of FAD with hNQO1. Open radiated circles indicate hydrophobic interactions. Hydrogen bonds are represented by dashed green lines; water molecules are shown as blue filled circles. Adapted from Li (1995) and Faig (2000).....	22
Figure 1.10	Mechanism of action of antitumor agents after bioreductive activation by human NQO1. Adapted from Siegel (2008).....	58
Figure 2.1	Cyclic voltammograms of naked quinones. Potential scans were conducted at a rate of 0.1 V s ⁻¹ at room temperature (22±2 °C) in a pH 7.1 0.1 M PB/0.1 M KCl buffer solution. A three-electrode cell was used containing a glassy carbon electrode (A=0.07 cm ²), a platinum counter electrode, and an Ag/AgCl (3M KCl) reference electrode (0.210 V vs. SHE). Potential sweeps started at 0.6 V to -0.6 and back to 0.6 V. Positive current peak corresponds to the reduction peak (<i>E</i> _{p,c}) and negative current corresponds to oxidation peak (<i>E</i> _{p,a}). Colored lines represent 4 trials performed on each quinone and dashed line represents the buffer solution.....	12
Figure 2.2	Cyclic voltammograms of quinones with a propionic acid side chain. Potential scans were conducted at a rate of 0.1 V s ⁻¹ at 22±2 °C in a pH 7.1 0.1 M PB/0.1 M KCl buffer solution. A three-electrode cell was used containing a glassy carbon electrode (A=0.07 cm ²), a platinum counter electrode, and an Ag/AgCl (3M KCl) reference electrode (0.210 V vs. SHE). Potential sweeps started at 0.6 V to -0.6 and back to 0.6 V. Positive current peak corresponds to the reduction peak (<i>E</i> _{p,c}) and negative	

current corresponds to oxidation peak ($E_{p,a}$). Colored lines represent 4 trials performed on each quinone and dashed lines represent the buffer solution.....63

Figure 2.3 Cyclic voltammograms of Q_{Me} -COOH. Potential scans were conducted at a rate of 0.1 V s^{-1} at $22 \pm 2 \text{ }^\circ\text{C}$ in the specified buffer solution. A three-electrode cell was used containing a glassy carbon electrode ($A=0.07 \text{ cm}^2$), a platinum counter electrode, and an Ag/AgCl (3M KCl) reference electrode (0.210 V vs. SHE). Potential sweeps started at 0.6 V to -0.6 and back to 0.6 V. Positive current peak corresponds to the reduction peak ($E_{p,c}$) and negative current corresponds to oxidation peak ($E_{p,a}$), and to the anodic peak of the lactone ($E_{p,l}$)66

Figure 3.1 Best prediction for the docked duroquinone in receptor 1 compared with the position of the duroquinone in the original crystal structure. Docked duroquinone (pink) differ from the original duroquinone (yellow) by 0.4530 \AA . Representation of amino acids (stick display; color by atom type, carbon atoms colored in purple) and FAD (sticks display; color by atom type, carbon atoms colored in cyan) in receptor 182

Figure 3.2 Structural frames of FlexX-docked quinones in the active site of *hNQO1*. Stick display in all the frames, FAD (color by atom type; carbon atoms colored in cyan), amino acids (color by atom type, carbon atoms colored in purple) and docked-quinones (color by atom type, carbon atoms in pink): (A) Q_{Br} -COOH, (B) Q_H -COOH, (C) Q_{Me} -COOH, (D) Q_{MeO} -COOH, (E) Q_{diMeO} -COOH, (F) Q' -COOH, (G) $Q_{nogemMe}$ -COOH, (H) Q_{Me-ETA} , (I) $Q_{(Me-N)}$ -COOH, and (J) $Q_{(n-pr-NH)}$ -COOH.....86

Figure 3.3 Correlation between the log (distance of the closer atom on the quinone ring with respect to N5 of FAD) and the log (k_{cat}/K_m).....89

Figure 4.1 UV-vis absorbance spectrum of 100% Q_{Me} -DOPE liposomes in pH 7.1 0.1 M PB/0.1 M KCl at room temperature. $\lambda_{max} = 264.9 \text{ nm}$ corresponds to the Q_{Me} headgroup and $\lambda_{max} = 497 \text{ nm}$ corresponds to the encapsulated calcein106

Figure 4.2 Stability of 100 μM 100% Q_{Me} -DOPE liposomes in the presence of 100 μM NADH. (\uparrow) the time for addition of 300 μL of 1 mM NADH solution. No leakage was observed as noted by the lack of increase in fluorescence intensity with time. (\bullet) time at which 100% Q_{Me} -DOPE liposomes were lysed with the addition of 15 μL of 30% (v/v) Triton X-100. (\blacklozenge) Instrument stopped by itself and was started again by me; no consequences observed on the measurement.....107

Figure 4.3 Instability of 100 μM 100% Q_{Me} -DOPE liposomes in the presence of 0.007% BSA. (\uparrow) the time for addition of 300 μL of 0.07% BSA solution into liposome solution. (\uparrow) the addition time for 100% Q_{Me} -DOPE liposomes into 0.007% BSA solution. (\bullet) time at which 100% Q_{Me} -DOPE liposomes were lysed with the addition of 15 μL of 30% (v/v) Triton X-100108

Figure 4.4	UV-vis absorbance spectrum of 97% Q _{Me} -DOPE/3% PEG ₂₀₀₀ -DOPE liposomes in pH 7.1 0.1 M PB/0.1 M KCl at room temperature. $\lambda_{\max} = 264.9$ nm corresponds to the Q _{Me} headgroup and $\lambda_{\max} = 497$ nm corresponds to the encapsulated calcein	109
Figure 4.5	Instability of 100 μ M 97% Q _{Me} -DOPE/3% PEG ₂₀₀₀ -DOPE liposomes in the presence of 0.007% BSA. (\uparrow) the time for addition of 300 μ L of 0.07% BSA solution into liposome solution. (\bullet) time at which 97% Q _{Me} -DOPE/3% PEG ₂₀₀₀ -DOPE liposomes were lysed with the addition of 15 μ L of 30% (v/v) Triton X-100	110
Figure 4.6	Instability of 100 μ M 97% Q _{Me} -DOPE/3% PEG ₂₀₀₀ -DOPE liposomes in the presence of 0.5 μ M hNQO1. (\uparrow) the time for addition of 300 μ L of 5 μ M hNQO1 solution into liposome solution. (\bullet) time at which 97% Q _{Me} -DOPE/3% PEG ₂₀₀₀ -DOPE liposomes were lysed with the addition of 15 μ L of 30% (v/v) Triton X-100	111
Figure 4.7	Instability of 100 μ M 97% Q _{Me} -DOPE/3% PEG ₂₀₀₀ -DOPE liposomes in the presence of 100 μ M NADH and 0.5 μ M hNQO1. (\uparrow) the addition time for 300 μ L of 5 μ M hNQO1 solution into liposome/NADH solution. (\bullet) time at which 97% Q _{Me} -DOPE/3% PEG ₂₀₀₀ -DOPE liposomes were lysed with the addition of 15 μ L of 30% (v/v) Triton X-100.....	112
Figure 4.8	Overlap of the calcein release curves for 100 μ M 97% Q _{Me} -DOPE/3% PEG ₂₀₀₀ -DOPE liposomes in the presence of 0.5 μ M hNQO1 (red line) and 100 μ M 97% Q _{Me} -DOPE/3% PEG ₂₀₀₀ -DOPE liposomes containing 100 μ M NADH in the presence of 0.5 μ M hNQO1 (blue line). (\uparrow) the addition time for 300 μ L of 5 μ M hNQO1 solution into liposome/NADH solution. (\bullet) time at which 97% Q _{Me} -DOPE/3% PEG ₂₀₀₀ -DOPE liposomes were lysed with the addition of 15 μ L of 30% (v/v) Triton X-100. Times were offset to compare the curves	112
Figure 4.9	Structure of DOPE and DOPC lipids.....	113
Figure 4.10	UV-vis absorbance spectrum of DOPC liposomes in pH 7.1 0.1 M PB/0.1 M KCl at room temperature. The peak of $\lambda_{\max} = 497$ nm corresponds to the encapsulated calcein.....	114
Figure 4.11	Stability of 100 μ M DOPC liposomes in the presence of 0.007% BSA. (\uparrow) the addition time for 300 μ L of 0.07% BSA solution into liposome solution. No leakage was observed as noted by the lack of increase in fluorescence intensity with time. (\bullet) time at which DOPC liposomes were lysed with the addition of 15 μ L of 30% (v/v) Triton X-100	115
Figure 4.12	Stability of 100 μ M DOPC liposomes in the presence of 0.5 μ M hNQO1. (\uparrow) the addition time for 300 μ L of 5 μ M hNQO1 solution into liposome solution. No leakage was observed as noted by the lack of increase in fluorescence intensity with time. (\bullet) time at which DOPC liposomes were lysed with the addition of 15 μ L of 30% (v/v) Triton X-100	115

- Figure 4.13** UV-vis absorbance spectrum of 90% Q_{Me}-DOPE/10% DOPC (blue line) and 80% Q_{Me}-DOPE/20% DOPC (red line) liposomes in pH 7.1 0.1 M PB/0.1 M KCl at room temperature. $\lambda_{\max} = 264.9$ nm corresponds to the Q_{Me} headgroup and $\lambda_{\max} = 497$ nm corresponds to the encapsulated calcein.....117
- Figure 4.14** Unstable behavior of 100 μ M 90% Q_{Me}-DOPE/10% DOPC and 100 μ M 80% Q_{Me}-DOPE/20% DOPC liposomes in the presence of 0.007% BSA. (\uparrow) the time for addition of 300 μ L of 0.07% BSA solution into the 90% Q_{Me}-DOPE/10% DOPC liposome solution. (\uparrow) the addition time for 80% Q_{Me}-DOPE/20% DOPC liposomes into 0.007% BSA solution. (\bullet) time at which 90% Q_{Me}-DOPE/10% DOPC and 80% Q_{Me}-DOPE/20% DOPC liposomes were lysed with the addition of 15 μ L of 30% (v/v) Triton X-100.....117
- Figure 4.15** Instability of 100 μ M 80% Q_{Me}-DOPE/20% DOPC liposomes in the presence of 0.5 μ M hNQO1. (\uparrow) the addition time for 300 μ L of 5 μ M hNQO1 solution into liposome solution. (\bullet) time at which 80% Q_{Me}-DOPE/20% DOPC liposomes were lysed with the addition of 15 μ L of 30% (v/v) Triton X-100118
- Figure 4.16** Calcein release curves of 100 μ M 90% Q_{Me}-DOPE/10% DOPC and 100 μ M 80% Q_{Me}-DOPE/20% DOPC by chemical reduction using 5 eq. of sodium dithionite. (\uparrow) the time for addition of sodium dithionite solution into the 90% Q_{Me}-DOPE/10% DOPC liposome solution. (\uparrow) the time for addition of sodium dithionite solution into the 80% Q_{Me}-DOPE/20% DOPC liposome solution. (\bullet) time at which 90% Q_{Me}-DOPE/10% DOPC and 80% Q_{Me}-DOPE/20% DOPC liposomes were lysed with the addition of 15 μ L of 30% (v/v) Triton X-100.....119
- Figure 4.17** UV-vis absorbance spectrum of 70% Q_{Me}-DOPE/30% CHO liposomes in pH 7.1 0.1 M PB/0.1 M KCl at room temperature. $\lambda_{\max} = 264.9$ nm corresponds to the Q_{Me} headgroup and $\lambda_{\max} = 497$ nm corresponds to the encapsulated calcein.....120
- Figure 4.18** Calcein release curves of 100 μ M 70% Q_{Me}-DOPE/30% CHO by chemical reduction using 5 eq. of sodium dithionite. The arrows (\uparrow and \uparrow) depict the time for addition of sodium dithionite solution into the 70% Q_{Me}-DOPE/30% CHO liposome solution for each trial. (\bullet) time at which 70% Q_{Me}-DOPE/30% CHO liposomes were lysed with the addition of 15 μ L of 30% (v/v) Triton X-100121
- Figure 4.19** Instability of 100 μ M 70% Q_{Me}-DOPE/30% CHO liposomes in the presence of 0.007% BSA. (\uparrow) the time for addition of liposome solution into the 0.007% BSA solution. (\bullet) time at which 70% Q_{Me}-DOPE/30% CHO liposomes were lysed with the addition of 15 μ L of 30% (v/v) Triton X-100122
- Figure 4.20** Instability of 100 μ M 70% Q_{Me}-DOPE/30% CHO liposomes in the presence of 0.5 μ M hNQO1. (\uparrow) the addition time for 300 μ L of 5 μ M hNQO1 solution into liposome solution. (\bullet) time at which 70% Q_{Me}-

	DOPE/30% CHO liposomes were lysed with the addition of 15 μL of 30% (v/v) Triton X-100.....	122
Figure 4.21	UV-vis spectra for hNQO1 assay (A) and hNQO1 inhibition assay (B). A) $\text{Q}_{\text{Me}}\text{-COOH}$ and NADH (blue line) and $\text{Q}_{\text{Me}}\text{-COOH}$ and NADH and hNQO1 after 1 min (pink line). B) $\text{Q}_{\text{Me}}\text{-COOH}$ and NADH (blue line) and $\text{Q}_{\text{Me}}\text{-COOH}$ and NADH and hNQO1 after 30 min (pink line), after 1 hour (green line) and after 4 hours (cyan line)	123
Figure 4.22	Instability of 100 μM 100% $\text{Q}_{\text{Me}}\text{-DOPE}$ liposomes in the presence of 0.25 μM hNQO1 (red line) and 0.25 μM inhibited hNQO1 (blue line). (\uparrow) the addition time for 300 μL of 2.5 μM hNQO1 or inhibited hNQO1 solution into liposome solution. (\bullet) time at which 100% $\text{Q}_{\text{Me}}\text{-DOPE}$ liposomes were lysed with the addition of 15 μL of 30% (v/v) Triton X-100	124
Figure 4.23	Instability of 100 μM 100% $\text{Q}_{\text{Me}}\text{-DOPE}$ liposomes in the presence of 0.25 μM hNQO1 (red line) and 0.25 μM hNQO2 (blue line). (\uparrow) the addition time for 300 μL of 2.5 μM hNQO1 or hNQO2 solution into liposome solution. (\bullet) time at which 100% $\text{Q}_{\text{Me}}\text{-DOPE}$ liposomes were lysed with the addition of 15 μL of 30% (v/v) Triton X-100.....	125
Figure 4.24	Stability of 100 μM 100% $\text{Q}_{\text{Me}}\text{-DOPE}$ liposomes in the presence of 0.25 μM heat inactivated hNQO1. (\uparrow) the addition time for 300 μL of 2.5 μM heat inactivated hNQO1 solution into liposome solution. (\bullet) time at which 100% $\text{Q}_{\text{Me}}\text{-DOPE}$ liposomes were lysed with the addition of 15 μL of 30% (v/v) Triton X-100.....	125

LIST OF SCHEMES

Scheme 2.1	Reduction of 1,4-benzoquinone to 1,4-hydroquinone	54
Scheme 2.2	Cyclization process of trimethyl-lock propionic acid 1,4-benzoquinones.....	55
Scheme 3.1	Reduction and cyclization process on quinone propionic acid triggers (QPA).....	73
Scheme 3.2	Hydride transfer mechanism on all possible atom sites on QPAs	83
Scheme 4.1	Proposed enzyme-responsive liposome system	101

LIST OF ABBREVIATIONS AND SYMBOLS

AAO	Amino acid oxidases
AELs	Anticancer ether lipids
AO	Aldehyde oxidase
AQ4N	1,4-bis [2-(dimethylamino-N-oxide) ethyl] amino-5,8-dihydroxyanthracene-9,10-dione
ARH019	3-hydroxymethyl-5-(2-methylaziridin-1-yl)-1-methyl-2-phenylindole-4,7-dione
AZQ	2,5-bis(carboethoxyamino)-3,6-diaziridinyl-1,4-benzoquinone
β -lap	β -lapachone
BSA	Bovine serum albumin
CHO	Cholesterol
CPR	Cytochrome P450 reductase
CSD	Cambridge Structural Database
CV	Cyclic voltammetry
CYPs	Cytochrome P450s
DAG	Diacylglycerol
DLS	Dynamic light scattering
DMXAA	5,6-dimethylxanthenone-4-acetic acid
DOPC	1,2-dioleoyl- <i>sn</i> -glycero-3-phosphocholine
DOPE	1,2-dioleoyl- <i>sn</i> -glycero-3-phosphoethanolamine
DPPC	1,2-dihexadecanoyl- <i>sn</i> -glycero-3-phosphocholine
DPPIsCho	1,2-dihexadec-1'-enyl- <i>sn</i> -glycero-3-phosphocholine

DPPC/DPPE-PEG ₂₀₀₀	1,2-dihexadecanoyl- <i>sn</i> -glycero-3-phosphocholine/1,2-dihexadecanoyl- <i>sn</i> -glycero-3-phosphoethanolamine- <i>N</i> -[methoxy(polyethylene glycol)-2000]
DTIC	Dacarbazine
ECM	Extracellular matrix
EPR	Enhanced permeability and retention
EO9	3-hydroxy-5-aziridinyl-1-methyl-2(1H-indole-4,7-indione)-propenol
ES936	5-methoxy-1,2-dimethyl-3-[(4-nitrophenoxy)methyl]indole-4,7-dione
FAA	flavone-8-acetic acid
FAD	Flavin adenine dinucleotide
FADH ₂	Reduced flavin adenine dinucleotide
FMN	Flavin mononucleotide
GDEPT	Gene directed enzyme prodrug therapy
IUdR	5-Iodo-2'-deoxyuridine
MeDZQ	2,5-diaziridinyl-3,6-dimethyl-1,4-benzoquinone
MeO-suc-AAPV	N-methoxy-succinyl-Ala-Ala-Pro-Val
MMC	Mitomycin C
MME	Methylester of melphalan
MPPs	Matrix metalloproteinases
MMP-2	Gelatinase A
MMP-9	Gelatinase B
<i>N</i> -Ac-4-S-CAP	<i>N</i> -acetyl-4-S-cysteaminyphenol
NADH	Reduced nicotinamide adenine dinucleotide
NADPH	Reduced nicotinamide adenine dinucleotide phosphate
NQO	NAD(P)H:quinone oxidoreductase
hNQO1	Human NAD(P)H:quinone oxidoreductase type-1

hNQO2	Human NAD(P)H:quinone oxidoreductase type-2
mNQO1	Mouse NAD(P)H:quinone oxidoreductase type-1
rNQO1	Rat NAD(P)H:quinone oxidoreductase type-1
rhNQO1	Recombinant human NAD(P)H:quinone oxidoreductase type-1
NQO3	Bacteria NAD(P)H:quinone oxidoreductase
NQO4	Fungi NAD(P)H:quinone oxidoreductase
NQO5	Archaeobacteria NAD(P)H:quinone oxidoreductase
PB	Phosphate buffer
PC	Phosphatidylcholine
PC-PLC	Phospholipase C
PE	Phosphatidylethanolamine
PEG	Poly(ethylene glycol)
PEG ₂₀₀₀ -DOPE	1,2-dioleoyl- <i>sn</i> -glycero-3-phosphoethanolamine- <i>N</i> - [methoxy(polyethyleneglycol)-2000]
PLA ₂	Phospholipase A ₂
PLA ₂ -I	PLA ₂ secretory pancreatic type
PLA ₂ -II	PLA ₂ non-pancreatic
cPLA ₂	PLA ₂ cytosolic
i PLA ₂	PLA ₂ cytosolic independent of Ca ²⁺
POPC	1-palmitoyl-2-oleoy- <i>sn</i> -glycero-3-phosphocholine
proAELs	AELs prodrugs
PS	Phosphatidylserine
QPAs	Quinone propionic acid triggers
Q-DOPE	Quinone attached to a DOPE lipid
Q _{Me} -DOPE	Methyl-substituted Q-DOPE

Q-liposomes	Quinone-based liposomes
RH1	2,5-diaziridinyl-3-(hydroxymethyl)-6-methyl-1,4-benzoquinone
RMSD	Root mean square deviation
SeCys	selenocysteine
SHE	Standard hydrogen electrode
SN	Streptonigrin
S-ProAEL	thio-ester anticancer ether lipid
SU5416	Melphalan semaxanib
TPZ	Tirapazamine
VDEPT	Virus directed enzyme prodrug therapy
Na ₂ S ₂ O ₄	Sodium dithionite
1,2-di- <i>O</i> -SPC	1,2- <i>O</i> -octadecyl- <i>sn</i> -glycero-3-phosphocholine
4-S-CAP	4-S-Cysteaminyphenol
5-FU	5-fluorouracil
17AG	17-amino-17-demethoxygeldanamycin
17-AAG	17-Allylamino-17-demethoxygeldanamycin
17-DMAG	17-demthoxy-17-[[2-(dimethylamino)ethyl]amino]-geldanamycin
ϵ	Molar extinction coefficient
$i_{p,a}$	Anode current peak
$i_{p,c}$	Cathode current peak
ΔE_p	Distance between cathode peak and anode peak
$E_{1/2}$	Half-wave potential
E°	Formal potential
$E_{p,c}$	Cathodic reduction peak
$E_{p,a}$	Anodic oxidation peak

λ_{ex}	Excitation wavelength
λ_{em}	Emission wavelength
T_{m}	Temperature at which lipids undergo phase transition from gel to liquid
K_{m}	Michaelis constant
V_{max}	Maximum velocity
k_{cat}	Catalytic constant
$k_{\text{cat}}/K_{\text{m}}$	Enzyme efficiency

ABSTRACT

For decades, there has been a lot of focus on the development of new carriers for drug delivery applications. From all of the carriers, stimuli-responsive liposomes have been studied extensively, but only a handful have been enzyme-responsive liposomes. Therefore, the field of endogenous proteins as activators of liposomes is a fertile field worthy of exploration.

The research described in this dissertation involves how structural changes on the quinone moiety altered their electronic properties, as well as their behavior toward the human enzyme NAD(P)H:quinone oxidoreductase type-1 (hNQO1, over expressed in certain tumor tissues), thus yielding a series of triggerable quinones to be used in the formation of enzyme-activated liposomes. The step-wise process to achieve the ultimate research objective includes: (1) measurement by cyclic voltammetry of the electronic properties of naked, propionic acid quinones and those attached to an ethanolamine handle, (2) detailed kinetics (Michaelis constant (K_m), maximum velocity (V_{max}), catalytic constant (k_{cat}), enzyme efficiency (k_{cat}/K_m)) and computational docking studies for a series of quinone derivatives against hNQO1, and (3) preparation of quinone-based liposomes and evaluation in the presence of the different components included in an hNQO1 assay.

Structural alterations on the quinone ring had an effect on their reduction behavior. Electrochemical studies exposed a trend in reduction potential; quinones with electron-withdrawing groups were easy to be reduced and the opposite happens to quinones with electron-donating groups. Enzyme and docking studies showed the different quinone responses obtained from the interaction of hNQO1 with structural-altered quinones. Liposome experiments provided all the obstacles that need to be overcome when designing an enzyme-responsive liposome system. The inclusion of 1,2-dioleoyl-*sn*-glycero-3-phosphocholine (DOPC) or cholesterol decreased the leakage of contents from the liposome systems. Gathering all this

information provided me a strong background on the fundamentals of structure-reactivity relationships between quinones and hNQO1 and their importance toward the design of a triggerable drug delivery system.

CHAPTER 1

INTRODUCTION

1.1 Research Goals and Aims

The goal of the research presented in this dissertation is the characterization of quinone trigger groups that are to be used to further develop enzyme-responsive liposomes. In particular, liposomes activated by human NAD(P)H:quinone oxidoreductase type-1 (hNQO1), an over-expressed enzyme in certain solid tumors (e.g. non-small cell lung, colon and pancreas tumors),¹⁻⁵ are targeted because they are expected to selectively deliver to the desired site more drug units per carrier than will a prodrug system.

The challenge of producing a prodrug or drug delivery system that actively releases its contents at the desired site but maintains its integrity in the bloodstream for long periods of time has been a continuing issue for researchers around the world over the past 30 years. Liposomes have been able to address one of those issues as a result of the addition of lipids possessing poly(ethylene glycol) chains (PEG) that have led to increased liposome circulation times in the body.⁶ PEGylated liposomes are able to circulate in the bloodstream for sufficient periods of times that they are able to accumulate at tumor sites via the enhanced permeability and retention (EPR) effect.^{7,8} Nevertheless, while drug-loaded PEGylated liposomes are in the circulatory system, non-specific interactions still occur, resulting in drug leakage from liposomes, an event that impacts healthy cells. Also, due to the slow nature of drug delivery at the target site, high concentration of liposomes is required, causing side effects, such as mucositis and hand-foot syndrome.⁹ In today's market, there are 11 approved liposomal formulations and 6 more currently in clinical development;¹⁰ however, none of those 17 liposomal formulations deliver their contents as a result of enzyme triggering. Therefore, the use of endogenous enzymes as an active stimulus for liposome contents release is a fertile field worthy of exploration.

Currently, extensive literature for enzyme-activated prodrugs is available;¹¹ this information has been an important contribution in the design of enzyme-responsive liposomes. However, the design and formulation of enzyme-responsive liposomes is still in the early stages. Only a few research groups have explored endogenous enzymes (e.g. elastase, alkaline phosphatase, phospholipase C, phospholipase A₂ (PLA₂) and matrix metalloproteinases (MMPs)) as trigger stimuli for liposome contents release.^{9,12,13}

The design of a liposome with triggerable groups that can be activated by an enzyme will allow for selective and site-specific controlled delivery of the liposomal contents. This scenario results in a lower frequency of drug administration and minimizes systemic side effects. The McCarley research group developed a redox-responsive liposome that contains a quinone head group and a fusogenic lipid, 1,2-dioleoyl-*sn*-glycero-3-phosphoethanolamine (DOPE).¹⁴ It was demonstrated that the liposomes are able to be opened and then release their contents as a result of a two-electron/two-proton chemical reduction, but their contents release has yet to be explored by a reductive enzyme.¹⁵ Among the different reductive enzymes used as stimuli for prodrug activation,^{16,17} NQO1 is an enzyme that specifically reduces quinones to hydroquinones by a two-electron/two-proton process.¹⁸ NQO1 has also been studied for bioreductive activation of anticancer drugs¹⁹ and prodrugs^{16,17} but to date has been investigated as a trigger for liposome contents release.

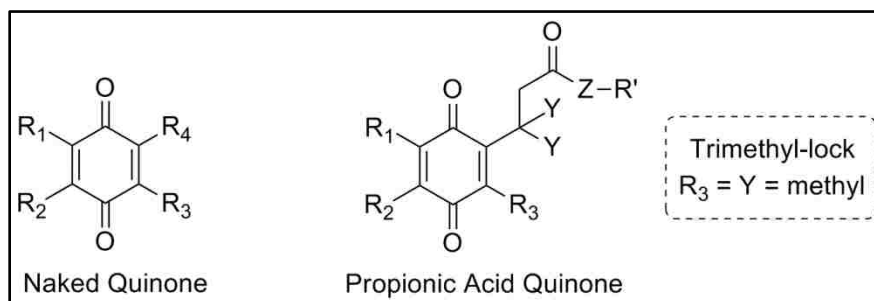


Figure 1.1. Illustration of quinone derivatives investigated in this dissertation.

The first aim of this research was the electrochemical characterization of a series of quinone derivatives: naked quinones (no propionic acid side chain), quinones containing a

propionic acid side chain, and quinones containing a trimethyl-lock motif ($R_3 = Y = \text{methyl}$), Figure 1.1. All quinones used underwent a two-electron/two-proton reduction process in aqueous media, and their electronic properties were measured by cyclic voltammetry (CV). Cyclic voltammetry is an electrochemical technique that provides information regarding the reduction potential and cyclization kinetics of the quinone derivatives. The main advantage of tuning the reduction potential of quinones is that these compounds can undergo reduction in a particular environment such as where a high concentration of NQO1 is available but remain inactive in healthy cells. It is crucial for the stability of quinone-based liposomes that their quinone derivatives have a reduction potential that can only be reduced by human NQO1, thus avoiding any non-specific reduction by other reducing species present inside the human body. Furthermore, the reduction/cyclization process resulting from quinone derivatives possessing the trimethyl-lock system is also believed to be dependent on the electronic properties of the quinones.

The second aim of this research was the characterization of quinone derivatives by enzyme assays and docking studies using the human enzyme NQO1. Enzyme kinetic assays gathered information on how structural changes of the quinone moiety affected the interaction between recombinant human NQO1 (rhNQO1) and the quinone derivatives. This information was based on the kinetic parameters K_m (Michaelis constant), V_{max} (maximum velocity), k_{cat} (catalytic constant), and k_{cat}/K_m (enzyme efficiency) extracted from the rhNQO1 assays. In addition, molecular docking studies were used to determine the possible interaction and optimum orientations between quinone derivatives and human NQO1.

The ultimate goal was the preparation of quinone-based liposome systems and observations of their behavior under rhNQO1 assay conditions. A variety of quinone-based liposome systems were prepared following a modified version of the well-known “lipid thin-film and extrusion” method.^{20,21} The stability of the quinone-liposome systems in the presence of

bovine serum albumin (BSA), reduced nicotinamide adenine dinucleotide (NADH) and rhNQO1 were investigated by fluorescence spectroscopy. As a probe, the self-quenching dye calcein was loaded into the liposome systems at concentrations where the dye is non-fluorescent. Liposome leakage caused by the introduction of BSA, NADH, or rhNQO1 to the liposome solution will result in the dilution of calcein and consequently a fluorescent signal is observed. In addition, chemical release curves for the new liposome formulations were investigated using the reducing agent sodium dithionite ($\text{Na}_2\text{S}_2\text{O}_4$). Calcein-loaded liposome formulations were characterized with UV-vis spectroscopy, dynamic light scattering (DLS) and zeta potential.

From the results in this work, there is a clear understanding of the structure-activity relationship of quinone derivatives with recombinant human NQO1 and the interaction between rhNQO1 assay contents and quinone-based liposome systems. These nanosizes structures are a promising tool as triggered release carriers because they hold potential for selectively unload their contents in a controlled manner at the desired site.

1.2 Prodrugs Activated by Endogenous Oxidoreductase Enzymes Other Than NQO1

Conventional chemotherapeutic drugs have been limited in their use due to low therapeutic index, and poor selectivity for tumor cells.¹¹ One of the most promising technologies to overcome this issue is the use of prodrugs where nontoxic drugs are carried and activated at the specific tumor site by over-expressed enzymes. Numerous tumor-associated enzymes have been exploited for prodrug activation in the field of gene- and virus-directed enzyme prodrug therapy (GDEPT, VDEPT), but effectiveness has been limited by insufficient transduction of tumor cells *in vivo*.^{11,22} Endogenous enzymes such as transferases, phosphorylases, kinases, hydrolases and oxidoreductases have also been investigated as a strategy to achieve local activation of prodrugs.¹¹ In the section that follows, the characteristics, localization and prodrug developments towards human oxidoreductases (except NQO1 that will be detailed reviewed in the last section) will be discussed.

1.2.1 Aldehyde Oxidase

Aldehyde oxidase (AO) is a homodimeric enzyme with a molecular mass of 300 kDa containing 1338 amino acids.²³⁻²⁵ Its structure contains flavin adenine dinucleotide (FAD), molybdenum, and heme-iron groups.^{11,23,25} This cytosolic protein is present in high levels in human liver, lung, adrenal, testis and prostate tissue; however, little is known about the difference in the concentration levels of AO between normal and tumor tissues.²⁶ AO oxidizes aldehydes to the corresponding acids using molecular oxygen, and it catalyzes the oxidation of pyrroles, pyridines, purines, pterins, and pyrimidines.¹¹

AO has been used in an attempt to increase organ selectivity of 5-ethynyluracil, a compound that prevents the rapid breakdown of 5-fluorouracil (5-FU), a well-known anticancer agent. Porter and co-workers assayed the 5-ethynyl-2(1H)-pyrimidinone as a potential liver-specific prodrug; however, their results showed lack of liver selectivity.²⁷ Later, Guo *et al.* synthesized a 5-fluoro-2-pyrimidinone prodrug to increase organ selectivity towards the liver. Even though the authors succeeded in their task, this prodrug had similar cytostatic activity as the conventional drug 5-FU.²⁸ AO has also been explored as an enzyme to increase the bioavailability of drugs. In this matter, a prodrug of the radiosensitizer 5-iodo-2'-deoxyuridine (IUdR) was developed; it exhibited promising results and is currently under phase I clinical trials.²⁹⁻³¹ Few attempts have been made to target AO as an enzyme that activates prodrugs, due to the wide distribution of this enzyme in humans.²⁷ Moreover, AO differs greatly in substrate specificity between species, and what may be promising in animal models is not always successful in humans.¹¹

1.2.2 Amino Acid Oxidases

Amino acid oxidases (AAO) are dimeric flavoproteins that contain FAD as a prosthetic group, and they stereoselectively catalyze the oxidative deamination (loss of an amine group) of amino acids to the corresponding α -keto acids, ammonia and hydrogen peroxide, as noted in

Figure 1.2.^{11,32-34} These enzymes also catalyze the β -elimination reactions of β -chloroalanine, β -cyanoalanine, and selenocysteine Se-conjugates (SeCys conjugates) that result in the production of chloride, cyanide, and selenols, along with the formation of pyruvate and ammonia.¹¹

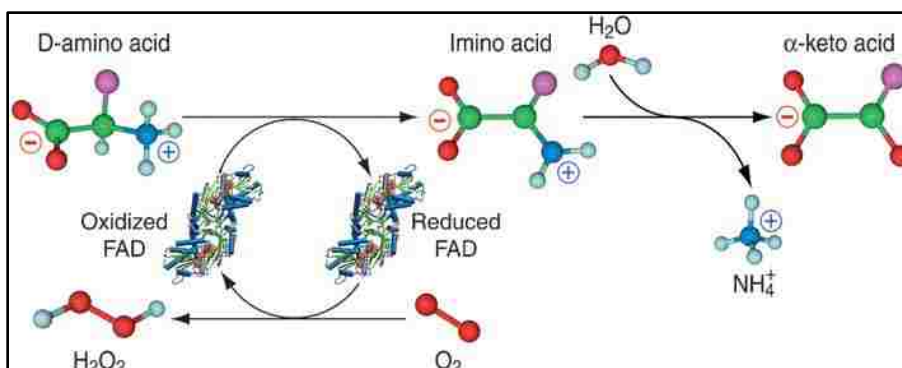


Figure 1.2. Mechanism of action of D-amino acid oxidase. Adapted from Pollegioni (2007).³²

LAAO (catalyzes the oxidative deamination of L-amino acids) has a molecular mass between 85 and 150 kDa, while the molecular mass range of DAAO (catalyzes the oxidative deamination of D-amino acids) is between 38 and 125 kDa.¹¹ High levels of AAO have been found in human tissues such as those of the kidney and liver, while low levels of AAO were found in brain tissue.³³

SeCys conjugates have been the most studied approach in the targeting of AAO.¹¹ Several Se-conjugates have been shown to possess chemopreventive and antitumor properties.^{34,35} So far, investigations on the β -elimination mechanism of Se-conjugates have been done with rat renal cytosol, rat and human kidney cytosol but targeting β -lyse enzymes.^{36,37} Later, Rooseboom *et. al.* demonstrated the activation of Se-conjugates by purified LAAO from *Crotalus adamanteous* and by DAAO from porcine kidney.³⁸ The activation of Se-conjugates is stereoselective, thus, it needs to be taken into account when designing a prodrug to activate DAAO or LAAO.

1.2.3 NADPH-Cytochrome P450 Reductase

Cytochrome P450 reductase (CPR) is a NADPH-ferrihemoprotein that catalyzes the reduction of cytochrome P450s, as well as the reduction of aldehydes (to form alcohols) and

quinones (to form semiquinone free radicals).¹¹ Human CPR is localized in the endoplasmic reticulum and has a molecular mass of approximately 82 kDa that includes 676 amino acids.^{39,40} CPR is a multidomain protein divided into a hydrophobic *N*-terminal domain, a flavin mononucleotide-binding (FMN) domain, and a FAD/NADPH binding domain (flavin adenine dinucleotide/nicotinamide adenine dinucleotide phosphate).^{41,42} The mechanism of this enzyme consists of accepting a pair of electrons from NADPH as a hydride ion, with FAD and FMN being the points of entry and exit, respectively. Then, these electrons are transferred to cytochrome P450s, or to aldehydes or quinones.⁴³ High levels of CPR were found in liver, lung, and small intestine based on immunohistochemical staining of human tissues.⁴⁴ CPR was also found in a variety of tumor cells, such as lung, breast, and liver.⁴⁵ However, only liver tumor cells were shown to have a significant increase in activity (2-fold) of CPR versus normal tissue.^{46,47} Moreover, in general, CPR activity is lower in tumor tissue than in the corresponding normal tissue.⁴⁸

CPR has been explored as a target for prodrug activation under hypoxic conditions (low oxygen levels) where the one-electron reduction of substrates by CPR generates toxic free radicals that cause cell damage. Studies on Chinese hamster ovary cells demonstrate CPR is the major enzyme that activates mitomycin C (MMC) and its analog porfiromycin under hypoxic conditions.^{49,50} In those studies, the hamster ovary cells were transfected with human CPR and compared with the parental cells. The authors found that porfiromycin exhibited greater cytotoxicity under hypoxic conditions than under aerobic conditions, while MMC had the same toxicity regardless of the oxygenation state.^{49,50} RH1 (2,5-diaziridinyl-3-(hydroxymethyl)-6-methyl-1,4-benzoquinone) prodrug was also demonstrated to be reduced by CPR of pig liver origin.⁵¹ However, studies in human cancer cell lines (T47D human breast cancer cells and T47D-P450 transfected with P450 Red gene) did not demonstrate any significant increase in

cytotoxicity after treatment with RH1.⁵² Therefore, human CPR does not appear to have a substantial contribution in the activation of RH1.

To date, the major focus on CPR-targeted prodrugs has been the bioreductive agent tirapazamine (TPZ). In the late 1980s, it was demonstrated that TPZ could be activated by CPR leading to DNA cleavage, as noted in Figure 1.3.^{11,17,53} Several *in vitro* investigations led to promising clinical trials; however, those results did not translate into *in vivo* success. It is believed poor drug penetration through the extravascular tumor was the key factor in affecting *in vivo* activity.^{11,17,53}

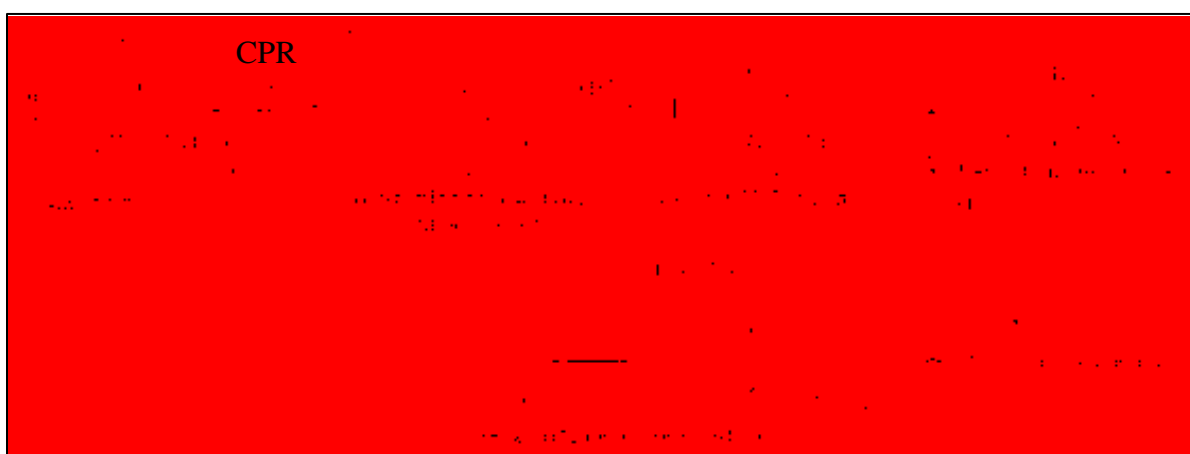


Figure 1.3. Reductive activation of TPZ. Adapted from Chen (2009).¹⁷

1.2.4 Cytochrome P450s

Cytochrome P450s (CYPs) consist of a family of several isoenzymes containing a heme prosthetic group that catalyzes the monooxygenation of a variety of substrates (from small molecules to large antibiotics) by incorporating one atom of molecular oxygen into a substrate and reducing the other oxygen atom to water.¹¹ CYPs accept electrons from either the enzyme CPR or from NADPH and use them in its catalytic cycle.¹¹ Human CYPs encoded by 57 genes are divided into families based on their homology in amino acid sequence identity.⁵⁴ The most important human isoenzymes are CYP1A1/2, 2C9/19, 2D6, 2E1 and 3A4.¹¹ Based on the three-dimensional structure availability, Johnson and Stout compared the structure of CYP2A6, 2C8, 2C9, and 3A4.⁵⁵ The investigation revealed that 3A4 and 2A6 share less than 40% amino acid

identity, whereas the active site of 2A6 is one-sixth the volume of that for 3A4. The authors also reported that 3A4 and 2C8 active sites are similar in size but different in shape, while the active site of 2C9 is larger than 2A6, but smaller than 2C8. The difference in active site architecture and chemical properties of the amino acids involved are probably the reasons why for all the CYPs, CYP3A4 contributes to over 60% of the metabolism of drugs reported to date.⁵⁴

Human CYPs are located in the endoplasmic reticulum, mainly in liver and adrenal gland tissues; however, low concentrations of CYPs were also found in kidney and testis tissues.⁵⁶ CYPs in general have lower levels in tumor tissues than in normal tissue,¹¹ yet higher levels of the enzyme isoforms CYP1A and CYP3A were found in tumors versus their corresponding normal tissues.⁵⁶

Most CYPs chemotherapeutic agents were not initially designed as prodrugs to target CYPs; however, later investigations demonstrated that they could be activated by CYPs.¹¹ That was the case for the example of 4-ipomeanol (1-(3-furyl)-4-hydroxy-1-pentanone) which is metabolized by CYP1A2, 3A3, and 3A4. Although bioactivation was demonstrated, 4-ipomeanol failed in clinical trials towards lung cancer.¹¹ Another example is Tegafur, a prodrug of 5-FU (anticancer drug) that was initially thought to be activated by thymidine phosphorylase and CYPs, but later it was demonstrated that Tegafur was mainly activated by CYPs.¹¹ Investigations revealed that the isoenzymes responsible for its activation are CYP1A2, 2A6, and 2C8/9.^{57,58} Dacarbazine (DTIC) is another CYP-activated prodrug used in the treatment of malignant melanoma and Hodgkin's lymphoma.⁵⁹ It has been demonstrated that isoforms CYP1A1, 1A2, and 2E1 account for the activation of DTIC.¹¹ However, in spite of the successful antitumor effect in rodents, an insufficient amount of antitumor activity was exhibited in humans.¹¹

To date, the major prodrug compounds activated by CYPs are oxazaphosphorines and 1,4-bis [2-(dimethylamino-*N*-oxide) ethyl] amino-5,8-dihydroxyanthracene-9,10-dione

(AQ4N).¹¹ Oxazaphosphorines, in particular cyclophosphamide, is the most used alkylating agent with widespread application in cancer therapy. This prodrug and its isomer are activated by the isoforms CYP2B6 and 3A4. Cyclophosphamide, along with its isomer ifosfamide, presented issues because of the high concentration of CYPs in liver and low levels in tumor cells.¹¹ Those obstacles were overcome by gene-directed enzyme prodrug therapy (GDEPT).⁶⁰

AQ4N is converted into a potent topoisomerase II inhibitor after bioreduction by CYPs (in particular the isoform 3A4) to AQ4, Figure 1.4.¹¹ AQ4 is also a high-affinity DNA-binding agent where its tertiary amine side chains ensure good uptake of the compound into the cells.¹⁷ AQ4 is currently in phase-2 clinical trials for brain tumor, chronic lymphocytic leukemia, and non-Hodgkin's lymphoma.¹⁷

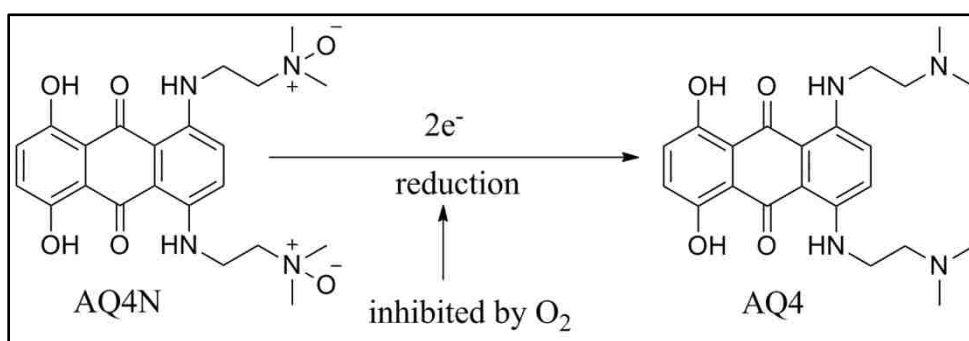


Figure 1.4. Reductive activation of AQ4N. Adapted from Chen (2009).¹⁷

The major drawbacks on targeting CYPs are their high concentration levels in liver and adrenal glands, their low turnover rates resulting in generally slow drug formation, and their low activity in tumor cells compared with normal cells. However, several prodrugs activated by CYPs are successfully used in the clinic.¹¹

1.2.5 Tyrosinase

Tyrosinase is a copper enzyme (two copper ions per enzyme molecule) that catalyzes the oxidation of L-tyrosine to the corresponding *o*-quinone dopaquinone as well as the oxidation of phenols and catechols to *o*-diphenols and *o*-quinones, respectively.^{11,61} This enzyme was found to have an approximate molecular mass of 67 kDa by SDS electrophoresis.⁶¹ The X-ray

structure of human tyrosinase has not yet been determined; however, the three-dimensional structure from *Streptomyces castaneoglobisporus* (gram-positive bacteria) has been solved, and it has been useful to describe in detail the tyrosinase catalytic mechanism, Figure 1.5.⁶² The authors proposed that first a peroxide ion is bridged to copper ions following a proton extraction from the phenolic hydroxyl to later have the deprotonated oxygen atom bound to copper. At this point, copper is hexa-coordinated and an *ortho*-carbon of the substrate is approached by the peroxide ion which adds one of the peroxide oxygens to the *ortho*-carbon of monophenol.

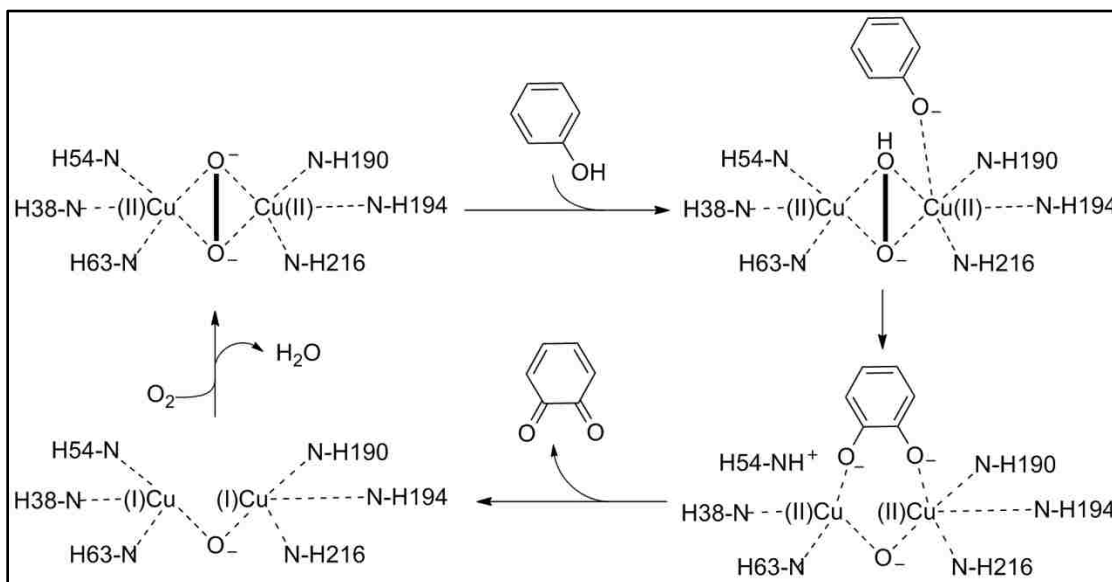


Figure 1.5. Catalytic mechanism of tyrosinase. Adapted from Matoba (2006).⁶²

Tyrosinase is responsible for skin pigmentation abnormalities and has the very peculiar property that it is only located in melanoma cells, making this enzyme a very attractive target for treatment of the cancer, melanoma.⁶³ The first prodrug dependent on tyrosinase activity was 2,4-dihydroxyphenylalanine.⁶⁴ This prodrug showed good selectivity towards tyrosinase-containing cells versus tyrosinase-lacking cells. In spite of these findings, the potential of 2,4-dihydroxyphenylalanine as a prodrug was not further evaluated.¹¹ 4-*S*-Cysteaminyphenol (4-*S*-CAP) and *N*-acetyl-4-*S*-cysteaminyphenol (*N*-Ac-4-*S*-CAP) are other two prodrugs that showed tyrosine-mediated cytotoxicity.¹¹ Later, analogs of *N*-Ac-4-*S*-CAP were synthesized and presented activities comparable to that of cisplatin, a well-known chemotherapy drug.⁶⁵ Phenyl-

and urea- mustard prodrugs were also synthesized and assayed for tyrosinase activity.^{66,67} The authors found a positive correlation between prodrug toxicity and tyrosinase activity. More recently, the stability of these prodrugs in the presence of phosphate buffer and bovine serum were evaluated;⁶⁸ the authors identified the urea prodrugs as the lead compounds for further studies.

1.3 Enzyme-Activated Liposomes

Currently marketed drug delivery systems based on liposomes and polymeric materials rely on passive diffusion or slow non-specific degradation of the liposomal carrier.⁹ To improve therapeutic efficiency, scientists have been putting their effort in designing carriers for active targeting (e.g. ligands on carrier surface) and active triggering (e.g. hyperthermia) to safely deliver carrier cargo to and at the desired site.⁹ These systems are composed of nanosize particles, ranging from liposomes to macromolecular dendrimers.^{6,13,69-71} It is not the intent of this dissertation to focus on each of these systems, but rather the few ones so far published that correspond to enzyme-responsive liposomes. The activation of liposomes by the endogenous enzymes elastase, alkaline phosphatase, phospholipase C, phospholipase A₂ and metalloproteinase, and their characteristics will be discussed below.

1.3.1 Elastase

Elastase is an enzyme released from the azurophil granules (cytoplasmic small particles in white blood cells) of activated neutrophils (50–70% of all white blood cells). Human neutrophil elastase has an approximate molecular mass of 30 kDa that includes 218 amino acids with two asparagine-linked carbohydrate side chains and four disulfide bonds.⁷² This enzyme became of particular interest in the activation of liposomes because it is ubiquitously present in inflammatory (e.g. rheumatoid arthritis,^{73,74} acute respiratory distress syndrome,⁷⁵ emphysema,⁷⁶ cystic fibrosis^{77,78}) and tumor (e.g. breast,⁷⁹ skin⁸⁰) tissues. Elastase has been used to activate enzyme-triggered liposomes where DOPE is capped with a short peptide sequence (e.g. *N*-Ac-

ala-ala) that is a substrate for the enzyme, Figure 1.6; stable non-fusogenic liposomes can be formed from *N*-Ac-ala-ala-DOPE.⁸¹ The stable peptide-DOPE liposome system became unstable upon cleavage of the peptide by elastase, resulting in liposome fusion with cells.

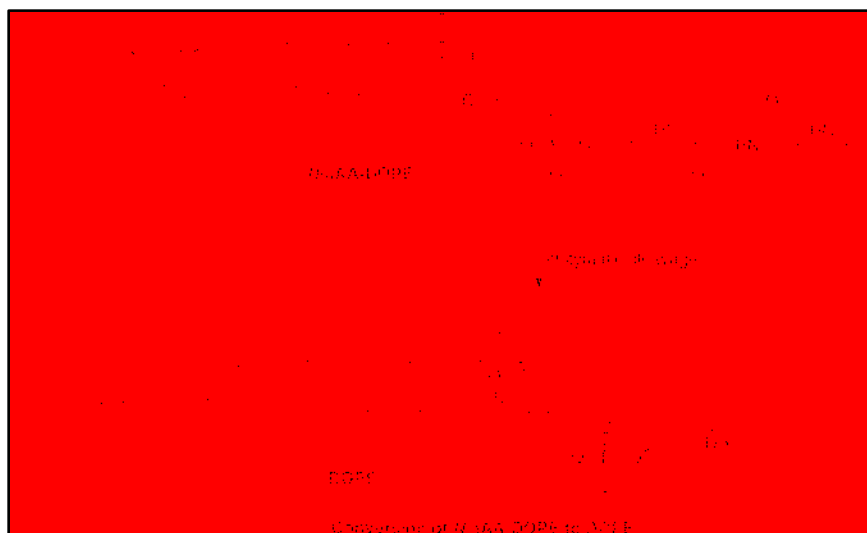


Figure 1.6. Cleavage of peptide-DOPE structure by elastase. Adapted from Pak (1998).⁸¹

This liposome system was further improved by attachment of a different peptide named *N*-methoxy-succinyl-ala-ala-pro-val (MeO-suc-AAPV) to the DOPE lipid that exhibited greater sensitivity and selectivity towards elastase than the previous peptide *N*-Ac-ala-ala. MeO-suc-AAPV-DOPE liposomes (250 μ M) were proved to be activated by 0.42 μ M elastase, an amount that is between 3 and 20 fold less than the amount found in cystic fibrosis tissue, with subsequent transfer of their aqueous content probes into adherent cells.⁸² The authors also observed that heat-inactivated elastase (95 °C for 1h) did not activate the MeO-suc-AAPV-DOPE liposomes. Other potential elastase substrates have been designed and are currently under development.¹²

1.3.2 Alkaline Phosphatase

Alkaline phosphatase is a non-specific phosphomonoesterase enzyme that is present in serum and on the cell membrane, as well as over-expressed in certain tumor tissues (e.g. testicular and ovarian).^{83,84} Its structure is the one of a dimeric metalloprotein with two Zn^{2+} ions and a Mg^{2+} ion in each active site.⁸⁵ The earlier demonstration on the ability of alkaline

phosphatase to activate prodrugs⁸⁶ and remove the phosphate group from a polysaccharide,⁸⁷ suggested the application of the enzyme to activate liposomes composed of phospholipid derivatives. Szoka and co-workers have been the only ones that took advantage of those results to design an alkaline phosphatase-sensitive liposome system composed of DOPE lipid and cholesterol phosphate derivatives.⁸⁸ They found that the liposome with the most sensitive behavior towards the enzyme exhibited a leakage of encapsulated fluorophore of 40% in 24 hours, while no leakage was observed in the presence of heat-inactivated enzyme.⁸⁸ The nature of the enzyme after being inactivated by heat could not be established because of the lack in information about the time and temperature at what the procedure was performed. The wide distribution of this enzyme in the body limited its use, unless the enzyme is directed to activate conjugated prodrugs (e.g. antibody).¹¹

1.3.3 Phospholipase C

Phospholipase C (PC-PLC) is an enzyme found in human gallbladder bile.^{89,90} High levels of PC-PLC have been found in rheumatoid arthritis tissues as well as in epithelial ovarian cancer cells and breast tumor cells.⁹¹⁻⁹³ The molecular mass of PC-PLC found in human monocytic U937 cell lines was 40kDa as determined by SDS gel electrophoresis.⁹¹ Later, a study on natural killer cells (NK cells) demonstrated the presence and subcellular localization of two PC-PLC isoforms with molecular masses of 40 and 66 kDa, respectively.⁹⁴ PC-PLC requires the presence of calcium ion as cofactor for its catalytic function for the hydrolysis of the phosphoester bond of lecithin to yield the amphiphile diacylglycerol (DAG) and the headgroup phosphocholine.⁹⁵⁻⁹⁷

This enzyme was the first catalytic agent to induce fusion of liposomes, an investigation done by Nieva and co-workers in the late 1980s.⁹⁵ The same investigation demonstrated that bilayer composition is critical. Phosphatidylethanolamine (PE) and cholesterol are essential, in addition to phosphatidylcholine (PC), for significant liposome fusion to occur at low levels of

phospholipase C.⁹⁵ In addition, it was later found that PC-PLC becomes inhibited by DAG, the end product, when DAG concentration is over 20 mol% in the liposome bilayer.⁹⁶ Contrary to the observation of Nieva, pure lecithin liposomes underwent aggregation and fusion with concomitant leakage of vesicle contents in the presence of PC-PLC, as reported by Luk.⁹⁸ However, in the fusion process described by Nieva, no leakage was observed.⁹⁵ In summary, PC-PLC-induced liposome fusion may be considered to happen in three steps: generation of DAG in the bilayer, aggregation of liposomes, and fusion of apposed membranes.⁹⁶

1.3.4 Phospholipase A₂ (PLA₂)

Phospholipase A₂ (PLA₂) and metalloproteinases have been the two enzymes most widely studied for liposome activation;¹³ the latter will be discussed in the next section. PLA₂ is an enzyme present in a wide variety of mammalian cells,^{99,100} and it hydrolyzes phosphoglycerides—such as phosphatidylcholine (PC), phosphatidylethanolamine (PE), and phosphatidylserine (PS)—at the acyl ester bond at the *sn*-2 position, yielding the corresponding lysophospholipid and fatty acid, as described in Figure 1.7.¹⁰¹

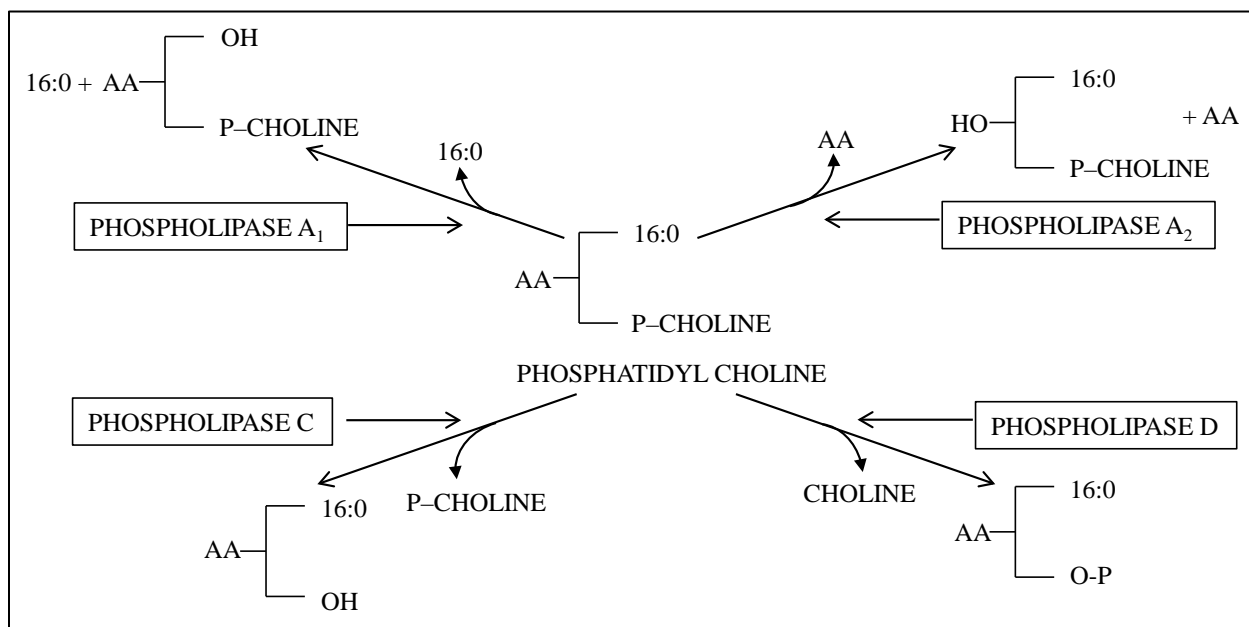


Figure 1.7. Mode of action of PLA₂ versus other phospholipases. AA = arachidonic acid. Adapted from Kaiser (1999).¹⁰¹

Mammalian PLA₂ is composed of three distinct isozymes: group I (PLA₂-I), group II (PLA₂-II), and cytosolic PLA₂ (cPLA₂).¹⁰² Group I is the secretory pancreatic type, with a molecular mass of approximately 14 kDa, and it requires millimolar amounts of Ca²⁺ for activation.¹⁰¹ The complete sequence of PLA₂-I consists of a single polypeptide chain of 125 amino acids with seven cross-linked disulfide bridges.¹⁰³ Group II is the non-pancreatic PLA₂ that can be further subdivided into secretory enzymes and membrane-associated enzymes.¹⁰² PLA₂-II has the same molecular mass and requirements of activation as PLA₂-I. The major difference is the absence of cysteine residues at position 11 and 77, along with the corresponding disulfide bridge in PLA₂-II. In spite of these differences, their respective active sites and hydrophobic regions are similar.¹⁰¹ Cytosolic PLA₂ enzymes have a molecular mass of approximately 80 kDa, with some being Ca²⁺ dependent (c PLA₂) enzymes and others are Ca²⁺ independent (i PLA₂) enzymes.¹⁰¹ An 85 kDa cPLA₂ was purified from human monocytic cell line (U937) and sequenced.¹⁰⁴ This cPLA₂ consisted of 749 amino acids and had no apparent disulfide bonds, in contrast to the PLA₂ enzymes found in Group I and II.¹⁰⁴ PLA₂ has been a target for cancer therapy because of its over expression in various types of cancer, such as pancreatic, breast, lung, stomach, and prostate; PLA₂-II is found in elevated concentrations in all types of cancer.^{9,101,105} In addition, high amounts of PLA₂-II in blood have been associated with systemic bacterial infections and malaria.¹⁰¹ Furthermore, it has been reported that elevated serum levels of PLA₂-II has been found in effusions from 47 patients with various cancers.¹⁰²

It has been essential to gain knowledge about the physical properties of liposomes (e.g. charge) and how that affects the substrate specificity towards PLA₂ for the rational design of a degradable drug delivery system. It was reported in the early 1990s that pig PLA₂ had a slight preference for anionic phospholipids (2–3 fold).¹⁰⁶ This preference was confirmed later by various investigations on the interaction of PLA₂-II and anionic membranes.¹⁰⁷⁻¹¹¹ Those investigations reported that the specificity of the enzyme for anionic membranes is a result of the

electrostatic nature of the active site of PLA₂-II that is high in cationic residues that provides non-specific electrostatic interactions that in turn promote surface binding. This specificity prevents PLA₂-II from interacting with unperturbed mammalian cells that are composed mostly of neutral lipids such as sphingomyelin, phosphatidylcholines, and cholesterol.¹¹⁰

PLA₂ has a fascinating feature of preference for aggregated lipid substrates, such as liposomes over lipid monomers.⁹ Thus, the design of liposomes with appropriate lipid composition will maximize PLA₂-II activity.¹¹² In addition, it has been proved that the addition of PEG modified lipids into the liposomal formulation did not preclude PLA₂ from binding to the liposome surface. On the contrary, PEG-lipid addition enhanced PLA₂ activity due to the anionic headgroup of the PEG-lipid.¹¹²⁻¹¹⁴

So far, the literature has presented two liposome designs: one is composed of different lipids and the other is formed by prodrug-lipid conjugates. Thompson and co-workers designed a cascade liposomal system that utilizes liposome photooxidation and contents release to activate PLA₂.¹¹⁵ This method employs a mixture of two liposomes, one composed of a photosensitive synthetic lipid, namely 1,2-dihexadec-1'-enyl-*sn*-glycero-3-phosphocholine (DPPICsCho) in conjunction with Ca²⁺, and the other composed of 1,2-dihexadecanoyl-*sn*-glycero-3-phosphocholine (DPPC) with the DPPC liposome containing the encapsulated fluorophore calcein. Upon light irradiation at 800 nm, the photosensitive liposome released Ca²⁺ ions thereby promoting PLA₂ activation which lead to a 50% calcein release in 40 min. A few years later, Davidsen *et al.* developed an experimental model using liposomes composed of 1,2-dihexadecanoyl-*sn*-glycero-3-phosphocholine/1,2-dihexadecanoyl-*sn*-glycero-3-phosphoethanolamine-*N*-[methoxy(poly(ethylene glycol))-2000], (DPPC/DPPE-PEG₂₀₀₀); these were activated by PLA₂ that caused destabilization of a second type of liposome inert to PLA₂ activity (mimicking stability of a target cell).¹¹⁶ Specifically, the generation of lysolipids and fatty acids by PLA₂ from a DPPC/DPPE-PEG₂₀₀₀ liposome caused cargo leakage from the inert

liposomes 1,2-*O*-octadecyl-*sn*-glycero-3-phosphocholine (1,2-di-*O*-SPC) that were in close proximity to the DPPC/DPPE-PEG₂₀₀₀ liposomes.

Anticancer ether lipids (AELs) are a class of drugs that inhibit tumor cell growth without causing mutagenic or myelosuppressive effects.⁹ However, the use of AELs was limited by severe hemolysis.⁹ In order to circumvent this issue, Andresen and co-workers synthesized AEL prodrugs (proAELs) to be included into a liposomal formulation sensitive to PLA₂.^{117,118} ProAEL liposomes successfully delivered the AELs into tumor cells showing no hemolytic toxicity.¹¹⁷⁻¹¹⁹ Very recently, Andresen *et al.* reported the synthesis of retinoid phospholipid prodrugs and proved that those pro-lipids can form liposomes sensitive to PLA₂. The ProAEL structures and their mechanism of release are represented in Figure 1.8. In addition to the work made by the Andresen group, Linderoth and co-workers reported the synthesis of a thio-ester anticancer ether lipid (S-ProAEL) and subsequent liposome formulations that were also sensitive to the enzyme PLA₂.¹²⁰

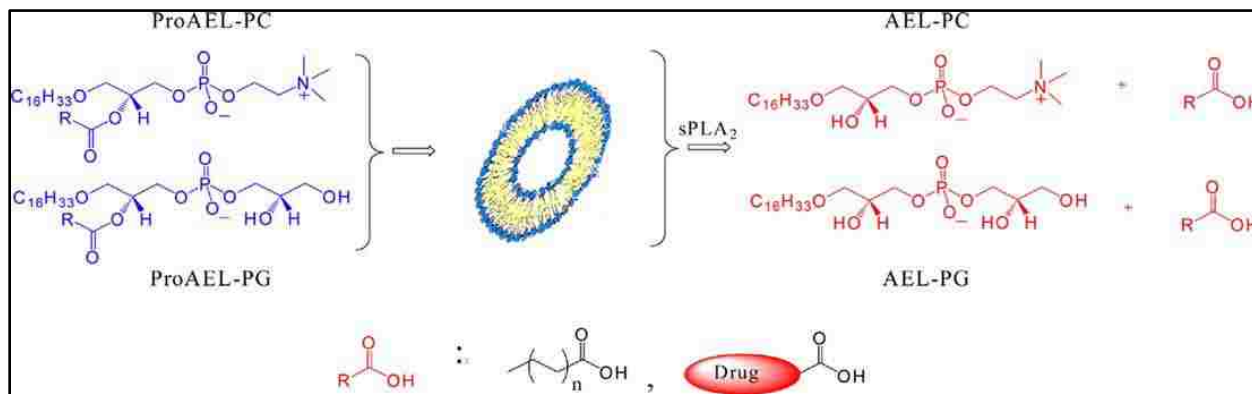


Figure 1.8. ProAELs structures and mechanism of AELs release in the presence of PLA₂. Adapted from Andresen (2005).⁹

1.3.5 Matrix Metalloproteinase (MMP)

Matrix metalloproteinases (MPPs) are zinc-dependent endopeptidases (they break peptide bonds of nonterminal amino acids) that together can degrade all components of the extracellular matrix (ECM).¹²¹ There are 21 members of the MMP family located in the membrane, as well as in the extracellular environment.¹²¹ Most of the MMPs secreted by cells are inactive zymogens

(or proenzyme, inactive enzyme precursors) that require proteolytical activation by tissue or plasma proteinases, bacterial proteinases or others MMPs.¹²¹ From the 21 MMPs known, MMP-2 (Gelatinase A) and MMP-9 (Gelatinase B) have been exploited for prodrug and liposome activation, because high levels of these enzymes are present in a variety of tumor cells, such as bladder, colorectal, gastric, lung, and ovarian with all of these causing poor prognosis and survival rate.¹²¹ MMP-2 has a molecular mass of 72 kDa in the inactive form and 62 kDa in the active form, while MMP-9 has a molecular mass of 92 kDa in the inactive form and 82 kDa in the active form.¹²² X-ray structures for both proenzymes have been reported.^{123,124} The structures of MMP-2 and MMP-9 are very similar; they both have two zinc ions in the catalytic site and three calcium ions in different parts of the enzyme.^{123,124} They also share the same number of domains consisting of the *N*-terminal propeptide domain (where the enzyme is activated), the catalytic domain (S1' pocket), the *C*-terminal domain and an additional three-tandem fibronectin type II (FnII) domain (4 versus 3 in the other MMPs).¹²⁴ The major differences between MMP-2 and MMP-9 rely on the side chain of Arg424 in MMP-9 that is angled slightly away from the S1' pocket when compared with the corresponding residue in MMP-2 (Thr424) and on the position of the second FnII domain.¹²⁴

The mode of action of the MMPs is cleavage of the peptide sequence, acetyl-L-prolyl-L-leucyl-glycyl-L-leucine (Ac-Pro-Leu-Gly-Leu), at the Gly-Leu bond.¹²⁵ Thus, prodrugs derivatized with that peptide should be substrates for MMP-2 and MMP-9, as envisioned by Kline and co-workers, who synthesized four peptides and four peptidomimetic compounds. From the 8 molecules synthesized, only two peptides were substrates for the enzymes, with one having higher cleavage rates for MMP-9.¹²⁵ Likewise, Chau *et al.* synthesized dextran-peptide-methotrexate conjugates for drug delivery in tumors that expressed MMP-2 and MMP-9. Pro-Val-Gly-Leu-Ile-Gly was the optimal peptide linker between the fully neutralized dextran and

the methotrexate drug.¹²⁶ This new peptide prodrug exhibited a bimolecular rate constant (k_{cat}/K_m) of $1.21 \times 10^5 \text{ M}^{-1} \text{ s}^{-1}$ for MMP-2 and $3.60 \times 10^3 \text{ M}^{-1} \text{ s}^{-1}$ for MMP-9.

Prodrug activation by MMPs gave the precedent for the design of triggerable liposomes capable of releasing their contents via MMP activation. Triple helical collagen-mimetic peptides conjugated to stearic acid (lipopeptides), along with 1,2-distearoyl-*sn*-glycero-3-phosphocholine (DSPC), were used to form the first liposomal formulation to be activated by MMP-9 which causes bilayer destabilization and release of liposomal contents.¹²⁷ In a later paper, the authors showed the mechanistic studies of liposomal formulations composed of three different lipopeptides integrated with 1-palmitoyl-2-oleoyl-*sn*-glycero-3-phosphocholine (POPC), 1,2-dioleoyl-*sn*-glycero-3-phosphocholine (DOPC) or DSPC lipids.¹²⁸ Those studies concluded that the rate and extent of leakage was dependent on MMP-9 concentration, and that upon MMP-9 activation, release of contents occurs due to lipid mismatch between the lipopeptide and the other lipids present in the liposome. Moreover, they proved that the lipopeptide liposomes did not release their contents in the presence of trypsin, even though the individual peptide is a substrate of the enzyme.¹²⁹ Recently, the same research group reported the release profile of liposome-encapsulated carboxyfluorescein in the presence of cancer cells.¹³⁰ They observed a 40% release in the presence of MCF7 cells (high levels of MMP-9) in 30 min versus a 10% release when liposomes were incubated with HT-29 cells (low levels of MMP-9) in the same amount of time.

In addition to the release mechanisms mentioned above, a different research group investigated the interactions between PEG-peptide-DOPE-liposomes and MMP-2.¹³¹ They found that MMP-2 hydrolyzed the peptide between PEG and DOPE. This indicates that the inclusion of PEG in the liposomal system to increase circulation time *in vivo* did not prevent MMP-2 from accessing the peptide substrate.

1.4 NAD(P)H:Quinone Oxidoreductase Type-1 (NQO1)

Prodrug activation by oxidoreductase enzymes other than NQO1, as well as enzyme-responsive liposomes, were discussed previously. This section will review NQO1 characteristics, as well as the different approaches to target NQO1 for cancer treatment.

1.4.1 Origin, Types, Structure, Mechanism, Location and Over Expression

NAD(P)H:quinone oxidoreductase Type-1 (NQO1, DT-diaphorase, EC 1.6.99.2) was accidentally discovered in 1955 and 1956 by Drs. Lars Ernster and Franco Navazio.^{132,133} The first published report (1958) of NQO1 described the enzyme as a soluble diaphorase found in animal tissue.¹³⁴ The term DT-diaphorase came later in order to differentiate NQO1 from other diaphorases specific to NADH¹³⁵ or NADPH.¹⁸ DT-diaphorase (NQO1) has the ability to accept electrons from the cofactors NADH (initially called DPNH) and NADPH (initially called TPNH).¹³⁶ Today, DT-diaphorase officially corresponds to NQO Type 1 (NQO1).¹³⁷ NQO has five genetic loci: NQO1 and NQO2 correspond to the human genes, as well as other mammals; NQO3 belongs to eubacteria; NQO4 belongs to fungi; and NQO5 belongs to archaeobacteria.¹³⁷

NQO1 is a homodimeric flavoprotein of 62 kDa containing 273 amino acids; each of the monomers has a non-covalently but tightly-attached FAD prosthetic group that remains bound during the catalytic cycle.^{138,139} The amino acid sequences and crystal structures of rat,¹³⁸ mouse¹³⁹ and human¹³⁹ NQO1s have been determined and are an important tool in identifying the similarities and differences among them.

In 1995, Li and co-workers reported the crystal structure of rat NQO1 (rNQO1) complexes with duroquinone and cibacron blue (2.1 Å resolution), where each subunit was shown to contain two separate domains: a major, catalytic domain (residues 1-220) folded in a predominantly α/β structure, and a small, C-terminal domain (residues 221-273).¹³⁸ The isoalloxazine moiety of the FAD interacts with different enzyme residues; the major interactions are those with aromatic residues Tyr104, Trp105, Phe106 and Leu103.¹³⁸ The oxygen atoms on

the isoalloxazine ring form hydrogen bonds with the –NH of Phe106 and Gly150, whereas the nitrogen atoms of the isoalloxazine ring form hydrogen bonds with the –NH of Gly149 and Trp105 as described in Figure 1.9.¹³⁸ The nicotinamide of NADP⁺ is stacked on top of the ring that contains the methyl groups of the isoalloxazine at a distance of approximately 3.4 Å. The nitrogen atom on the amine attached to the carbonyl group on the NADP⁺ makes hydrogen bonds with the –OHs (hydroxyl groups) of Tyr126 and Tyr128.¹³⁸

Fifteen years later, the crystal structure of human NQO1 (hNQO1) containing only the FAD prosthetic group (1.7 Å resolution), as well as the crystal structure of mouse NQO1 (mNQO1, 2.8 Å resolution) revealed that most of the FAD-enzyme interactions in human and mouse NQO1 are highly homologous to those described in the structure of rat NQO1, Figure 1.9.¹³⁹ The residues' interaction with the cofactor of NQO1 were identified in the rNQO1/NADP⁺ structure; however, in human and mouse NQO1s, residues in loop 9 shift their positions by several Å, thereby closing the cleft. Moreover, Tyr128 retrocedes from the cleft, resulting in widening of the cleft by 0.5 Å in hNQO1 relative to rNQO1.¹³⁹

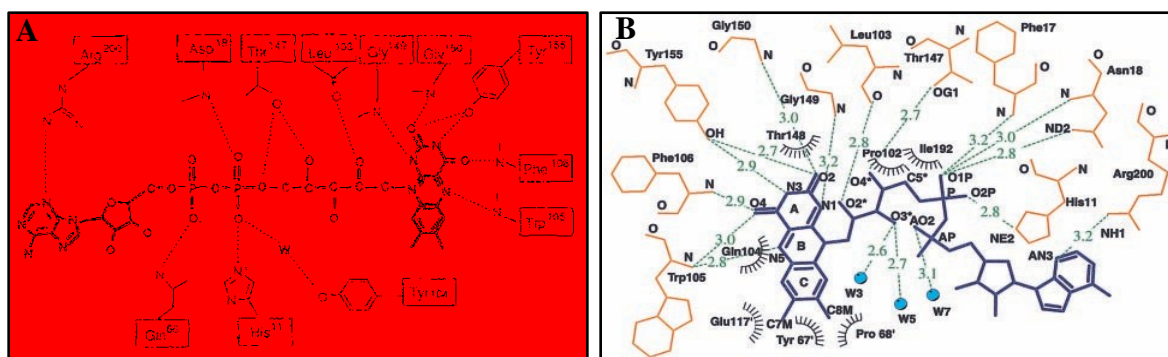


Figure 1.9. Schematic representation of FAD interactions with rat NQO1 (A) and human NQO1 (B). A) Shows hydrogen bonds of FAD with residues. W means water. B) Shows hydrogen bonds and van der Waals interactions of FAD with hNQO1. Open radiated circles indicate hydrophobic interactions. Hydrogen bonds are represented by dashed green lines; water molecules are shown as blue filled circles. Adapted from Li (1995)¹³⁸ and Faig (2000).¹³⁹

Overall, the sequence and structural similarities between hNQO1 and mNQO1 and hNQO1 and rNQO1 are both 86%, while it is 94% between mNQO1 and rNQO1.¹³⁹ The 86% similarity between rat and human NQO1 accounts for a difference of 37 amino acids.¹⁴⁰ The

major differences involve the replacement of Tyr104 present in the rNQO1 with Gln104 in the hNQO1 and mNQO1 structures, along with the absence of several water molecules in the rNQO1.¹³⁹ Comparison of the X-ray structures of hNQO1 and mNQO1 versus rNQO1 shows replacement of the bulky aromatic residue (Tyr104) with a smaller aliphatic residue (Gln104) increases the space in the binding pocket of hNQO1 and mNQO1, thus allowing the dimethylbenzene ring of the FAD (ring C in Figure 1.9 (B)) to be located 0.5–0.7 Å deeper in the enzyme cavity.^{139,140} Those differences are reflected by the ability of NQO1 to activate different antitumor compounds, such as Mitomycin C and Streptonigrin (both with 5-fold lower rates for hNQO1 versus rNQO1).¹⁴¹ In addition, Walton *et al.* have found that rNQO1 and hNQO1 catalyzed the reduction of menadione with a similar K_m (1.4–3.1 μM) but the V_{max} was 7 to 8-fold lower for hNQO1.¹⁴² The same authors found that rNQO1 readily reduced the antitumor agent, EO9; however, no activity could be detected with hNQO1.¹⁴² Mutation studies replacing residues in rNQO1 with the human sequence and residues in hNQO1 with the rat sequence have shown that amino acid 104 (Tyr in rat and Gln in human) accounts for the catalytic differences between hNQO1 and rNQO1.¹⁴³ Therefore, it is important to assay quinoid substrates with human NQO1 and not to rely on the data described for rat NQO1.

The catalytic site has three distinct regions in all types of NQO1: one that binds to FAD, one that binds to the adenine ribose portion of NAD(P), and one that binds to either the hydride acceptor (substrate) or the hydride donor (NADH or NADPH).¹³⁹ The binding pocket where the substrate and the cofactor bind has an internal wall (Phe106, Gly174, Phe178, Trp105), a floor (isoalloxazine ring), a roof (Tyr126, Tyr128) and an entrance (Gly149, Gly150, His194, Pro68).¹³⁹ The non-occupied substrate binding pocket is 10 Å wide, 9 Å deep and 4 Å high.¹³⁹ Comparison of the X-ray structure of apo-hNQO1 (no quinone substrate present) with that of the hNQO1/duroquinone complex shows that duroquinone binds to the enzyme mainly by hydrophobic interactions, and that the plane of the quinone ring stacks 3.5 Å from the

isoalloxazine ring of hNQO1.¹³⁹ It also revealed that Tyr128 adopts different conformations, resulting in opening and closing of the binding site.¹³⁹

NQO1 follows a ping-pong mechanism where the cofactor (NADH or NADPH) binds to NQO1 and donates a hydride to reduce FAD to FADH₂. Then, the cofactor leaves the binding pocket and a quinone binds to NQO1 and gets reduced to hydroquinone.¹⁸ This direct two-electron reduction of quinones is unique among the reductive enzymes.^{18,144} In the X-ray structure of the hNQO1/duroquinone complex, it is shown that the closest distances from the flavin N5 (hydride donor) to the possible atom acceptors (of the hydride ion) in the quinone are 4.5 Å to oxygen, 4.1 Å to carbon, and 3.55 Å to the other carbon.¹³⁹ The details of the reduction of quinone to hydroquinone by the NQO1 mechanism are not fully understood, but it is believed residues Tyr155 and His161 play an important role in the charge stabilization of NQO1 during the hydride transfer process.^{138,145}

For the most part, NQO1 is located in the cytosol of cells, but it has also been found in the nucleus,¹⁴⁶ membrane,¹⁴⁷ endoplasmic reticulum,¹⁴⁸ mitochondria,^{18,149} and in the extracellular environment.¹⁵⁰ In human tissue, NQO1 has been primarily detected in epithelial and endothelial cells,^{3,4,151} and it is over expressed in various solid tumors, such as those of the liver (20 to 50-fold),¹ lung (12 to 18-fold),^{3,11} pancreas,¹⁵² colon (3 to 4-fold)¹¹ and breast (3-fold).¹¹ For that reason, hNQO1 is a promising target for bioreductive activation of therapeutic agents.

1.4.2 Inhibitors of Human NQO1

NQO1 is considered a detoxifying enzyme because it prevents superoxide formation by reducing quinone radicals (before they react with molecular oxygen to form superoxides) to the less damaging hydroquinone compounds.^{153,154} Therefore, deactivation of NQO1 will lead to superoxide accumulation and cell death. Dicoumarol is the best known competitive inhibitor for NQO1 with respect to the cofactors NADH and NADPH.¹⁸ The major problem with the use of

dicoumarol is its non-specific nature and ability to inhibit other enzymes besides hNQO1.^{155,156} In addition, the effective concentration of dicoumarol that is required to inhibit NQO1 depends on the efficiency of the second substrate based on the NQO1 ping-pong mechanism.¹⁵⁵ Few research groups have been investigating different quinone derivatives as inhibitors of NQO1 to use them as a possible route for cancer treatment.

The tumor blood-flow inhibitors flavone-8-acetic acid (FAA) and 5,6-dimethylxanthenone-4-acetic acid (DMXAA) were reported by Phillips as competitive inhibitors of hNQO1 with respect to NADH.¹⁵⁷ DMXAA and FAA presented relatively high K_i values (20 μM and 75 μM); however, therapeutically-achievable levels of DMXAA and FAA would be sufficient to inhibit hNQO1 activity *in vivo* (IC_{50} of 49.6 μM and 110.9 μM).¹⁵⁷ It was also reported that 3.55 mM of FAA exhibited only 6.51% inhibition on cytochrome b_5 activity while DMXAA was found to partially inhibit cytochrome b_5 (25% inhibition). The authors also found that 1.77 mM of FAA partially inhibited cytochrome P450 while 2 mM of DMXAA had only an 8.9% inhibition on the same enzyme.¹⁵⁷

Ross and collaborators reported in 2001 a more specific inhibitor (ES936) for hNQO1.¹⁵⁸ ES936 is a mechanism-based inhibitor that depends on NADH to deactivate hNQO1.¹⁵⁸ Incubation of ES936 (2 μM) with NADH (100 μM) and hNQO1 (2 $\mu\text{g}\cdot\text{mL}^{-1}$) resulted in more than 99% inhibition of enzyme activity in less than 5 min.¹⁵⁸ X-ray, ESI-LC/MS/MS and MALDI-TOFMS analysis confirmed alkylation on one of the tyrosine residues (Tyr126 or Tyr128) in the active site of hNQO1.¹⁵⁸ Later, ES936 analogs were investigated by Ross and coworkers as possible inhibitors of hNQO1.¹⁵⁹ Growth inhibition activity in MIA PaCa-2 cells and computational-based molecular docking simulations revealed that ES936 and analog 2 were the best inhibitors of hNQO1 (~95% inhibition) and they stopped cell growth (IC_{50} of approximately 0.63 μM and 0.64 μM).¹⁵⁹ Analogs 5, 6, and 7 were found to be good inhibitors (~90% inhibition) of hNQO1, but they were not effective in stopping cell growth.¹⁵⁹

In 2006, Bryce *et al.* identified novel inhibitors of hNQO1 from the National Cancer Institute (NCI) compound database.¹⁶⁰ They applied a virtual screening on thousands of compounds and narrowed them down to 28 for biological activity testing towards recombinant human NQO1. From those 28 compounds, only the most potent inhibitor (NSC645827) had an observed IC_{50} of $0.7 \mu\text{M}$ that was comparable with that of dicoumarol ($IC_{50} = 0.45 \mu\text{M}$ in the presence of BSA).¹⁶⁰ In 2007, the same research group investigated 26 coumarin analogs as inhibitors of hNQO1 from the NCI database.¹⁶¹ Analogs were assayed in the presence and absence of BSA, providing information on the effect of nonspecific protein binding. In the case of dicoumarol, it was found that the $IC_{50} = 0.45 \mu\text{M}$ in the presence of BSA and $IC_{50} = 0.005 \mu\text{M}$ in the absence of BSA towards recombinant human NQO1, confirming its non-specific nature.¹⁶¹ The best inhibitors in the presence of BSA towards recombinant human NQO1 comparable to dicoumarol were compound 2, 22, and 23 having IC_{50} values of $0.35 \mu\text{M}$, $0.65 \mu\text{M}$ and $0.60 \mu\text{M}$, respectively.¹⁶¹ Cell growth inhibition studies on MIA PaCa-2 cell lines in the presence of dicoumarol, compound 2, 22 and 23 gave IC_{50} values of 75, 190, 150 and $140 \mu\text{M}$, respectively.¹⁶¹ A few years later in a continued study on coumarin analogs, Bryce and collaborators investigated 29 dicoumarol analogs (with greater water solubility) as potential hNQO1 inhibitors.¹⁶² From those 29 analogs, several of them had IC_{50} values comparable or even better than the IC_{50} value of dicoumarol towards recombinant human NQO1; however, none of the analogs were as toxic as dicoumarol when incubated with MIA PaCa-2 or HCT116 cell lines.¹⁶² More recently, Bryce and colleagues reported a range of triazoloacridin-6-ones (structurally related to NSC645827) as novel inhibitors of hNQO1.¹⁶³ In this work, all of the fifteen compounds were assayed in the absence of BSA and had an IC_{50} far from dicoumarol's IC_{50} value of $0.005 \mu\text{M}$ towards recombinant hNQO1.¹⁶³

In summary, ES936 and analog 2 have been the only reported mechanism inhibitors of hNQO1, with IC_{50} values comparable to that of dicoumarol. In spite of the effort made by

research groups to find better inhibitors on structurally similar dicoumarol compounds, dicoumarol is still the most potent inhibitor of hNQO1. Today, there are a handful of X-ray structures of hNQO1/inhibitor complexes that has been solved to gain an understanding of the mechanism of action of the different inhibitors and for the development and identification of additional potent inhibitors of hNQO1.^{158,162,164}

1.4.3 Bioreductive Drugs Activated by Human NQO1

NQO1 is known to reductively activate anticancer agents, such as mitomycins (MMC), aziridinyl benzoquinones (AZQ, MeDZQ, RH1), indolequinone EO9, streptonigrin, β -lapachone and benzoquinone ansamycins.^{19,43,154,165,166} The mechanism of action of those antitumor agents depends on the reactivity of the corresponding hydroquinone, Figure 1.10.⁴³

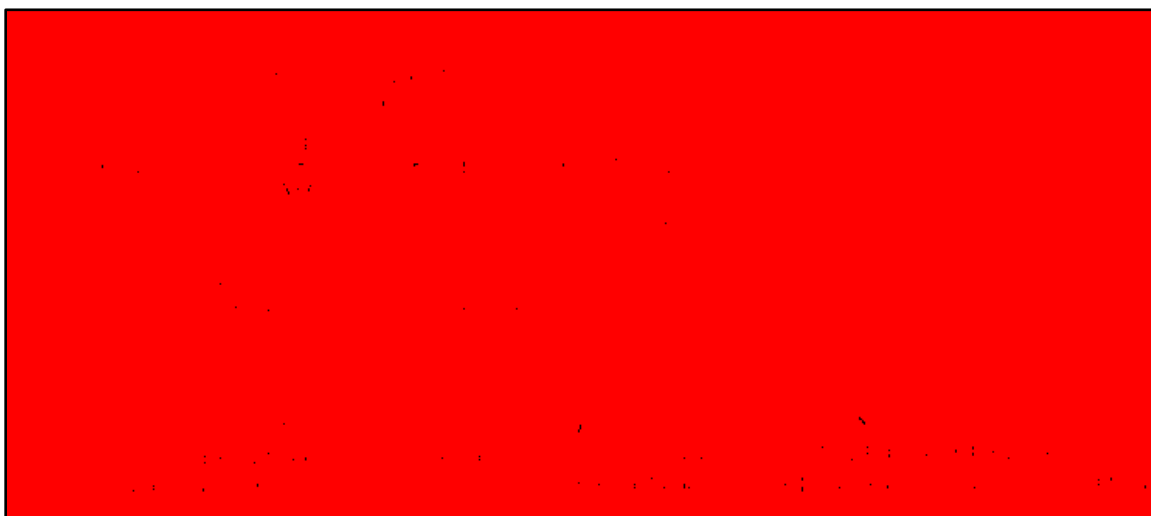


Figure 1.10. Mechanism of action of antitumor agents after bioreductive activation by human NQO1. Adapted from Siegel (2008).⁴³

Mitomycin C (MMC) is one of a series of mitomycin antibiotics isolated in the late 1950s.¹⁶⁷ It was found to be effective towards different human tumors,¹⁶⁸ but there has been controversy with respect to hNQO1 activation of MMC. In the presence of air, hNQO1 activates MMC in a pH-dependent manner;^{169,170} however, under hypoxic conditions, hNQO1 detoxifies the drug.¹⁶⁵ Despite this controversy, there is agreement that hNQO1 is the enzyme that activates MMC which in turn results in DNA crosslinking. Experiments with HT-29 (high

hNQO1 expression) and BE (deficient hNQO1 expression) cells have shown that cells with high expression of hNQO1 are about 6-fold more sensitive to MMC.¹⁷⁰ However, it has become evident that superior substrates for hNQO1 exist, and that the response to MMC *in vivo* cannot be predicted on the basis of hNQO1 activity.^{19,171,172}

EO9 is an indolequinone antitumor drug developed to undergo bioreductive activation similar to MMC.^{43,173} Beall *et al.* found that EO9 was a good substrate for hNQO1, having a K_m value of 13.6 μM and a k_{cat} value of 778 min^{-1} . They also observed that the reduction rate of EO9 by hNQO1 was 50% faster than that of MMC at a 50 μM quinone concentration.¹⁷² However, EO9 failed to demonstrate a significant antitumor response in clinical trials because its poor pharmacokinetics properties, such as short half-life and poor tissue penetration.^{17,174,175}

Aziridinybenzoquinones are another class of DNA alkylating quinones. In this series, MeDZQ was found to have a better response than AZQ toward killing HT-29 human cell (high hNQO1 expression) with IC_{50} values of 0.075 and 7.6 μM , respectively.¹⁷⁶ The same compounds were tested later against recombinant hNQO1. It was observed that MeDZQ was an excellent substrate with a reduction rate of 860 $\mu\text{mol}\cdot\text{min}^{-1}\cdot\mu\text{mol}^{-1}$, while the AZQ reduction rate was 160 $\mu\text{mol}\cdot\text{min}^{-1}\cdot\mu\text{mol}^{-1}$, both at a 100 μM quinone concentration.¹⁴¹ However, MeDZQ's use was limited by its poor solubility.¹⁹ A few years later, Ross and coworkers identified a new azidinybenzoquinone, RH1, as an NQO1-directed antitumor agent.¹⁷⁷ RH1 had an increased solubility versus MeDZQ and was found to be more effective than MeDZQ towards recombinant human NQO1 at a 50 μM quinone concentration (NADH oxidation rates RH1 = 45.2 $\mu\text{mol}\cdot\text{min}^{-1}\cdot\text{mg}^{-1}$ and MeDZQ = 21.6 $\mu\text{mol}\cdot\text{min}^{-1}\cdot\text{mg}^{-1}$).¹⁷⁷ RH1 toxicity was confirmed toward high expression NQO1 human cell lines (H460 and HT29), with IC_{50} values of 0.002 and 0.011 μM , respectively.¹⁷⁷ It was also reported that bioreductive activation of RH1 by other reductive enzymes would be unlikely because high concentrations of RH1 (0.5 μM) will be required for that to happen, while 0.05 μM of RH1 is already enough to produce 100% DNA

cross-linking on human blood mononuclear cells.¹⁷⁸ RH1 has also proven to be efficient against paediatric tumor cell lines.¹⁷⁹ Furthermore, RH1 has recently completed Phase I trials in adults in the United Kingdom and further clinical evaluation is ongoing.¹⁷⁹

Streptonigrin (SN) and β -lapachone (β -lap) are examples of redox-cycling quinones.⁴³ Streptonigrin was found to be the best substrate when compared to MeDZQ and EO9 towards recombinant hNQO1 with a K_m value of 35.6 μ M and a k_{cat} value of 7,320 min^{-1} (MeDZQ values were 33.2 μ M and 3940 min^{-1} and EO9 values were 13.6 μ M and 778 min^{-1}).¹⁷² The same study reported SN as the antitumor agent with better selectivity ratios (86-fold more toxic) when compared with the IC_{50} of human cell lines H596 (deficient in NQO1) with H460 (high NQO1 expression).¹⁷² In addition, it was reported that SN was much more cytotoxic towards human colon carcinoma cell line HT-29 with high NQO1 expression than human colon carcinoma BE (deficient NQO1 activity).¹⁸⁰ In the 1960s, clinical use of SN was limited by myelotoxicity.^{181,182} β -lap was found to have enhanced cytotoxicity towards breast cancer cells expressing NQO1 versus deficient NQO1 cell line. It was determined that 4 μ M of β -lap was sufficient to kill over 99% of the cells with high NQO1 content.¹⁸³ β -lap was also found to be an efficient cytotoxic compound towards human pancreatic cancer cells (MIA PaCa-2) that over-express NQO1.^{184,185}

Benzoquinone ansamycin compounds such as geldanamycin, 17-AAG, 17-DMAG, and 17AG have been identified as substrates for hNQO1; these compounds generate a hydroquinone that inhibits the heat shock protein 90 (HSP90), causing degradation of several important oncogenic client proteins.^{43,186} In two independent *in vitro* studies between the lead geldanamycin derivative 17-AAG and human cancer cell lines, a positive relationship was observed between hNQO1 expression level and growth inhibition by 17-AAG.¹⁸⁷ Moreover, Guo and coworkers have reported a detailed study of the reduction of 17-AAG to 17-AAGH₂ by hNQO1 and its 12-fold increase in growth inhibition towards MDA468/NQ16 cells (high

hNQO1 content) versus MDA468 cells (deficient hNQO1 content) based on its IC₅₀ values.¹⁸⁸ A year later, Guo and coworkers extended their detailed study to the reduction 17-AAG analogs by hNQO1 and found that these analogs also presented higher sensitivity towards MDA468/NQ16 cells versus MDA468 cells.¹⁸⁹ 17-AAG and 17-DMAG (a more water soluble derivative of 17-AAG) were found to be the most sensitive compounds in the series and are currently in clinical trials.¹⁸⁹

Out of all the bioreductive drugs mentioned above, just a few like RH1 are still in clinical trials. The structures of the different bioreductive drugs that did not make it out of the clinical trials have been taken as models to design analogs that could have better response in cancer treatments.¹⁹⁰ In the last 15 years, several research groups have emphasized their work on the structure–activity relationships between antitumor agents such as indolequinones,¹⁹¹⁻¹⁹⁵ benzoquinone mustards,^{196,197} benzimidazoles,¹⁹⁸ quinolinequinones,¹⁹⁹ lavendamycins²⁰⁰ and human NQO1 with the aim of finding new therapeutic agents. Among the antitumor compounds, indolequinone analogs received the most attention as a possible prodrug system.^{16,190} Following this strategy, Borch *et al.* examined the delivery of phosphoramidate mustards attached to indolequinones by hNQO1 activation. The authors found that compounds substituted at the 2-position were excellent substrates for hNQO1 ($k_{\text{cat}}/K_{\text{m}} = (2-5) \times 10^6 \text{ M}^{-1} \cdot \text{s}^{-1}$) and potent inhibitors of cell growth with GI₅₀ (growth inhibition) values in the low micromolar to nanomolar range.²⁰¹ To date, none of the analogs developed have been approved for clinical use.¹⁷ In addition, the X-ray structure of three antitumor quinones (ARH019, RH1, EO9) complexed with human NQO1 were reported to improve the knowledge regarding the interaction of model compounds and hNQO1.²⁰²

1.4.4 Prodrugs Presenting the Trimethyl-Lock System Activated by Human NQO1

This section will focus on the quinone moieties, which after being reduced by hNQO1; release their cytotoxic agents by intramolecular cyclization facilitated by the presence of the trimethyl-lock system.

Chikhale *et al.* investigated benzoquinone-prodrugs (TDDS) that can selectively deliver the anticancer drug methylester of melphalan (MME) based on their electronic nature.^{203,204} The authors found that TDDS presenting less negative reduction potential had a higher amount of TDDS reduced under reductive chemical conditions and the extent of drug-delivery was proportional to the amount of TDDS reduced.²⁰³ In their follow up paper, they reported TDDS reduction by purified hNQO1 and found that the H-TDDS analog had the fastest rate of reduction followed by the Br-TDDS analog based on their $t_{1/2}$ values of 3 min and 15 min, respectively.²⁰⁴

In 2007, Volpato *et al.* reported the human NQO1 activation of a benzoquinone prodrug conjugated to a 4-aminophenyl nitrogen mustard with a K_m value of $\sim 3 \mu\text{M}$ and a V_{max} value of $\sim 12 \mu\text{mol}\cdot\text{min}^{-1}\cdot\text{mg}^{-1}$.²⁰⁵ The authors identified the formation of lactone and 4-aminophenyl nitrogen mustard using LC/MS after the prodrug was reduced by hNQO1 in a cell free assay. In addition, chemosensitivities studies show the prodrug is selectively toxic to cells that have elevated levels of NQO1 (H460) versus cells that are NQO1-deficient (BE) with IC_{50} values of $36 \mu\text{M}$ and greater than a $100 \mu\text{M}$, respectively.²⁰⁵

More recently, Moody and colleagues reported a benzoquinone prodrug conjugated to an antiangiogenic agent (SU5416) derivative as a potent inhibitor of the vascular endothelial growth factor (VEGF).²⁰⁶ The authors proved 100% inhibition of VEGF-stimulated angiogenesis in HUEVs (human umbilical vein endothelial cells with NQO1 expression) by addition of $10 \mu\text{M}$ of two different benzoquinone prodrugs conjugated with SU5416.

1.5 References

- (1) Cresteil, T.; Jaiswal, A. K., High-Levels of Expression of the Nad(P)H-Quinone Oxidoreductase (Nqo1) Gene in Tumor-Cells Compared to Normal-Cells of the Same Origin. *Biochem. Pharmacol.* **1991**, *42* (5), 1021-1027.
- (2) Fitzsimmons, S. A.; Workman, P.; Grever, M.; Paull, K.; Camalier, R.; Lewis, A. D., Reductase Enzyme Expression across the National Cancer Institute Tumor Cell Line Panel: Correlation with Sensitivity to Mitomycin C and E09. *J. Natl. Cancer Inst.* **1996**, *88* (5), 259-269.
- (3) Siegel, D.; Franklin, W. A.; Ross, D., Immunohistochemical Detection of Nad(P)H : Quinone Oxidoreductase in Human Lung and Lung Tumors. *Clin. Cancer Res.* **1998**, *4* (9), 2065-2070.
- (4) Siegel, D.; Ross, D., Immunodetection of Nad(P)H : Quinone Oxidoreductase 1 (Nqo1) in Human Tissues. *Free Radical Biol. Med.* **2000**, *29* (3-4), 246-253.
- (5) Jamieson, D.; Wilson, K.; Pridgeon, S.; Margetts, J. P.; Edmondson, R. J.; Leung, H. Y.; Knox, R.; Boddy, A. V., Nad(P)H : Quinone Oxidoreductase1 and Nrh : Quinone Oxidoreductase 2 Activity and Expression in Bladder and Ovarian Cancer and Lower Nrh : Quinone Oxidoreductase 2 Activity Associated with an Nqo2 Exon 3 Single-Nucleotide Polymorphism. *Clin. Cancer Res.* **2007**, *13* (5), 1584-1590.
- (6) Kaasgaard, T.; Andresen, T. L., Liposomal Cancer Therapy: Exploiting Tumor Characteristics. *Expert Opin. Drug Deliv.* **2010**, *7* (2), 225-243.
- (7) Maeda, H.; Wu, J.; Sawa, T.; Matsumura, Y.; Hori, K., Tumor Vascular Permeability and the Epr Effect in Macromolecular Therapeutics: A Review. *J. Controlled Release* **2000**, *65* (1-2), 271-284.
- (8) Maeda, H., Tumor-Selective Delivery of Macromolecular Drugs Via the Epr Effect: Background and Future Prospects. *Bioconjugate Chem.* **2010**, *21* (5), 797-802.
- (9) Andresen, T. L.; Jensen, S. S.; Jorgensen, K., Advanced Strategies in Liposomal Cancer Therapy: Problems and Prospects of Active and Tumor Specific Drug Release. *Prog. Lipid Res.* **2005**, *44* (1), 68-97.
- (10) Zhang, L.; Gu, F. X.; Chan, J. M.; Wang, A. Z.; Langer, R. S.; Farokhzad, O. C., Nanoparticles in Medicine: Therapeutic Applications and Developments. *Clin. Pharmacol. Ther.* **2008**, *83* (5), 761-769.

- (11) Rooseboom, M.; Commandeur, J. N. M.; Vermeulen, N. P. E., Enzyme-Catalyzed Activation of Anticancer Prodrugs. *Pharmacol. Rev.* **2004**, *56* (1), 53-102.
- (12) Meers, P., Enzyme-Activated Targeting of Liposomes. *Advanced Drug Delivery Reviews* **2001**, *53* (3), 265-272.
- (13) Andresen, T. L.; Thompson, D. H.; Kaasgaard, T., Enzyme-Triggered Nanomedicine: Drug Release Strategies in Cancer Therapy (Invited Review). *Mol. Membr. Biol.* **2010**, *27* (7), 353-363.
- (14) Hafez, I. M.; Cullis, P. R., Roles of Lipid Polymorphism in Intracellular Delivery. *Advanced Drug Delivery Reviews* **2001**, *47* (2-3), 139-148.
- (15) Ong, W.; Yang, Y. M.; Cruciano, A. C.; McCarley, R. L., Redox-Triggered Contents Release from Liposomes. *J. Am. Chem. Soc.* **2008**, *130* (44), 14739-14744.
- (16) Jaffar, M.; Abou-Zeid, N.; Bai, L.; Mrema, I.; Robinson, I.; Tanner, R.; Stratford, I. J., Quinone Bioreductive Prodrugs as Delivery Agents. *Curr. Drug Delivery* **2004**, *1*, 345-350.
- (17) Chen, Y.; Hu, L. Q., Design of Anticancer Prodrugs for Reductive Activation. *Med. Res. Rev.* **2009**, *29* (1), 29-64.
- (18) Ernster, L., Dt-Diaphorase - a Historical Review. *Chem. Scripta* **1987**, *27A*, 1-13.
- (19) Danson, S.; Ward, T. H.; Butler, J.; Ranson, M., Dt-Diaphorase: A Target for New Anticancer Drugs. *Cancer Treatment Reviews* **2004**, *30* (5), 437-449.
- (20) Szoka, F.; Papahadjopoulos, D., Comparative Properties and Methods of Preparation of Lipid Vesicles (Liposomes). *Annu. Rev. Biophys. Bio.* **1980**, *9*, 467-508.
- (21) Avanti Polar Lipids. <http://avantilipids.com/>.
- (22) de Groot, F. M. H.; Damen, E. W. P.; Scheeren, H. W., Anticancer Prodrugs for Application in Monotherapy: Targeting Hypoxia, Tumor-Associated Enzymes, and Receptors. *Curr. Med. Chem.* **2001**, *8* (9), 1093-1122.
- (23) Moriwaki, Y.; Yamamoto, T.; Higashino, K., Distribution and Pathophysiologic Role of Molybdenum-Containing Enzymes. *Histol. Histopathol.* **1997**, *12* (2), 513-524.

- (24) Alfaro, J. F.; Joswig-Jones, C. A.; Ouyang, W.; Nichols, J.; Crouch, G. J.; Jones, J. P., Purification and Mechanism of Human Aldehyde Oxidase Expressed in Escherichia Coli. *Drug Metab. Dispos.* **2009**, *37* (12), 2393-2398.
- (25) Al-Salmy, H. S., Individual Variation in Hepatic Aldehyde Oxidase Activity. *Iubmb Life* **2001**, *51* (4), 249-253.
- (26) Moriwaki, Y.; Yamamoto, T.; Takahashi, S.; Tsutsumi, Z.; Hada, T., Widespread Cellular Distribution of Aldehyde Oxidase in Human Tissues Found by Immunohistochemistry Staining. *Histol. Histopathol.* **2001**, *16* (3), 745-753.
- (27) Porter, D. J. T.; Harrington, J. A.; Almond, M. R.; Lowen, G. T.; Zimmerman, T. P.; Spector, T., 5-Ethynyl-2(1h)-Pyrimidinone - Aldehyde Oxidase-Activation to 5-Ethynyluracil, a Mechanism-Based Inactivator of Dihydropyrimidine Dehydrogenase. *Biochem. Pharmacol.* **1994**, *47* (7), 1165-1171.
- (28) Guo, X.; Lernertung, M.; Chen, H. X.; Chang, C. N.; Zhu, J. L.; Chang, C. P.; Pizzorno, G.; Lin, T. S.; Cheng, Y. C., 5-Fluoro-2-Pyrimidinone, a Liver Aldehyde Oxidase-Activated Prodrug of 5-Fluorouracil. *Biochem. Pharmacol.* **1995**, *49* (8), 1111-1116.
- (29) Kinsella, T. J.; Kunugi, K. A.; Vielhuber, K. A.; Mcculloch, W.; Liu, S. H.; Cheng, Y. C., An in-Vivo Comparison of Oral 5-Iodo-2'-Deoxyuridine and 5-Iodo-2-Pyrimidinone-2'-Deoxyribose Toxicity, Pharmacokinetics, and DNA Incorporation in Athymic Mouse-Tissues and the Human Colon-Cancer Xenograft, Hct-116. *Cancer Res.* **1994**, *54* (10), 2695-2700.
- (30) Kinsella, T. J.; Kunugi, K. A.; Vielhuber, K. A.; Potter, D. M.; Fitzsimmons, M. E.; Collins, J. M., Preclinical Evaluation of 5-Iodo-2-Pyrimidinone-2 '-Deoxyribose as a Prodrug for 5-Iodo-2 '-Deoxyuridine-Mediated Radiosensitization in Mouse and Human Tissues. *Clin. Cancer Res.* **1998**, *4* (1), 99-109.
- (31) Kinsella, T. J.; Schupp, J. E.; Davis, T. W.; Berry, S. E.; Hwang, H. S.; Warren, K.; Balis, F.; Barnett, J.; Sands, H., Preclinical Study of the Systemic Toxicity and Pharmacokinetics of 5-Iodo-2-Deoxypyrimidinone-2 '-Deoxyribose as a Radiosensitizing Prodrug in Two, Non-Rodent Animal Species: Implications for Phase I Study Design. *Clin. Cancer Res.* **2000**, *6* (9), 3670-3679.
- (32) Pollegioni, L.; Piubelli, L.; Sacchi, S.; Pilone, M. S.; Molla, G., Physiological Functions of D-Amino Acid Oxidases: From Yeast to Humans. *Cell Mol. Life Sci.* **2007**, *64* (11), 1373-1394.

- (33) Holme, D. J.; Goldberg, D. M., Development of a Fluorometric Assay for Amino-Acid Oxidase Activity and Its Application to the Study of Human-Tissues. *Biochem. Med.* **1982**, 28 (1), 51-61.
- (34) Ip, C., Lessons from Basic Research in Selenium and Cancer Prevention. *J. Nutr.* **1998**, 128 (11), 1845-1854.
- (35) Ip, C.; Zhu, Z. J.; Thompson, H. J.; Lisk, D.; Ganther, H. E., Chemoprevention of Mammary Cancer with Se-Allylselenocysteine and Other Selenoamino Acids in the Rat. *Anticancer Res.* **1999**, 19, 2875-2880.
- (36) Andreadou, I.; Menge, W. M. P. B.; Commandeur, J. N. M.; Worthington, E. A.; Vermeulen, N. P. E., Synthesis of Novel Se-Substituted Selenocysteine Derivatives as Potential Kidney Selective Prodrugs of Biologically Active Selenol Compounds: Evaluation of Kinetics of Beta-Elimination Reactions in Rat Renal Cytosol. *J. Med. Chem.* **1996**, 39 (10), 2040-2046.
- (37) Rooseboom, M.; Vermeulen, N. P. E.; Andreadou, I.; Commandeur, J. N. M., Evaluation of the Kinetics of Beta-Elimination Reactions of Selenocysteine Se-Conjugates in Human Renal Cytosol: Possible Implications for the Use as Kidney Selective Prodrugs. *J. Pharmacol. Exp. Ther.* **2000**, 294 (2), 762-769.
- (38) Rooseboom, M.; Vermeulen, N. P. E.; van Hemert, N.; Commandeur, J. N. M., Bioactivation of Chemopreventive Selenocysteine Se-Conjugates and Related Amino Acids by Amino Acid Oxidases Novel Route of Metabolism of Selenoamino Acids. *Chem. Res. Toxicol.* **2001**, 14 (8), 996-1005.
- (39) Haniu, M.; Mcmanus, M. E.; Birkett, D. J.; Lee, T. D.; Shively, J. E., Structural and Functional-Analysis of NADPH-Cytochrome-P-450 Reductase from Human-Liver - Complete Sequence of Human Enzyme and NADPH-Binding Sites. *Biochemistry* **1989**, 28 (21), 8639-8645.
- (40) Osawa, Y.; Higashiyama, T.; Nakamura, T., Species Specificity of Estrogen Biosynthesis in Pregnancy - Immunochemical Difference of Placental NADPH-Cytochrome C (P-450) Reductase in Human, Baboon and Horse. *J. Steroid Biochem. Mol. Biol.* **1981**, 15, 449-452.
- (41) Zhao, Q.; Modi, S.; Smith, G.; Paine, M.; McDonagh, P. D.; Wolf, C. R.; Tew, D.; Lian, L. Y.; Roberts, G. C. K.; Driessen, H. P. C., Crystal Structure of the Fmn-Binding Domain of Human Cytochrome P450 Reductase at 1.93 Angstrom Resolution. *Protein Sci.* **1999**, 8 (2), 298-306.

- (42) Aigrain, L.; Pompon, D.; Morera, S.; Truan, G., Structure of the Open Conformation of a Functional Chimeric NADPH Cytochrome P450 Reductase. *EMBO Reports* **2009**, *10* (7), 742-747.
- (43) Siegel, D.; Reigan, P.; Ross, D., One- and Two-Electron-Mediated Reduction of Quinones: Enzymology and Toxicological Implications. *Biotechnology: Pharmaceutical Aspects* **2008**, *9*, 169-197.
- (44) Hall, P. D.; Stupans, I.; Burgess, W.; Birkett, D. J.; McManus, M. E., Immunohistochemical Localization of NADPH-Cytochrome-P450 Reductase in Human-Tissues. *Carcinogenesis* **1989**, *10* (3), 521-530.
- (45) Yu, L. J.; Matias, J.; Scudiero, D. A.; Hite, K. M.; Monks, A.; Sausville, E. A.; Waxman, D. J., P450 Enzyme Expression Patterns in the NCI Human Tumor Cell Line Panel. *Drug Metab. Dispos.* **2001**, *29* (3), 304-312.
- (46) de Cerain, A. L.; Marin, A.; Idoate, M. A.; Tunon, M. T.; Bello, J., Carbonyl Reductase and NADPH Cytochrome P450 Reductase Activities in Human Tumoral Versus Normal Tissues. *Eur. J. Cancer* **1999**, *35* (2), 320-324.
- (47) Plewka, D.; Plewka, A.; Nowaczyk, G.; Kaminski, M.; Rutlowski, T.; Ludyga, T.; Ziaja, K., Neoplastic Lesions of the Human Liver in Relation to the Activity of the Cytochrome P-450 Dependent Monooxygenase System. *Med. Sci. Monit.* **2000**, *6* (2), 244-248.
- (48) Forkert, P. G.; Lord, J. A.; Parkinson, A., Alterations in Expression of Cyp1a1 and NADPH-Cytochrome P450 Reductase During Lung Tumor Development in Swr/J Mice. *Carcinogenesis* **1996**, *17* (1), 127-132.
- (49) Belcourt, M. F.; Hodnick, W. F.; Rockwell, S.; Sartorelli, A. C., Differential Toxicity of Mitomycin C and Porfiromycin to Aerobic and Hypoxic Chinese Hamster Ovary Cells Overexpressing Human NADPH: Cytochrome C (P-450) Reductase. *Proc. Natl. Acad. Sci. U. S. A.* **1996**, *93* (1), 456-460.
- (50) Belcourt, M. F.; Hodnick, W. F.; Rockwell, S.; Sartorelli, A. C., Exploring the Mechanistic Aspects of Mitomycin Antibiotic Bioactivation in Chinese Hamster Ovary Cells Overexpressing NADPH : Cytochrome C (P-450) Reductase and DT-Diaphorase. *Adv. Enzyme Regul.* **1998**, *38*, 111-133.
- (51) Nemeikaite-Ceniene, A.; Sarlauskas, J.; Anusevicius, Z.; Nivinskas, H.; Cenas, N., Cytotoxicity of Rh1 and Related Aziridinylbenzoquinones: Involvement of Activation by NAD(P)H : Quinone Oxidoreductase (Nqo1) and Oxidative Stress. *Arch. Biochem. Biophys.* **2003**, *416* (1), 110-118.

- (52) Begleiter, A.; Leith, M. K.; Patel, D.; Hasinoff, B. B., Role of NADPH Cytochrome P450 Reductase in Activation of Rh1. *Cancer Chemother. Pharmacol.* **2007**, *60* (5), 713-723.
- (53) McKeown, S. R.; Cowent, R. L.; Williams, K. J., Bioreductive Drugs: From Concept to Clinic. *Clin. Oncol.* **2007**, *19* (6), 427-442.
- (54) Cashman, J. R., Some Distinctions between Flavin-Containing and Cytochrome P450 Monooxygenases. *Biochem. Biophys. Res. Commun.* **2005**, *338* (1), 599-604.
- (55) Johnson, E. F.; Stout, C. D., Structural Diversity of Human Xenobiotic-Metabolizing Cytochrome P450 Monooxygenases. *Biochem. Biophys. Res. Commun.* **2005**, *338* (1), 331-336.
- (56) Patterson, L. H.; McKeown, S. R.; Robson, T.; Gallagher, R.; Raleigh, S. M.; Orr, S., Antitumour Prodrug Development Using Cytochrome P450 (Cyp) Mediated Activation. *Anti-Cancer Drug Des.* **1999**, *14* (6), 473-486.
- (57) Komatsu, T.; Yamazaki, H.; Shimada, N.; Nakajima, M.; Yokoi, T., Roles of Cytochromes P450 1a2, 2a6, and 2c8 in 5-Fluorouracil Formation from Tegafur, an Anticancer Prodrug, in Human Liver Microsomes. *Drug Metab. Dispos.* **2000**, *28* (12), 1457-1463.
- (58) Ikeda, K.; Yoshisue, K.; Matsushima, E.; Nagayama, S.; Kobayashi, K.; Tyson, C. A.; Chiba, K.; Kawaguchi, Y., Bioactivation of Tegafur to 5-Fluorouracil Is Catalyzed by Cytochrome P-450 2a6 in Human Liver Microsomes in Vitro. *Clin. Cancer Res.* **2000**, *6* (11), 4409-4415.
- (59) Kopf, D.; Goretzki, P. E.; Lehnert, H., Clinical Management of Malignant Adrenal Tumors. *J. Cancer Res. Clin. Oncol.* **2001**, *127* (3), 143-155.
- (60) Patterson, A. V.; Saunders, M. P.; Greco, O., Prodrugs in Genetic Chemoradiotherapy. *Curr. Pharm. Des.* **2003**, *9* (26), 2131-2154.
- (61) Nishioka, K., Particulate Tyrosinase of Human Malignant-Melanoma - Solubilization, Purification Following Trypsin Treatment, and Characterization. *Eur. J. Biochem.* **1978**, *85* (1), 137-146.
- (62) Matoba, Y.; Kumagai, T.; Yamamoto, A.; Yoshitsu, H.; Sugiyama, M., Crystallographic Evidence That the Dinuclear Copper Center of Tyrosinase Is Flexible During Catalysis. *J. Biol. Chem.* **2006**, *281* (13), 8981-8990.

- (63) Pawelek, J.; Korner, A.; Bergstrom, A.; Bologna, J., New Regulators of Melanin Biosynthesis and the Auto-Destruction of Melanoma-Cells. *Nature* **1980**, 286 (5773), 617-619.
- (64) Morrison, M. E.; Yagi, M. J.; Cohen, G., Invitro Studies of 2,4-Dihydroxyphenylalanine, a Prodrug Targeted against Malignant-Melanoma Cells. *Proc. Natl. Acad. Sci. U. S. A.* **1985**, 82 (9), 2960-2964.
- (65) Lant, N. J.; McKeown, P.; Kelland, L. R.; Rogers, P. M.; Robins, D. J., Synthesis and Antimelanoma Activity of Analogues of N-Acetyl-4-S-Cysteaminylphenol. *Anti-Cancer Drug Des.* **2000**, 15 (4), 295-302.
- (66) Jordan, A. M.; Khan, T. H.; Osborn, H. M. I.; Photiou, A.; Riley, P. A., Melanocyte-Directed Enzyme Prodrug Therapy (Mdept): Development of a Targeted Treatment for Malignant Melanoma. *Bioorg. Med. Chem.* **1999**, 7 (9), 1775-1780.
- (67) Jordan, A. M.; Khan, T. H.; Malkin, H.; Osborn, H. M. I.; Photiou, A.; Riley, P. A., Melanocyte-Directed Enzyme Prodrug Therapy (Mdept): Development of Second Generation Prodrugs for Targeted Treatment of Malignant Melanoma. *Bioorg. Med. Chem.* **2001**, 9 (6), 1549-1558.
- (68) Knaggs, S.; Malkin, H.; Osborn, H. M. I.; Williams, N. A. O.; Yaqoob, P., New Prodrugs Derived from 6-Aminodopamine and 4-Aminophenol as Candidates for Melanocyte-Directed Enzyme Prodrug Therapy (Mdept). *Org. Biomol. Chem.* **2005**, 3 (21), 4002-4010.
- (69) Tarahovsky, Y. S., "Smart" Liposomal Nanocontainers in Biology and Medicine. *Biochemistry (Moscow)* **2010**, 75 (7), 811-824.
- (70) Danhier, F.; Feron, O.; Preat, V., To Exploit the Tumor Microenvironment: Passive and Active Tumor Targeting of Nanocarriers for Anti-Cancer Drug Delivery. *J. Controlled Release* **2010**, 148 (2), 135-146.
- (71) Zhang, H. B.; Wang, G. J.; Yang, H. A., Drug Delivery Systems for Differential Release in Combination Therapy. *Expert Opin. Drug Deliv.* **2011**, 8 (2), 171-190.
- (72) Sinha, S.; Watorek, W.; Karr, S.; Giles, J.; Bode, W.; Travis, J., Primary Structure of Human Neutrophil Elastase. *Proc. Natl. Acad. Sci. U. S. A.* **1987**, 84 (8), 2228-2232.
- (73) Alhaik, N.; Lewis, D. A.; Struthers, G., Neutral Protease, Collagenase and Elastase Activities in Synovial-Fluids from Arthritic Patients. *Agents Actions* **1984**, 15 (3-4), 436-442.

- (74) Gysen, P.; Malaise, M.; Gaspar, S.; Franchimont, P., Measurement of Proteoglycans, Elastase, Collagenase and Protein in Synovial-Fluid in Inflammatory and Degenerative Arthropathies. *Clin. Rheumatol.* **1985**, *4* (1), 39-50.
- (75) Tate, R. M.; Repine, J. E., Neutrophils and the Adult Respiratory-Distress Syndrome. *Am. Rev. Respir. Dis.* **1983**, *128* (3), 552-559.
- (76) Janoff, A., Elastases and Emphysema - Current Assessment of the Protease-Antiprotease Hypothesis. *Am. Rev. Respir. Dis.* **1985**, *132* (2), 417-433.
- (77) Suter, S.; Schaad, U. B.; Roux, L.; Nydegger, U. E.; Waldvogel, F. A., Granulocyte Neutral Proteases and Pseudomonas Elastase as Possible Causes of Airway Damage in Patients with Cystic-Fibrosis. *J. Infect. Dis.* **1984**, *149* (4), 523-531.
- (78) Birrer, P.; Mcelvaney, N. G.; Rudeberg, A.; Sommer, C. W.; Liechtigallati, S.; Kraemer, R.; Hubbard, R.; Crystal, R. G., Protease-Antiprotease Imbalance in the Lungs of Children with Cystic-Fibrosis. *Am J. Resp. Crit. Care* **1994**, *150* (1), 207-213.
- (79) Yamashita, J. I.; Ogawa, M.; Ikei, S.; Omachi, H.; Yamashita, S. I.; Saishoji, T.; Nomura, K.; Sato, H., Production of Immunoreactive Polymorphonuclear Leukocyte Elastase in Human Breast-Cancer Cells - Possible Role of Polymorphonuclear Leukocyte Elastase in the Progression of Human Breast-Cancer. *Br. J. Cancer* **1994**, *69* (1), 72-76.
- (80) Starcher, B.; O'Neal, P.; Granstein, R. D.; Beissert, S., Inhibition of Neutrophil Elastase Suppresses the Development of Skin Tumors in Hairless Mice. *J. Invest. Dermatol.* **1996**, *107* (2), 159-163.
- (81) Pak, C. C.; Ali, S.; Janoff, A. S.; Meers, P., Triggerable Liposomal Fusion by Enzyme Cleavage of a Novel Peptide-Lipid Conjugate. *Biochim. Biophys. Acta* **1998**, *1372* (1), 13-27.
- (82) Pak, C. C.; Erukulla, R. K.; Ahl, P. L.; Janoff, A. S.; Meers, P., Elastase Activated Liposomal Delivery to Nucleated Cells. *Biochim. Biophys. Acta* **1999**, *1419* (2), 111-126.
- (83) Simopoulos, T. T.; Jencks, W. P., Alkaline-Phosphatase Is an Almost Perfect Enzyme. *Biochemistry* **1994**, *33* (34), 10375-10380.
- (84) Millan, J. L.; Fishman, W. H., Biology of Human Alkaline-Phosphatases with Special Reference To Cancer. *Crit. Rev. Clin. Lab. Sci.* **1995**, *32* (1), 1-39.

- (85) Sowadski, J. M.; Handschumacher, M. D.; Murthy, H. M. K.; Foster, B. A.; Wyckoff, H. W., Refined Structure of Alkaline-Phosphatase from Escherichia-Coli at 2.8-Å Resolution. *J. Mol. Biol.* **1985**, *186* (2), 417-433.
- (86) Deonarain, M. P.; Epenetos, A. A., Targeting Enzymes for Cancer-Therapy - Old Enzymes in New Roles. *Br. J. Cancer* **1994**, *70* (5), 786-794.
- (87) Poelstra, K.; Bakker, W. W.; Klok, P. A.; Hardonk, M. J.; Meijer, D. K. F., A Physiologic Function for Alkaline Phosphatase: Endotoxin Detoxification. *Lab. Invest.* **1997**, *76* (3), 319-327.
- (88) Davis, S. C.; Szoka, F. C., Cholesterol Phosphate Derivatives: Synthesis and Incorporation into a Phosphatase and Calcium-Sensitive Triggered Release Liposome. *Bioconjugate Chem.* **1998**, *9* (6), 783-792.
- (89) Pattinson, N. R., Identification of a Phosphatidylcholine Active Phospholipase-C in Human Gallbladder Bile. *Biochem. Biophys. Res. Commun.* **1988**, *150* (2), 890-896.
- (90) Pattinson, N. R.; Willis, K. E., Effect of Phospholipase-C on Cholesterol Solubilization in Model Bile - a Concanavalin-a Binding Nucleation-Promoting Factor from Human Gallbladder Bile. *Gastroenterology* **1991**, *101* (5), 1339-1344.
- (91) Clark, M. A.; Shorr, R. G. L.; Bomalski, J. S., Antibodies Prepared to Bacillus-Cereus Phospholipase-C Cross-React with a Phosphatidylcholine Preferring Phospholipase-C in Mammalian-Cells. *Biochem. Biophys. Res. Commun.* **1986**, *140* (1), 114-119.
- (92) Spadaro, F.; Ramoni, C.; Mezzanzanica, D.; Miotti, S.; Alberti, P.; Cecchetti, S.; Iorio, E.; Dolo, V.; Canevari, S.; Podo, F., Phosphatidylcholine-Specific Phospholipase C Activation in Epithelial Ovarian Cancer Cells. *Cancer Res.* **2008**, *68* (16), 6541-6549.
- (93) Glunde, K.; Jie, C.; Bhujwala, Z. M., Molecular Causes of the Aberrant Choline Phospholipid Metabolism in Breast Cancer. *Cancer Res.* **2004**, *64* (12), 4270-4276.
- (94) Ramoni, C.; Spadaro, F.; Menegon, M.; Podo, F., Cellular Localization and Functional Role of Phosphatidylcholine-Specific Phospholipase C in Nk Cells. *J. Immunol.* **2001**, *167* (5), 2642-2650.
- (95) Nieva, J. L.; Goni, F. M.; Alonso, A., Liposome Fusion Catalytically Induced by Phospholipase-C. *Biochemistry* **1989**, *28* (18), 7364-7367.

- (96) Nieva, J. L.; Goni, F. M.; Alonso, A., Phospholipase C-Promoted Membrane-Fusion - Retroinhibition by the End-Product Diacylglycerol. *Biochemistry* **1993**, *32* (4), 1054-1058.
- (97) Goni, F. M.; Alonso, A., Membrane Fusion Induced by Phospholipase C and Sphingomyelinases. *Biosci. Rep.* **2000**, *20* (6), 443-463.
- (98) Luk, A. S.; Kaler, E. W.; Lee, S. P., Phospholipase-C-Induced Aggregation and Fusion of Cholesterol Lecithin Small Unilamellar Vesicles. *Biochemistry* **1993**, *32* (27), 6965-6973.
- (99) Van den Bosch, H., Intracellular Phospholipases A. *Biochim. Biophys. Acta* **1980**, *604* (2), 191-246.
- (100) Takayama, K.; Kudo, I.; Kim, D. K.; Nagata, K.; Nozawa, Y.; Inoue, K., Purification and Characterization of Human Platelet Phospholipase-A2 Which Preferentially Hydrolyzes an Arachidonoyl Residue. *FEBS Lett.* **1991**, *282* (2), 326-330.
- (101) Kaiser, E., Phospholipase a(2): Its Usefulness in Laboratory Diagnostics. *Crit. Rev. Clin. Lab. Sci.* **1999**, *36* (2), 65-163.
- (102) Abe, T.; Sakamoto, K.; Kamohara, H.; Hirano, Y.; Kuwahara, N.; Ogawa, M., Group II Phospholipase A2 Is Increased in Peritoneal and Pleural Effusions in Patients with Various Types of Cancer. *Int. J. Cancer* **1997**, *74* (3), 245-250.
- (103) Verheij, H. M.; Westerman, J.; Sternby, B.; Dehaas, G. H., The Complete Primary Structure of Phospholipase-A2 from Human-Pancreas. *Biochim. Biophys. Acta* **1983**, *747* (1-2), 93-99.
- (104) Sharp, J. D.; White, D. L.; Chiou, X. G.; Goodson, T.; Gamboa, G. C.; McClure, D.; Burgett, S.; Hoskins, J.; Skatrud, P. L.; Sportsman, J. R.; Becker, G. W.; Kang, L. H.; Roberts, E. F.; Kramer, R. M., Molecular-Cloning and Expression of Human Ca²⁺-Sensitive Cytosolic Phospholipase-A2. *J. Biol. Chem.* **1991**, *266* (23), 14850-14853.
- (105) Laye, J. P.; Gill, J. H., Phospholipase a(2) Expression in Tumours: A Target for Therapeutic Intervention? *Drug Discov. Today* **2003**, *8* (15), 710-716.
- (106) Ghomashchi, F.; Yu, B. Z.; Berg, O.; Jain, M. K.; Gelb, M. H., Interfacial Catalysis by Phospholipase-A2 - Substrate-Specificity in Vesicles. *Biochemistry* **1991**, *30* (29), 7318-7329.

- (107) Buckland, A. G.; Wilton, D. C., Anionic Phospholipids, Interfacial Binding and the Regulation of Cell Functions. *Biochim. Biophys. Acta* **2000**, *1483* (2), 199-216.
- (108) Canaan, S.; Nielsen, R.; Ghomashchi, F.; Robinson, B. H.; Gelb, M. H., Unusual Mode of Binding of Human Group Iia Secreted Phospholipase a(2) to Anionic Interfaces as Studied by Continuous Wave and Time Domain Electron Paramagnetic Resonance Spectroscopy. *J. Biol. Chem.* **2002**, *277* (34), 30984-30990.
- (109) Bezzine, S.; Bollinger, J. G.; Singer, A. G.; Veatch, S. L.; Keller, S. L.; Gelb, M. H., On the Binding Preference of Human Groups Iia and X Phospholipases a(2) for Membranes with Anionic Phospholipids. *J. Biol. Chem.* **2002**, *277* (50), 48523-48534.
- (110) Leidy, C.; Linderoth, L.; Andresen, T. L.; Mouritsen, O. G.; Jorgensen, K.; Peters, G. H., Domain-Induced Activation of Human Phospholipase a(2) Type Iia: Local Versus Global Lipid Composition. *Biophys. J.* **2006**, *90* (9), 3165-3175.
- (111) Gadd, M. E.; Biltonen, R. L., Characterization of the Interaction of Phospholipase a(2) with Phosphatidylcholine-Phosphatidylglycerol Mixed Lipids. *Biochemistry* **2000**, *39* (32), 9623-9631.
- (112) Jorgensen, K.; Davidsen, J.; Mouritsen, O. G., Biophysical Mechanisms of Phospholipase A2 Activation and Their Use in Liposome-Based Drug Delivery. *FEBS Lett.* **2002**, *531* (1), 23-27.
- (113) Jorgensen, K.; Vermehren, C.; Mouritsen, O. G., Enhancement of Phospholipase a(2) Catalyzed Degradation of Polymer Grafted Peg-Liposomes: Effects of Lipopolymer-Concentration and Chain-Length. *Pharm. Res.* **1999**, *16* (9), 1491-1493.
- (114) Davidsen, J.; Vermehren, C.; Frokjaer, S.; Mouritsen, O. G.; Jorgensen, K., Drug Delivery by Phospholipase a(2) Degradable Liposomes. *Int. J. Pharm.* **2001**, *214* (1-2), 67-69.
- (115) Wymer, N. J.; Gerasimov, O. V.; Thompson, D. H., Cascade Liposomal Triggering: Light-Induced Ca²⁺ Release from Dipalmitoylcholine Liposomes Triggers Pla(2)-Catalyzed Hydrolysis and Contents Leakage from Dppc Liposomes. *Bioconjugate Chem.* **1998**, *9* (3), 305-308.
- (116) Davidsen, J.; Jorgensen, K.; Andresen, T. L.; Mouritsen, O. G., Secreted Phospholipase a(2) as a New Enzymatic Trigger Mechanism for Localised Liposomal Drug Release and Absorption in Diseased Tissue. *Biochim. Biophys. Acta* **2003**, *1609* (1), 95-101.

- (117) Andresen, T. L.; Davidsen, J.; Begtrup, M.; Mouritsen, O. G.; Jorgensen, K., Enzymatic Release of Antitumor Ether Lipids by Specific Phospholipase A2 Activation of Liposome-Forming Prodrugs. *J. Med. Chem.* **2004**, *47* (7), 1694-1703.
- (118) Jensen, S. S.; Andresen, T. L.; Davidsen, J.; Hoyrup, P.; Shnyder, S. D.; Bibby, M. C.; Gill, J. H.; Jorgensen, K., Secretory Phospholipase a(2) as a Tumor-Specific Trigger for Targeted Delivery of a Novel Class of Liposomal Prodrug Anticancer Etherlipids. *Mol. Cancer Ther.* **2004**, *3* (11), 1451-1458.
- (119) Andresen, T. L.; Jensen, S. S.; Kaasgaard, T.; Jorgensen, K., Triggered Activation and Release of Liposomal Prodrugs and Drugs in Cancer Tissue by Secretory Phospholipase A2. *Curr. Drug Delivery* **2005**, *2*, 353-362.
- (120) Linderoth, L.; Fristrup, P.; Hansen, M.; Melander, F.; Madsen, R.; Andresen, T. L.; Peters, G. H., Mechanistic Study of the Spla(2)-Mediated Hydrolysis of a Thio-Ester Pro Anticancer Ether Lipid. *J. Am. Chem. Soc.* **2009**, *131* (34), 12193-12200.
- (121) Vihinen, P.; Kahari, V. M., Matrix Metalloproteinases in Cancer: Prognostic Markers and Therapeutic Targets. *Int. J. Cancer* **2002**, *99* (2), 157-166.
- (122) Olson, M. W.; Gervasi, D. C.; Mobashery, S.; Fridman, R., Kinetic Analysis of the Binding of Human Matrix Metalloproteinase-2 and -9 to Tissue Inhibitor of Metalloproteinase (Timp)-1 and Timp-2. *J. Biol. Chem.* **1997**, *272* (47), 29975-29983.
- (123) Morgunova, E.; Tuuttila, A.; Bergmann, U.; Isupov, M.; Lindqvist, Y.; Schneider, G.; Tryggvason, K., Structure of Human Pro-Matrix Metalloproteinase-2: Activation Mechanism Revealed. *Science* **1999**, *284* (5420), 1667-1670.
- (124) Elkins, P. A.; Ho, Y. S.; Smith, W. W.; Janson, C. A.; D'Alessio, K. J.; McQueney, M. S.; Cummings, M. D.; Romanic, A. M., Structure of the C-Terminally Truncated Human Prommp9, a Gelatin-Binding Matrix Metalloproteinase. *Acta Crystallogr D* **2002**, *58*, 1182-1192.
- (125) Kline, T.; Torgov, M. Y.; Mendelsohn, B. A.; Cervený, C. G.; Senter, P. D., Novel Antitumor Prodrugs Designed for Activation by Matrix Metalloproteinases-2 and-9. *Mol. Pharmaceut.* **2004**, *1* (1), 9-22.
- (126) Chau, Y.; Tan, F. E.; Langer, R., Synthesis and Characterization of Dextran-Peptide-Methotrexate Conjugates for Tumor Targeting Via Mediation by Matrix Metalloproteinase Ii and Matrix Metalloproteinase Ix. *Bioconjugate Chem.* **2004**, *15* (4), 931-941.

- (127) Sarkar, N. R.; Rosendahl, T.; Krueger, A. B.; Banerjee, A. L.; Benton, K.; Mallik, S.; Srivastava, D. K., "Uncorking" of Liposomes by Matrix Metalloproteinase-9. *Chem. Commun.* **2005**, (8), 999-1001.
- (128) Elegbede, A. I.; Banerjee, J.; Hanson, A. J.; Tobwala, S.; Ganguli, B.; Wang, R. Y.; Lu, X. N.; Srivastava, D. K.; Mallik, S., Mechanistic Studies of the Triggered Release of Liposomal Contents by Matrix Metalloproteinase-9. *J. Am. Chem. Soc.* **2008**, *130* (32), 10633-10642.
- (129) Sarkar, N.; Banerjee, J.; Hanson, A. J.; Elegbede, A. I.; Rosendahl, T.; Krueger, A. B.; Banerjee, A. L.; Tobwala, S.; Wang, R. Y.; Lu, X. N.; Mallik, S.; Srivastava, D. K., Matrix Metalloproteinase-Assisted Triggered Release of Liposomal Contents. *Bioconjugate Chem.* **2008**, *19* (1), 57-64.
- (130) Banerjee, J.; Hanson, A. J.; Gadam, B.; Elegbede, A. I.; Tobwala, S.; Ganguly, B.; Wagh, A. V.; Muhonen, W. W.; Law, B.; Shabb, J. B.; Srivastava, D. K.; Mallik, S., Release of Liposomal Contents by Cell-Secreted Matrix Metalloproteinase-9. *Bioconjugate Chem.* **2009**, *20* (7), 1332-1339.
- (131) Terada, T.; Iwai, M.; Kawakami, S.; Yamashita, F.; Hashida, M., Novel Peg-Matrix Metalloproteinase-2 Cleavable Peptide-Lipid Containing Galactosylated Liposomes for Hepatocellular Carcinoma-Selective Targeting. *J. Controlled Release* **2006**, *111* (3), 333-342.
- (132) Ernster, L.; Navazio, F., Studies on Tpn-Linked Oxidations .1. Pathways of Isocitrate Oxidation in Rat Liver Mitochondria. *Biochim. Biophys. Acta* **1957**, *26* (2), 408-415.
- (133) Navazio, F.; Ernster, B. B.; Ernster, L., Studies on Tpn-Linked Oxidations .2. The Quantitative Significance of Liver Lactic Dehydrogenase as a Catalyzer of Tpnh-Oxidation. *Biochim. Biophys. Acta* **1957**, *26* (2), 416-421.
- (134) Ernster, L.; Navazio, F., Soluble Diaphorase in Animal Tissues. *Acta Chem. Scand.* **1958**, *12* (3), 595-595.
- (135) Straub, F. B., Isolation and Properties of a Flavoprotein from Heart Muscle Tissue. *Biochem. J.* **1939**, *33*, 787-792.
- (136) Ernster, L.; Ljunggren, M.; Danielson, L., Purification and Some Properties of a Highly Dicumaryl-Sensitive Liver Diaphorase. *Biochem. Biophys. Res. Commun.* **1960**, *2* (2), 88-92.

- (137) Vasiliou, V.; Ross, D.; Nebert, D. W., Update of the Nad(P)H:Quinone Oxidoreductase (Nqo) Gene Family. *Human Genomics* **2006**, *2*, 329-335.
- (138) Li, R.; Bianchet, M. A.; Talalay, P.; Amzel, L. M., The Three-Dimensional Structure of Nad(P)H:Quinone Reductase, a Flavoprotein Involved in Cancer Chemoprotection and Chemotherapy: Mechanism of the Two-Electron Reduction. *Proceedings of the National Academy of Science* **1995**, *92*, 8846-8850.
- (139) Faig, M.; Bianchet, M. A.; Talalay, P.; Chen, S.; Winski, S.; Ross, D.; Amzel, L. M., Structures of Recombinant Human and Mouse Nad(P)H : Quinone Oxidoreductases: Species Comparison and Structural Changes with Substrate Binding and Release. *Proc. Natl. Acad. Sci. U. S. A.* **2000**, *97* (7), 3177-3182.
- (140) Skelly, J. V.; Sanderson, M. R.; Suter, D. A.; Baumann, U.; Read, M. A.; Gregory, D. S. J.; Bennett, M.; Hobbs, S. M.; Neidle, S., Crystal Structure of Human Dt-Diaphorase: A Model for Interaction with the Cytotoxic Prodrug 5-(Aziridin-1-Yl)-2,4-Dinitrobenzamide (Cb1954). *J. Med. Chem.* **1999**, *42* (21), 4325-4330.
- (141) Beall, H. D.; Mulcahy, R. T.; Siegel, D.; Traver, R. D.; Gibson, N. W.; Ross, D., Metabolism of Bioreductive Antitumor Compounds by Purified Rat and Human Dt-Diaphorases. *Cancer Res.* **1994**, *54* (12), 3196-3201.
- (142) Walton, M. I.; Smith, P. J.; Workman, P., The Role of Nad(P)H - Quinone Reductase (Ec 1.6.99.2, Dt-Diaphorase) in the Reductive Bioactivation of the Novel Indoloquinone Antitumor Agent Eo9. *Cancer Communications* **1991**, *3* (7), 199-206.
- (143) Chen, S.; Knox, R.; Wu, K.; Deng, P. S. K.; Zhou, D. J.; Bianchet, M. A.; Amzel, L. M., Molecular Basis of the Catalytic Differences among Dt-Diaphorase of Human, Rat, and Mouse. *J. Biol. Chem.* **1997**, *272* (3), 1437-1439.
- (144) Iyanagi, T.; Yamazaki, I., One-Electron-Transfer Reactions in Biochemical Systems .5. Difference in Mechanism of Quinone Reduction by Nadh Dehydrogenase and Nad(P)H Dehydrogenase (Dt-Diaphorase). *Biochim. Biophys. Acta* **1970**, *216* (2), 282-294.
- (145) Bianchet, M. A.; Erdemli, S. B.; Amzel, L. M., Structure, Function, and Mechanism of Cytosolic Quinone Reductases. *Vitam Horm* **2008**, *78*, 63-84.
- (146) Winski, S. L.; Koutalos, Y.; Bentley, D. L.; Ross, D., Subcellular Localization of Nad(P)H : Quinone Oxidoreductase 1 in Human Cancer Cells. *Cancer Res.* **2002**, *62* (5), 1420-1424.

- (147) Villalba, J. M.; Navarro, F.; Arroyo, A.; Martin, S. F.; Bello, R. I.; de Cabo, R.; Burgess, J. R.; Navas, P., Protective Role of Ubiquinone in Vitamin E and Selenium-Deficient Plasma Membranes. *Biofactors* **1999**, *9* (2-4), 163-170.
- (148) Dallner, G.; Orrenius, S.; Bergstrand, A., Isolation and Properties of Rough and Smooth Vesicles from Rat Liver. *J. Cell Biol.* **1963**, *16* (2), 426-430.
- (149) Ernster, L., Dt Diaphorase. *Methods Enzymol.* **1967**, *10*, 309-317.
- (150) Sreerama, L.; Hedge, M. W.; Sladek, N. E., Identification of a Class 3 Aldehyde Dehydrogenase in Human Saliva and Increased Levels of This Enzyme, Glutathione S-Transferases, and Dt-Diaphorase in the Saliva of Subjects Who Continually Ingest Large Quantities of Coffee or Broccoli. *Clin. Cancer Res.* **1995**, *1* (10), 1153-1163.
- (151) Siegel, D.; Ryder, J.; Ross, D., Nad(P)H: Quinone Oxidoreductase 1 Expression in Human Bone Marrow Endothelial Cells. *Toxicol. Lett.* **2001**, *125* (1-3), 93-98.
- (152) Awadallah, N. S.; Dehn, D.; Shah, R. J.; Nash, S. R.; Chen, Y. K.; Ross, D.; Bentz, J. S.; Shroyer, K. R., Nqo1 Expression in Pancreatic Cancer and Its Potential Use as a Biomarker. *Appl. Immunohistochem. Mol. Morphol.* **2008**, *16* (1), 24-31.
- (153) Dinkova-Kostova, L. T.; Talalay, P., Persuasive Evidence That Quinone Reductase Type 1 (Dt Diaphorase) Protects Cells against the Toxicity of Electrophiles and Reactive Forms of Oxygen. *Free Radical Biol. Med.* **2000**, *29* (3-4), 231-240.
- (154) Ross, D., Quinone Reductases Multitasking in the Metabolic World. *Drug Metab. Rev.* **2004**, *36* (3-4), 639-654.
- (155) Preusch, P. C.; Siegel, D.; Gibson, N. W.; Ross, D., A Note on the Inhibition of Dt-Diaphorase by Dicoumarol. *Free Radical Biol. Med.* **1991**, *11* (1), 77-80.
- (156) Ross, D.; Siegel, D.; Beall, H.; Prakash, A. S.; Mulcahy, R. T.; Gibson, N. W., Dt-Diaphorase in Activation and Detoxification of Quinones - Bioreductive Activation of Mitomycin-C. *Cancer Metast. Rev.* **1993**, *12* (2), 83-101.
- (157) Phillips, R. M., Inhibition of Dt-Diaphorase (Nad(P)H : Quinone Oxidoreductase, Ec 1.6.99.2) by 5,6-Dimethylxanthone-4-Acetic Acid (Dmxaa) and Flavone-8-Acetic Acid (Faa): Implications for Bioreductive Drug Development. *Biochem. Pharmacol.* **1999**, *58* (2), 303-310.

- (158) Winski, S. L.; Faig, M.; Bianchet, M. A.; Siegel, D.; Swann, E.; Fung, K.; Duncan, M. W.; Moody, C. J.; Amzel, L. M.; Ross, D., Characterization of a Mechanism-Based Inhibitor of Nad(P)H: Quinone Oxidoreductase 1 by Biochemical, X-Ray Crystallographic, and Mass Spectrometric Approaches. *Biochemistry* **2001**, *40* (50), 15135-15142.
- (159) Reigan, P.; Colucci, M. A.; Siegel, D.; Chilloux, A.; Moody, C. J.; Ross, D., Development of Indolequinone Mechanism-Based Inhibitors of Nad(P)H : Quinone Oxidoreductase 1 (Nqo1): Nqo1 Inhibition and Growth Inhibitory Activity in Human Pancreatic Mia Paca-2 Cancer Cells. *Biochemistry* **2007**, *46* (20), 5941-5950.
- (160) Nolan, K. A.; Timson, D. J.; Stratford, I. J.; Bryce, R. A., In Silico Identification and Biochemical Characterization of Novel Inhibitors of Nqo1. *Bioorg. Med. Chem. Lett.* **2006**, *16* (24), 6246-6254.
- (161) Nolan, K. A.; Zhao, H.; Faulder, P. F.; Frenkel, A. D.; Timson, D. J.; Siegel, D.; Ross, D.; Burke, T. R.; Stratford, I. J.; Bryce, R. A., Coumarin-Based Inhibitors of Human Nad(P)H : Quinone Oxidoreductase-1. Identification, Structure-Activity, Off-Target Effects and in Vitro Human Pancreatic Cancer Toxicity. *J. Med. Chem.* **2007**, *50* (25), 6316-6325.
- (162) Nolan, K. A.; Doncaster, J. R.; Dunstan, M. S.; Scott, K. A.; Frenkel, A. D.; Siegel, D.; Ross, D.; Barnes, J.; Levy, C.; Leys, D.; Whitehead, R. C.; Stratford, I. J.; Bryce, R. A., Synthesis and Biological Evaluation of Coumarin-Based Inhibitors of Nad(P)H: Quinone Oxidoreductase-1 (Nqo1). *J. Med. Chem.* **2009**, *52* (22), 7142-7156.
- (163) Nolan, K. A.; Humphries, M. P.; Barnes, J.; Doncaster, J. R.; Caraher, M. C.; Tirelli, N.; Bryce, R. A.; Whitehead, R. C.; Stratford, I. J., Triazoloacridin-6-Ones as Novel Inhibitors of the Quinone Oxidoreductases Nqo1 and Nqo2. *Bioorg. Med. Chem.* **2010**, *18*, 696-706.
- (164) Asher, G.; Dym, O.; Tsvetkov, P.; Adler, J.; Shaul, Y., The Crystal Structure of Nad(P)H Quinone Oxidoreductase 1 in Complex with Its Potent Inhibitor Dicoumarol. *Biochemistry* **2006**, *45* (20), 6372-6378.
- (165) Gutierrez, P. L., The Role of Nad(P)H Oxidoreductase (Dt-Diaphorase) in the Bioactivation of Quinone-Containing Antitumor Agents: A Review. *Free Radical Biol. Med.* **2000**, *29* (3-4), 263-275.
- (166) Asche, C., Antitumour Quinones. *Mini-Rev. Med. Chem.* **2005**, *5* (5), 449-467.
- (167) Hata, T.; Sano, Y.; Sugawara, R.; Matsumae, A.; Kanamori, K.; Shima, T.; Hoshi, T., Mitomycin, a New Antibiotic from Streptomyces .1. *J. Antibiot.* **1956**, *9* (4), 141-146.

- (168) Crooke, S. T.; Bradner, W. T., Mitomycin-C - Review. *Cancer Treatment Reviews* **1976**, 3 (3), 121-139.
- (169) Pan, S. S.; Akman, S. A.; Forrest, G. L.; Hipsher, C.; Johnson, R., The Role of Nad(P)H - Quinone Oxidoreductase in Mitomycin C-Resistant and Porfiromycin-Resistant Hct 116 Human Colon-Cancer Cells. *Cancer Chemother. Pharmacol.* **1992**, 31 (1), 23-31.
- (170) Siegel, D.; Gibson, N. W.; Preusch, P. C.; Ross, D., Metabolism of Mitomycin-C by Dt-Diaphorase - Role in Mitomycin-C-Induced DNA Damage and Cytotoxicity in Human Colon-Carcinoma Cells. *Cancer Res.* **1990**, 50 (23), 7483-7489.
- (171) Phillips, R. M.; Burger, A. M.; Loadman, P. M.; Jarrett, C. M.; Swaine, D. J.; Fiebig, H. H., Predicting Tumor Responses to Mitomycin C on the Basis of Dt-Diaphorase Activity or Drug Metabolism by Tumor Homogenates: Implications for Enzyme-Directed Bioreductive Drug Development. *Cancer Res.* **2000**, 60 (22), 6384-6390.
- (172) Beall, H. D.; Murphy, A. M.; Siegel, D.; Hargreaves, R. H. J.; Butler, J.; Ross, D., Nicotinamide Adenine-Dinucleotide (Phosphate)Quinone Oxidoreductase (Dt-Diaphorase) as a Target for Bioreductive Antitumor Quinones - Quinone Cytotoxicity and Selectivity in Human Lung and Breast-Cancer Cell-Lines. *Mol. Pharmacol.* **1995**, 48 (3), 499-504.
- (173) Oostveen, E. A.; Speckamp, W. N., Mitomycin Analogs .1. Indoloquinones as (Potential) Bisalkylating Agents. *Tetrahedron* **1987**, 43 (1), 255-262.
- (174) Dirix, L. Y.; Tonnesen, F.; Cassidy, J.; Epelbaum, R.; Huinink, W. W. T.; Pavlidis, N.; Sorio, R.; Gamucci, T.; Wolff, I.; TeVelde, A.; Lan, J.; Verweij, J., Eo9 Phase II Study in Advanced Breast, Gastric, Pancreatic and Colorectal Carcinoma by the Eortc Early Clinical Studies Group. *Eur. J. Cancer* **1996**, 32A (11), 2019-2022.
- (175) Pavlidis, N.; Hanauske, A. R.; Gamucci, T.; Smyth, J.; Lehnert, M.; teVelde, A.; Lan, J.; Verweij, J., A Randomized Phase II Study with Two Schedules of the Novel Indoloquinone Eo9 in Non-Small-Cell Lung Cancer: A Study of the Eortc Early Clinical Studies Group (EcsG). *Ann Oncol* **1996**, 7 (5), 529-531.
- (176) Gibson, N. W.; Hartley, J. A.; Butler, J.; Siegel, D.; Ross, D., Relationship between Dt-Diaphorase-Mediated Metabolism of a Series of Aziridinybenzoquinones and DNA Damage and Cytotoxicity. *Mol. Pharmacol.* **1992**, 42 (3), 531-536.
- (177) Winski, S. L.; Hargreaves, R. H. J.; Butler, J.; Ross, D., A New Screening System for Nad(P)H : Quinone Oxidoreductase (Nqo1)-Directed Antitumor Quinones: Identification of a New Aziridinybenzoquinone, Rh1, as a Nqo1-Directed Antitumor Agent. *Clin. Cancer Res.* **1998**, 4 (12), 3083-3088.

- (178) Yan, C.; Kepa, J. K.; Siegel, D.; Stratford, I. J.; Ross, D., Dissecting the Role of Multiple Reductases in Bioactivation and Cytotoxicity of the Antitumor Agent 2,5-Diaziridinyl-3-(Hydroxymethyl)-6-Methyl-1,4-Benzoquinone (Rh1). *Mol. Pharmacol.* **2008**, *74* (6), 1657-1665.
- (179) Hussein, D.; Holt, S. V.; Brookes, K. E.; Klymenko, T.; Adamski, J. K.; Hogg, A.; Estlin, E. J.; Ward, T.; Dive, C.; Makin, G. W. J., Preclinical Efficacy of the Bioreductive Alkylating Agent Rh1 against Paediatric Tumours. *Br. J. Cancer* **2009**, *101* (1), 55-63.
- (180) Beall, H. D.; Liu, Y. F.; Siegel, D.; Bolton, E. M.; Gibson, N. W.; Ross, D., Role of Nad(P)H:Quinone Oxidoreductase (Dt-Diaphorase) in Cytotoxicity and Induction of DNA Damage by Streptonigrin. *Biochem. Pharmacol.* **1996**, *51* (5), 645-652.
- (181) Hackethal, C.; Burchenal, J. H.; Golbey, R. B.; Tan, C. T. C.; Karnofsky, D. A., Clinical Observations on Effects of Streptonigrin in Patients with Neoplastic Disease. *Antibiot. Chemother.* **1961**, *11* (3), 178-183.
- (182) Humphrey, E. W.; Blank, N., Clinical Experience with Streptonigrin. *Cancer Chemother. Rep.* **1961**, (12), 99-103.
- (183) Pink, J. J.; Planchon, S. M.; Tagliarino, C.; Varnes, M. E.; Siegel, D.; Boothman, D. A., Nad(P)H : Quinone Oxidoreductase Activity Is the Principal Determinant of Beta-Lapachone Cytotoxicity. *J. Biol. Chem.* **2000**, *275* (8), 5416-5424.
- (184) Ough, M.; Lewis, A.; Bey, E. A.; Gao, J. M.; Ritchie, J. M.; Bornmann, W.; Boothman, D. A.; Oberley, L. W.; Cullen, J. J., Efficacy of Beta-Lapachone in Pancreatic Cancer Treatment - Exploiting the Novel, Therapeutic Target Nqo1. *Cancer Biol. Ther.* **2005**, *4* (1), 95-102.
- (185) Li, L. S.; Bey, E. A.; Dong, Y.; Meng, J. R.; Patra, B.; Yan, J. S.; Xie, X. J.; Brekken, R. A.; Barnett, C. C.; Bornmann, W. G.; Gao, J. M.; Boothman, D. A., Modulating Endogenous Nqo1 Levels Identifies Key Regulatory Mechanisms of Action of Beta-Lapachone for Pancreatic Cancer Therapy. *Clin. Cancer Res.* **2011**, *17* (2), 275-285.
- (186) Workman, P., Overview: Translating Hsp90 Biology into Hsp90 Drugs. *Curr. Cancer Drug Targets* **2003**, *3*, 297-300.
- (187) Kelland, L. R.; Sharp, S. Y.; Rogers, P. M.; Myers, T. G.; Workman, P., Dt-Diaphorase Expression and Tumor Cell Sensitivity to 17-Allylamino,17-Demethoxygeldanamycin, an Inhibitor of Heat Shock Protein 90. *J. Natl. Cancer Inst.* **1999**, *91* (22), 1940-1949.

- (188) Guo, W. C.; Reigan, P.; Siegel, D.; Zirrolli, J.; Gustafson, D.; Ross, D., Formation of 17-Allylamino-Demethoxygeldanamycin (17-Aag) Hydroquinone by Nad(P)H : Quinone Oxidoreductase 1: Role of 17-Aag Hydroquinone in Heat Shock Protein 90 Inhibition. *Cancer Res.* **2005**, *65* (21), 10006-10015.
- (189) Guo, W. C.; Reigan, P.; Siegel, D.; Zirrolli, J.; Gustafson, D.; Ross, D., The Bioreduction of a Series of Benzoquinone Ansamycins by Nad(P)H : Quinone Oxidoreductase 1 to More Potent Heat Shock Protein 90 Inhibitors, the Hydroquinone Ansamycins. *Mol. Pharmacol.* **2006**, *70* (4), 1194-1203.
- (190) Colucci, M. A.; Moody, C. J.; Couch, G. D., Natural and Synthetic Quinones and Their Reduction by the Quinone Reductase Enzyme Nqo1: From Synthetic Organic Chemistry to Compounds with Anticancer Potential. *Org. Biomol. Chem.* **2008**, *6* (4), 637-656.
- (191) Phillips, R. M., Bioreductive Activation of a Series of Analogues of 5-Aziridinyl-3-Hydroxymethyl-1-Methyl-2-[1h-Indole-4,7-Dione] Prop-Beta-En-Alpha-Ol (Eo9) by Human Dt-Diaphorase. *Biochem. Pharmacol.* **1996**, *52* (11), 1711-1718.
- (192) Beall, H. D.; Winski, S.; Swann, E.; Hudnott, A. R.; Cotterill, A. S.; O'Sullivan, N.; Green, S. J.; Bien, R.; Siegel, D.; Ross, D.; Moody, C. J., Indolequinone Antitumor Agents: Correlation between Quinone Structure, Rate of Metabolism by Recombinant Human Nad(P)H : Quinone Oxidoreductase, and in Vitro Cytotoxicity. *J. Med. Chem.* **1998**, *41* (24), 4755-4766.
- (193) Phillips, R. M.; Naylor, M. A.; Jaffar, M.; Doughty, S. W.; Everett, S. A.; Breen, A. G.; Choudry, G. A.; Stratford, I. J., Bioreductive Activation of a Series of Indolequinones by Human Dt-Diaphorase: Structure-Activity Relationships. *J. Med. Chem.* **1999**, *42* (20), 4071-4080.
- (194) Swann, E.; Barraja, P.; Oberlander, A. M.; Gardipee, W. T.; Hudnott, A. R.; Beall, H. D.; Moody, C. J., Indolequinone Antitumor Agents: Correlation between Quinone Structure and Rate of Metabolism by Recombinant Human Nad(P)H : Quinone Oxidoreductase. Part 2. *J. Med. Chem.* **2001**, *44* (20), 3311-3319.
- (195) Newsome, J. J.; Swann, E.; Hassani, M.; Bray, K. C.; Slawin, A. M. Z.; Beall, H. D.; Moody, C. J., Indolequinone Antitumour Agents: Correlation between Quinone Structure and Rate of Metabolism by Recombinant Human Nad(P)H : Quinone Oxidoreductase. *Org. Biomol. Chem.* **2007**, *5* (10), 1629-1640.
- (196) Fourie, J.; Oleschuk, C. J.; Guziec, F.; Guziec, L.; Fiterman, D. J.; Monterrosa, C.; Begleiter, A., The Effect of Functional Groups on Reduction and Activation of Quinone Bioreductive Agents by Dt-Diaphorase. *Cancer Chemother. Pharmacol.* **2002**, *49* (2), 101-110.

- (197) Begleiter, A.; El-Gabalawy, N.; Lange, L.; Leith, M. K.; Guziec, L. J.; Guziec Jr, F. S., A Model for Nad(P)H:Quinoneoxidoreductase 1 (Nqo1) Targeted Individualized Cancer Chemotherapy. *Drug Target Insights* **2009**, *4*, 1-8.
- (198) Suleman, A.; Skibo, E. B., A Comprehensive Study of the Active Site Residues of Dt-Diaphorase: Rational Design of Benzimidazolediones as Dt-Diaphorase Substrates. *J. Med. Chem.* **2002**, *45* (6), 1211-1220.
- (199) Fryatt, T.; Pettersson, H. I.; Gardipee, W. T.; Bray, K. C.; Green, S. J.; Slawin, A. M. Z.; Beall, H. D.; Moody, C. J., Novel Quinolinequinone Antitumor Agents: Structure-Metabolism Studies with Nad(P)H : Quinone Oxidoreductase (Nqo1). *Bioorg. Med. Chem.* **2004**, *12* (7), 1667-1687.
- (200) Hassani, M.; Cai, W.; Koelsch, K. H.; Holley, D. C.; Rose, A. S.; Olang, F.; Lineswala, J. P.; Holloway, W. G.; Gerdes, J. M.; Behforouz, M.; Beall, H. D., Lavendamycin Antitumor Agents: Structure-Based Design, Synthesis, and Nad(P)H : Quinone Oxidoreductase 1 (Nqo1) Model Validation with Molecular Docking and Biological Studies. *J. Med. Chem.* **2008**, *51* (11), 3104-3115.
- (201) Hernick, M.; Flader, C.; Borch, R. F., Design, Synthesis, and Biological Evaluation of Indolequinone Phosphoramidate Prodrugs Targeted to Dt-Diaphorase. *J. Med. Chem.* **2002**, *45* (16), 3540-3548.
- (202) Faig, M.; Bianchet, M. A.; Winski, S.; Hargreaves, R.; Moody, C. J.; Hudnott, A. R.; Ross, D.; Amzel, L. M., Structure-Based Development of Anticancer Drugs: Complexes of Nad(P)H : Quinone Oxidoreductase 1 with Chemotherapeutic Quinones. *Structure* **2001**, *9* (8), 659-667.
- (203) Gharat, L.; Visser, P.; Brummelhuis, M.; Guiles, R.; Chikhale, P., Reductive Activation of Conformationally-Constrained, Anticancer Drug Delivery Systems. *Med. Chem. Res.* **1998**, *8* (7), 444-456.
- (204) Weerapreeyakul, N.; Visser, P.; Brummelhuis, M.; Gharat, L.; Chikhale, P. J., Reductive and Bioreductive Activation Is Controlled by Electronic Properties of Substituents in Conformationally-Constrained Anticancer Drug Delivery Systems. *Med. Chem. Res.* **2000**, *10* (3), 149-163.
- (205) Volpato, M.; Abou-Zeid, N.; Tanner, R. W.; Glassbrook, L. T.; Taylor, J.; Stratford, I.; Loadman, P.; Jaffar, M.; Phillips, R. M., Chemical Synthesis and Biological Evaluation of a Nad(P)H:Quinone Oxidoreductase-1-Targeted Tripartite Quinone Drug Delivery System. *Mol. Cancer Ther.* **2007**, *6* (12), 3122-3130.

- (206) Moody, C. J.; Maskell, L.; Blanche, E. A.; Colucci, M. A.; Whatmore, J. L., Synthesis and Evaluation of Prodrugs for Anti-Angiogenic Pyrrolylmethylidenyl Oxindoles. *Bioorg. Med. Chem. Lett.* **2007**, *17* (6), 1575-1578.

CHAPTER 2

ELECTROCHEMICAL BEHAVIOR OF QUINONE DERIVATIVES POTENTIALLY USABLE FOR DRUG DELIVERY APPLICATIONS

2.1 Introduction

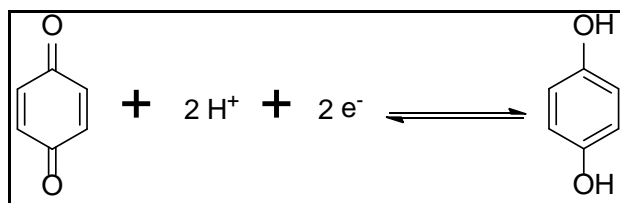
Quinones are known to be electrochemically active and undergo a two-electron, two-proton reduction in aqueous media where the pH is below the pKa of the corresponding hydroquinone¹ as presented in Scheme 2.1. Electrochemical techniques, such as cyclic voltammetry (CV), can provide important thermodynamic as well as kinetic information on quinone-related compounds.² The electrochemical properties of quinones can be tuned by subtle structural changes of the quinone moiety by adding a functional group or a handle, such as a propionic acid chain; in that way, the electronic properties of these compounds can be affected and a change in their reduction potential is possible.

The goal of this work is to construct a series of quinone derivatives with various electronic properties that will be later tested with the human enzyme NAD(P)H:quinone oxidoreductase type 1 (hNQO1), which is known to reduce quinones to hydroquinones;³⁻⁵ thus these quinones may be used as triggers for endogenous target activation. More explicitly, the research in the McCarley group focusses on the use of quinone triggers in the formation of enzyme-responsive liposomes for drug delivery applications. It is known that the half-wave reduction potential of the flavin adenine dinucleotide (FAD) center of rat NQO1 is -0.159 V vs. the standard hydrogen electrode (SHE).⁶ This enzyme follows a ping-pong mechanism using reduced nicotinamide adenine dinucleotide (NADH) or reduced nicotinamide adenine dinucleotide phosphate (NADPH) as the electron source. It is also known that the reduction potentials of NADH/NAD^+ and $\text{NADPH}/\text{NADP}^+$ are -0.310 V and -0.320 V versus SHE, respectively.^{7,8}

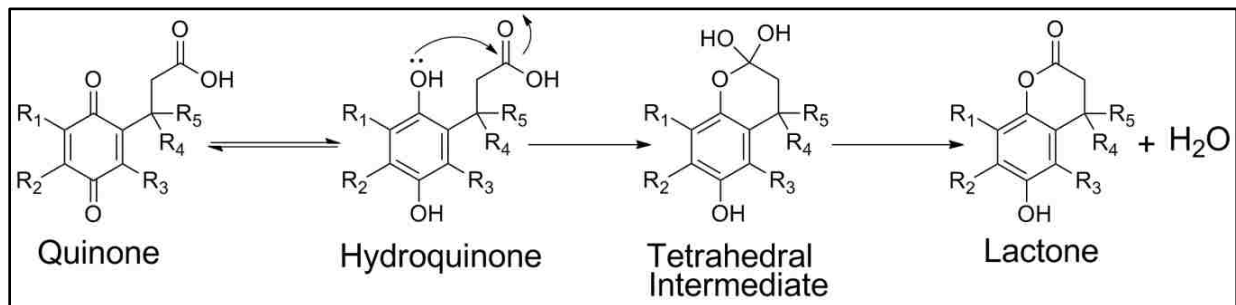
To successfully assess the quinones as substrates of hNQO1, it is necessary that their reduction potential be more positive than -0.159 V, but not so positive that the quinone substrate is possibly reduced directly by NADH or NADPH, as previously demonstrated in the literature for simple quinones.⁸ In addition, it is important to tune the reduction potential of quinone triggers to prevent non-specific interactions with potential reducing species that are endogenous in biological environments, such as glutathione ($E_{1/2} = -0.22$ V vs. SHE)⁹ and ascorbate ($E_{1/2} = 0.051$ vs. SHE),¹⁰ so as to avoid the opening of liposomes at undesired locations. The thermodynamic parameters of cathodic reduction peak ($E_{p,c}$), anodic oxidation peak ($E_{p,a}$) and half-wave potential ($E_{1/2}$) of quinone derivatives were measured. The half-wave potentials were calculated using Equation 2.1.

$$E_{\frac{1}{2}} = \left(\frac{\Delta E_p}{2} \right) + E_{p,c} \quad \text{Equation 2.1}$$

Moreover, it has been well established in earlier works that quinones possessing a trimethyl-lock system ($R_3 = R_4 = R_5 = \text{CH}_3$) experience an intramolecular cyclization passing through a tetrahedral intermediate after being reduced to the corresponding hydroquinone and forming the lactone compound as is depicted in Scheme 2.2.¹¹ Such a reduction/cyclization process for propionic acid quinones is also thought to be dependent on the reduction potential (electronic properties) of the corresponding quinone; thus, the rate constant for the disappearance of hydroquinone was calculated using the peak current ratios ($i_{p,a}/i_{p,c}$) and their evaluation by the Nicholson and Shain method.^{12,13} Therefore, it may be possible to estimate the time for release of a target, such as a drug to be delivered after reduction occurs on the quinone moiety.



Scheme 2.1. Reduction of 1,4-benzoquinone to 1,4-hydroquinone.



Scheme 2.2. Cyclization process of trimethyl-lock propionic acid 1,4-benzoquinones.

2.2 Experimental Section

2.2.1 Materials and Methods

Quinone synthesis was previously described by a colleague in our group.¹⁴ Cyclic voltammetry (CV) experiments were performed with a computer-controlled EG&G PAR model 273 A potentiostat (Princeton, NJ). The electrochemical cell was composed of three electrodes: a (pretreated) glassy-carbon working electrode ($A=0.07 \text{ cm}^2$, CH Instruments, Austin, TX), a homemade 99.9 % platinum counter electrode ($d=0.05 \text{ cm}$), and an Ag/AgCl (3.0 M KCl, CH Instruments) reference electrode. The procedure starts with the polishing of the carbon electrode on a Buehler microcloth with 1 micron alpha alumina slurry micropolish, followed by pretreatment of this electrode by applying +1.5 V for 10 minutes while the electrode is immersed in the buffer solution used for the evaluation of the quinones. Polishing the working electrode eliminates any species that the electrode may absorb, and pretreatment activates the surface of the electrode, permitting a reproducible electron transfer at the working electrode surface.¹⁵ Scans were conducted at a rate of 0.1 V s^{-1} at room temperature ($22\pm 2 \text{ }^\circ\text{C}$) in a degassed 0.1 M phosphate buffer (PB)/0.1 M KCl (pH=7.1). Each solution was degassed with nitrogen for 10 min before obtaining the voltammogram. Before the quinone was tested, the buffer was scanned to confirm a clear background with no unexpected peaks present. Each individual quinone was tested on a different day, with 4 replicates per day. Between replicates, no polishing or cleaning of the electrodes was performed. Quinone solutions contained 1% ethanol or were sufficiently

soluble, solutions were sonicated for 30 min to ensure complete dissolution in the buffer solution; quinone concentrations ranged from 0.3 to 1×10^{-3} M.

2.3 Results and Discussion

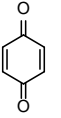
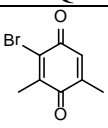
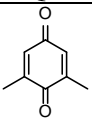
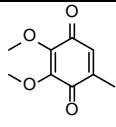
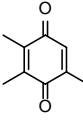
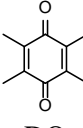
2.3.1 Thermodynamic Parameters of Naked Quinones

In Table 2.1 are summarized the thermodynamic results for six naked (not containing propionic acid) quinones whose voltammograms are presented in Figure 2.1. It can be noted that all of the naked quinones, except the Q_{Br} , deviated from the ideal peak separation (ΔE_p) of 30 mV that corresponds to a total two proton/two electron reversible system.¹⁶ Instead, these compounds follow the behavior of a quasireversible system, which may be due to the slow electron transfer kinetics at the electrode surface.¹⁷⁻¹⁹ Therefore, the half-wave potential ($E_{1/2}$) of each of the naked quinones was used as an approximation of the formal potential (E°) in these systems.

Theoretically, quinones with electron withdrawing groups (EWG) attached to the ring will possess a more positive reduction potential (easier to reduce); while for quinones with electron donating groups (EDG), the opposite should happen. In Table 2.1, it can be seen that 1,4-benzoquinone is the easiest quinone to be reduced with a peak cathodic potential ($E_{p,c}$) of 0.286 V and an $E_{1/2}$ of 0.326 V. When functional groups are added to the benzoquinone, its potential changes following a trend close to our expectations with $E_{1/2}$ values of 0.220 V for Q_{Br} , 0.212 V for Q_H , 0.196 V for Q_{diMeO} , 0.155 V for Q_{Me} , and 0.078 V for DQ. Q_{Br} , where bromine has the property of withdrawing electron density from the quinone moiety by the inductive effect, has a more positive $E_{p,c}$ and $E_{1/2}$ than the hydrogen, methoxy and methyl analogs, as I anticipated. Even though the trend was clear, when comparing the Q_{Br} to the Q_H , the difference in the half-way potential was only 0.008 V more positive for the bromine analog. This similarity of potential between Q_H and Q_{Br} may be explained by the inductive effect of the bromine being counteracted by a resonance effect and a lone pair contribution to the electron density of the

quinone moiety by the halogen as reported in earlier work.²⁰ Another interesting observation was the dimethoxy substituted quinone case; Q_{diMeO} was expected to be more negative than the methyl analog due to its strong resonance effect; however, the opposite was observed. A colleague in our group determined the crystal structure of Q_{diMeO} and observed that one of the methoxy groups is twisted from the quinone plane when two methoxy groups are adjacent on the quinone ring.¹⁴ Such a conformation for the Q_{diMeO} results in a decrease of the resonance effect. This finding was supported by previous research groups that came to the same conclusion for quinones where two adjacent methoxy groups are present.^{21,22}

Table 2.1. Thermodynamic results for naked quinones. Potential scans were conducted at a rate of 0.1 V s^{-1} at $22 \pm 2 \text{ }^\circ\text{C}$ in a pH 7.1 0.1 M PB/0.1 M KCl buffer solution. A three-electrode cell was used containing a glassy carbon electrode, a platinum counter electrode, and an Ag/AgCl (3M KCl) reference electrode. Potentials were converted to values versus the standard hydrogen electrode (SHE) by adding 0.210 V.²³ Results are reported as the mean of 4 replicates \pm one standard deviation.

Quinone	$E_{\text{p,c}}$ (V) vs. SHE	$E_{\text{p,a}}$ (V) vs. SHE	ΔE_{p} (V)	$E_{1/2}$ (V) vs. SHE
 BQ	0.286 \pm 0.001	0.365 \pm 0.001	0.079 \pm 0.001	0.326 \pm 0.001
 Q_{Br}	0.202 \pm 0.000	0.239 \pm 0.001	0.037 \pm 0.001	0.220 \pm 0.001
 Q_{H}	0.176 \pm 0.000	0.249 \pm 0.000	0.073 \pm 0.000	0.212 \pm 0.001
 Q_{diMeO}	0.143 \pm 0.000	0.249 \pm 0.003	0.106 \pm 0.003	0.196 \pm 0.002
 Q_{Me}	0.107 \pm 0.001	0.204 \pm 0.000	0.097 \pm 0.001	0.155 \pm 0.001
 DQ	0.033 \pm 0.001	0.123 \pm 0.001	0.090 \pm 0.000	0.078 \pm 0.001

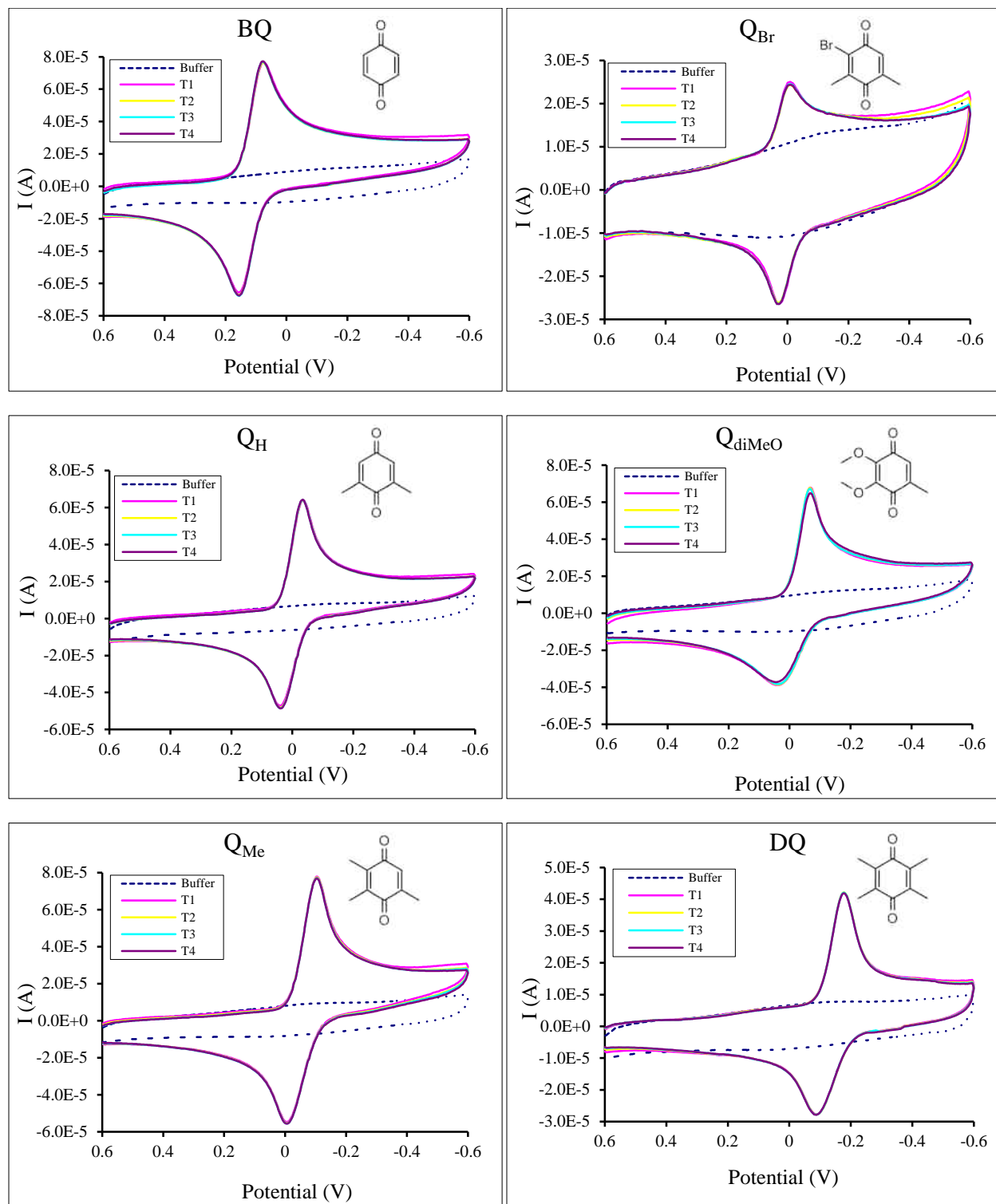


Figure 2.1. Cyclic voltammograms of naked quinones. Potential scans were conducted at a rate of 0.1 V s^{-1} at room temperature ($22 \pm 2 \text{ }^\circ\text{C}$) in a pH 7.1 0.1 M PB/0.1 M KCl buffer solution. A three-electrode cell was used containing a glassy carbon electrode ($A=0.07 \text{ cm}^2$), a platinum counter electrode, and an Ag/AgCl (3M KCl) reference electrode (0.210 V vs. SHE).²³ Potential sweeps started at 0.6 V to -0.6 and back to 0.6 V. Positive current peak corresponds to the reduction peak ($E_{p,c}$) and negative current corresponds to oxidation peak ($E_{p,a}$). Colored lines represent 4 trials performed on each quinone and dashed line represents the buffer solution.

2.3.2 Thermodynamic Parameters of Propionic Acid Quinones and Q_{Me}-ETA

In Table 2.2 are shown the thermodynamic values for eleven propionic acid quinones and one quinone propionic acid derivatized with an ethanolamine group. In Figure 2.2 are contained the voltammograms for each of the quinone compounds mentioned above. All the quinones in Table 2.2, with the only exception being NQ-COOH, had a ΔE_p ranging between 0.242 V and 0.446 V meaning, that these systems are electron-transfer irreversible. This is not surprising, as the quinone propionic units have disturbed benzoquinone rings,¹⁴ while the conversely hydroquinone rings are expected to be planar.²⁴ Thus, there is a significant change in ring geometry during the electron-transfer process that should lead to kinetics sluggishness.

To compare the electronic properties of the various quinones, the reduction peak ($E_{p,c}$) was selected, as it is a better approximation for the reduction potential than $E_{1/2}$ for this type of system. In Table 2.2, the first 10 quinones are subdivided into two groups: quinones without a trimethyl lock system (quinones 1–3) and quinones possessing it (quinone 4–10). In the first group (NQ-COOH, Q'-COOH, Q_{nogemMe}-COOH), the $E_{p,c}$ decreases from 0.249 V to 0.004 V when methyl groups are added to the quinone ring, as expected because methyl functions as an electron donating group and will provide electron density to the ring, resulting in a lower reduction potential for the quinone (harder to be reduced). In the second group are quinones where the only difference is the functional group at the 2-position on the ring. How much an electron donating or withdrawing group affects the reduction of quinones is represented clearly in this series. When a halogen (Br or I) is attached to the quinone propionic acid, the $E_{p,c}$ is –0.026 V and –0.047 V, respectively, and thus are the easier quinones to reduce in the series. When an electron donating group, such as methoxy or methyl, is present, the $E_{p,c}$ value shifts negatively to –0.107 V and –0.125 V, respectively. It is interesting to observe that the more negative value of $E_{p,c}$ between Q_{MeO}-COOH and Q_{Me}-COOH, corresponds to the methyl analog and not to the methoxy analog, as it was expected. This result, opposite to what it was

anticipated, may be due to the not planar conformation that a methoxy group (hindered by a methyl at the 3-position) can acquire with respect to the quinone ring which will decrease the electron density contribution that the methoxy group can bring to the quinone.²² Moreover, when the functional group at the 2-position on the quinone ring is an *n*-propyl amine or a methyl amine, the reduction peak shifts even further negative achieving a value of -0.188 V and -0.219 V respectively. Such a strong electron density on the quinone moiety makes them the hardest in this series to be reduced. The last quinones in Table 2.2 are $Q_{\text{diMeO-COOH}}$ and $Q_{\text{Me-ETA}}$. The $E_{\text{p,c}}$ of $Q_{\text{diMeO-COOH}}$ differs by only 0.012 V from $Q_{\text{MeO-COOH}}$, meaning that addition of an adjacent methoxy group does not alter the electronic properties, probably because the quinone can receive electron density from just one methoxy group, as stated before for the naked quinones. In the case of $Q_{\text{Me-ETA}}$, the electronics are virtually the same as $Q_{\text{Me-COOH}}$, meaning that the nature of the propionic acid side chain (neutral or anionic at pH 7.1) does not impact electronic properties of the quinone moiety, as judged by voltammetry.

Finally, when comparing the naked quinone, such is duroquinone, to the $Q_{\text{noGemMe-COOH}}$ with a propionic acid handle, the reduction peak moves to the negative side by 0.029 V. Likewise, when compared Q_{Me} to $Q'\text{-COOH}$, having a propionic acid handle that includes the presence of germinal methyls, the reduction peak moves to the negative side by 0.085 V. Moreover, the reduction peak of $Q_{\text{Me-COOH}}$, presenting the trimethyl-lock, compared with the reduction peak of duroquinone, is 0.158 V more negative. This confirms the fact that the addition of a handle makes the quinones more difficult to be reduced and that this difficulty increases as the handle includes germinal methyls or the whole trimethyl-lock system is present. The reason for the furthest shift of $E_{\text{p,c}}$ to the negative side, is that the trimethyl-lock induces conformational strain onto the quinone ring, resulting in a deviation from a typical planar conformation by roughly 20° . These observations were made from X-ray crystallography on

each of these compounds¹⁴ and supported by a previous study by Wang *et al.* that also described the strain caused by the trimethyl-lock system.²⁵

Table 2.2. Thermodynamic results for propionic acid quinones. Potential scans were conducted at a rate of 0.1 V s⁻¹ at 22±2 °C in a pH 7.1 0.1 M PB/0.1 M KCl buffer solution. A three-electrode cell was used containing a glassy carbon electrode, a platinum counter electrode, and an Ag/AgCl (3M KCl) reference electrode. Potentials were converted to standard hydrogen electrode (SHE) by adding 210 mV.²³ Results are reported as the mean of 4 replicates ± one standard deviation. ^aThe anodic peak potential of lactone oxidation, $E_{p,l}$, is reported for those propionic acid quinones that exhibit this voltammetric feature.

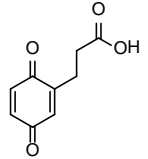
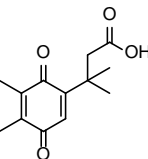
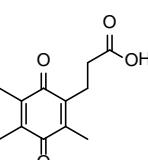
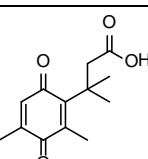
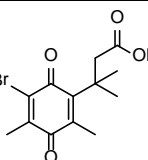
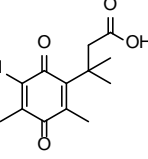
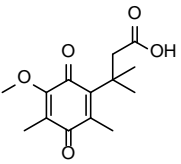
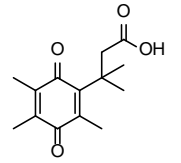
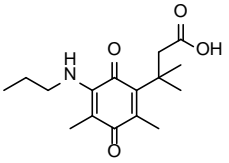
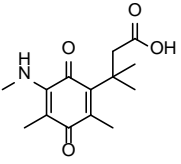
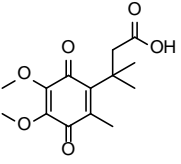
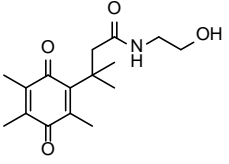
Quinone	$E_{p,c}$ (V) vs. SHE	$E_{p,a}$ (V) vs. SHE	ΔE_p (V)	$E_{1/2}$ (V) vs. SHE	$E_{p,l}$ (V) vs. SHE ^a
 NQ-COOH	0.249±0.002	0.321±0.001	0.072±0.003	0.285±0.001	N/A
 Q'-COOH	0.022±0.001	0.267±0.001	0.245±0.001	0.144±0.001	N/A
 Q _{nogemMe} -COOH	0.004±0.002	0.281±0.002	0.277±0.003	0.143±0.002	N/A
 Q _H -COOH	-0.019±0.002	0.253±0.002	0.272±0.001	0.117±0.002	0.659±0.002
 Q _{Br} -COOH	-0.026±0.001	0.216±0.003	0.242±0.004	0.095±0.001	0.706±0.002
 Q _I -COOH	-0.047±0.003	0.289±0.005	0.336±0.008	0.121±0.001	0.711±0.003

Table 2.2 continued.

Quinone	$E_{p,c}$ (V) vs. SHE	$E_{p,a}$ (V) vs. SHE	ΔE_p (V)	$E_{1/2}$ (V) vs. SHE	$E_{p,l}$ (V) vs. SHE
 $Q_{MeO-COOH}$	-0.107 ± 0.002	0.303 ± 0.002	0.410 ± 0.003	0.098 ± 0.001	0.612 ± 0.003
 $Q_{Me-COOH}$	-0.125 ± 0.001	0.218 ± 0.005	0.343 ± 0.007	0.047 ± 0.002	0.615 ± 0.003
 $Q_{n-pr-NH-COOH}$	-0.188 ± 0.001	0.144 ± 0.002	0.332 ± 0.003	-0.022 ± 0.001	0.640 ± 0.004
 $Q_{Me-N-COOH}$	-0.219 ± 0.002	0.165 ± 0.002	0.384 ± 0.005	-0.027 ± 0.001	0.618 ± 0.003
 $Q_{diMeO-COOH}$	-0.095 ± 0.000	0.351 ± 0.002	0.446 ± 0.002	0.128 ± 0.001	0.694 ± 0.004
 Q_{Me-ETA}	-0.118 ± 0.002	0.199 ± 0.000	0.317 ± 0.002	0.041 ± 0.001	0.640 ± 0.003

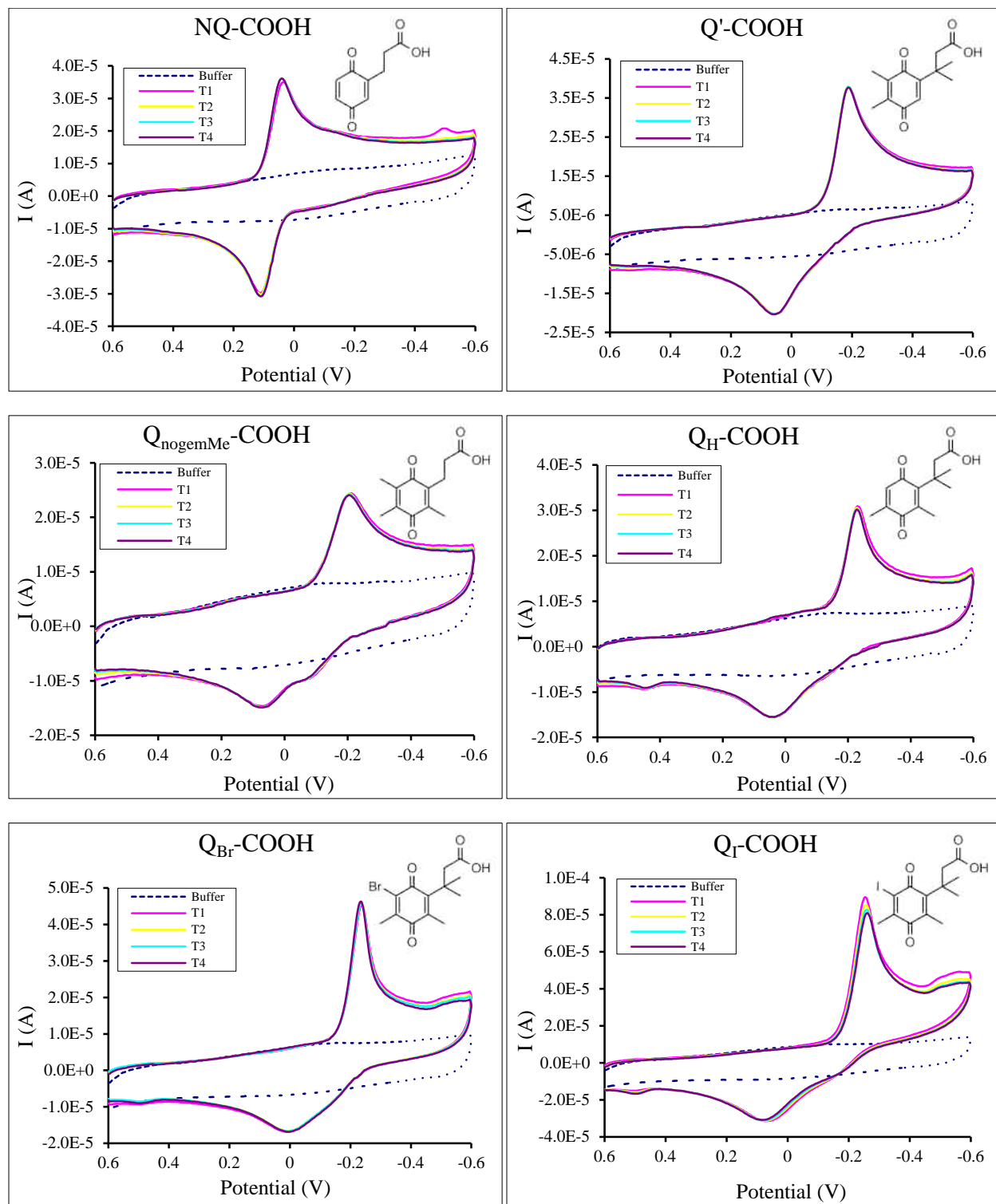
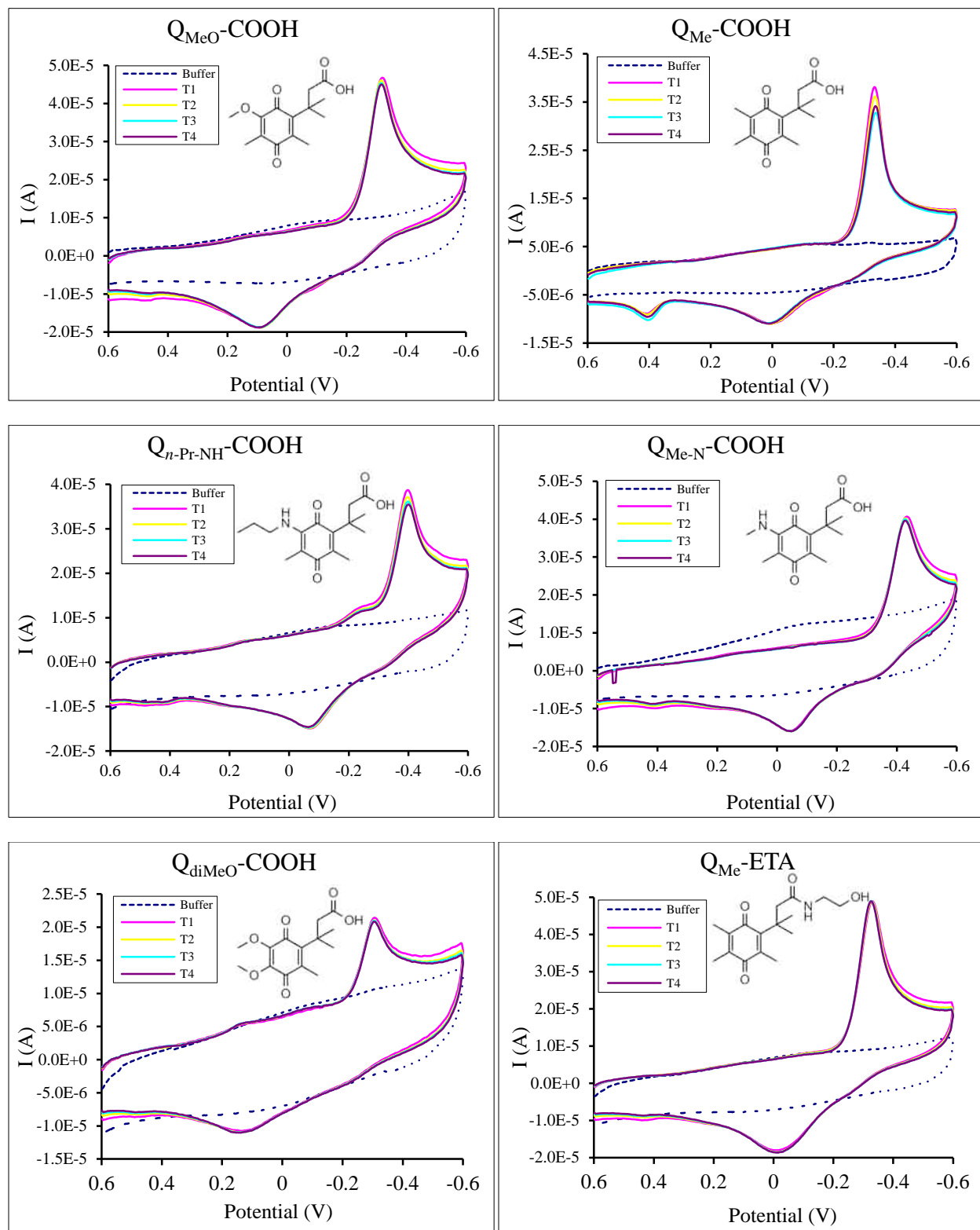


Figure 2.2. Cyclic voltammograms of quinones with a propionic acid side chain. Potential scans were conducted at a rate of 0.1 V s^{-1} at $22 \pm 2 \text{ }^\circ\text{C}$ in a pH 7.1 0.1 M PB/0.1 M KCl buffer solution. A three-electrode cell was used containing a glassy carbon electrode ($A=0.07 \text{ cm}^2$), a platinum counter electrode, and an Ag/AgCl (3M KCl) reference electrode (0.210 V vs. SHE).²³ Potential sweeps started at 0.6 V to -0.6 and back to 0.6 V. Positive current peak corresponds to the reduction peak ($E_{p,c}$) and negative current corresponds to oxidation peak ($E_{p,a}$). Colored lines represent 4 trials performed on each quinone and dashed lines represent the buffer solution.

Figure 2.2 continued.



2.3.3 Propionic Acid Quinones and Their Cyclization Behavior

Earlier voltammograms of propionic acid quinones containing the trimethyl-lock system dissolved in 50% acetonitrile/buffer solutions, showed a lactone peak appearing when Q_H -COOH is reduced to its corresponding hydroquinone.²⁶ The cyclic voltammetry data obtained here in aqueous buffer electrolyte on our trimethyl-lock quinones, led to observation of a lactone peak ($E_{p,l}$) when these quinones were reduced to their hydroquinones under the experimental conditions used here. However, quinone propionic acid where the trimethyl-lock is absent (NQ-COOH, Q'-COOH, Q_{nogemMe} -COOH) does not present a lactone peak. Such a difference between the quinone propionic acid is due to the fact that when the trimethyl-lock system is absent, the cyclization rate is significantly slower, as was reported previously in our group and in earlier works.^{24,27-30} In Scheme 2.2 is presented the reaction sequence for the lactone formation. It is important to our final goal not only to determine the ease of reduction of our quinones but also to find the rate at what hydroquinone disappear to become a lactone. In this matter, the peak current ratio for quinone reduction and hydroquinone oxidation was measured for all the propionic acid quinone and subsequently predicted according to Nicholson and Shain for a chemical step following electron transfer.¹³ As a result, the rate constant for the disappearance of hydroquinone, called k_f was obtained. In Table 2.3 are presented the rate for the disappearance of hydroquinone after reduction of the quinone. The results from Table 2.3 revealed that quinones with no trimethyl-lock have the slowest rate among the propionic acid series ($\text{NQ-COOH} = 0.02 \text{ s}^{-1}$, $Q_{\text{nogemMe}}\text{-COOH} = 0.08 \text{ s}^{-1}$, $Q'\text{-COOH} = 0.13 \text{ s}^{-1}$). Those values confirm the rate enhancement produced by the trimethyl-lock presence when lactone is form by the cyclization of propionic acid quinones.

Table 2.3. Rate constant for the disappearance of propionic acid hydroquinones. ^aRatio measured between peaks current where the potential scan was conducted at a rate of 0.1 V s^{-1} at $22 \pm 2 \text{ }^\circ\text{C}$ in a pH 7.1 0.1 M PB/0.1 M KCl buffer solution. ^bRatio measured between peaks current where the potential scan was conducted at a rate of 1 V s^{-1} $22 \pm 2 \text{ }^\circ\text{C}$ in a 0.1 M PBS / 0.1 M KCl pH 7.1 buffer solution. A three-electrode cell was used containing a glassy carbon electrode, a platinum counter electrode, and an Ag/AgCl (3M KCl) reference electrode.

Quinone	$k_f \text{ (s}^{-1}\text{)}$
NQ-COOH	0.02 ^a
Q _{nogemMe} -COOH	0.08 ^a
Q'-COOH	0.13 ^a
Q _H -COOH	0.19 ^a
Q _{MeO} -COOH	0.27 ^a
Q _{diMeO} -COOH	0.29 ^a
Q _{Me-N} -COOH	0.37 ^a
Q _{n-pr-NH} -COOH	0.39 ^a
Q _{Me} -COOH	1.0 ^b
Q _I -COOH	1.8 ^b
Q _{Br} -COOH	2.4 ^b

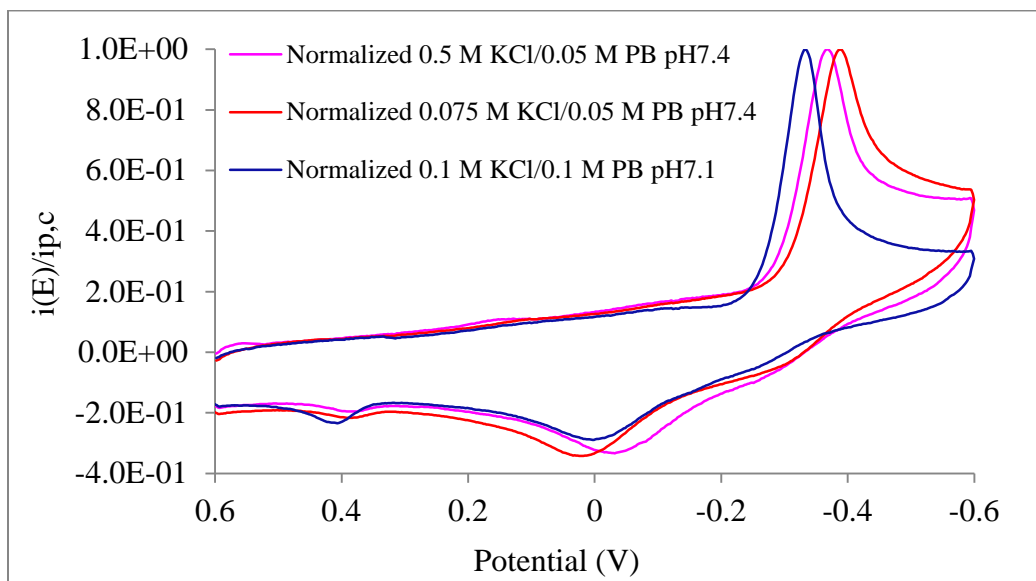


Figure 2.3. Cyclic voltammograms of Q_{Me}-COOH. Potential scans were conducted at a rate of 0.1 V s^{-1} at $22 \pm 2 \text{ }^\circ\text{C}$ in the specified buffer solution. A three-electrode cell was used containing a glassy carbon electrode ($A=0.07 \text{ cm}^2$), a platinum counter electrode, and an Ag/AgCl (3M KCl) reference electrode (0.210 V vs. SHE).²³ Potential sweeps started at 0.6 V to -0.6 and back to 0.6 V . Positive current peak corresponds to the reduction peak ($E_{p,c}$) and negative current corresponds to oxidation peak ($E_{p,a}$), and to the anodic peak of the lactone ($E_{p,l}$).

To conclude the study on the cyclization rate of propionic acid quinones, the influence of buffer catalysis and salt concentration was investigated for $Q_{Me}-COOH$. In Figure 2.3 is clearly shown that the increase in buffer concentration increases the rate of cyclization as seen by the bigger size on the lactone peak and the change on the current peak ratio. On the other hand, adding more salt does not have an effect on the current ratio peak, thus, no impact is seen in the cyclization rate.

2.4 Conclusions

The electronic properties of six naked quinones, eleven propionic acid quinones, and a quinone propionic acid with an ethanolamine handle were characterized by cyclic voltammetry. In all cases, it was demonstrated that structural changes on the quinone moiety altered their reduction behavior. In the case of naked and trimethyl-lock propionic acid quinones, their reduction potentials were changed by addition of different functional groups to the benzoquinone moiety. Both type of quinones followed the same trend where quinones with a halogen had the more positive (or less negative) reduction potential, and quinones with a group that donates electron density to the ring, such as methyl, methoxy or amine, had more negative reduction potentials. However, it seems that halogens donate some electron density to the quinone ring because their reduction potentials with respect to their hydrogen variant were very close (-0.026 V vs. -0.019 V). A similar conclusion was reached for iodo, chloride and bromine substituted quinones in Novak work.²⁰ I also observed that propionic acid quinones without the presence of the trimethyl-lock system had a more positive reduction potential and more easily reduced than those where the trimethyl-lock system is present. The contorted strain produced onto the quinone ring by the trimethyl-lock makes the transfer of electrons more difficult. Although, quinone derivatives are harder to reduce when the trimethyl lock is present, its inclusion is fundamental to create quinones that can have a fast cyclization, as seen previously by in our group and by other research groups.^{24,27-30} In Figure 2.3, it is stated that an increase in buffer

concentration increases the cyclization rate but that no impact is seen when more salt is present into the solution. As shown in Table 2.3, quinone propionic acids without the presence of trimethyl lock had the slowest rate for the disappearance of the hydroquinone after reduction of the quinone moiety occurred. It is important to mention that the nature of the handle does not alter the reduction potential of the quinone as seen when comparing $Q_{Me}-COOH$ versus $Q_{Me}-ETA$. From our summarized results, I can conclude that halogen, hydrogen, methyl, and methoxy trimethyl-lock propionic acid quinones can be assayed against the human enzyme NQO1 without further concerns of non-enzymatic reduction with the aim of finding possible trigger-quinones for enzyme activation.

2.5 References

- (1) Bailey, S. I.; Ritchie, I. M., A Cyclic Voltammetric Study of the Aqueous Electrochemistry of Some Quinones. *Electrochim. Acta* **1985**, *30* (1), 3-12.
- (2) Goulart, M. O. F.; Hillard, E. A.; de Abreu, F. C.; Ferreira, D. C. M.; Jaouen, G.; Amatore, C., Electrochemical Parameters and Techniques in Drug Development, with an Emphasis on Quinones and Related Compounds. *Chem. Commun.* **2008**, (23), 2612-2628.
- (3) Ernster, L.; Ljunggren, M.; Danielson, L., Dt Diaphorase .1. Purification from Soluble Fraction of Rat-Liver Cytoplasm, and Properties. *Biochim. Biophys. Acta* **1962**, *58* (2), 171-188.
- (4) Ernster, L., Dt Diaphorase. *Methods Enzymol.* **1967**, *10*, 309-317.
- (5) Lind, C.; Cadenas, E.; Hochstein, P.; Ernster, L., Dt-Diaphorase: Purification, Properties, and Function. *Methods Enzymol.* **1990**, *186*, 287-301.
- (6) Tedeschi, G.; Chen, S.; Massey, V., Dt-Diaphorase - Redox Potential, Steady-State, and Rapid Reaction Studies. *J. Biol. Chem.* **1995**, *270* (3), 1198-1204.
- (7) Carlson, B. W.; Miller, L. L., Mechanism of the Oxidation of Nadh by Quinones - Energetics of One-Electron and Hydride Routes. *J. Am. Chem. Soc.* **1985**, *107* (2), 479-485.

- (8) Butler, J.; Hoey, B. M., The One-Electron Reduction Potential of Several Substrates Can Be Related to Their Reduction Rates by Cytochrome-P-450 Reductase. *Biochim. Biophys. Acta* **1993**, *1161* (1), 73-78.
- (9) Reipa, V., Direct Spectroelectrochemical Titration of Glutathione. *Bioelectrochemistry* **2004**, *65* (1), 47-49.
- (10) Ball, E. G., Studies on Oxidation-Reduction Xxiii. Ascorbic Acid. *J. Biol. Chem.* **1937**, *118* (1), 219-239.
- (11) Carpino, L. A.; Triolo, S. A.; Berglund, R. A., Reductive Lactonization of Strategically Methylated Quinone Propionic-Acid Esters and Amides. *J. Org. Chem.* **1989**, *54* (14), 3303-3310.
- (12) Nicholson, R. S.; Shain, I., Theory of Stationary Electrode Polarography - Single Scan and Cyclic Methods Applied to Reversible, Irreversible, and Kinetic Systems. *Anal. Chem.* **1964**, *36* (4), 706-723.
- (13) Nicholson, R. S., Semiempirical Procedure for Measuring with Stationary Electrode Polarography Rates of Chemical Reactions Involving Product of Electron Transfer. *Anal. Chem.* **1966**, *38* (10), 1406.
- (14) Carrier, N. H. Redox-Active Liposome Delivery Agents with Highly Controllable Stimuli-Responsive Behavior. Ph.D. Dissertation, Louisiana State University, Baton Rouge, LA, 2011.
- (15) Engstrom, R. C., Electrochemical Pretreatment of Glassy-Carbon Electrodes. *Anal. Chem.* **1982**, *54* (13), 2310-2314.
- (16) Mabbott, G. A., An Introduction to Cyclic Voltammetry. *J. Chem. Educ.* **1983**, *60* (9), 697-702.
- (17) Smith, D. K.; Quan, M.; Sanchez, D.; Wasylkiw, M. F., Voltammetry of Quinones in Unbuffered Aqueous Solution: Reassessing the Roles of Proton Transfer and Hydrogen Bonding in the Aqueous Electrochemistry of Quinones. *J. Am. Chem. Soc.* **2007**, *129* (42), 12847-12856.
- (18) Tommos, C.; Hay, S.; Westerlund, K., Redox Characteristics of a De Novo Quinone Protein. *J. Phys. Chem. B* **2007**, *111* (13), 3488-3495.

- (19) Rich, P. R., The Quinone Chemistry of Bc Complexes. *Bba-Bioenergetics* **2004**, 1658 (1-2), 165-171.
- (20) Novak, I.; Kovac, B., Electronic Structure of Substituted Benzoquinones and Quinonechloroimides. *J. Phys. Chem. A* **2008**, 112 (14), 3061-3065.
- (21) Silverman, J.; Stam-Thole, I.; Stam, C. H., Crystal and Molecular Structure of 2-Methyl-4,5-Dimethoxy Para Quinone (Fumigatin Methyl Ether), C₉H₁₀O₄. *Acta Cryst. B-Struc.* **1971**, B 27 (Oct15), 1846-1851.
- (22) Burie, J. R.; Boullais, C.; Nonella, M.; Mioskowski, C.; Nabadryk, E.; Breton, J., Importance of the Conformation of Methoxy Groups on the Vibrational and Electrochemical Properties of Ubiquinones. *J. Phys. Chem. B* **1997**, 101 (33), 6607-6617.
- (23) Friis, E. P.; Andersen, J. E. T.; Madsen, L. L.; Bonander, N.; Moller, P.; Ulstrup, J., Dynamics of Pseudomonas Aeruginosa Azurin and Its Cys3ser Mutant at Single-Crystal Gold Surfaces Investigated by Cyclic Voltammetry and Atomic Force Microscopy. *Electrochim. Acta* **1998**, 43 (9), 1114-1122.
- (24) Karaman, R., A New Mathematical Equation Relating Activation Energy to Bond Angle and Distance: A Key for Understanding the Role of Acceleration in Lactonization of the Trimethyl-Lock System. *Bioorg. Chem.* **2009**, 37, 11-25.
- (25) Wang, B.; Nicolaou, M. G.; Liu, S.; Borchardt, R. T., Structural Analysis of a Facile Lactonization System Facilitated by a "Trimethyl Lock". *Bioorg. Chem.* **1996**, 24 (1), 39-49.
- (26) Amsberry, K. L.; Borchardt, R. T., Amine Prodrugs Which Utilize Hydroxy Amide Lactonization .1. A Potential Redox-Sensitive Amide Prodrug. *Pharm. Res.* **1991**, 8 (3), 323-330.
- (27) Ong, W.; Yang, Y. M.; Cruciano, A. C.; McCarley, R. L., Redox-Triggered Contents Release from Liposomes. *J. Am. Chem. Soc.* **2008**, 130 (44), 14739-14744.
- (28) Amsberry, K. L.; Borchardt, R. T., The Lactonization of 2'-Hydroxyhydrocinnamic Acid-Amides: A Potential Prodrug for Amines. *J. Org. Chem.* **1990**, 55 (23), 5867-5877.
- (29) Milstien, S.; Cohen, L. A., Stereopopulation Control .1. Rate Enhancement in Lactonizations of Ortho-Hydroxyhydrocinnamic Acids. *J. Am. Chem. Soc.* **1972**, 94 (26), 9158-9165.

- (30) Caswell, M.; Schmir, G. L., Formation and Hydrolysis of Lactones of Phenolic-Acids. *J. Am. Chem. Soc.* **1980**, *102* (14), 4815-4821.

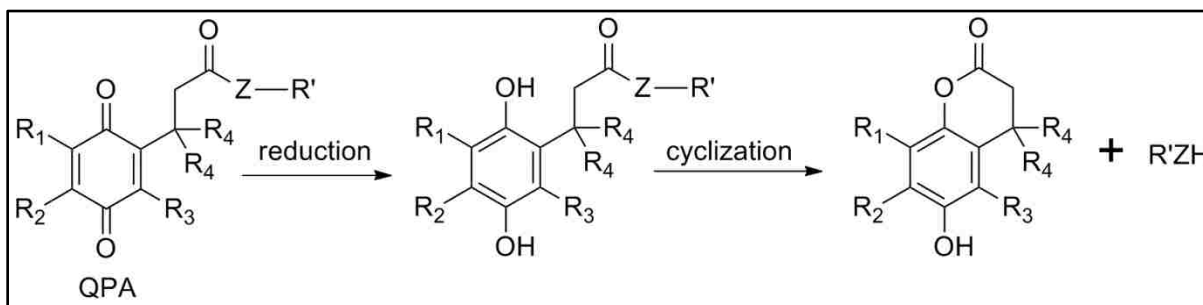
CHAPTER 3

TRIGGERABLE QUINONES ACTIVATED BY NAD(P)H:QUINONE OXIDOREDUCTASE TYPE I (NQO1) FOR POTENTIAL DRUG DELIVERY APPLICATIONS

3.1 Introduction

In the last two decades, there has been remarkable interest in the activation of drug delivery systems and cellular process by enzymes associated with inflammatory diseases and cancer.¹ The latter has been addressed in two ways: 1) using such endogenous, unregulated proteins to selectively activate antitumor compounds,² prodrugs,³⁻⁶ and very recently liposomes⁷⁻¹³ and 2) deactivating the enzyme which causes cell death through accumulation of damaged species, such as superoxide.¹⁴ Among the enzymes used as stimuli for these therapeutic routes, a significant research effort has been directed at a subgroup of reductase enzymes, of which NAD(P)H: quinone oxidoreductase-1 (NQO1, DT-diaphorase, EC 1.6.99.2)^{15,16} has become of great interest.¹⁷ This homodimeric flavoprotein is unique among reductases, as it catalyzes the direct two-electron reduction of a wide variety quinones using NADH or NADPH as cofactor¹⁵. NQO1 is located mainly in the cytosol of cells, but can also be found in the nucleus, endoplasmic reticulum, membrane and mitochondria, as well as extracellularly.^{15,18-24} The over-expression of human NQO1 in certain tumor tissues (e.g. non-small cell lung, pancreas and colon)²⁵⁻²⁹ makes it a valuable target for activating stimuli-responsive drug delivery systems based on quinone derivatives. As a result, many groups have been actively studying its molecular structure using crystallography methods so as to improve our understanding about its nature (e.g. human code 1D4A),³⁰ as well as its behavior with substrates or inhibitors (e.g. duroquinone-enzyme code 1DXO).³⁰⁻³⁵ Importantly, the ability of NQO1 to reductively activate sophisticated quinone and quinoidal compounds such as antitumor compounds³⁶ and prodrugs³⁷ has been studied a great deal in the past. However, the interaction of rhNQO1 with simple quinones or quinones useful for trigger groups in prodrugs and delivery vehicles, has to date not been studied.

Trigger groups that upon activation by a reductive stimulus are subsequently cleaved from a targeted group,⁶ hold much promise in the development of endogenously-triggered prodrugs and drug delivery vehicles, such as liposomes. Our group has shown that reductively-activated liposomes can have their contents delivered upon self-cleavage of the reduced quinone headgroup of the fusogenic lipids composing the liposomes.³⁸ The key step of this delivery process is the initial reduction of the cleavable quinone head group, which should be controlled by the structure of the trimethyl-locked quinone propionic acid trigger (QPA), Scheme 3.1.



Scheme 3.1. Reduction and cyclization process on quinone propionic acid triggers (QPA).

Variants of the QPA trigger groups have also been investigated for prodrugs, such those based on mustard³⁹ and oxindoles.⁴⁰ Tunability in the reductive triggering of QPA groups for either prodrug or liposome delivery applications will be achieved by substituent variation at R_1 , R_2 , and R_3 (Scheme 3.1). Although others groups have previously demonstrated that simple quinones can be tuned for better interaction with rat NQO1,⁴¹⁻⁴³ and there exist a good number of reports on structure-relationship activity⁴⁴⁻⁵¹ and docking studies of NQO1 inhibitors and substrates for anticancer therapy,^{14,32,52-56} there is little data in the literature for the interaction of simple quinones with recombinant human NQO1. Volpato *et al.* found that rhNQO1 activated an aromatic nitrogen mustard prodrug containing the QPA group with $R_1=R_2=R_3=R_4=CH_3$.³⁹ In this paper, we examine a good number of QPA derivatives as potential substrates for human NQO1. We report detailed solution-phase kinetic parameters, as well as molecular docking studies, to help understand how these quinones interact with hNQO1. Using the known crystal

structure of the hNQO1-duroquinone complex (1DXO),³⁰ six different receptors (changing interface radius, oxidation state of cofactor, and method to define active site) were defined. Quinone derivatives were docked in each receptor to see if there was any difference on the outcomes and to have a better prediction for the orientation of our quinones into the active site of hNQO1. Furthermore, we intended to correlate the experimental free energies extracted from the kinetic assays with the theoretical free energies from the docking studies.

3.2 Experimental Section

3.2.1 Materials

Recombinant human enzyme NAD(P)H:quinone oxidoreductase-1 (EC 1.6.99.2) (rhNQO1), nicotinamide adenine dinucleotide reduced (β -NADH) and bovine serum albumin (BSA) were purchased from Sigma (D1315, N8129, A3294). Potassium dihydrogen phosphate (KH_2PO_4 , Fluka 60219), dipotassium hydrogen phosphate (K_2HPO_4 , Fisher P288), potassium chloride (KCl, Sigma P9541) and potassium hydroxide pellets (KOH, Mallinckrodt) were used to make the buffer. Ethyl alcohol (200 Proof-Absolute-Anhydrous) was purchased from Pharmaco-AAPER. Nanopure water was obtained from a Nanopure Diamond Barnstead System (18.2 M Ω -cm). Quinone substrates were synthesized as previously described or as outlined in the Appendix.⁵⁷ The quartz 96-well microplate used in the enzyme assays was purchased from Hellma (730.009-QG). FLUOstar Optima plate reader from BMG Labtech was used to follow NADH consumption during the enzyme assay.

3.2.2 Enzyme Kinetic Assay

Enzyme activities were determined using UV-vis spectroscopy by adapting a previous assay⁵⁸ to a 96-well plate reader. The oxidation of NADH at 340 nm was measured using an experimental determined extinction coefficient of 4390 M⁻¹cm⁻¹ (Table A.1 and Figure A.1). Kinetic experiments were performed on three different days with at least three replicates of each condition performed. The assay solution consisted of 0.1 M PB/0.1 M KCl buffer solution at pH

7.10 containing 0.007% of bovine serum albumin, 100 μL of appropriate concentration of quinone substrate, 50 μL of a 400 μM NADH solution, and 50 μL of enzyme solution (0.11–3.00 μg). The total assay volume was 200 μL . All stock quinone solutions were prepared by dissolving each quinone in ethanol (100 μL) with subsequent dilution to 10.00 \pm 0.02 mL with 0.007% BSA solution. Quinone solutions of the desired concentrations were made by taking the appropriate volume from the quinone stock solution and diluting it to 10.00 \pm 0.02 mL in a volumetric flask. The solutions were kept at room temperature (22 \pm 2 $^{\circ}\text{C}$), in the dark, for approximately 2 hours before the experiments were started. Once the 96-well plate was filled with the assay solutions, except the NADH solution, it was placed into the instrument and left to sit for 5 min before starting the measurements. The enzyme reaction was started by automated dispensing of the NADH solution, and the absorbance change at 340 nm was measured for 1.6 min at room temperature (22 to 26 $^{\circ}\text{C}$). The linear portion of the absorbance vs. time graphs (the first 20 seconds to 1 min) were fitted and slopes were calculated. The average slopes from the replicates was used to calculate the kinetic parameters, with the Q-test being applied so as to reject values outside of the 90% confidence level.⁵⁹ Plots of velocity versus quinone concentration were used to obtain K_m and V_{max} values from non-linear least squares analysis.⁶⁰ T-test was applied to the close values in the kinetic parameters so as to see if they were statistically different at the 95% confidence level.⁶¹ Due to instrument sensitivity, quinones with K_m values lower than 15 μM could only be estimated.

3.2.3 Molecular Docking

Docking studies were performed using FlexX from LeadIT (1.3.0 version).⁶²⁻⁶⁹ Quinone structures were prepared in Chemdraw3D and subsequently minimized using Sybyl-X (Version 1.1.1) using the Tripos force field for suitable bond distances and angles and the Gasteiger-Hückel method for charge calculation. Enzyme coordinates used in the FlexX software were obtained from The Protein Data Bank (code: 1DXO). A molecular visualization system called

PyMOL was used to prepare the docking frames. Construction of six different receptors was done with the FlexX software by selecting the active site containing amino acids from monomer A and C of the enzyme crystal structure. Two water molecules were present in each of the receptors. Receptor 1 includes FAD (as it is in the X-ray coordinates) as a cofactor with duroquinone as the reference ligand (X-ray coordinates edited by FlexX for correct atom hybridization and bond type) and the binding site is defined within an interface of 6 Å encompassing the reference ligand. Receptor 2 includes FADH₂ (FAD X-ray coordinates modified) as a cofactor with duroquinone as the reference ligand (X-ray coordinates edited by FlexX for correct atom hybridization and bond type) and the binding site is defined within an interface of 6 Å encompassing the reference ligand. Receptor 3 is the same as Receptor 1 but has an interface radius of 8 Å. Receptor 4 is the same as Receptor 2 but has an interface radius of 8 Å. Receptor 5 includes FAD as a cofactor with the active site defined by a sphere of 8.5 Å with N5 from FAD as its center. Receptor 6 includes FADH₂ as a cofactor with the active site defined by a sphere of 8.5 Å with N5 from FADH₂ as its center.

In FlexX flexible docking calculations, the initial position of the substrate is outside the active site. Then, an algorithm for fragmenting the quinone substrate is executed, and a base fragment is automatically selected and placed in the active site on which an incremental construction algorithm is performed. From these calculations, each substrate examined using different receptors, has a set of solutions where the closest poses (based on score, position and interactions with the protein) were selected for detailed investigation. On these selected poses, the influence of the cofactor state (oxidized FAD or reduced FADH₂ form), receptor radius, and the inclusion or not of a reference ligand was studied. In addition, the total score was used as an estimate of the free energy of binding and was subsequently used to plot theoretical free energies of binding versus experimental free energies of binding ($\Delta G = -RT \ln K_m$).⁶³

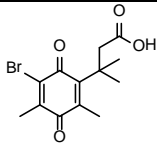
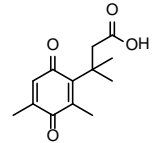
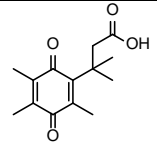
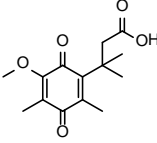
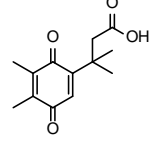
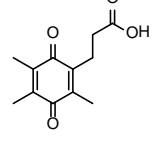
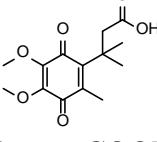
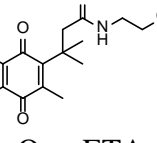
The docking method is based on the experimental observed range of nonbonded contact geometries revealed by statistical analysis of the Cambridge Structural Database (CSD), the analysis of the CSD is used to define the range of allowed angles and dihedrals describing the nonbonded contact geometry.⁷⁰ The program discards any solution with electrostatic repulsion (based on a threshold limit distance). The scoring function accounts for hydrogen bonds, ionic interactions, hydrophobic contact surface, and the number of rotatable bonds in the substrate. The limitations of the scoring function is that it does not account for differences in binding strengths between various neutral hydrogen bonds or ionic interactions, and it does not include the conformational energy of the substrate.^{63,70} The FlexX algorithm breaks down the substrate into fragments where one is automatically elected as the base fragment,⁶⁶ and then the fragments are connected flexibly during docking in an incremental way.⁶⁵ In the triangle algorithm, triangles of interaction centers are formed using the base fragment, and those are mapped onto triangle points lying on the receptor's surface. As an alternative to the triangle algorithm, a line algorithm is used when only two interactions exist simultaneously between the substrate and the enzyme. The receptor is rigid and the ligand is flexible for both algorithms. The scoring function is a modification of Böhm's function.⁶⁶⁻⁶⁸

3.3 Results and Discussion

3.3.1 Kinetic Studies on Triggerable Quinones

All the rhNQO1 kinetic parameters for the different quinone derivatives studied here are presented in Table 3.1. To compare our data, we divided our complete list of quinone derivatives into 3 groups: a) changing the substituents at the 2-position (R_1) on the quinone ring for the trimethyl lock series ($R_3=R_4=CH_3$), b) presence versus absence of the trimethyl lock system, and c) charged versus neutral quinone propionic acid.

Table 3.1. Kinetic parameters for the reduction of quinone derivatives by hNQO1. Values are the mean \pm one standard deviation for three independent determinations.

Quinone	K_m (μM)	V_{max} ($\mu\text{mol}\cdot\text{min}^{-1}\cdot\text{mg}^{-1}$ of hNQO1)	k_{cat} (min^{-1})	k_{cat}/K_m ($\text{min}^{-1}\cdot\mu\text{M}^{-1}$)
 Q_{Br}-COOH	41 \pm 8	88 \pm 7	5500 \pm 400	133 \pm 28
 Q_H-COOH	50 \pm 11	83 \pm 8	5100 \pm 500	103 \pm 25
 Q_{Me}-COOH	158 \pm 41	38 \pm 5	2400 \pm 300	15 \pm 4
 Q_{MeO}-COOH	447 \pm 102	42 \pm 5	2600 \pm 300	6 \pm 1
 Q[']-COOH	20 \pm 3	78 \pm 3	4800 \pm 200	242 \pm 37
 Q_{nogemMe}-COOH	5 \pm 1	66 \pm 4	4100 \pm 200	853 \pm 178
 Q_{diMeO}-COOH	376 \pm 87	14 \pm 1	800 \pm 100	2 \pm 0.5
 Q_{Me}-ETA	132 \pm 32	60 \pm 7	3700 \pm 400	28 \pm 7

- Changing the Substituent at the 2-position on the Quinone Ring–Trimethyl Lock Series.

We obtained the kinetic parameters for four quinones that differ in their functional group at the 2-position on the quinone ring (bromine, hydrogen, methyl, methoxy). Of this group, Q_{Br}-COOH (R₁=Br) and Q_H-COOH (R₁=H) appear to be the best substrates based on its K_m , V_{max} and k_{cat}/K_m values. The Michaelis constant values of $K_m = 41 \mu\text{M}$ (Q_{Br}-COOH) and $K_m = 50 \mu\text{M}$ (Q_H-COOH), as well as, the maximum velocity values of $V_{max} = 88 \mu\text{mol}\cdot\text{min}^{-1}\cdot\text{mg}^{-1}$ (Q_{Br}-COOH) and $V_{max} = 83 \mu\text{mol}\cdot\text{min}^{-1}\cdot\text{mg}^{-1}$ (Q_H-COOH) were found to be statistically equal at the 95% confidence level. Both Q_{Br}-COOH and Q_H-COOH are efficient substrates for rhNQO1, based on their k_{cat}/K_m values of $133 \text{ min}^{-1}\cdot\mu\text{M}^{-1}$ and $103 \text{ min}^{-1}\cdot\mu\text{M}^{-1}$, respectively. In the case of Q_{Me}-COOH, there are two clear effects on the kinetic parameters as a consequence of the presence of a methyl group at the 2-position of the quinone ring. First, the presence of the methyl group increases the electron density of the quinone core (due to its electron donating character) possibly making the analog less wishful to accept the electrons that come from the enzyme cofactor FADH₂. Second and more prominent, the methyl substituent causes steric interactions between the quinone ring and the hNQO1 active site, resulting in an unfavorable alignment and position of the quinone, causing lower binding, thus lowering the reduction rate. Steric hindrance at R₁ position on the quinone ring has been previously observed to be an important factor in changing the rate of reduction between human NQO1 and structures such as indolequinones and benzoquinone mustard compounds.^{48,51,56} Lastly, Q_{MeO}-COOH has a very similar turnover rate compared to its methyl analog, and even though the methoxy group has a higher electron-donating ability, the alignment of this group with respect to the quinone ring reduces its power and make it behaves as a methyl. The alignment distortion is caused by the methyl group at the 3-position of the quinone ring, because when a hydrogen is placed instead, the methoxy group adopt a coplanar conformation with the quinone ring that permits fully contribution of the electron density.^{71,72} However, the K_m value of the Q_{MeO}-COOH differs from

that of its methyl analog because the methoxy group is a bulkier substituent than methyl. Consequently, steric interactions between the quinone and the hNQO1 active site, lead to decreased $Q_{\text{MeO-COOH}}$ binding affinity, resulting in it being the worst substrate for hNQO1 in this series. To complete the enzyme kinetic analysis of different functional groups at R_1 position on the quinone rings, attempts were made to investigate $Q_{\text{Me-N-COOH}}$ and $Q_{\text{n-pr-NH-COOH}}$ responses toward rhNQO1 but the results obtained are not reliable because both substrates absorb at the wavelength (340 nm) that NADH consumption is measured.

- Special Note to $Q_{\text{diMeO-COOH}}$.

Although this analog possesses the trimethyl-lock structural motif, $Q_{\text{diMeO-COOH}}$ does not fall into the category discussed above, because it does not have a methyl group at the 3-position on the quinone ring. However, it was synthetically readily achievable and so it was investigated. The presence of one more methoxy group versus $Q_{\text{MeO-COOH}}$ does not alter the K_m value, which are statistically equal. However, the V_{max} value of $Q_{\text{diMeO-COOH}}$ is 1/3 times that of the quinone with only one methoxy group, $Q_{\text{MeO-COOH}}$ ($V_{\text{max}}=42 \mu\text{mol}\cdot\text{min}^{-1}\cdot\text{mg}^{-1}$). The cause associated with the rate difference, may be the presence of adjacent methoxy groups in the $Q_{\text{diMeO-COOH}}$ analog. It has been reported before that when methoxy groups are in adjacent locations on the quinone ring, one of them is coplanar to the quinone ring, and the other one is not.^{71,72} Therefore, the quinone ring will receive full electron density contribution from the coplanar methoxy group making the quinone not as happy to receive electrons. Moreover, the steric hindrance caused by the second methoxy group, which is a bulkier group than a methyl at R_2 position on the quinone ring, could also affect the reduction rate of the quinone by hNQO1.

- The Presence *versus* the Absence of the Trimethyl-Lock Motif in the Quinone.

$Q_{\text{Br-COOH}}$, $Q_{\text{H-COOH}}$, $Q_{\text{Me-COOH}}$ and $Q_{\text{MeO-COOH}}$ all contain the trimethyl-lock motif, whereas $Q^{\cdot}\text{-COOH}$ and $Q_{\text{nogemMe-COOH}}$ do not. All quinone structures are shown in Table 3.1. In $Q^{\cdot}\text{-COOH}$, a hydrogen is present (instead of a methyl) at the 5-position on the

quinone ring and its observed Michaelis constant of 20 μM , it is substantially lower than that of $\text{Q}_{\text{Me}}\text{-COOH}$ that possesses the trimethyl-lock motif (158 μM). In addition, $\text{Q}_{\text{H}}\text{-COOH}$ and $\text{Q}'\text{-COOH}$, both have a hydrogen group on the quinone ring but the difference in position of that hydrogen at R_1 and R_3 , respectively, make QH-COOH a trimethyl-lock derivative and $\text{Q}'\text{-COOH}$ not. This difference is reflected on the K_{m} value of 50 μM for QH-COOH and 20 μM for $\text{Q}'\text{-COOH}$, resulting the last one a better substrate toward the hNQO1 enzyme. This change in affinity can be explained by the ease of the trimethyl-lock strain when hydrogen is placed on the quinone ring on the same side as the propionic acid chain. To further probe the effect of the trimethyl-lock motif, a quinone with no germinal methyl groups on the propionic side chain was examined, $\text{Q}_{\text{nogemMe}}\text{-COOH}$. It was found that $\text{Q}_{\text{nogemMe}}\text{-COOH}$ was even more specific toward the enzyme, as stated by its K_{m} value of roughly 5 μM (K_{m} values lower than 15 μM could only be estimated).

- The Role of Charged Quinone *versus* Neutral Quinone.

To investigate the effect of a neutral quinone in the active site, versus a negatively-charged quinone, we studied a quinone with an ethanolamine ($\text{Q}_{\text{Me}}\text{-ETA}$) attached to the propionic acid group via an amide bond (with a $\text{p}K_{\text{a}}$ around 10)⁷³ and compared its hNQO1 values obtained for the $\text{Q}_{\text{Me}}\text{-COOH}$ that is anionic at physiological pH.⁷⁴ $\text{Q}_{\text{Me}}\text{-ETA}$ presents a higher maximum velocity; however, the Michaelis constant values (K_{m}) are statistically equal, therefore, no significant difference is presented in binding affinity. The increase of 22 $\mu\text{mol}\cdot\text{min}^{-1}\cdot\text{mg}^{-1}$ in maximum velocity for the $\text{Q}_{\text{Me}}\text{-ETA}$ could be due to the absence of charge on the molecule or to the longer extended chain that $\text{Q}_{\text{Me}}\text{-ETA}$ presents, that permits a different arrangement of the quinone-ethanolamine derivative into the active site of the enzyme. This hypothesis will be later discussed by analysis of the docking outcomes.

3.3.2 Docking Studies on Triggerable Quinones

In order to validate the docking methods used for the various quinone propionic acids, we examined docking results for duroquinone. It was found that excellent results were achieved with all of the receptors, with an observed root mean square deviation (RMSD) $< 0.5 \text{ \AA}$ for the best prediction and a RMSD $< 1.34 \text{ \AA}$ for the lowest score. In all of these outcomes, it was found that the orientation of the duroquinone was very similar, with differences of less than $1.2 \text{ kJ}\cdot\text{mol}^{-1}$ from the lowest energy to the 20th lowest energy in each receptor. In Figure 3.1, the best pose for duroquinone is shown and compared with the original crystal structure.

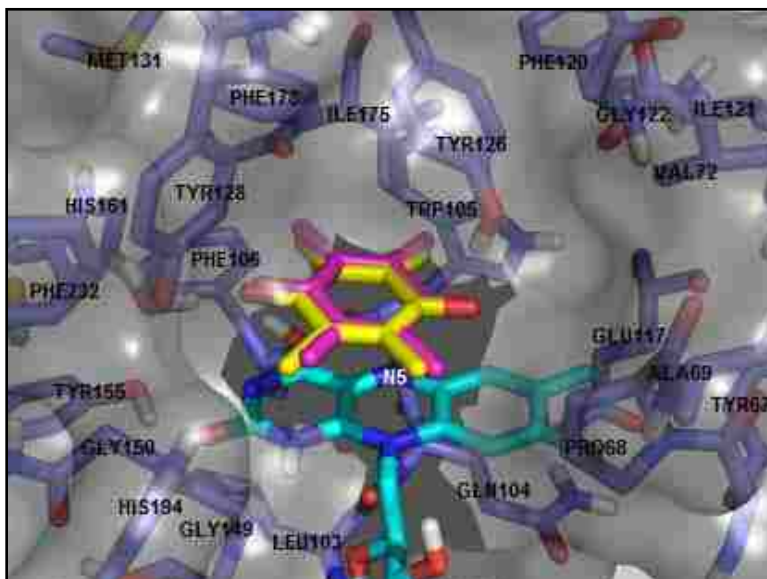
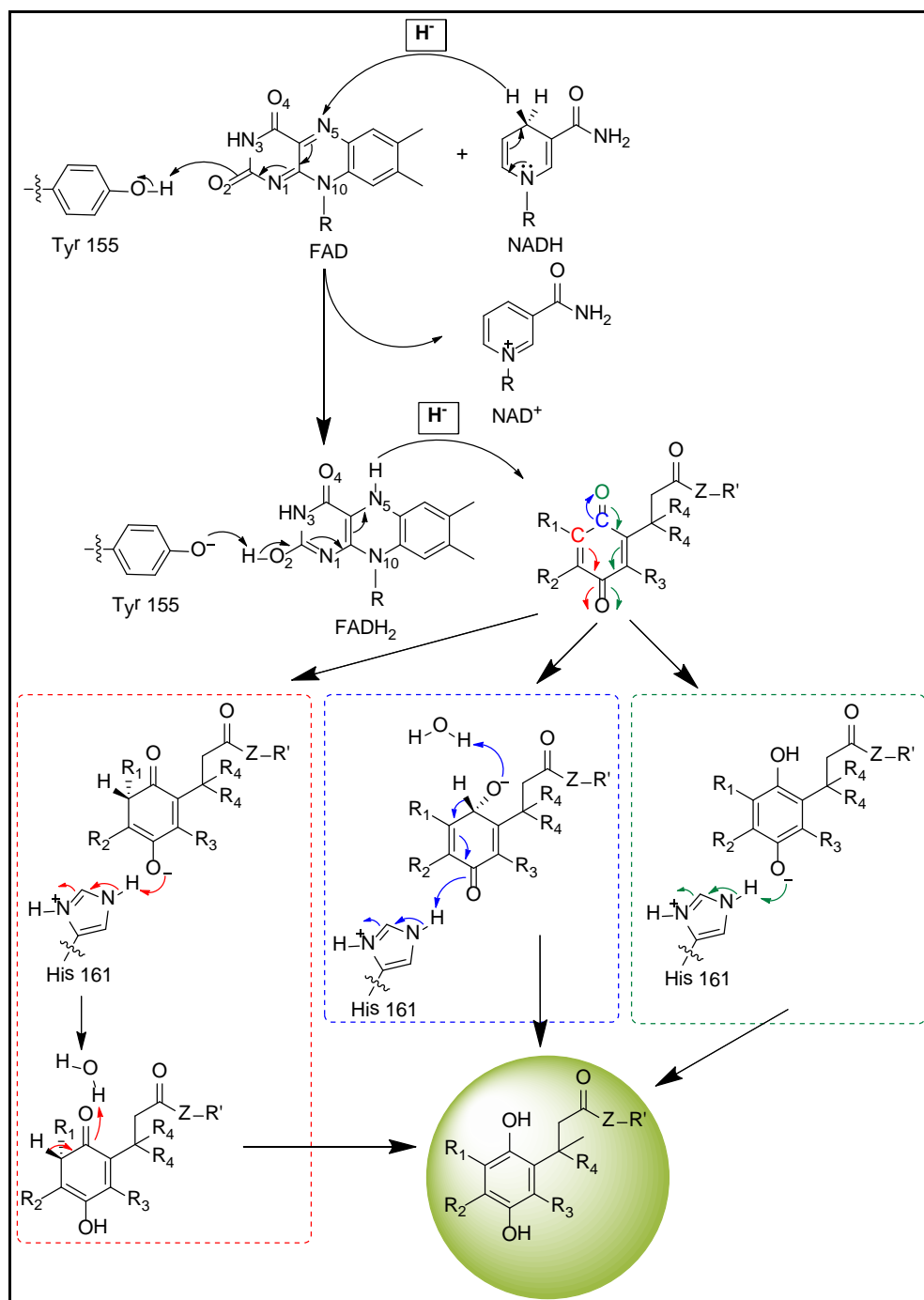


Figure 3.1. Best prediction for the docked duroquinone in receptor 1 compared with the position of the duroquinone in the original crystal structure. Docked duroquinone (pink) differ from the original duroquinone (yellow) by 0.4530 \AA . Representation of amino acids (stick display; color by atom type, carbon atoms colored in purple) and FAD (sticks display; color by atom type, carbon atoms colored in cyan) in receptor 1.

- Which Receptor Gives the Best Prediction?

In docking, the way in which a receptor is defined affects in different ways the predictions of substrate interactions. It is important to know what amino acids are to be included (defined by the radius of interaction), and the cofactor oxidation state must also be selected. For the catalyzed NQO1 reduction of quinones with NADH, there is still much debate as to where

the negative charge stays after the first hydride transfer happens. The most prominent proposal is that in which the negative charge stays on O2 and then this oxygen gets protonated to become an OH and the hydride is transferred to form FADH₂.^{37,75,76} Scheme 3.2 represents the charge relay process and the possible atom sites on the quinone moiety where the hydride can be transferred to.



Scheme 3.2. Hydride transfer mechanism on all possible atom sites on QPAs.

There are also concerns about the geometry of FAD versus FADH₂ and how the protonation can affect its conformation. In the literature, it is reported that the conformation of FADH₂ changes to a butterfly-like shape in solution (versus planar for FAD), but in most modeling structures FADH₂ retains its planar conformation.^{30,75} To elucidate the possible influence of all these factors on the computed interactions between the QPAs and hNQO1, a variety of receptors were defined and evaluated. All the QPAs tested in the kinetic assays were docked in the active site of hNQO1. In addition, the QPA amine derivatives, Q_{N-Me}-COOH and Q_{n-pr-NH}-COOH, were also docked in the active site of hNQO1 with the aim of predicting their position and binding energy because of the lack of kinetic data for them.

- FAD (Oxidized) *versus* FADH₂ (Reduced).

The outcome solutions from docking the quinone analogs in different receptors, having the active site FAD or FADH₂ as cofactor, were examined. For this, we compared the results from receptor 1 versus receptor 2, receptor 3 versus receptor 4, and receptor 5 versus receptor 6. In all cases, the positions of the quinones were the same. The only slight difference was the energy score. For the lowest energy score a slight increase of 0.6 kJ·mol⁻¹ was observed for the outcome solution of the receptor containing FAD versus the receptor containing FADH₂ and for the best prediction energy the increase was of 0.8 kJ·mol⁻¹.

- Interface Radius of 6 Å *versus* Interface Radius of 8 Å.

The binding conformations of the quinone analogs were examined where the only difference was the interface radius of the active site. We compared receptor 1 versus receptor 3 and receptor 2 versus receptor 4. In this case, the orientation of the quinone analogs in all the receptors mentioned above were the same, and the outcome solution with the lowest score energy for the duroquinone in each receptor differ by only 1 kJ·mol⁻¹.

- Defining Active Site (Reference Ligand *versus* Sphere).

The binding conformations of the quinone analogs were examined by defining the active site differently. In the case of receptor 3 and 4, the ligand bound to the enzyme was used as reference ligand (duroquinone) and had an interface radius of 8 Å defined from its position. In the case of receptor 5 and 6, the nitrogen N5 from the cofactor FAD or FADH₂ was used as the sphere center and had an interface radius of 8.5 Å defined from it. We compared receptor 3 versus receptor 5 and receptor 4 versus receptor 6. In these scenarios, the outcome with the lowest score and the best prediction differ in their orientations only for duroquinone but not for the other quinone analogs. However, the outcome for the lowest energy value and the one associated with the best orientation is different for all of the quinones. The lower energy score is smaller by 1 kJ·mol⁻¹ in the receptors where the active site is defined by the 8.5 Å radius sphere. The best prediction corresponds to the quinone located deeper in the receptors 5 and 6. In this case the energy is 0.6 kJ·mol⁻¹ lower than in receptors 3 and 4. We conclude that in this case for quinone analogs, even though there is a difference in score energy, this difference is minimal and does not affect the outcome. Therefore, there is no apparent effect of active site definition on quinone positions or score energies.

After comparing all the receptors, we observed that there is no effect of the oxidation state of the cofactor or of the interface radius in the docking outcomes. There is little influence on the docking solutions when the active site was defined in different ways. While the observed difference in the docking outcomes was major for duroquinone, the rest of the quinone analogs were unaffected. In Figures A.5 and A.6 are represented the lower score frame of Q_{Br}-COOH (representative example of outcomes for all of the quinone analogs) in each of the receptors, and its corresponding poseview so as to help to visually support the conclusions made above. These conclusions are also based on data in Table A.2 that contains the lowest score energies for Q_{Br}-COOH in all the receptors.

The docking solutions of receptor 1 were used to compare the quinone analogs among themselves, and those outcomes are an accurate representation of what happened in all the receptors, Figure 3.2.

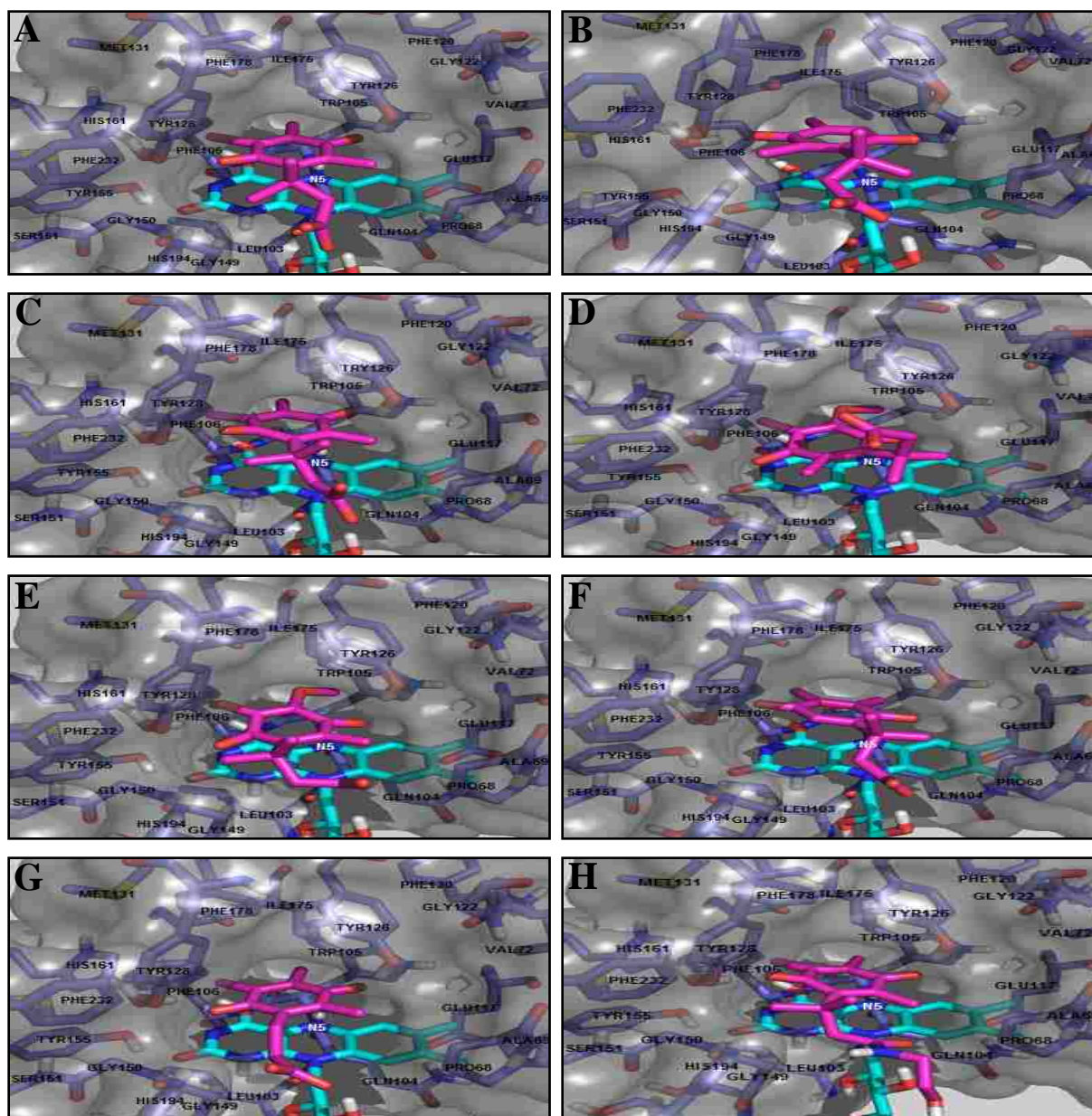
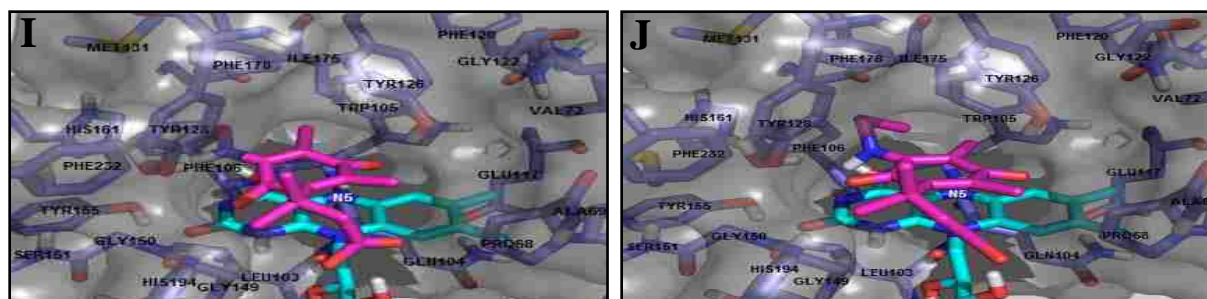


Figure 3.2. Structural frames of FlexX-docked quinones in the active site of *hNQO1*. Stick display in all the frames, FAD (color by atom type; carbon atoms colored in cyan), amino acids (color by atom type, carbon atoms colored in purple) and docked-quinones (color by atom type, carbon atoms in pink): (A) $Q_{Br-COOH}$, (B) Q_{H-COOH} , (C) $Q_{Me-COOH}$, (D) $Q_{MeO-COOH}$, (E) $Q_{diMeO-COOH}$, (F) $Q'-COOH$, (G) $Q_{nogemMe-COOH}$, (H) Q_{Me-ETA} , (I) $Q_{(Me-N)-COOH}$, and (J) $Q_{(n-pr-NH)-COOH}$.

Figure 3.2 continued.



It was observed that Q_{Br} -COOH, Q_H -COOH and Q_{Me} -COOH all lay parallel to the isoalloxazine ring of the FAD cofactor, but the carbon site of the quinone for the possible hydride transfer is different due to the slight variance in the binding orientation with respect to FAD. In the case of the methoxy and amine quinone derivatives, they do not bind as tightly as the other quinone analogs. The obvious possible explanation for this is that the bulky substituents on the ring need more space, thereby preventing these analogs from venturing as deeply into the active site. Other research groups reported in the past that a bulky amine at 2-position of the quinone ring for indolequinones and quinolinequinones, decreased tremendously the reduction rate of these compounds with hNQO1 making them not a good substrate for this enzyme.^{46,47,49}

Furthermore, the theoretical binding energies from these docking outcomes were used in an attempted correlation with the experimental binding affinities. The experimental binding energies were calculated using the free energy equation $\Delta G = RT \ln K$,⁶³ so as to plot $|\Delta G$ (experimental)| versus $|\Delta G$ (theoretical)|. To our disappointment, there was no clear correlation between these values (Figure A.7). However, this is not surprising based on the controversy that exist in the literature about whether or not docking binding energies can be correlated with experimental reactivity.^{35,53-55,77} In addition, other attempts were made to correlate reactivity with the information extracted from the docking outcomes. The only correlation observed was the one between the log (atom distance) and the log (k_{cat}/K_m) as seen in Figure 3.3. The atom distance corresponds to the distance between the closer atom on the quinone ring and the N5

atom of FAD. This correlation indicates that the closer the atoms on the quinone are to receive a hydride from the N5 of FAD, the more reactive the quinone derivative will be with hNQO1. Based on this observation, the reactivity of the amine derivatives with hNQO1 should be similar to the one observed for the methoxy analogs.

Energy results for the more accurate score of each quinone and the distance from N5 of the FAD center in hNQO1 to the possible hydride transfer atoms of the quinone substrates⁷⁸ are presented in Table 3.2. It can be deduced that the hydride transfer for most of the quinones will be accepted by the carbon atom, except in the case of the quinones containing methoxy groups where the orientation favors a hydride transfer to the carbonyl oxygen. In the case of the amine-quinone derivatives, no conclusion can be made because the preferred site for Q_(N-Me)-COOH is the oxygen and the preferred site for Q_(n-pr-NH)-COOH is the carbon.

Table 3.2. Energy score and distance from N5 of FAD to the possible hydride transfer atoms. Atoms closer in distance to N5 are highlighted in red.

Quinone	Score (kJ·mol ⁻¹)	d [N5-C](Å)	d [N5-C=O](Å)	d [N5-O](Å)
Q _{Br} -COOH	- 25.2018	3.25	3.47	3.58
Q _H -COOH	- 24.0028	3.40	4.11	4.50
Q _{Me} -COOH	-26. 4276	3.58	3.54	3.71
Q _{MeO} -COOH	-20.3317	3.83	3.90	3.50
Q _{diMeO} -COOH	-28.3849	4.05	4.05	3.68
Q'-COOH	-26.9646	3.18	3.81	3.92
Q _{nogemMe} -COOH	-25.8435	3.22	3.49	3.68
Q _{Me} -ETA	-28.4801	3.43	3.73	3.81
Q _(N-Me) -COOH	-24.8434	3.95	3.90	3.45
Q _(n-pr-NH) -COOH	-20.9808	3.68	4.36	4.32

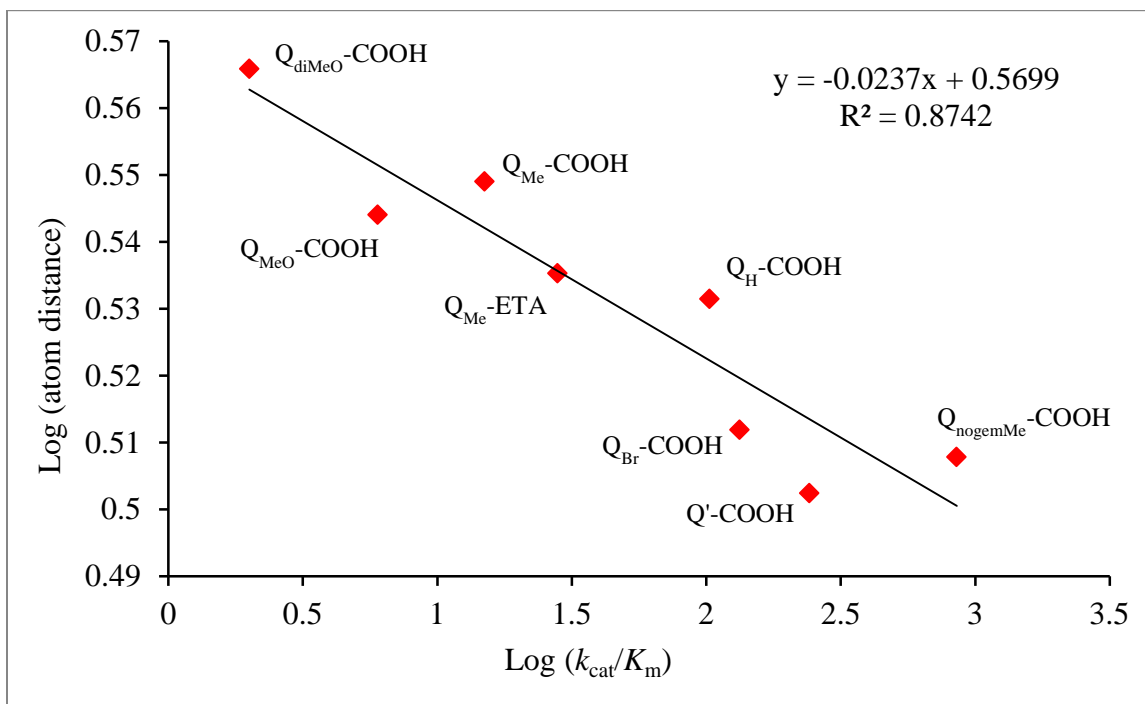


Figure 3.3. Correlation between the log (distance of the closer atom on the quinone ring with respect to N5 of FAD) and the log (k_{cat}/K_m).

Superimposed images of the quinones containing trimethyl-lock motif (Figure A.2), quinones with the trimethyl-lock motif present and absent (Figure A.3) and quinones differing on the molecule charge (Figure A.4), were prepared to see if there was any correlation between the kinetic results and the docking studies. In Figure A.2, it was found that $Q_{Br}-COOH$ holds the deepest location into the active site, whereas $Q_{MeO}-COOH$ penetrates the least deep. These observations are in accordance with the kinetic data for these quinone series. In Figure A.3, $Q_{nogemMe}-COOH$ is the closest to the FAD and $Q_{Me}-COOH$ the one located further from the isoalloxazine ring. These observations agree with the order of reactivity of these compounds with hNQO1. In Figure A.4, the longer chain present in the $Q_{Me}-ETA$ permits the quinone to accede to a deeper location in the active site of the enzyme. This could be the cause for the increase of $22 \mu\text{mol}\cdot\text{min}^{-1}\cdot\text{mg}^{-1}$ in maximum velocity for the $Q_{Me}-ETA$.

3.4 Conclusions

In conclusion, we studied the reduction of eight quinone derivatives by human recombinant NQO1 using a 96-well microplate enzyme assay and obtained kinetic parameters K_m and V_{max} having excellent reproducibility. Minor alterations in structure resulted in significant changes in the kinetic parameters; for example $Q_{Br}-COOH$ is much more active at a low concentration than is $Q_{Me}-COOH$, and so is the case for $Q_{Me}-COOH$ versus $Q_{MeO}-COOH$, and $Q_{MeO}-COOH$ versus $Q_{diMeO}-COOH$. $Q_{Br}-COOH$ appears to be the preferred substrate among the quinones containing the trimethyl-lock system based on its higher k_{cat}/K_m value of $133 \text{ min}^{-1}\cdot\mu\text{M}^{-1}$. It is also notable that sterics seems to predominate over electronic effects among the trimethyl-lock series, an outcome similar in nature for the benzoquinone mustards.^{48,51} As far as the best substrate in Table 3.1, the quinone without the geminal methyls is the most efficient of all with the highest product formation at small concentration of reactant ($k_{cat}/K_m = 853 \text{ min}^{-1}\cdot\mu\text{M}^{-1}$). This conclusion guides us to believe that the presence of the trimethyl-lock affects the geometry of the quinone ring, which has somewhat of an effect on the interaction of the quinone with the active site of the enzyme.

The docking studies completed on ten quinone derivatives suggested that small modifications of the quinone core alter the ability of the quinone to be reduced by the enzyme, results that are in agreement with those of indolequinones.⁵⁶ Based on the kinetic and modeling studies with the QPAs, hNQO1 can accommodate a range of quinones having characteristics binding affinities. The unsuccessful correlation between experimental binding energy versus theoretical binding energy makes us think that, in order to quantitatively analyze the influence of a functional group in the quinone core, experimental assays are required. However, we were able to qualitatively visualize the different positions of the quinone trimethyl-lock series in the active site, and our results are in qualitative agreement with the experimental binding values (strongest toward weakest $Q_{Br} > Q_H > Q_{Me} > Q_{MeO}$). In the same manner, we obtained the same

qualitative correlation for quinones either containing or lacking the trimethyl-lock ($Q_{\text{no gemMe}} > Q' > Q_{\text{Me}}$). Lastly, docking and kinetics studies revealed that the presence of a longer side chain attached to the quinone (i.e. $Q_{\text{Me}}\text{-ETA}$ versus $Q_{\text{Me}}\text{-COOH}$) can cause the quinone core to penetrate deeper into the active site. This suggest that addition of spacers to the quinone derivatives⁷⁹ may increase quinone-enzyme binding and perhaps the enzyme rate of conversion.

The combination of the experimental kinetic and theoretical docking data support our predictions: changing functional groups on the quinone ring affects how deep the quinone is located in the active site of the enzyme, and this difference in position has consequences on the binding affinity and on the hydride transfer rate. Overall, this analysis will enrich the knowledge for simple quinones and hNQO1 interactions, providing valuable information for the design of enzyme triggerable systems.

3.5 References

- (1) Andresen, T. L.; Jensen, S. S.; Jorgensen, K., Advanced Strategies in Liposomal Cancer Therapy: Problems and Prospects of Active and Tumor Specific Drug Release. *Prog. Lipid Res.* **2005**, *44* (1), 68-97.
- (2) Asche, C., Antitumour Quinones. *Mini-Rev. Med. Chem.* **2005**, *5* (5), 449-467.
- (3) de Groot, F. M. H.; Damen, E. W. P.; Scheeren, H. W., Anticancer Prodrugs for Application in Monotherapy: Targeting Hypoxia, Tumor-Associated Enzymes, and Receptors. *Curr. Med. Chem.* **2001**, *8* (9), 1093-1122.
- (4) Jaffar, M.; Abou-Zeid, N.; Bai, L.; Mrema, I.; Robinson, I.; Tanner, R.; Stratford, I. J., Quinone Bioreductive Prodrugs as Delivery Agents. *Curr. Drug Delivery* **2004**, *1*, 345-350.
- (5) Rooseboom, M.; Commandeur, J. N. M.; Vermeulen, N. P. E., Enzyme-Catalyzed Activation of Anticancer Prodrugs. *Pharmacol. Rev.* **2004**, *56* (1), 53-102.
- (6) Chen, Y.; Hu, L. Q., Design of Anticancer Prodrugs for Reductive Activation. *Med. Res. Rev.* **2009**, *29* (1), 29-64.

- (7) Davis, S. C.; Szoka, F. C., Cholesterol Phosphate Derivatives: Synthesis and Incorporation into a Phosphatase and Calcium-Sensitive Triggered Release Liposome. *Bioconjugate Chem.* **1998**, *9* (6), 783-792.
- (8) Davidsen, J.; Vermehren, C.; Frokjaer, S.; Mouritsen, O. G.; Jorgensen, K., Drug Delivery by Phospholipase a(2) Degradable Liposomes. *Int. J. Pharm.* **2001**, *214* (1-2), 67-69.
- (9) Jorgensen, K.; Davidsen, J.; Mouritsen, O. G., Biophysical Mechanisms of Phospholipase A2 Activation and Their Use in Liposome-Based Drug Delivery. *FEBS Lett.* **2002**, *531* (1), 23-27.
- (10) Davidsen, J.; Jorgensen, K.; Andresen, T. L.; Mouritsen, O. G., Secreted Phospholipase a(2) as a New Enzymatic Trigger Mechanism for Localised Liposomal Drug Release and Absorption in Diseased Tissue. *Biochim. Biophys. Acta* **2003**, *1609* (1), 95-101.
- (11) Meers, P., Enzyme-Activated Targeting of Liposomes. *Advanced Drug Delivery Reviews* **2001**, *53* (3), 265-272.
- (12) Sarkar, N.; Banerjee, J.; Hanson, A. J.; Elegbede, A. I.; Rosendahl, T.; Krueger, A. B.; Banerjee, A. L.; Tobwala, S.; Wang, R. Y.; Lu, X. N.; Mallik, S.; Srivastava, D. K., Matrix Metalloproteinase-Assisted Triggered Release of Liposomal Contents. *Bioconjugate Chem.* **2008**, *19* (1), 57-64.
- (13) Banerjee, J.; Hanson, A. J.; Gadam, B.; Elegbede, A. I.; Tobwala, S.; Ganguly, B.; Wagh, A. V.; Muhonen, W. W.; Law, B.; Shabb, J. B.; Srivastava, D. K.; Mallik, S., Release of Liposomal Contents by Cell-Secreted Matrix Metalloproteinase-9. *Bioconjugate Chem.* **2009**, *20* (7), 1332-1339.
- (14) Reigan, P.; Colucci, M. A.; Siegel, D.; Chilloux, A.; Moody, C. J.; Ross, D., Development of Indolequinone Mechanism-Based Inhibitors of Nad(P)H : Quinone Oxidoreductase 1 (Nqo1): Nqo1 Inhibition and Growth Inhibitory Activity in Human Pancreatic Mia Paca-2 Cancer Cells. *Biochemistry* **2007**, *46* (20), 5941-5950.
- (15) Ernster, L., Dt-Diaphorase - a Historical Review. *Chem. Scripta* **1987**, *27A*, 1-13.
- (16) Ernster, L.; Navazio, F., Soluble Diaphorase in Animal Tissues. *Acta Chem. Scand.* **1958**, *12* (3), 595-595.
- (17) Siegel, D.; Reigan, P.; Ross, D., One- and Two-Electron-Mediated Reduction of Quinones: Enzymology and Toxicological Implications. *Biotechnology: Pharmaceutical Aspects* **2008**, *9*, 169-197.

- (18) Winski, S. L.; Koutalos, Y.; Bentley, D. L.; Ross, D., Subcellular Localization of Nad(P)H : Quinone Oxidoreductase 1 in Human Cancer Cells. *Cancer Res.* **2002**, *62* (5), 1420-1424.
- (19) Villalba, J. M.; Navarro, F.; Arroyo, A.; Martin, S. F.; Bello, R. I.; de Cabo, R.; Burgess, J. R.; Navas, P., Protective Role of Ubiquinone in Vitamin E and Selenium-Deficient Plasma Membranes. *Biofactors* **1999**, *9* (2-4), 163-170.
- (20) Ernster, L., Dt Diaphorase. *Methods Enzymol.* **1967**, *10*, 309-317.
- (21) Nakamura, M.; Hayashi, T., One-Electron and 2-Electron Reduction of Quinones by Rat-Liver Subcellular-Fractions. *J. Biochem.-Tokyo* **1994**, *115* (6), 1141-1147.
- (22) Siegel, D.; McGuinness, S. M.; Winski, S. L.; Ross, D., Genotype-Phenotype Relationships in Studies of a Polymorphism in Nad(P)H : Quinone Oxidoreductase 1. *Pharmacogenetics* **1999**, *9*, 113-121.
- (23) Sreerama, L.; Hedge, M. W.; Sladek, N. E., Identification of a Class 3 Aldehyde Dehydrogenase in Human Saliva and Increased Levels of This Enzyme, Glutathione S-Transferases, and Dt-Diaphorase in the Saliva of Subjects Who Continually Ingest Large Quantities of Coffee or Broccoli. *Clin. Cancer Res.* **1995**, *1* (10), 1153-1163.
- (24) Reicks, M. M.; Appelt, L. C., Soy Induces Phase Ii Enzymes but Does Not Inhibit Dimethylbenz[a]Anthracene-Induced Carcinogenesis in Female Rats. *J. Nutr.* **1999**, *129* (10), 1820-1826.
- (25) Cresteil, T.; Jaiswal, A. K., High-Levels of Expression of the Nad(P)H-Quinone Oxidoreductase (Nqo1) Gene in Tumor-Cells Compared to Normal-Cells of the Same Origin. *Biochem. Pharmacol.* **1991**, *42* (5), 1021-1027.
- (26) Fitzsimmons, S. A.; Workman, P.; Grever, M.; Paull, K.; Camalier, R.; Lewis, A. D., Reductase Enzyme Expression across the National Cancer Institute Tumor Cell Line Panel: Correlation with Sensitivity to Mitomycin C and E09. *J. Natl. Cancer Inst.* **1996**, *88* (5), 259-269.
- (27) Siegel, D.; Franklin, W. A.; Ross, D., Immunohistochemical Detection of Nad(P)H : Quinone Oxidoreductase in Human Lung and Lung Tumors. *Clin. Cancer Res.* **1998**, *4* (9), 2065-2070.
- (28) Siegel, D.; Ross, D., Immunodetection of Nad(P)H : Quinone Oxidoreductase 1 (Nqo1) in Human Tissues. *Free Radical Biol. Med.* **2000**, *29* (3-4), 246-253.

- (29) Jamieson, D.; Wilson, K.; Pridgeon, S.; Margetts, J. P.; Edmondson, R. J.; Leung, H. Y.; Knox, R.; Boddy, A. V., Nad(P)H : Quinone Oxidoreductase1 and Nrh : Quinone Oxidoreductase 2 Activity and Expression in Bladder and Ovarian Cancer and Lower Nrh : Quinone Oxidoreductase 2 Activity Associated with an Nqo2 Exon 3 Single-Nucleotide Polymorphism. *Clin. Cancer Res.* **2007**, *13* (5), 1584-1590.
- (30) Faig, M.; Bianchet, M. A.; Talalay, P.; Chen, S.; Winski, S.; Ross, D.; Amzel, L. M., Structures of Recombinant Human and Mouse Nad(P)H : Quinone Oxidoreductases: Species Comparison and Structural Changes with Substrate Binding and Release. *Proc. Natl. Acad. Sci. U. S. A.* **2000**, *97* (7), 3177-3182.
- (31) Li, R.; Bianchet, M. A.; Talalay, P.; Amzel, L. M., The Three-Dimensional Structure of Nad(P)H:Quinone Reductase, a Flavoprotein Involved in Cancer Chemoprotection and Chemotherapy: Mechanism of the Two-Electron Reduction. *Proceedings of the National Academy of Science* **1995**, *92*, 8846-8850.
- (32) Faig, M.; Bianchet, M. A.; Winski, S.; Hargreaves, R.; Moody, C. J.; Hudnott, A. R.; Ross, D.; Amzel, L. M., Structure-Based Development of Anticancer Drugs: Complexes of Nad(P)H : Quinone Oxidoreductase 1 with Chemotherapeutic Quinones. *Structure* **2001**, *9* (8), 659-667.
- (33) Winski, S. L.; Faig, M.; Bianchet, M. A.; Siegel, D.; Swann, E.; Fung, K.; Duncan, M. W.; Moody, C. J.; Amzel, L. M.; Ross, D., Characterization of a Mechanism-Based Inhibitor of Nad(P)H: Quinone Oxidoreductase 1 by Biochemical, X-Ray Crystallographic, and Mass Spectrometric Approaches. *Biochemistry* **2001**, *40* (50), 15135-15142.
- (34) Asher, G.; Dym, O.; Tsvetkov, P.; Adler, J.; Shaul, Y., The Crystal Structure of Nad(P)H Quinone Oxidoreductase 1 in Complex with Its Potent Inhibitor Dicoumarol. *Biochemistry* **2006**, *45* (20), 6372-6378.
- (35) Nolan, K. A.; Doncaster, J. R.; Dunstan, M. S.; Scott, K. A.; Frenkel, A. D.; Siegel, D.; Ross, D.; Barnes, J.; Levy, C.; Leys, D.; Whitehead, R. C.; Stratford, I. J.; Bryce, R. A., Synthesis and Biological Evaluation of Coumarin-Based Inhibitors of Nad(P)H: Quinone Oxidoreductase-1 (Nqo1). *J. Med. Chem.* **2009**, *52* (22), 7142-7156.
- (36) Danson, S.; Ward, T. H.; Butler, J.; Ranson, M., Dt-Diaphorase: A Target for New Anticancer Drugs. *Cancer Treatment Reviews* **2004**, *30* (5), 437-449.
- (37) Colucci, M. A.; Moody, C. J.; Couch, G. D., Natural and Synthetic Quinones and Their Reduction by the Quinone Reductase Enzyme Nqo1: From Synthetic Organic Chemistry to Compounds with Anticancer Potential. *Org. Biomol. Chem.* **2008**, *6* (4), 637-656.

- (38) Ong, W.; Yang, Y. M.; Cruciano, A. C.; McCarley, R. L., Redox-Triggered Contents Release from Liposomes. *J. Am. Chem. Soc.* **2008**, *130* (44), 14739-14744.
- (39) Volpato, M.; Abou-Zeid, N.; Tanner, R. W.; Glassbrook, L. T.; Taylor, J.; Stratford, I.; Loadman, P.; Jaffar, M.; Phillips, R. M., Chemical Synthesis and Biological Evaluation of a Nad(P)H:Quinone Oxidoreductase-1-Targeted Tripartite Quinone Drug Delivery System. *Mol. Cancer Ther.* **2007**, *6* (12), 3122-3130.
- (40) Moody, C. J.; Maskell, L.; Blanche, E. A.; Colucci, M. A.; Whatmore, J. L., Synthesis and Evaluation of Prodrugs for Anti-Angiogenic Pyrrolylmethylidenyl Oxindoles. *Bioorg. Med. Chem. Lett.* **2007**, *17* (6), 1575-1578.
- (41) Anusevicius, Z.; Sarlauskas, J.; Cenas, N., Two-Electron Reduction of Quinones by Rat Liver Nad(P)H : Quinone Oxidoreductase: Quantitative Structure-Activity Relationships. *Arch. Biochem. Biophys.* **2002**, *404* (2), 254-262.
- (42) Cenas, N.; Anusevicius, Z.; Nivinskas, H.; Miseviciene, L.; Sarlauskas, J., Structure-Activity Relationship in Two-Electron Reduction of Quinones. *Methods Enzymol.* **2004**, *382*, 258-277.
- (43) Zhou, Z. G.; Fisher, D.; Spidel, J.; Greenfield, J.; Patson, B.; Fazal, A.; Wigal, C.; Moe, O. A.; Madura, J. D., Kinetic and Docking Studies of the Interaction of Quinones with the Quinone Reductase Active Site. *Biochemistry* **2003**, *42* (7), 1985-1994.
- (44) Beall, H. D.; Murphy, A. M.; Siegel, D.; Hargreaves, R. H. J.; Butler, J.; Ross, D., Nicotinamide Adenine-Dinucleotide (Phosphate)Quinone Oxidoreductase (Dt-Diaphorase) as a Target for Bioreductive Antitumor Quinones - Quinone Cytotoxicity and Selectivity in Human Lung and Breast-Cancer Cell-Lines. *Mol. Pharmacol.* **1995**, *48* (3), 499-504.
- (45) Phillips, R. M., Bioreductive Activation of a Series of Analogues of 5-Aziridiny-3-Hydroxymethyl-1-Methyl-2-[1h-Indole-4,7-Dione] Prop-Beta-En-Alpha-Ol (Eo9) by Human Dt-Diaphorase. *Biochem. Pharmacol.* **1996**, *52* (11), 1711-1718.
- (46) Beall, H. D.; Winski, S.; Swann, E.; Hudnott, A. R.; Cotterill, A. S.; O'Sullivan, N.; Green, S. J.; Bien, R.; Siegel, D.; Ross, D.; Moody, C. J., Indolequinone Antitumor Agents: Correlation between Quinone Structure, Rate of Metabolism by Recombinant Human Nad(P)H : Quinone Oxidoreductase, and in Vitro Cytotoxicity. *J. Med. Chem.* **1998**, *41* (24), 4755-4766.
- (47) Swann, E.; Barraja, P.; Oberlander, A. M.; Gardipee, W. T.; Hudnott, A. R.; Beall, H. D.; Moody, C. J., Indolequinone Antitumor Agents: Correlation between Quinone Structure

- and Rate of Metabolism by Recombinant Human Nad(P)H : Quinone Oxidoreductase. Part 2. *J. Med. Chem.* **2001**, *44* (20), 3311-3319.
- (48) Fourie, J.; Oleschuk, C. J.; Guziec, F.; Guziec, L.; Fiterman, D. J.; Monterrosa, C.; Begleiter, A., The Effect of Functional Groups on Reduction and Activation of Quinone Bioreductive Agents by Dt-Diaphorase. *Cancer Chemother. Pharmacol.* **2002**, *49* (2), 101-110.
- (49) Fryatt, T.; Pettersson, H. I.; Gardipee, W. T.; Bray, K. C.; Green, S. J.; Slawin, A. M. Z.; Beall, H. D.; Moody, C. J., Novel Quinolinequinone Antitumor Agents: Structure-Metabolism Studies with Nad(P)H : Quinone Oxidoreductase (Nqo1). *Bioorg. Med. Chem.* **2004**, *12* (7), 1667-1687.
- (50) Newsome, J. J.; Swann, E.; Hassani, M.; Bray, K. C.; Slawin, A. M. Z.; Beall, H. D.; Moody, C. J., Indolequinone Antitumour Agents: Correlation between Quinone Structure and Rate of Metabolism by Recombinant Human Nad(P)H : Quinone Oxidoreductase. *Org. Biomol. Chem.* **2007**, *5* (10), 1629-1640.
- (51) Begleiter, A.; El-Gabalawy, N.; Lange, L.; Leith, M. K.; Guziec, L. J.; Guziec Jr, F. S., A Model for Nad(P)H:Quinoneoxidoreductase 1 (Nqo1) Targeted Individualized Cancer Chemotherapy. *Drug Target Insights* **2009**, *4*, 1-8.
- (52) Skelly, J. V.; Sanderson, M. R.; Suter, D. A.; Baumann, U.; Read, M. A.; Gregory, D. S. J.; Bennett, M.; Hobbs, S. M.; Neidle, S., Crystal Structure of Human Dt-Diaphorase: A Model for Interaction with the Cytotoxic Prodrug 5-(Aziridin-1-Yl)-2,4-Dinitrobenzamide (Cb1954). *J. Med. Chem.* **1999**, *42* (21), 4325-4330.
- (53) Suleman, A.; Skibo, E. B., A Comprehensive Study of the Active Site Residues of Dt-Diaphorase: Rational Design of Benzimidazolediones as Dt-Diaphorase Substrates. *J. Med. Chem.* **2002**, *45* (6), 1211-1220.
- (54) Hassani, M.; Cai, W.; Koelsch, K. H.; Holley, D. C.; Rose, A. S.; Olang, F.; Lineswala, J. P.; Holloway, W. G.; Gerdes, J. M.; Behforouz, M.; Beall, H. D., Lavendamycin Antitumor Agents: Structure-Based Design, Synthesis, and Nad(P)H : Quinone Oxidoreductase 1 (Nqo1) Model Validation with Molecular Docking and Biological Studies. *J. Med. Chem.* **2008**, *51* (11), 3104-3115.
- (55) Nolan, K. A.; Humphries, M. P.; Barnes, J.; Doncaster, J. R.; Caraher, M. C.; Tirelli, N.; Bryce, R. A.; Whitehead, R. C.; Stratford, I. J., Triazoloacridin-6-Ones as Novel Inhibitors of the Quinone Oxidoreductases Nqo1 and Nqo2. *Bioorg. Med. Chem.* **2010**, *18*, 696-706.

- (56) Phillips, R. M.; Naylor, M. A.; Jaffar, M.; Doughty, S. W.; Everett, S. A.; Breen, A. G.; Choudry, G. A.; Stratford, I. J., Bioreductive Activation of a Series of Indolequinones by Human Dt-Diaphorase: Structure-Activity Relationships. *J. Med. Chem.* **1999**, *42* (20), 4071-4080.
- (57) Carrier, N. H. Redox-Active Liposome Delivery Agents with Highly Controllable Stimuli-Responsive Behavior. Ph.D. Dissertation, Louisiana State University, Baton Rouge, LA, 2011.
- (58) Osman, A. M.; Boeren, S., Studies on the Dt-Diaphorase-Catalysed Reaction Employing Quinones as Substrates: Evidence for a Covalent Modification of Dt-Diaphorase by Tetrachloro-P-Benzoquinone. *Chem.-Biol. Interact.* **2004**, *147* (1), 99-108.
- (59) Harris, D. C., Statistics. In *Quantitative Chemical Analysis*, 7th ed.; Byrd, M. L., Ed. W. H. Freeman and Company, New York: 2007; p 65.
- (60) Cleland, W. W., Statistical Analysis of Enzyme Kinetic Data. *Methods Enzymol.* **1979**, *63*, 103-138.
- (61) Harris, D. C., Statistics. In *Quantitative Chemical Analysis*, 7th ed.; Byrd, M. L., Ed. W. H. Freeman and Company, New York: 2007; p 59.
- (62) Bohm, H. J., The Computer-Program Ludi - a New Method for the Denovo Design of Enzyme-Inhibitors. *J. Comput. Aid. Mol. Des.* **1992**, *6* (1), 61-78.
- (63) Bohm, H. J., The Development of a Simple Empirical Scoring Function to Estimate the Binding Constant for a Protein Ligand Complex of Known 3-Dimensional Structure. *J. Comput. Aid. Mol. Des.* **1994**, *8* (3), 243-256.
- (64) Rarey, M.; Wefing, S.; Lengauer, T., Placement of Medium-Sized Molecular Fragments into Active Sites of Proteins. *J. Comput. Aid. Mol. Des.* **1996**, *10* (1), 41-54.
- (65) Rarey, M.; Kramer, B.; Lengauer, T.; Klebe, G., A Fast Flexible Docking Method Using an Incremental Construction Algorithm. *J. Mol. Biol.* **1996**, *261* (3), 470-489.
- (66) Rarey, M.; Kramer, B.; Lengauer, T., Multiple Automatic Base Selection: Protein-Ligand Docking Based on Incremental Construction without Manual Intervention. *J. Comput. Aid. Mol. Des.* **1997**, *11* (4), 369-384.
- (67) Kramer, B.; Rarey, M.; Lengauer, T., Casp2 Experiences with Docking Flexible Ligands Using Flexx. *Proteins* **1997**, 221-225.

- (68) Kramer, B.; Rarey, M.; Lengauer, T., Evaluation of the Flexx Incremental Construction Algorithm for Protein-Ligand Docking. *Proteins* **1999**, *37* (2), 228-241.
- (69) Rarey, M.; Kramer, B.; Lengauer, T., Docking of Hydrophobic Ligands with Interaction-Based Matching Algorithms. *Bioinformatics* **1999**, *15* (3), 243-250.
- (70) Bohm, H. J., Ludi - Rule-Based Automatic Design of New Substituents for Enzyme-Inhibitor Leads. *J. Comput. Aid. Mol. Des.* **1992**, *6* (6), 593-606.
- (71) Burie, J. R.; Boullais, C.; Nonella, M.; Mioskowski, C.; Nabedryk, E.; Breton, J., Importance of the Conformation of Methoxy Groups on the Vibrational and Electrochemical Properties of Ubiquinones. *J. Phys. Chem. B* **1997**, *101* (33), 6607-6617.
- (72) Silverman, J.; Stam-Thole, I.; Stam, C. H., Crystal and Molecular Structure of 2-Methyl-4,5-Dimethoxy Para Quinone (Fumigatin Methyl Ether), C₉H₁₀O₄. *Acta Cryst. B-Struc.* **1971**, *B 27* (Oct15), 1846-1851.
- (73) Robitaille, P. M. L.; Robitaille, P. A.; Brown, G. G.; Brown, G. G., An Analysis of the Ph-Dependent Chemical-Shift Behavior of Phosphorus-Containing Metabolites. *J. Magn. Reson.* **1991**, *92* (1), 73-84.
- (74) Milstien, S.; Cohen, L. A., Stereopopulation Control .1. Rate Enhancement in Lactonizations of Ortho-Hydroxyhydrocinnamic Acids. *J. Am. Chem. Soc.* **1972**, *94* (26), 9158-9165.
- (75) Cavelier, G.; Amzel, L. M., Mechanism of Nad(P)H : Quinone Reductase: Ab Initio Studies of Reduced Flavin. *Proteins* **2001**, *43* (4), 420-432.
- (76) Deller, S.; Macheroux, P.; Sollner, S., Flavin-Dependent Quinone Reductases. *Cell Mol. Life Sci.* **2008**, *65* (1), 141-160.
- (77) Nolan, K. A.; Timson, D. J.; Stratford, I. J.; Bryce, R. A., In Silico Identification and Biochemical Characterization of Novel Inhibitors of Nqo1. *Bioorg. Med. Chem. Lett.* **2006**, *16* (24), 6246-6254.
- (78) Carlson, B. W.; Miller, L. L., Mechanism of the Oxidation of Nadh by Quinones - Energetics of One-Electron and Hydride Routes. *J. Am. Chem. Soc.* **1985**, *107* (2), 479-485.

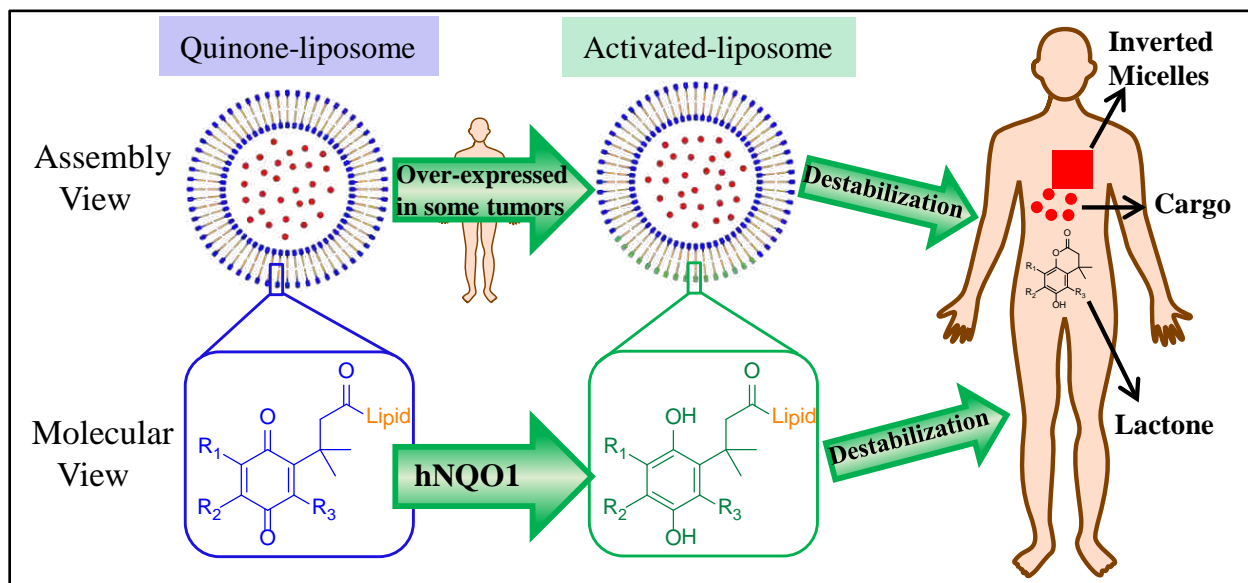
- (79) Tranoy-Opalinski, I.; Fernandes, A.; Thomas, M.; Gesson, J. P.; Papot, S., Design of Self-Immolative Linkers for Tumour-Activated Prodrug Therapy. *Anti-Cancer Agent Me* **2008**, 8 (6), 618-637.

CHAPTER 4

QUINONE TRIGGER-BASED LIPIDS FOR FORMING ENZYME-RESPONSIVE LIPOSOMES AND THEIR RESPONSE TOWARD hNQO1 ASSAY CONDITIONS

4.1 Introduction

In general, quinones have been applied to different systems with the aim of improving therapeutic responses in the area of targeting cancer, such is the case for antitumor compounds and prodrugs; both being activated by reductive enzymes.¹⁻³ The McCarley research group went a step further from prodrugs and designed a quinone-based liposome system to be specifically activated by the human reductive enzyme NAD(P)H:quinone oxidoreductase type-1 (hNQO1), which is over-expressed in certain solid tumors,⁴⁻⁷ with the objective of adding more deliverable drug units per delivery carrier. Such liposome systems have been proved by the McCarley group to open by chemical reduction under bench-top conditions.⁸ However, these liposomes still need to be assayed against the human enzyme NQO1 for the development of enzyme-responsive liposomes. Initial information was extracted from the characterization of trimethyl-lock quinone derivatives by cyclic voltammetry (chapter 2), enzyme assays and docking (chapter 3). With such knowledge in hand, it was expected that contents release would occur for quinone-based liposomes (Q-liposomes) upon hNQO1 activation (reduction) of the quinone headgroup to the hydroquinone, and as a result, destabilization of the liposome bilayer would lead to cargo release, Scheme 4.1. In order to clearly demonstrate liposome opening through this enzyme mechanism, first proper control experiments needed to be done wherein in the dye-containing liposomes are examined in the sole presence of bovine serum albumin (BSA), reduced nicotinic adenine dinucleotide (NADH), and hNQO1, common components of the NQO1 assay.⁹ Those control experiments will provide knowledge on the interaction between quinone-liposome systems and hNQO1 assay components.



Scheme 4.1. Proposed enzyme-responsive liposome system.

4.2 Experimental Section

4.2.1 Materials

Potassium dihydrogen phosphate (KH_2PO_4 , Fluka 60219), dipotassium hydrogen phosphate (K_2HPO_4 , Fisher P288), potassium chloride (KCl, Sigma P9541) and potassium hydroxide pellets (KOH, Mallinckrodt) were used to make the buffer. Recombinant human enzyme NAD(P)H:quinone oxidoreductase type 1 and type 2 (rhNQO1 and rhNQO2), nicotinamide adenine dinucleotide reduced (β -NADH) and bovine serum albumin (BSA) were purchased from Sigma Aldrich (D1315, Q0380, N8129, A3294). Triton X-100 (> 99% pure, Sigma T8787) was also purchased from Sigma Aldrich. Calcein (85% pure, Acros Organics) was purchased from Fisher Scientific. 1,2-dioleoyl-*sn*-glycero-3-phosphoethanolamine (DOPE), 1,2-dioleoyl-*sn*-glycero-3-phosphoethanolamine-*N*-[methoxy(polyethyleneglycol)-2000] (PEG₂₀₀₀-DOPE), 1,2-dioleoyl-*sn*-glycero-3-phosphocholine (DOPC), and cholesterol (CHO) were purchased from Avanti Polar Lipids and used without further purification. Sephadex Fine G-50 was purchased from GE Healthcare. NORM-JECT syringes were purchased from Fisher Scientific. Nanopure water was obtained from a Nanopure Diamond Barnstead system (18.2 M Ω ·cm). Q-DOPE syntheses and characterizations were published previously.¹⁰ The

instrument used was a Perkin-Elmer LS 55 Fluorescence Spectrometer with a PTP-1 Fluorescence Peltier System and PCB 1500 Water Peltier System (PerkinElmer, Waltham, MA).

4.2.2 Calcein-loaded Liposome Preparation

Liposomes were prepared using a modified version of the well-known lipid thin-film and extrusion method.^{11,12} Around 20 mL of pH 7.1 0.1M phosphate buffer (PB)/0.1 M KCl was placed under argon to degas. 1–3 mg of quinone-DOPE (taken out of the freezer 20 min before weighing) was dissolved in a minimal amount of chloroform (approximately 1 mL). Depending on the liposome system to be prepared, appropriate amounts of PEG₂₀₀₀-DOPE, DOPC, or cholesterol were weighed, and subsequently dissolved in certain volume of chloroform to reach the desired concentration for later addition to the Q-DOPE solution. Then, the solution was transferred into a 10-mL (14/20) ground joint test tube. Chloroform was removed by rotary evaporation for 15 min, and a thin film layer was formed at the bottom of the tube. The lipid film was further dried under high vacuum for 1 hour. While the lipid was drying, a 40 mM calcein solution in degassed buffer was prepared. Approximately 248 mg of calcein and 70 mg of potassium hydroxide were added into a vial followed by addition of 8 mL of degassed pH 7.1 0.1 M PB/0.1 M KCl buffer solution. The mixture was sonicated to help dissolve the solids, yielding an orange solution. Titration with KOH solution (KOH pellets and pH 7.1 0.1 M PB/0.1 M KCl buffer) gave the desired pH of 7.1. The calcein solution was transferred to a 10-mL volumetric flask and filled with degassed buffer to the calibration mark. Dried lipids were hydrated in 1 mL of calcein solution by vortexing the mixture for 30 seconds and allowed to stand every 2 min for a total of 30 min. The hydrated lipids went through six-freeze thaw cycles using an acetone/dry ice bath and a warm water-bath. At this point, an Avanti Mini-Extruder (Avanti Polar Lipids, Alabaster, AL) was assembled and rinsed with buffer and then with calcein solution before injection of the lipid solution into the extruder. A total of 19 extrusions were performed at room temperature (22 ± 2 °C) using one 100-nm diameter pore Whatman

Nucleopore polycarbonate track-etched membrane. Free calcein was separated from liposome-encapsulated calcein by column centrifugation method, as follows 100–250 μL of solution was added to a 3-mL syringe with glass-cotton frit, packed with Sephadex Fine G-50 and then centrifuged for 3 min at 500 x g . Solutions of liposome-encapsulated calcein were stored in an amber vial under argon and then placed in the refrigerator at 8 °C for subsequent experiments. Liposome-encapsulated calcein solutions are stable for up to 5 days.

4.2.3 Characterization of Calcein-loaded Liposomes

Liposome sizes (diameters) were measured using dynamic light scattering from backscattered light intensities (173°, 633-nm red laser) at 25 °C in a Zetasizer Nano ZS (Malvern Instruments, Worcestershire, U. K.) particle analyzer. No significant size differences were found previously between calcein-loaded liposomes and calcein-free liposomes.⁸ Liposome charge was obtained by measuring the zeta potential at 25 °C in a folded capillary zeta potential cell using a Smoluchowski model.

4.2.4 Stability and Calcein Release Experiments

10 μL of calcein-loaded liposomes and 990 μL of pH 7.1 0.1 M PB/0.1 M KCl buffer solution were added to a 1-cm quartz cuvette, and an absorbance scan was performed at room temperature from 200 to 600 nm in a Varian Cary 50 Bio UV-Visible Spectrophotometer. The peak at 497 nm corresponds to the encapsulated calcein, and its absorbance ranged from 0.06 to 0.1 a.u. depending on the liposome system. The peak at 264.9 nm corresponded to the Q_{Me} headgroup absorbance, when it was equal to 0.55 a.u., meant that the lipid concentration was 100 μM based on a $\epsilon_{265} = 5500 \text{ M}^{-1}$ for the Q_{Me} headgroup.¹³ A ratio between this value and the absorbance value measured for a particular experiment containing Q_{Me} -DOPE gave the corresponding amount of liposome solution needed to have 100 μM liposome in a 3-mL volume. In these liposome stability experiments, different assay components were present in the 4-sided transparent cuvette by the time the fluorescent experiment start. All fluorescence intensity

experiments were performed at 25 °C on a Perkin-Elmer LS 55 Fluorescence Spectrometer with a PTP-1 Fluorescence Peltier System and PCB 1500 Water Peltier System. The excitation wavelength was $\lambda_{\text{ex}} = 490$ nm, and the emission wavelength was $\lambda_{\text{em}} = 515$ nm, both with a slit width of 2.5 nm. Data was acquired every 1 min with a 0.1 second integration time; the total experimental time varied from 1 hour to 24 hours. To avoid detector saturation, two neutral density filters (ND 0.3 and ND 0.5, Omega Optics, Brattleboro, VT) were placed inside the instrument so as to reduce the total transmission to 16% of the original intensity. The percent of calcein release was calculated as follows:

$$\% \text{ Leakage} = \frac{(F_t - F_0)}{(F_{100} - F_0)} * 100 \quad \text{Equation 4.1}$$

F_0 is the intensity value that corresponds to the point before addition of the assay component (BSA, NADH, hNQO1, dithionite, liposomes) where there is a 0% leakage. F_t corresponds to the fluorescence intensity observed at the point in time after addition of the assay component. F_{100} is the fluorescence intensity observed after addition of 15 μL of 30% (v/v) Triton X-100 that ensures lysing of the liposomes for release of all calcein.

4.2.4.1 Bovine Serum Albumin

When BSA was tested with the different liposome systems, the concentration of liposomes was calculated as described in Section 4.2.4. BSA solutions were made using a 10-mL volumetric flask containing pH 7.1 0.1 M PB/0.1 M KCl and 0.7 mg or 7 mg of BSA, corresponding to a 1 μM or 10 μM BSA solutions. The experiment started by addition of liposome solution to the already present BSA solution in the cuvette or the other way around. In both cases the same result was observed, reaffirming that the addition order had no effect on the outcome. Fluorescence at 515 nm was recorded upon addition of either component.

4.2.4.2 Reduced Nicotine Adenine Dinucleotide

When NADH was tested with the different liposome systems, the concentration of liposomes was calculated as described in Section 4.2.4. NADH solutions were made using a 10-

mL volumetric flask containing pH 7.1 0.1 M PB/0.1 M KCl and 7.25 mg of NADH, corresponding to a 1 mM solution. 300 μ L of 1 mM NADH solution were added to the cuvette and fluorescence as a function of time was recorded.

4.2.4.3 Human NAD(P)H:Quinone Oxidoreductase Type 1 (hNQO1) and Type 2 (hNQO2)

The reaction started when 300 μ L of hNQO1 solution were added to the liposome solution in the 4-sided transparent cuvette. The amount of enzyme used in the experiment was calculated based on hNQO1 enzyme kinetics assays carried out previously on Q_{Me}-COOH. Enzyme solutions were prepared from a 50 μ L frozen enzyme aliquot (2 mg·mL⁻¹) added to 275 μ L of pH 7.1 0.1 M PB/0.1 M KCl buffer to yield a 5 μ M solution. For inhibition experiments, 599 μ L of pH 7.1 0.1 M PB/0.1 M KCl buffer containing NADH (100 μ M) and ES936 (30 μ M) were added to the hNQO1 enzyme (50 μ L frozen aliquot), and this solution was incubated at room temperature for 30 min prior to its addition to the 4-sided transparent cuvette. For heat inactivation of hNQO1, the enzyme was heated at 85 °C for 25 min, and then 300 μ L were added to the liposome solution. hNQO2 experiments were performed as described for hNQO1 but using an enzyme concentration of 2.5 μ M. Fluorescence at 515 nm was recorded upon addition of either component

4.2.4.4 Sodium Dithionite

Around 15 mL of buffer was purged with argon for 20 min. The appropriate amount of liposome solution and degassed buffer were mixed to yield a total volume of 3 mL and then added to a 4-sided cuvette with a screw-cap septum; the solution was purged with argon for 10 min. The cuvette was taken to the room where the fluorescence instrument is located, and the experiment was started. Approximate 5.3 mg of dithionite was added to an amber-septum vial and then purged with argon for 1 min. To the degassed vial containing dithionite, 1 mL of degassed buffer was added. The oxygen-free dithionite solution was taken to the fluorometer room and an appropriate amount of this solution was injected into the cuvette using a 50- μ L

Gastight syringe (Hamilton, Reno, NV). After injection, the cuvette was shaken, and then the time-dependent fluorescence was recorded.

4.3 Results and Discussion

4.3.1 Stability and Calcein Release for Q-DOPE Liposome Systems

4.3.1.1 Liposomes Composed of 100% Q_{Me}-DOPE

Q_{Me}-DOPE liposomes have been extensively studied in the McCarley group, and their contents release curves were reported previously upon addition of dithionite.^{8,10,13} Therefore, there was an imminent curiosity to see how they will behave under hNQO1 assay conditions. The appropriate amounts of Q_{Me}-DOPE liposome, NADH and BSA solutions were calculated as outlined in Section 4.2. The absorbance spectrum of 100% Q_{Me}-DOPE liposomes is presented in Figure 4.1. In this spectrum is clearly observed the quinone headgroup peak ($\lambda_{\max} = 264.9$ nm) used to calculate the liposome concentration as well as the necessary value for the encapsulated calcein peak ($\lambda_{\max} = 497$ nm) to avoid detector saturation.

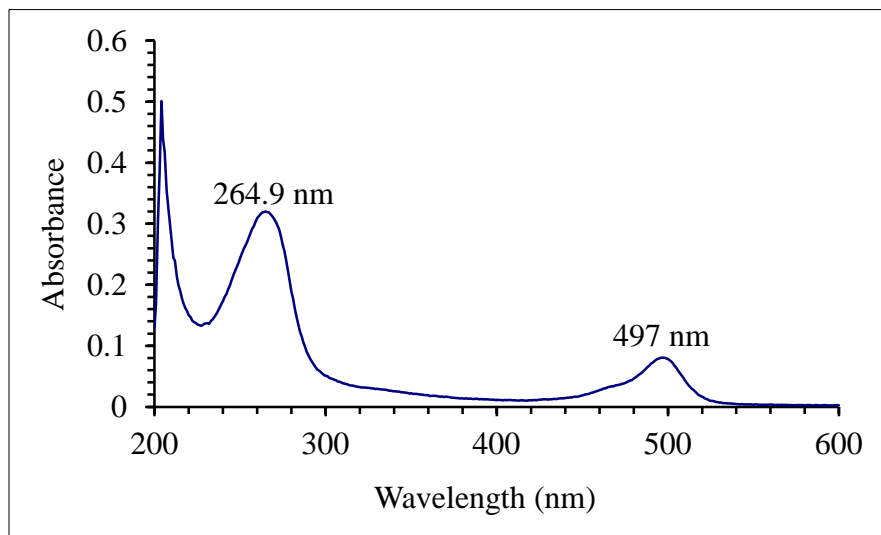


Figure 4.1. UV-vis absorbance spectrum of 100% Q_{Me}-DOPE liposomes in pH 7.1 0.1 M PB/0.1 M KCl at room temperature. $\lambda_{\max} = 264.9$ nm corresponds to the Q_{Me} headgroup and $\lambda_{\max} = 497$ nm corresponds to the encapsulated calcein.

The first experiment intended to verify if the presence of NADH, an hNQO1 electron donor during the ping-pong mechanism,⁹ has any impact on the liposome stability. In Figure 4.2

is shown the behavior of 100% Q_{Me}-DOPE liposome upon addition of 300 μ L of 1 mM NADH solution. To our satisfaction, liposomes were stable up to 18 hours (the maximum time measured) in the presence of the hNQO1 cofactor. The stability of the liposomes in the presence of NADH confirms the absence of direct reduction between the quinone headgroup and the cofactor. In this matter, any liposome opening should be caused by the enzymatic reduction of the quinone headgroup as illustrated in Scheme 4.1.

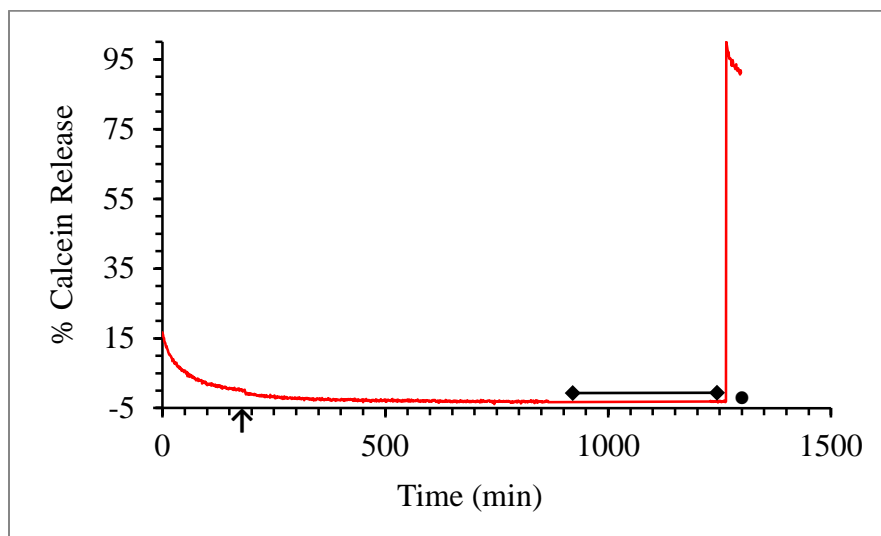


Figure 4.2. Stability of 100 μ M 100% Q_{Me}-DOPE liposomes in the presence of 100 μ M NADH. (\uparrow) the time for addition of 300 μ L of 1 mM NADH solution. No leakage was observed as noted by the lack of increase in fluorescence intensity with time. (\bullet) time at which 100% Q_{Me}-DOPE liposomes were lysed with the addition of 15 μ L of 30% (v/v) Triton X-100. (\blacklozenge) Instrument stopped by itself and was started again by me; no consequences observed on the measurement.

The next enzyme assay component to be tested against the liposomes was BSA, which has been mentioned numerous times as an NQO1 activator in a way that to this date is not fully understood.¹⁴ In Figure 4.3 are displayed both trials made on this liposome system with addition of only BSA solution. Unfortunately, they were not stable in the presence of this protein. Trial 1 exhibited a calcein leakage of 44% in 3 hours and 61% in 16 hours and 30 min while trial 2 resulted in a calcein leakage of 54% in 3 hours and 71% in 15 hours and 12 min. The shape of the release curves varied because of the different order of addition between the liposomes and the BSA solution; in both cases this did not affect the % calcein leakage results. The fast release

rate of contents for the 100% Q_{Me} -DOPE system took us by surprise based on the previous knowledge of the interaction of liposomes with BSA solutions.

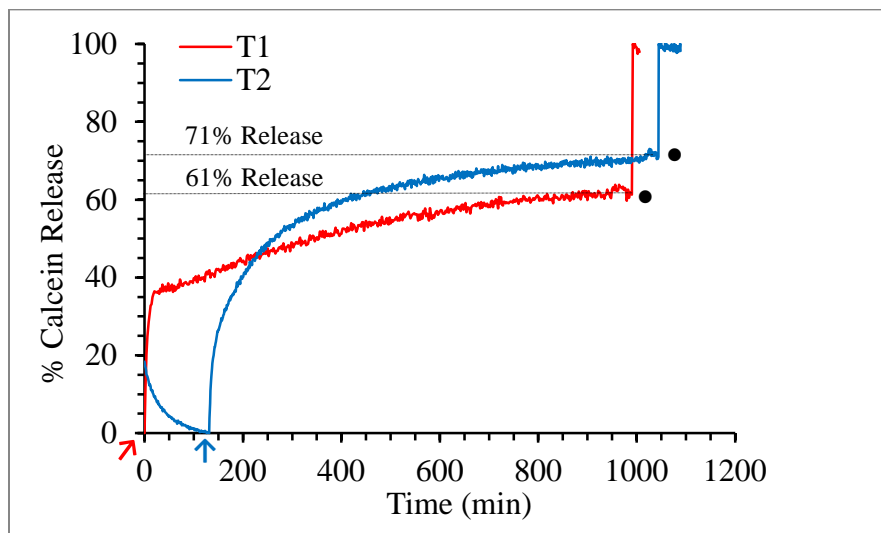


Figure 4.3. Instability of 100 μ M 100% Q_{Me} -DOPE liposomes in the presence of 0.007% BSA. (\uparrow) the time for addition of 300 μ L of 0.07% BSA solution into liposome solution. (\uparrow) the addition time for 100% Q_{Me} -DOPE liposomes into 0.007% BSA solution. (\bullet) time at which 100% Q_{Me} -DOPE liposomes were lysed with the addition of 15 μ L of 30% (v/v) Triton X-100.

Kim and co-workers described that egg phosphatidylcholine (PC) liposomes had a percent leakage of ca. 13% in 5 hours and ca. 18% in 10 hours when incubated with approximate 8 μ M BSA solution (in TES buffer pH 7.4) at 37 $^{\circ}$ C.¹⁵ In addition, Guo and Szoka depicted their liposome system (DSPE-PEG/DOPE 1:9) to have a leakage of 13% in 4 hours and 20% in 12 hours in the presence of 75% of fetal serum albumin (in pH 7.4 0.05 M PB/0.1 M NaCl).¹⁶ Because of the instability of the 100% Q_{Me} -DOPE liposomes toward the protein BSA, other liposome formulations were investigated with the objective of finding the system that would be assay against hNQO1.

4.3.1.2 Liposomes Composed of 97% Q_{Me} -DOPE/3% PEG₂₀₀₀-DOPE

Based on the previous results with 100% Q_{Me} -DOPE liposomes, the liposome formulation was adjusted by including 3% of a lipid attached to poly(ethylene glycol), PEG-DOPE in the mixture. It is well known that PEG lipids stabilize liposomes containing PEGs of 2,000 MW with respect to non-specific protein absorption and disruption. Due to the properties

of PEG lipids, long-circulation liposomes, known as “Stealth Liposomes,” have helped improved the therapeutic efficiency of liposomes as drug delivery carriers with reported circulatory half-lives of up to 45 hours.^{17,18} Q_{Me} -DOPE, BSA, NADH and hNQO1 solutions were prepared as described in Section 4.2. PEG₂₀₀₀-DOPE was obtained from Avanti Polar Lipids and dissolved in an appropriate amount of chloroform previous to its addition to chloroform solutions of Q_{Me} -DOPE solution. The absorbance spectrum of 97% Q_{Me} -DOPE/3% PEG₂₀₀₀-DOPE liposomes is presented in Figure 4.4 and look exactly as the one in Figure 4.1. Thus, as expected, the addition of PEG₂₀₀₀-DOPE did not introduce extra peak that could interfere with the fluorescence experiments. The quinone headgroup peak as well as the encapsulated calcein peak is observed as seen previously for 100% Q_{Me} -DOPE liposomes. The new formulation was tested with BSA to see its impact on liposome stability. In Figure 4.5 is shown the behavior of 97% Q_{Me} -DOPE/3% PEG₂₀₀₀-DOPE liposomes upon addition of BSA solution. Even with 3% polyethylene glycol in the liposome formulation, the liposomes were not stable when they came in contact with BSA. The calcein leakage was 59% in 3 hours and 77% in 15 hours and 45 min.

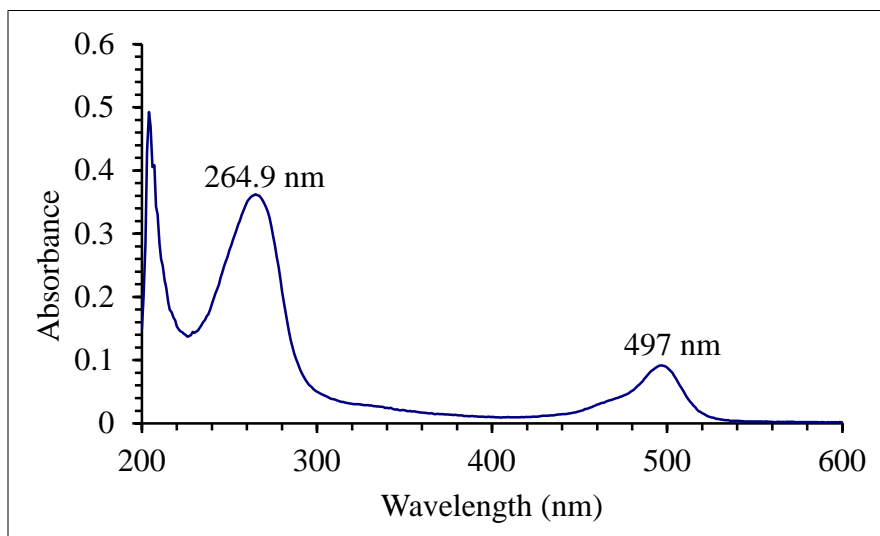


Figure 4.4. UV-vis absorbance spectrum of 97% Q_{Me} -DOPE/3% PEG₂₀₀₀-DOPE liposomes in pH 7.1 0.1 M PB/0.1 M KCl at room temperature. $\lambda_{max} = 264.9$ nm corresponds to the Q_{Me} headgroup and $\lambda_{max} = 497$ nm corresponds to the encapsulated calcein.

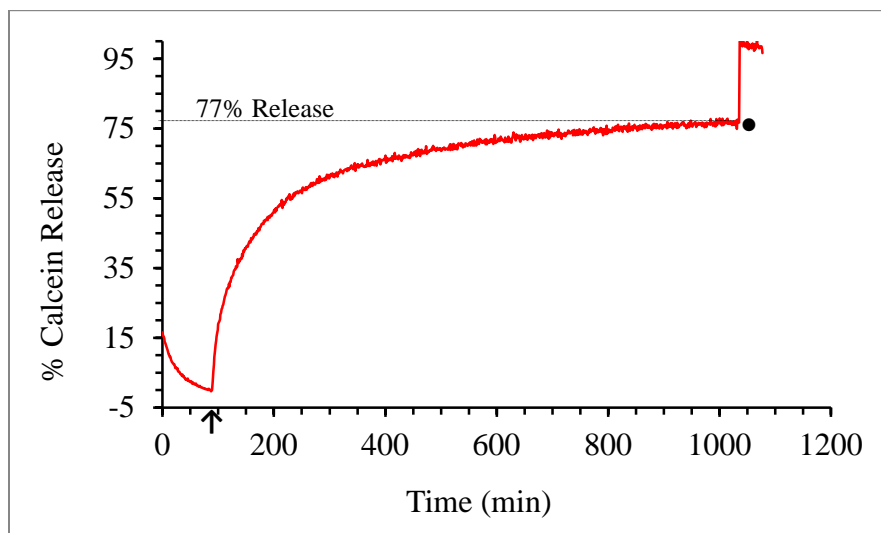


Figure 4.5. Instability of 100 μ M 97% Q_{Me}-DOPE/3% PEG₂₀₀₀-DOPE liposomes in the presence of 0.007% BSA. (\uparrow) the time for addition of 300 μ L of 0.07% BSA solution into liposome solution. (\bullet) time at which 97% Q_{Me}-DOPE/3% PEG₂₀₀₀-DOPE liposomes were lysed with the addition of 15 μ L of 30% (v/v) Triton X-100.

At this point, two hypotheses can be presented for the way that BSA interacts with the Q-DOPE liposomes: 1) the attraction of BSA to the liposomes is based on surface-charge interactions or/and 2) the attraction of BSA to the liposomes is based on hydrophobic interactions between the protein and the lipid bilayer. Hypothesis 1 is less feasible based on the fact that BSA is a negatively charged protein at pH 7.1 (isoelectric point between 4.5–4.9)¹⁹⁻²¹ and the liposomes also present a highly negative surface charge (Table 4.1), thus, electrostatic interactions at pH 7.1 should be minimal or none. Sweet and Zull indicated that other factors, besides electrostatic interactions, are involved in the interaction of BSA with phospholipid membranes.²¹ The same authors later stated that electrostatic interactions between negatively charged membranes and BSA would be more probably near or below the isoelectric point of BSA (4.5–4.9).¹⁹ In addition, Kim and co-workers came to the conclusion that BSA attacks the lipid bilayer whether it is at the inner or at the outer phase of the bilayer and induces leakage of the entrapped materials.¹⁵ Therefore, it is more probable that BSA caused the release of calcein from the liposomes by penetrating into the lipid bilayer. The observations that Sweet and Zull found for

their systems¹⁹ made me think of the possibility that hNQO1, with an isoelectric point of 8.91,²² could have electrostatic interactions with our negative liposomes and induce leakage of contents by a different mechanism than the one proposed on Figure 4.1. Therefore, the 97% Q_{Me}-DOPE/3% PEG₂₀₀₀-DOPE liposomes were evaluated in the presence of only hNQO1.

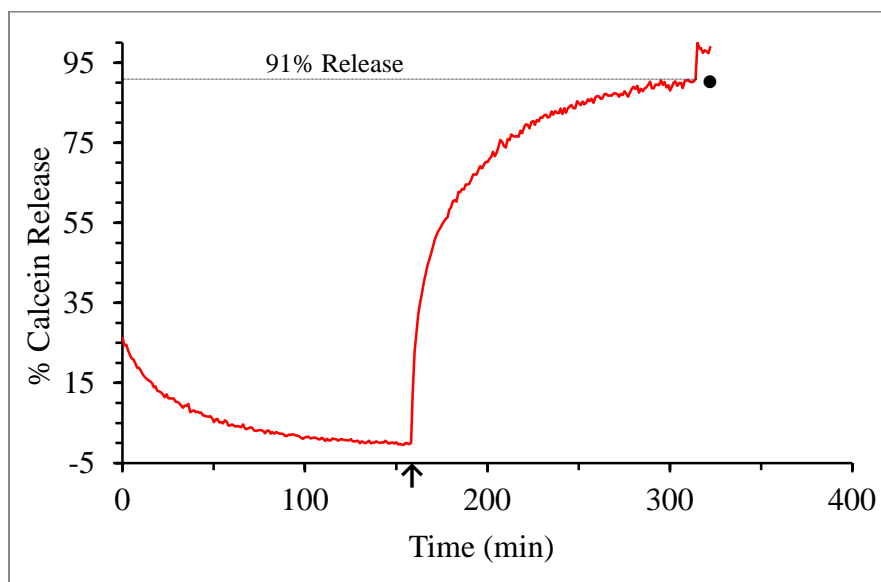


Figure 4.6. Instability of 100 μM 97% Q_{Me}-DOPE/3% PEG₂₀₀₀-DOPE liposomes in the presence of 0.5 μM hNQO1. (\uparrow) the time for addition of 300 μL of 5 μM hNQO1 solution into liposome solution. (\bullet) time at which 97% Q_{Me}-DOPE/3% PEG₂₀₀₀-DOPE liposomes were lysed with the addition of 15 μL of 30% (v/v) Triton X-100.

Upon inspection of Figure 4.6, a calcein release of 80% was observed in 70 min and 91% in 2 hours and 36 min after exposure of 97% Q_{Me}-DOPE/3% PEG₂₀₀₀-DOPE liposomes to hNQO1. In fact, the calcein release rate provoked by hNQO1 was faster than the one caused by BSA. Such a difference in the release rate could be a consequence of the apparent different mechanisms for the proteins acting on the liposomes. Human NQO1 seems to interact by surface charge attractions that would disrupt the liposomes (faster release), while on the other hand, BSA seems to interact by penetrating the lipid bilayer (slower release).

At this moment, the attention was focused on the fact that the liposome opened by the sole presence of the enzyme by a path different from the one proposed in Scheme 4.1. In this regard, another experiment using hNQO1 and NADH was performed to see if the rate of leakage

was increased from the results obtained in Figure 4.6. The addition of NADH provides the necessary component for the enzyme to act through its ping-pong mechanism.⁹

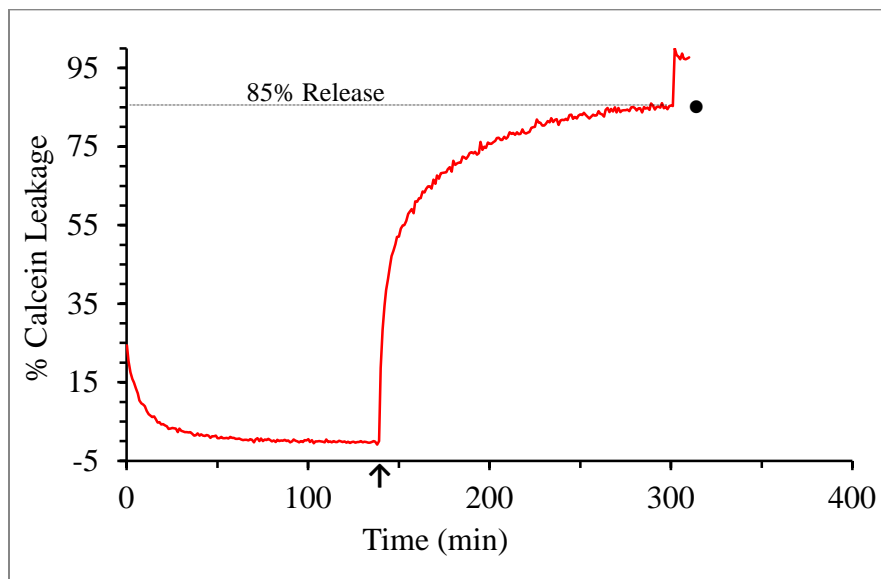


Figure 4.7. Instability of 100 μM 97% Q_{Me} -DOPE/3% PEG_{2000} -DOPE liposomes in the presence of 100 μM NADH and 0.5 μM hNQO1. (\uparrow) the addition time for 300 μL of 5 μM hNQO1 solution into liposome/NADH solution. (\bullet) time at which 97% Q_{Me} -DOPE/3% PEG_{2000} -DOPE liposomes were lysed with the addition of 15 μL of 30% (v/v) Triton X-100.

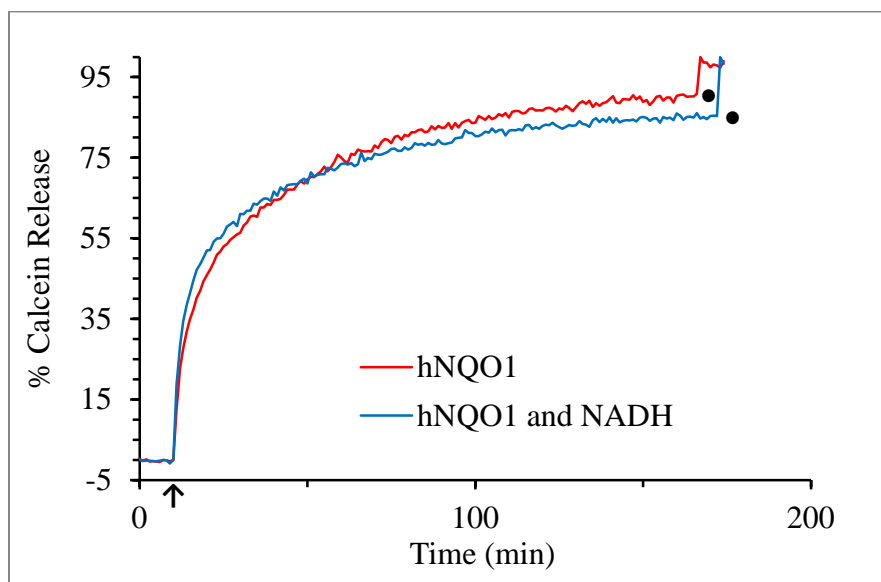


Figure 4.8. Overlap of the calcein release curves for 100 μM 97% Q_{Me} -DOPE/3% PEG_{2000} -DOPE liposomes in the presence of 0.5 μM hNQO1 (red line) and 100 μM 97% Q_{Me} -DOPE/3% PEG_{2000} -DOPE liposomes containing 100 μM NADH in the presence of 0.5 μM hNQO1 (blue line). (\uparrow) the addition time for 300 μL of 5 μM hNQO1 solution into liposome/NADH solution. (\bullet) time at which 97% Q_{Me} -DOPE/3% PEG_{2000} -DOPE liposomes were lysed with the addition of 15 μL of 30% (v/v) Triton X-100. Times were offset to compare the curves.

In Figure 4.7 is displayed the behavior of 97% Q_{Me}-DOPE/3% PEG₂₀₀₀-DOPE liposomes in the presence of NADH and hNQO1, showing minimal difference with respect to Figure 4.6. In fact, both curves can be almost overlapped as shown in Figure 4.8.

The instability of 97% Q_{Me}-DOPE/3% PEG₂₀₀₀-DOPE liposomes in the presence of bovine serum albumin and hNQO1 lead me to investigate more liposome formulations with the aim of finding one that is stable under hNQO1 assay conditions.

4.3.1.3 DOPC Liposomes

The new liposome formulation described in this section is devoid of the Q_{Me}-DOPE lipid; no quinone headgroup is present in this liposome system. In that way, I could investigate how much the presence of the Q_{Me} headgroup affected liposome leakage when they came in contact with BSA or hNQO1. Unfortunately, DOPE lipids do not form stable liposomes at pH 7.1,^{23,24} therefore, DOPC lipids were used instead. DOPC has a similar structure to DOPE, with the difference being the polar group as illustrated in Figure 4.9; therefore, the fluidity of the bilayer is not changed because the transition temperature of the lipids are very similar (T_m DOPE = -16 °C and T_m DOPC = -20 °C).

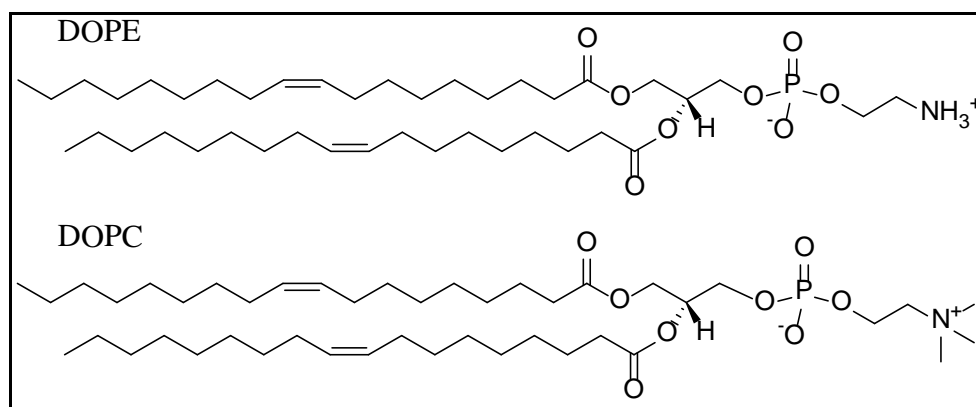


Figure 4.9. Structure of DOPE and DOPC lipids.

In Figure 4.10 is presented the absorbance spectrum of DOPC liposomes containing calcein. As can be seen, the quinone peak at 264.9 nm is absent, as expected, and the peak at 497 nm corresponds to the encapsulated calcein. In effect, the encapsulated calcein peak was

used to approximate the concentration of this liposome formulation to be 100 μM as it was for our previous experiments. DOPC liposomes were tested in the presence of BSA and also with hNQO1.

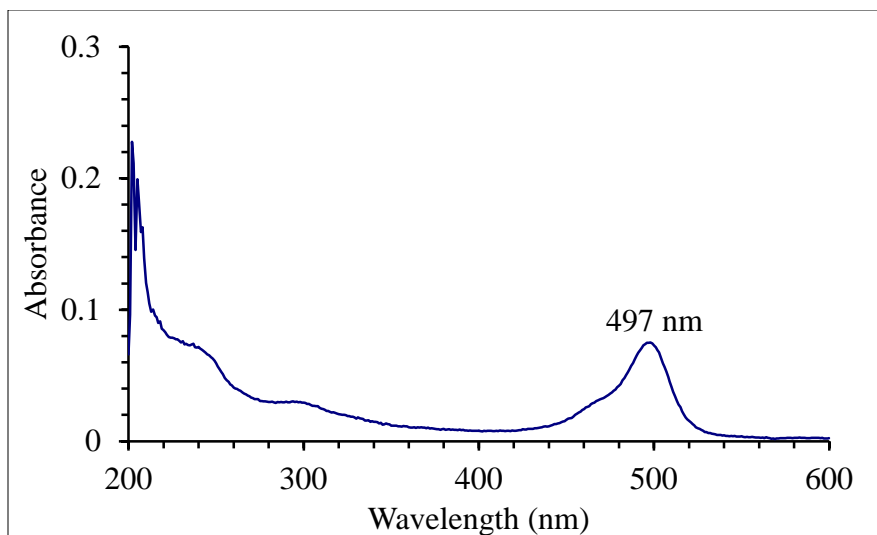


Figure 4.10. UV-vis absorbance spectrum of DOPC liposomes in pH 7.1 0.1 M PB/0.1 M KCl at room temperature. The peak of $\lambda_{\text{max}} = 497$ nm corresponds to the encapsulated calcein.

In Figure 4.11 is shown the stable behavior of DOPC liposomes with BSA for almost 17 hours. The lack of interaction between BSA and DOPC liposomes, lead me to believe that the Q_{Me} headgroup played an important role in liposome leakage. In the previous section, I referred to BSA as a protein that interacts with liposomes through the lipid bilayer; it could happen that in the Q_{Me} -DOPE liposome systems, the hydrophobic quinone mediated the interaction between BSA and the liposome membrane, permitting the protein to penetrate the Q_{Me} -DOPE liposome system.

In Figure 4.12 is displayed the stability of DOPC liposomes in the presence of hNQO1 for approximately 15 hours. The absence of interaction between DOPC liposomes and hNQO1 could be credited to two things: 1) the almost neutral surface charge of DOPC liposomes (Table 4.1) and/or 2) the absence of the Q_{Me} headgroup in the liposome formulation. The first one would definitely decrease any electrostatic interaction that the positively charged enzyme could have with the slightly negative charge liposomes, and the second one would lead me to the

option that hNQO1 could just embrace the quinone headgroup of the liposomes inducing bilayer destabilization and liposome leakage.

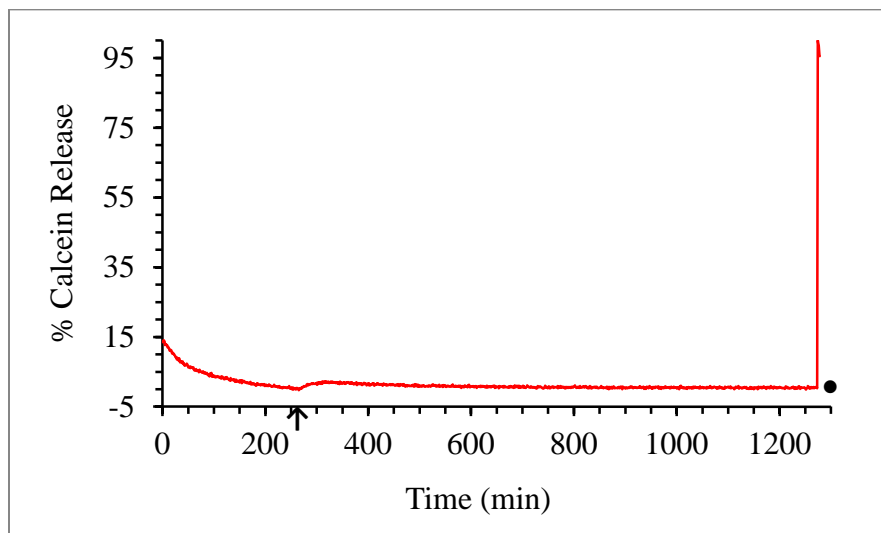


Figure 4.11. Stability of 100 μM DOPC liposomes in the presence of 0.007% BSA. (\uparrow) the addition time for 300 μL of 0.07% BSA solution into liposome solution. No leakage was observed as noted by the lack of increase in fluorescence intensity with time. (\bullet) time at which DOPC liposomes were lysed with the addition of 15 μL of 30% (v/v) Triton X-100.

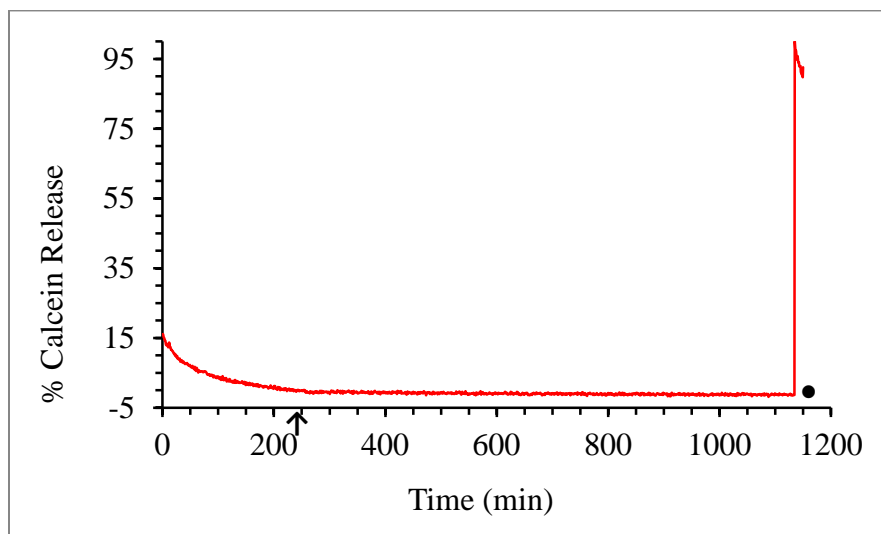


Figure 4.12. Stability of 100 μM DOPC liposomes in the presence of 0.5 μM hNQO1. (\uparrow) the addition time for 300 μL of 5 μM hNQO1 solution into liposome solution. No leakage was observed as noted by the lack of increase in fluorescence intensity with time. (\bullet) time at which DOPC liposomes were lysed with the addition of 15 μL of 30% (v/v) Triton X-100.

The stability of DOPC liposomes toward both proteins proved the fact that Q_{Me} headgroup played a significant role in the instability of Q-DOPE liposomes toward BSA and hNQO1. For the development of enzyme-responsive liposomes the presence of quinone

headgroups into the liposome formulation is essential because of the inherent substrate affinity of hNQO1 towards quinones.⁹ Therefore, a potential solution for liposome stability is to create liposomes based on mixtures of Q_{Me}-DOPE and DOPC lipids.

4.3.1.4 Liposomes Composed of 90% Q_{Me}-DOPE/10% DOPC and 80% Q_{Me}-DOPE/20% DOPC

With the intent of finding a stable system that contains Q_{Me}-DOPE, two different formulations that included DOPC were prepared as described in Section 4.2. Those formulations were intended to decrease the amount of Q_{Me}-DOPE and consequently decrease the leakage of liposomes when they come in contact with BSA or hNQO1. In addition, a calcein release experiment initiated by chemical reduction using dithionite (which resembles the reduction by hNQO1) was also performed with the aim to demonstrate that these liposome formulations also follow the proposed mechanism illustrated in Scheme 4.1. In Figure 4.13 is shown the absorbance spectrum for 90% Q_{Me}-DOPE/10% DOPC and 80% Q_{Me}-DOPE/20% DOPC liposomes. It is observed that both liposome formulations exhibited the peak at 264.9 nm that corresponds to the quinone head group and the peak at 497 nm that corresponds to the calcein encapsulated in the liposomes. In Figure 4.14 is revealed the behavior of 90% Q_{Me}-DOPE/10% DOPC and 80% Q_{Me}-DOPE/20% DOPC liposomes in the presence of BSA. The 90% Q_{Me}-DOPE/10% DOPC system had a calcein leakage of 40% in 66 min while 80% Q_{Me}-DOPE/20% DOPC liposomes had a calcein leakage of 13% in 3 hours and 31% in 11 hours and 24 min. Both examples show that decreasing the amount of Q_{Me}-DOPE helps to slow down the leakage process when BSA is present. The reasonable stability observed for 80% Q_{Me}-DOPE/20% DOPC liposomes in the presence of BSA, provides hope for testing the same system with hNQO1.

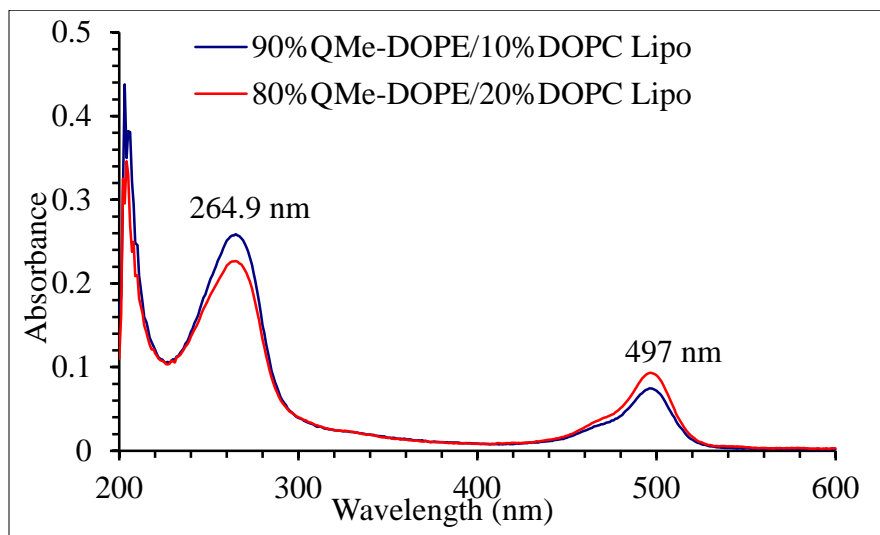


Figure 4.13. UV-vis absorbance spectrum of 90% Q_{Me}-DOPE/10% DOPC (blue line) and 80% Q_{Me}-DOPE/20% DOPC (red line) liposomes in pH 7.1 0.1 M PB/0.1 M KCl at room temperature. $\lambda_{\max} = 264.9$ nm corresponds to the Q_{Me} headgroup and $\lambda_{\max} = 497$ nm corresponds to the encapsulated calcein.

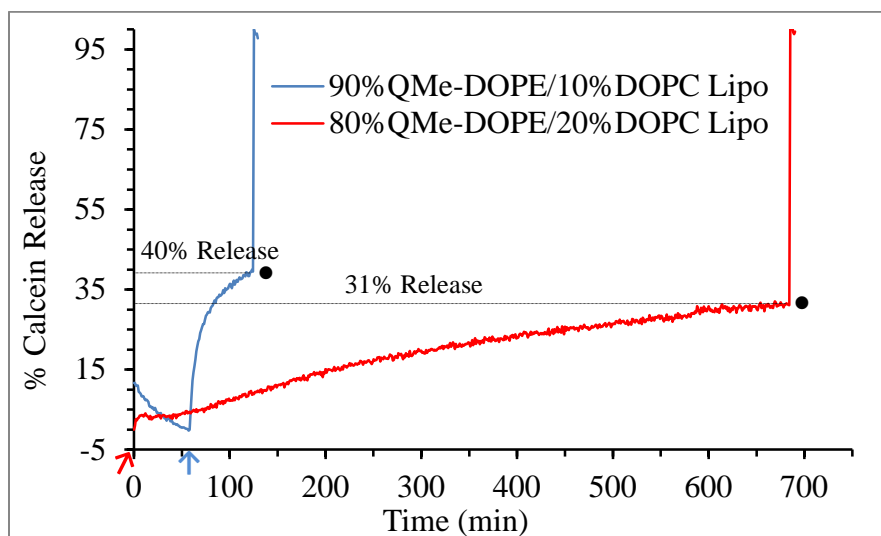


Figure 4.14. Unstable behavior of 100 μ M 90% Q_{Me}-DOPE/10% DOPC and 100 μ M 80% Q_{Me}-DOPE/20% DOPC liposomes in the presence of 0.007% BSA. (\uparrow) the time for addition of 300 μ L of 0.07% BSA solution into the 90% Q_{Me}-DOPE/10% DOPC liposome solution. (\uparrow) the addition time for 80% Q_{Me}-DOPE/20% DOPC liposomes into 0.007% BSA solution. (\bullet) time at which 90% Q_{Me}-DOPE/10% DOPC and 80% Q_{Me}-DOPE/20% DOPC liposomes were lysed with the addition of 15 μ L of 30% (v/v) Triton X-100.

In Figure 4.15 is displayed the behavior of 80% Q_{Me}-DOPE/20% DOPC liposomes in the presence of hNQO1. These liposomes experienced a calcein release of 48% in 70 min and 68% in 3 hours. Although these liposomes are not stable in the sole presence of the enzyme, the rate of leakage is decreased when compared with the previous liposome formulations that contained

Q_{Me} -DOPE. The inclusion of DOPC lipids in the liposome formulation resulted in reduced leakage in an inverse relationship, with more DOPC being present leading to less calcein release.

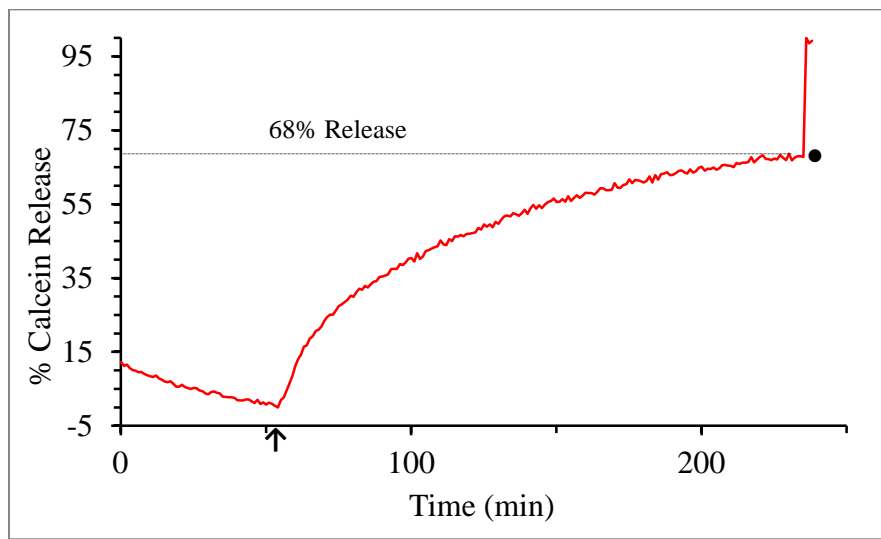


Figure 4.15. Instability of 100 μ M 80% Q_{Me} -DOPE/20% DOPC liposomes in the presence of 0.5 μ M hNQO1. (\uparrow) the addition time for 300 μ L of 5 μ M hNQO1 solution into liposome solution. (\bullet) time at which 80% Q_{Me} -DOPE/20% DOPC liposomes were lysed with the addition of 15 μ L of 30% (v/v) Triton X-100.

After performing the stability experiments, it was important to see how the Q_{Me} -DOPE/DOPC liposomes behave when they are opened by chemical reduction. In that way, I could predict the time that liposomes will take to open and deliver their cargo by the proposed mechanism, and see if adding more DOPC lipids to the liposome mixture was feasible. The calcein release curves for both formulations for sodium dithionite addition are shown in Figure 4.16. Upon introduction of the reducing agent into the liposome solution, a “lag” phase happened that corresponds to the reduction of the Q_{Me} headgroup and its detachment from the DOPE lipid. Such action initiates a bilayer destabilization (as labeled in Scheme 4.1), and subsequent opening of the liposome occurred as noticed by the increase in fluorescence intensity.

The 90% Q_{Me} -DOPE/10% DOPC liposomes exhibited a lag time of 31 minutes, and reached a maximum in 20 min, with a total calcein release of 63%. However, the 80% Q_{Me} -DOPE/20% DOPC liposomes experienced a lag time of 38 min and took 3 hours to reach the maximum with a total calcein release of 55%.

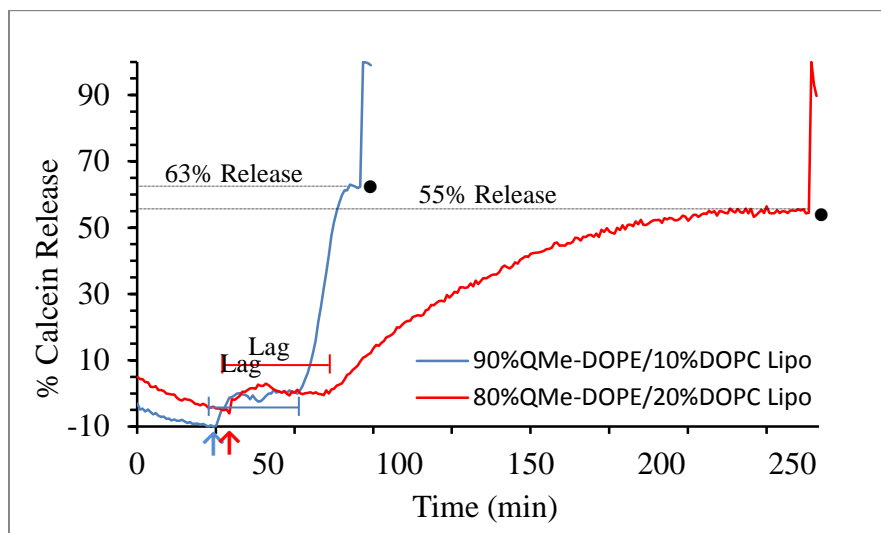


Figure 4.16. Calcein release curves of 100 μM 90% $\text{Q}_{\text{Me}}\text{-DOPE}/10\%$ DOPC and 100 μM 80% $\text{Q}_{\text{Me}}\text{-DOPE}/20\%$ DOPC by chemical reduction using 5 eq. of sodium dithionite. (\uparrow) the time for addition of sodium dithionite solution into the 90% $\text{Q}_{\text{Me}}\text{-DOPE}/10\%$ DOPC liposome solution. (\uparrow) the time for addition of sodium dithionite solution into the 80% $\text{Q}_{\text{Me}}\text{-DOPE}/20\%$ DOPC liposome solution. (\bullet) time at which 90% $\text{Q}_{\text{Me}}\text{-DOPE}/10\%$ DOPC and 80% $\text{Q}_{\text{Me}}\text{-DOPE}/20\%$ DOPC liposomes were lysed with the addition of 15 μL of 30% (v/v) Triton X-100.

The increase in DOPC content from 10% to 20% in the liposome formulation caused the lag time to rise by 7 minutes and the time to reach maximum contents release to be reached 160 min later. The important decrease in the rate at which calcein is released required me to take a different approach for the formulation of $\text{Q}_{\text{Me}}\text{-DOPE}$ liposomes, because it was anticipated that the amount of DOPC content necessary to make the system more stable toward proteins will create liposomes not suitable for hNQO1 enzyme assay (too slow to open).

4.3.1.5 Liposomes Composed of 70% $\text{Q}_{\text{Me}}\text{-DOPE}/30\%$ Cholesterol (CHO)

The results in Section 4.3.1.4 directed me to look for a new liposome system that is stable in the presence of BSA and hNQO1. A review by Pagano and Weinstein published in 1978 described that up to 50% of cholesterol can be added to liposomes to decrease their leakage.²⁵ It was also mentioned in the literature that the addition of CHO decreases liposome fluidity and permeability of contents across the membrane.^{25,26} CHO-containing liposomes were prepared as described in Section 4.2. In Figure 4.17 is shown the absorbance spectrum for 70% $\text{Q}_{\text{Me}}\text{-DOPE}/30\%$ CHO liposomes and as seen previously no unpredicted peaks are present.

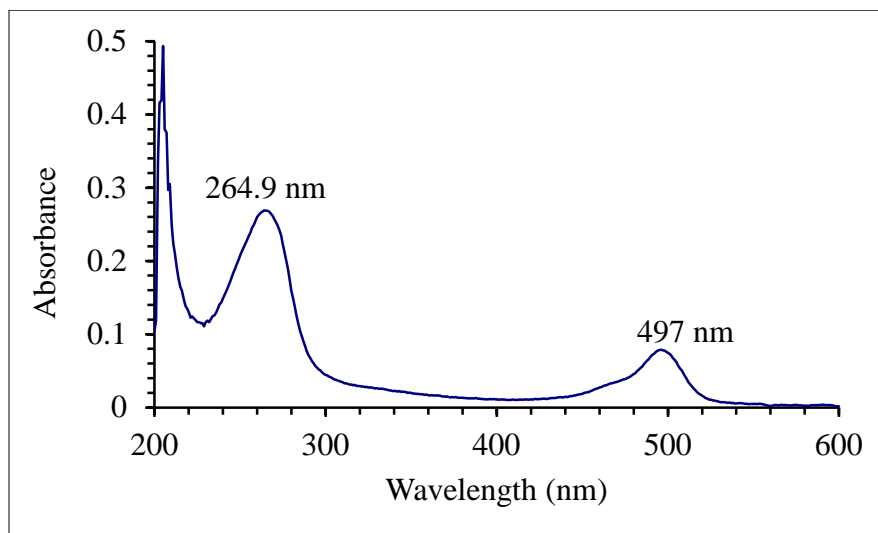


Figure 4.17. UV-vis absorbance spectrum of 70% Q_{Me}-DOPE/30% CHO liposomes in pH 7.1 0.1 M PB/0.1 M KCl at room temperature. $\lambda_{\text{max}} = 264.9$ nm corresponds to the Q_{Me} headgroup and $\lambda_{\text{max}} = 497$ nm corresponds to the encapsulated calcein.

To make sure that CHO does not prevent liposomes from opening, the calcein release profile of 70% Q_{Me}-DOPE/30% CHO liposomes opened by chemical reduction was investigated. In Figure 4.18 are presented the calcein release curves for 70% Q_{Me}-DOPE/30% CHO liposomes caused by sodium dithionite. Upon introduction of the reducing agent into the liposomes solution, a “lag” phase is noted where the reduction of the Q_{Me} headgroup and its detachment from the DOPE lipid occurs. Such action initiates bilayer destabilization (as labeled in Scheme 4.1) and opening of the liposome as noticed by the increase in fluorescence intensity. The current liposome system exhibited a lag time of 27 min and took 12 min to reach the fluorescence maximum with an average calcein release of 71%. It is interesting to notice that when cholesterol was included in the mixture, the release of contents happened much faster than when DOPC was present at the same level in the formulation. In addition, the “lag” phase differed a little in shape from the one observed for Q_{Me}-DOPE/DOPC liposomes in Figure 4.16.

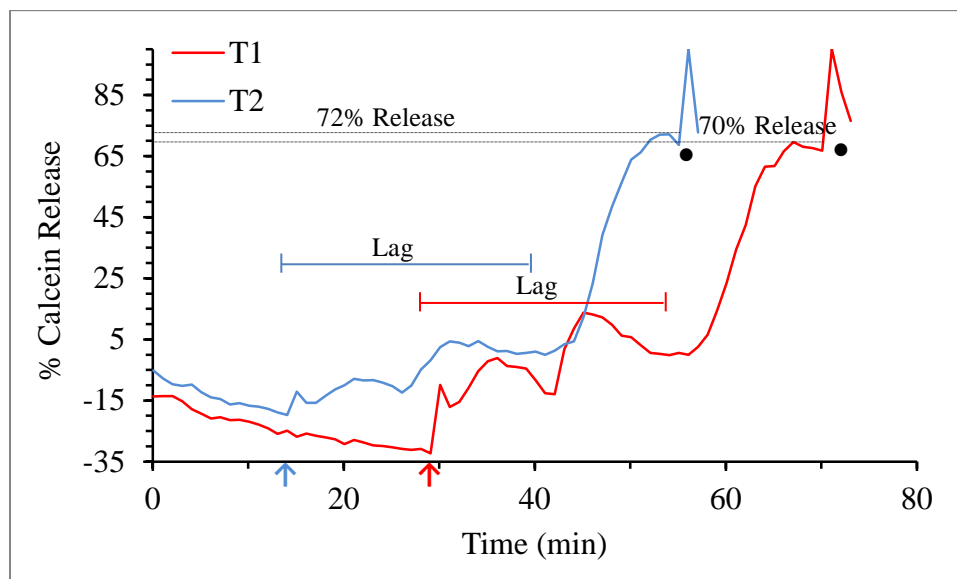


Figure 4.18. Calcein release curves of 100 μM 70% Q_{Me} -DOPE/30% CHO by chemical reduction using 5 eq. of sodium dithionite. The arrows (\uparrow and \uparrow) depict the time for addition of sodium dithionite solution into the 70% Q_{Me} -DOPE/30% CHO liposome solution for each trial. (\bullet) time at which 70% Q_{Me} -DOPE/30% CHO liposomes were lysed with the addition of 15 μL of 30% (v/v) Triton X-100.

After confirming that the CHO-containing liposomes opened upon chemical reduction, stability experiments were performed on these systems. As a rule, the first experiment made on the new liposome system was to test the integrity of it in the presence of BSA. In Figure 4.19 is shown the behavior of 70% Q_{Me} -DOPE/30% CHO liposomes in the presence of BSA. As it was expected, calcein leakage was lower than in the other formulations with a 15% in 1 hour and 20% in 3 hours and 10 min. The favorable results with liposomes containing CHO agreed with the statement previously made on the mechanism of action of cholesterol by other scientists because its inclusion diminished the penetration of the BSA molecules into the lipid bilayer resulting in less leakage of liposome contents.²⁶

After the satisfactory behavior of the liposomes with BSA, the next obvious step was to test them with hNQO1. Displayed in Figure 4.20 is presented the behavior of 70% Q_{Me} -DOPE/30% CHO liposomes with hNQO1. Unfortunately, the enzyme still caused a liposome leakage of 47% in 1 hour and 61% in 3 hours.

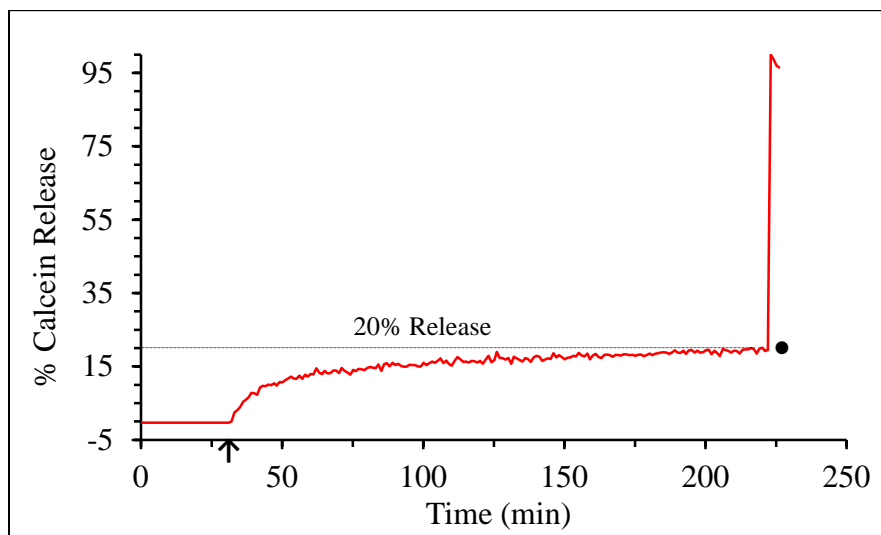


Figure 4.19. Instability of 100 μM 70% Q_{Me} -DOPE/30% CHO liposomes in the presence of 0.007% BSA. (\uparrow) the time for addition of liposome solution into the 0.007% BSA solution. (\bullet) time at which 70% Q_{Me} -DOPE/30% CHO liposomes were lysed with the addition of 15 μL of 30% (v/v) Triton X-100.

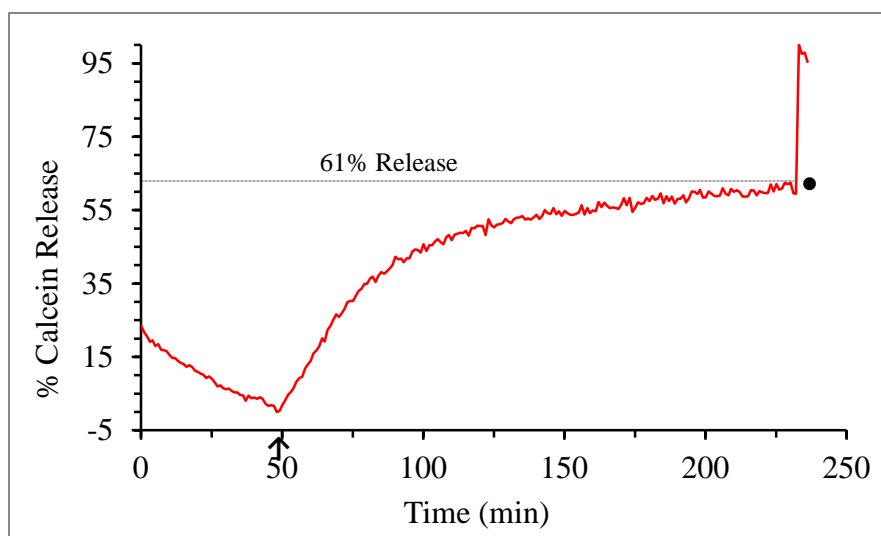


Figure 4.20. Instability of 100 μM 70% Q_{Me} -DOPE/30% CHO liposomes in the presence of 0.5 μM hNQO1. (\uparrow) the addition time for 300 μL of 5 μM hNQO1 solution into liposome solution. (\bullet) time at which 70% Q_{Me} -DOPE/30% CHO liposomes were lysed with the addition of 15 μL of 30% (v/v) Triton X-100.

The difference in observed behavior between BSA and hNQO1 with the CHO-liposomes confirmed the previous hypothesis of the mechanisms in which the proteins interact with the liposome system. For BSA, it is clear that hydrophobic interactions are the driving force in the BSA-liposome contact. On the other hand, hNQO1 attacks the liposomes by electrostatic

interactions or by just embracing the quinone headgroup which causes bilayer destabilization and liposome leakage.

A series of 3 experiments was performed on 100% Q_{Me}-DOPE liposomes to have more knowledge about the mode of interaction between hNQO1 and the liposomes. The first experiment corresponds to the interaction of inhibited hNQO1 with the liposomes. 100% Q_{Me}-DOPE liposomes were assayed with 0.25 μM hNQO1 and also with inhibited 0.25 μM hNQO1. Human NQO1 is known to be completely inhibited by ES936, an inhibitor that alkylates one of the tyrosine residues in the active site of the enzyme.^{27,28} The results of UV-vis experiments for Q_{Me}-COOH (quinone headgroup of the Q_{Me}-DOPE lipid), hNQO1, NADH and ES936 confirmed the mode of action of ES936, as seen in Figure 4.21. If hNQO1 inhibition prevents liposome leakage, then it will be clear that the mechanism of action of hNQO1 is the embracing of the quinone headgroup by the enzyme.

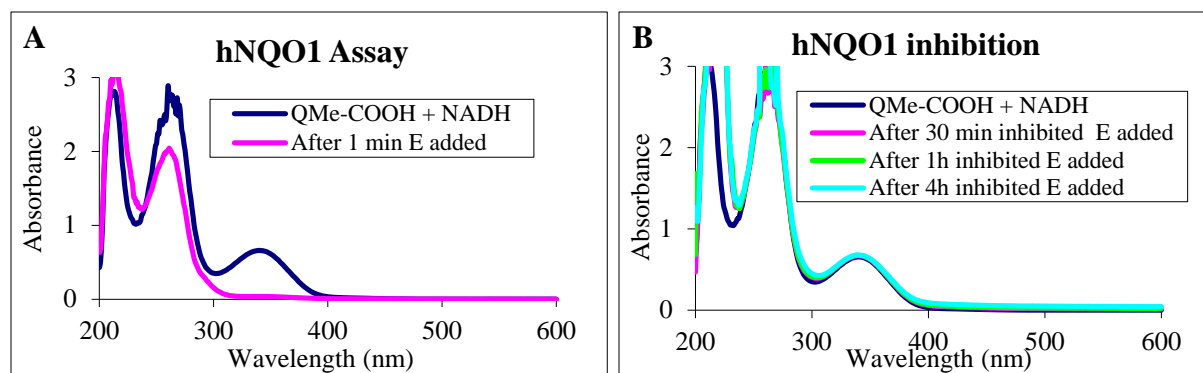


Figure 4.21. UV-vis spectra for hNQO1 assay (A) and hNQO1 inhibition assay (B). A) Q_{Me}-COOH and NADH (blue line) and Q_{Me}-COOH and NADH and hNQO1 after 1 min (pink line). B) Q_{Me}-COOH and NADH (blue line) and Q_{Me}-COOH and NADH and hNQO1 after 30 min (pink line), after 1 hour (green line) and after 4 hours (cyan line).

The behavior of 100% Q_{Me}-DOPE liposomes with inhibited hNQO1 is shown in Figure 4.22. It is clear that inhibition of hNQO1 by ES936 did not preclude the enzyme from causing a liposome leakage as noted by the observed 56% release of contents in 2 hours and 3 min, while 54% calcein leakage was seen with the non-inhibited hNQO1.

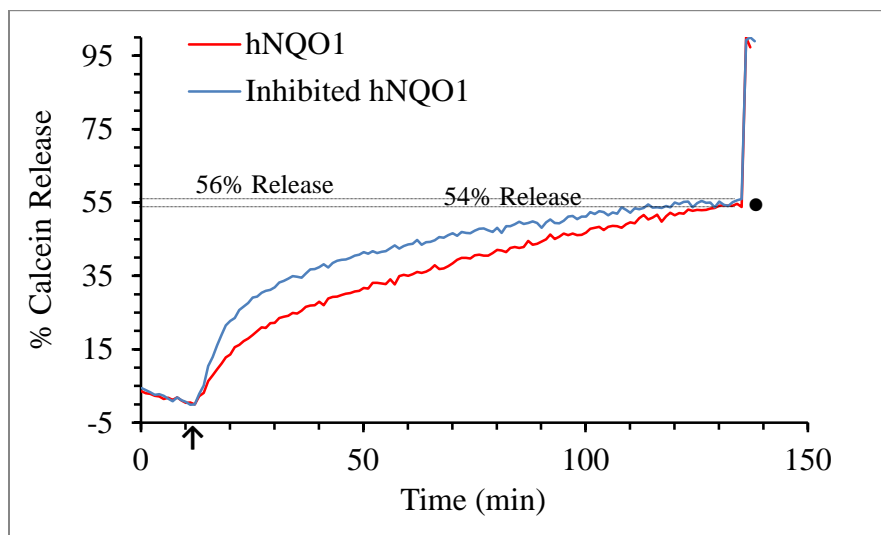


Figure 4.22. Instability of 100 μM 100% Q_{Me} -DOPE liposomes in the presence of 0.25 μM hNQO1 (red line) and 0.25 μM inhibited hNQO1 (blue line). (\uparrow) the addition time for 300 μL of 2.5 μM hNQO1 or inhibited hNQO1 solution into liposome solution. (\bullet) time at which 100% Q_{Me} -DOPE liposomes were lysed with the addition of 15 μL of 30% (v/v) Triton X-100.

A second experiment to see if electrostatic interaction was the factor of attraction between hNQO1 (isoelectric point of 8.91)²² and the 100% Q_{Me} -DOPE liposomes was performed using the human enzyme NQO2 with an isoelectric point of 5.87 that will have a negative charge under the experimental conditions.²² The protein sequences of hNQO1 and hNQO2 can be aligned without insertions or deletions, and are 49% identical over their shared length.^{29,30} The major differences are that hNQO2 is 43 amino acids shorter than hNQO1 at the C-terminal domain and 10 amino acids present at the C-terminal domain of hNQO2 have no sequence homology with the corresponding residues in hNQO1.^{29,30} Also hNQO2 uses dihydronicotinamide riboside (NRH) instead of NAD(P)H as an electron donor.^{29,30} Therefore, the active sites of hNQO1 and hNQO2, both having the FAD prosthetic group are very similar in nature. If hNQO2 provokes liposome leakage, then electrostatic interactions would not be the driving force for the hNQO1-liposome interactions.

In Figure 4.23 is shown the behavior of hNQO2 versus hNQO1 in the presence of 100% Q_{Me} -DOPE liposomes. hNQO1 caused a calcein leakage of 54% in 2 hours and 3 min while hNQO2 caused a calcein leakage of 37% in the same amount of time. It is clear that hNQO2

caused liposome leakage in a very similar manner to that of hNQO1, indicating that the quinone is the reason why liposomes open in the presence of these enzymes and not surface charge interactions.

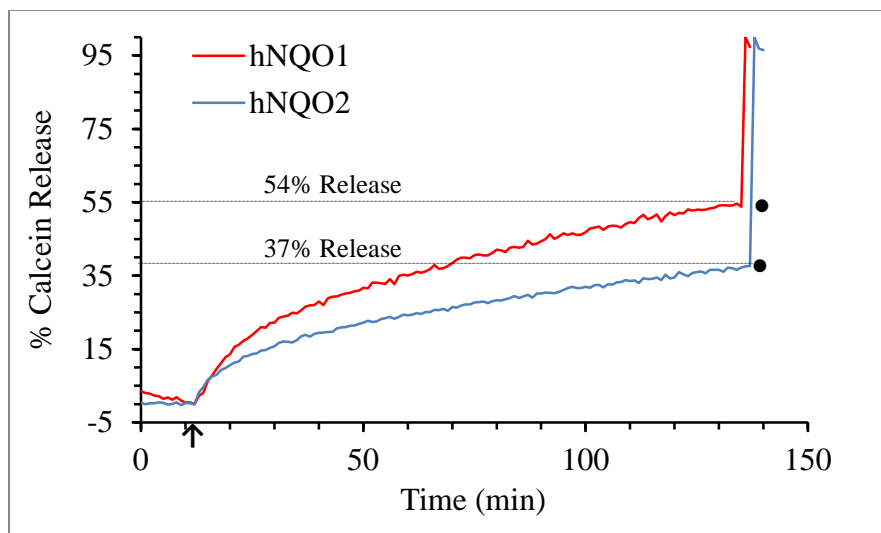


Figure 4.23. Instability of 100 μM 100% Q_{Me} -DOPE liposomes in the presence of 0.25 μM hNQO1 (red line) and 0.25 μM hNQO2 (blue line). (\uparrow) the addition time for 300 μL of 2.5 μM hNQO1 or hNQO2 solution into liposome solution. (\bullet) time at which 100% Q_{Me} -DOPE liposomes were lysed with the addition of 15 μL of 30% (v/v) Triton X-100.

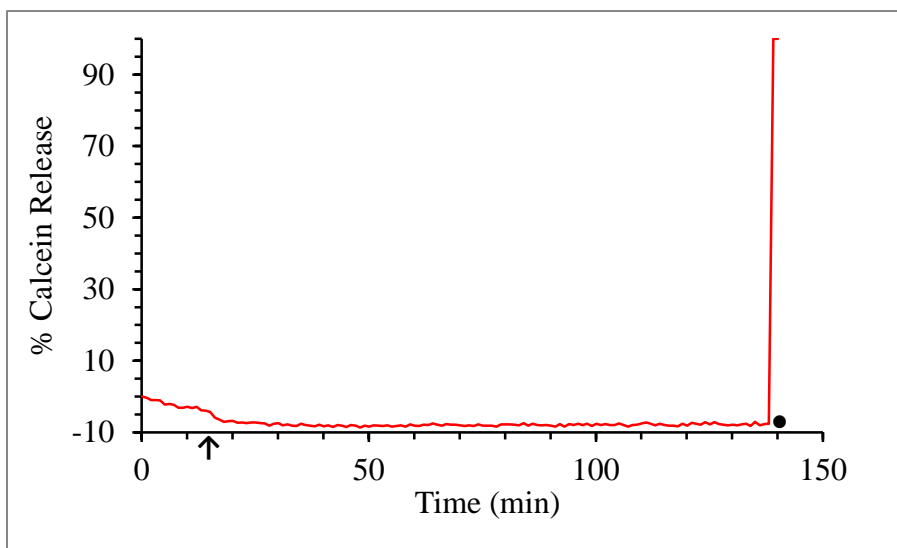


Figure 4.24. Stability of 100 μM 100% Q_{Me} -DOPE liposomes in the presence of 0.25 μM heat inactivated hNQO1. (\uparrow) the addition time for 300 μL of 2.5 μM heat inactivated hNQO1 solution into liposome solution. (\bullet) time at which 100% Q_{Me} -DOPE liposomes were lysed with the addition of 15 μL of 30% (v/v) Triton X-100.

The last experiment of the series of 3 performed on the 100% Q_{Me} -DOPE liposomes was heat inactivation of hNQO1 and its behavior with the liposomes. In Figure 4.24 is shown no

content release for Q-DOPE liposomes in the presence of heat-inactivated hNQO1, indicating that the active site of the enzyme is the one responsible for the calcein leakage from the 100% Q_{Me}-DOPE liposomes. These three experiments performed on 100% Q_{Me}-DOPE liposomes demonstrate that the mechanism of interaction between hNQO1 and quinone-based liposomes is through the quinone head group.

In summary, after examining all the quinone-based liposome formulations, there is still the need of a stable system in the sole presence of hNQO1.

4.3.2 DLS and Zeta Potential of Q-DOPE Liposome Systems

Liposome diameters and surface charge were measured for each of the liposome systems to help me understand the interaction of BSA and hNQO1 with liposomes. In Table 4.1 are presented the average values of diameter and zeta potential for each system.

In general, the Q_{Me}-DOPE liposome systems fall in the expected range of 100–120 nm, as previously reported in the McCarley group.^{10,13} DOPC liposomes are almost identical in diameter to the 100% Q_{Me}-DOPE liposomes, with values that overlap considering the error associated with them. The equal value in diameter between the liposome systems indicates that the size of the liposomes has no effect on their interaction with the proteins.

Table 4.1 Average diameters and zeta potentials of Q_{Me}-DOPE liposome systems. Experiments performed at 25 °C in pH 7.1 0.1M PB/0.1M KCl. Results are the average of 3 determinations ± one standard deviation. ^aPolydispersity indexes ≤ 0.3 are considered acceptable. ^bReference 2; pH 7.4 0.05 M PB/0.075 M KCl. ^cMeasurement done by Dr. Martin Loew.

Liposome System	Avg. Diameter (nm)	Avg. PDI ^a	Avg. Zeta Potential (mV)
100% Q _{Me} -DOPE	123±1	0.06±0.02	-60±3 ^b
97% Q _{Me} -DOPE / 3% PEG ₂₀₀₀ -DOPE	117±1 ^c	0.12±0.01 ^c	not measured
100% DOPC	126±3	0.06±0.02	-7±2
90% Q _{Me} -DOPE / 10% DOPC	112±1	0.08±0.02	-48±4
80% Q _{Me} -DOPE / 20% DOPC	119±1	0.09±0.01	-52±2
70% Q _{Me} -DOPE / 30% CHO	119±2	0.20±0.05	-50±3

The surface charge values for all the Q_{Me} -DOPE liposome systems measured in pH 7.1 0.1 M PB/0.1 M KCl ranged between -44 to -53 mV. The zeta potential of 100% Q_{Me} -DOPE liposome system (-60 mV) was measured by a colleague in 0.05 M PB/0.075 M KCl pH 7.4.¹⁰ The surface charge of DOPC was measured to be -7 mV, much less negative than the systems that included Q_{Me} -DOPE. The consistency of negative surface charge in all Q_{Me} -DOPE liposome systems is an indicative of the potent attraction of hNQO1 (isoelectric point 8.91)²² at pH 7.1 to those liposomes; interaction that is not observed with DOPC liposomes. It also supports the hypothesis that BSA (isoelectric point 4.5–4.7)^{19,20} would rather interact with the Q_{Me} -DOPE liposome systems by penetrating into the lipid bilayer (hydrophobic interactions) than by surface charge interactions.

4.4 Conclusions

Five different liposome formulations containing Q_{Me} -DOPE and one containing 100% DOPC were tested against the common components of an hNQO1 assay. To my disappointment, none of the formulations were completely stable in the presence of BSA or hNQO1. However, important conclusions can be made from the results obtained, and they are summarized in Table 4.2. All the liposomes systems had an average diameter between 100 and 130 nm as previously seen in the McCarley group for similar systems.¹⁰ Also, the liposome systems containing Q_{Me} -DOPE lipids experienced a negative surface charge between -44 and -53 mV, while 100% DOPC liposomes presented an almost neutral surface charge of -7 mV. After examining the stability experiments, it is clear that the inclusion of the Q_{Me} headgroup facilitates the interaction of BSA with the lipid membrane as seen by the absence of leakage of DOPC liposomes. Likewise, the interaction of hNQO1 with the liposomes is also mediated by the presence of Q_{Me} headgroup as seen by the different experiments performed on the quinone based liposome systems. The chemical release profiles of new quinone-based liposome systems were investigated and different results were seen depending on the nature of the liposome components.

The liposomal formulation with 10% DOPC and 90% QMe-DOPE presented a much faster calcein release rate than the formulation with 20% DOPE and 80% QMe-DOPE (63% in 20 min versus 55% in 3 hours). From these results I can infer that only a 10% increase in DOPC content caused significant changes on the mechanism of release of the liposomes. On the other hand, the inclusion of 30% of cholesterol in the liposome mixture did not decrease the rate of calcein release (71% in 12 min) but did affect the mechanism of release as concluded by comparing these release profiles versus the chemical release profile for 100% Q_{Me}-DOPE liposomes performed by a colleague in the McCarley group at pH 7.4 0.05 M PB/0.075 M KCl.¹³ The examination of a variety of liposome formulations reflected the important quality of liposome that it is its versatility to change the outcome by incorporation of different lipids. This versatility can be explored further with the aim of finding a liposomal formulation that would only open by the mechanism described in Scheme 4.1.

4.5 References

- (1) Asche, C., Antitumour Quinones. *Mini-Rev. Med. Chem.* **2005**, 5 (5), 449-467.
- (2) Jaffar, M.; Abou-Zeid, N.; Bai, L.; Mrema, I.; Robinson, I.; Tanner, R.; Stratford, I. J., Quinone Bioreductive Prodrugs as Delivery Agents. *Curr. Drug Delivery* **2004**, 1, 345-350.
- (3) Chen, Y.; Hu, L. Q., Design of Anticancer Prodrugs for Reductive Activation. *Med. Res. Rev.* **2009**, 29 (1), 29-64.
- (4) Cresteil, T.; Jaiswal, A. K., High-Levels of Expression of the Nad(P)H-Quinone Oxidoreductase (Nqo1) Gene in Tumor-Cells Compared to Normal-Cells of the Same Origin. *Biochem. Pharmacol.* **1991**, 42 (5), 1021-1027.
- (5) Siegel, D.; Franklin, W. A.; Ross, D., Immunohistochemical Detection of Nad(P)H : Quinone Oxidoreductase in Human Lung and Lung Tumors. *Clin. Cancer Res.* **1998**, 4 (9), 2065-2070.

Table 4.2. Summarized results from calcein release, DLS, and zeta potential experiments performed on Q_{Me}-DOPE liposome systems at 25 °C in pH 7.1 0.1 M PB/0.1 M KCl. ^aReference 2; pH 7.4 0.05 M PB/0.075 M KCl. ^bMeasurement done by Dr. Martin Loew.

	100%Q _{Me} -DOPE	97%Q _{Me} -DOPE 3%PEG ₂₀₀₀	100%DOPC	90%Q _{Me} -DOPE 10% DOPC	80%Q _{Me} -DOPE 20% DOPC	70%Q _{Me} -DOPE 30% CHO
0.007%BSA	50% in 3h	60% in 3h	Stable for 17 h	40% in 1h 6 min	13% in 3 h	20% in 3h 10 min
100 μM NADH	Stable for 18 h					
0.5 μM hNQO1		80% in 1h 10 min	Stable for 15 h		48% in 1h 10 min	47% in 1h
0.5 μM hNQO1 100 μM NADH		77% in 1h 10 min				
0.25 μM hNQO1	54% in 2h 3 min					
0.25 μM hNQO2	37% in 2h 3 min					
0.25 μM inhibited hNQO1	56% in 2h 3 min					
5 eq. Na ₂ S ₂ O ₄				31 min lag time 20 min reach max 63% in 20 min	38 min lag time 3h reach max 55% in 3h	27 min lag time 12 min reach max 71% in 12 min
Diameter (nm)	123±1 (n=3)	117±1 ^b (n=3)	126±3 (n=3)	112±1 (n=3)	119±1 (n=3)	119±2 (n=3)
Zeta Pot. (mV)	-60±3 ^a (n=3)		-7±2 (n=3)	-48±4 (n=3)	-52±2 (n=3)	-50±3 (n=3)

- (6) Siegel, D.; Ross, D., Immunodetection of Nad(P)H : Quinone Oxidoreductase 1 (Nqo1) in Human Tissues. *Free Radical Biol. Med.* **2000**, *29* (3-4), 246-253.
- (7) Jamieson, D.; Wilson, K.; Pridgeon, S.; Margetts, J. P.; Edmondson, R. J.; Leung, H. Y.; Knox, R.; Boddy, A. V., Nad(P)H : Quinone Oxidoreductase1 and Nrh : Quinone Oxidoreductase 2 Activity and Expression in Bladder and Ovarian Cancer and Lower Nrh : Quinone Oxidoreductase 2 Activity Associated with an Nqo2 Exon 3 Single-Nucleotide Polymorphism. *Clin. Cancer Res.* **2007**, *13* (5), 1584-1590.
- (8) Ong, W.; Yang, Y. M.; Cruciano, A. C.; McCarley, R. L., Redox-Triggered Contents Release from Liposomes. *J. Am. Chem. Soc.* **2008**, *130* (44), 14739-14744.
- (9) Ernster, L., Dt-Diaphorase - a Historical Review. *Chem. Scripta* **1987**, *27A*, 1-13.
- (10) Carrier, N. H. Redox-Active Liposome Delivery Agents with Highly Controllable Stimuli-Responsive Behavior. Ph.D. Dissertation, Louisiana State University, Baton Rouge, LA, 2011.
- (11) Szoka, F.; Papahadjopoulos, D., Comparative Properties and Methods of Preparation of Lipid Vesicles (Liposomes). *Annu. Rev. Biophys. Bio.* **1980**, *9*, 467-508.
- (12) Avanti Polar Lipids. <http://avantilipids.com/>.
- (13) Forsythe, J. Kinetics and Mechanisms of Release by Redox-Active Liposomes in Drug Delivery. Ph.D. Dissertation, Louisiana State University, Baton Rouge, LA, 2011.
- (14) Ernster, L.; Ljunggren, M.; Danielson, L., Dt Diaphorase .1. Purification from Soluble Fraction of Rat-Liver Cytoplasm, and Properties. *Biochim. Biophys. Acta* **1962**, *58* (2), 171-188.
- (15) Kim, C.-K.; Kim, H.-S.; Lee, B.-J.; Han, J.-H., Effect of Bovine Serum Albumin on the Stability of Methotrexate-Encapsulated Liposomes. *Arch. Pharm. Res.* **1991**, *14* (4), 336-341.
- (16) Szoka, F. C.; Guo, X., Steric Stabilization of Fusogenic Liposomes by a Low-Ph Sensitive Peg-Diortho Ester-Lipid Conjugate. *Bioconjugate Chem.* **2001**, *12* (2), 291-300.
- (17) Lasic, D. D.; Needham, D., The “Stealth” Liposome: A Prototypical Biomaterial. *Chem. Rev.* **1995**, *95* (8), 2601-2628.

- (18) Moghimi, S. M.; Szebeni, J., Stealth Liposomes and Long Circulating Nanoparticles: Critical Issues in Pharmacokinetics, Opsonization and Protein-Binding Properties. *Prog. Lipid Res.* **2003**, *42* (6), 463-478.
- (19) Sweet, C.; Zull, J. E., The Binding of Serum Albumin to Phospholipid Liposomes. *Biochim. Biophys. Acta* **1970**, *219*, 253-262.
- (20) Wilkins, D. J.; Ottewill, R. H., On the Flocculation of Sheep Leucocytes: 1. Electrophoretic Studies. *J. Theor. Biol.* **1962**, *2* (2), 165-175.
- (21) Sweet, C.; Zull, J. E., Activation of Glucose Diffusion from Egg Lecithin Liquid Crystals by Serum Albumin. *Biochim. Biophys. Acta* **1969**, *173* (1), 94-103.
- (22) Phosphositeplus Homepage. <http://www.phosphosite.org/proteinAction.do?id=14721>.
- (23) Hafez, I. M.; Cullis, P. R., Roles of Lipid Polymorphism in Intracellular Delivery. *Advanced Drug Delivery Reviews* **2001**, *47* (2-3), 139-148.
- (24) Pak, C. C.; Ali, S.; Janoff, A. S.; Meers, P., Triggerable Liposomal Fusion by Enzyme Cleavage of a Novel Peptide-Lipid Conjugate. *Biochim. Biophys. Acta* **1998**, *1372* (1), 13-27.
- (25) Pagano, R. E.; Weinstein, J. N., Interactions of Liposomes with Mammalian Cells. *Annu. Rev. Biophys. Bio.* **1978**, *7*, 435-468.
- (26) Kim, C.-K.; Park, D.-K., Stability and Drug Release Properties of Liposomes Containing Cytarabine as a Drug Carrier. *Arch. Pharm. Res.* **1987**, *10* (2), 75-79.
- (27) Winski, S. L.; Faig, M.; Bianchet, M. A.; Siegel, D.; Swann, E.; Fung, K.; Duncan, M. W.; Moody, C. J.; Amzel, L. M.; Ross, D., Characterization of a Mechanism-Based Inhibitor of Nad(P)H: Quinone Oxidoreductase 1 by Biochemical, X-Ray Crystallographic, and Mass Spectrometric Approaches. *Biochemistry* **2001**, *40* (50), 15135-15142.
- (28) Reigan, P.; Colucci, M. A.; Siegel, D.; Chilloux, A.; Moody, C. J.; Ross, D., Development of Indolequinone Mechanism-Based Inhibitors of Nad(P)H : Quinone Oxidoreductase 1 (Nqo1): Nqo1 Inhibition and Growth Inhibitory Activity in Human Pancreatic Mia Paca-2 Cancer Cells. *Biochemistry* **2007**, *46* (20), 5941-5950.

- (29) Wu, K. B.; Knox, R.; Sun, X. Z.; Joseph, P.; Jaiswal, A. K.; Zhang, D.; Deng, P. S. K.; Chen, S., Catalytic Properties of Nad(P)H:Quinone Oxidoreductase-2 (Nqo2), a Dihyronicotinamide Riboside Dependent Oxidoreductase. *Arch. Biochem. Biophys.* **1997**, 347 (2), 221-228.
- (30) Foster, C. E.; Bianchet, M. A.; Talalay, P.; Zhao, Q. J.; Amzel, L. M., Crystal Structure of Human Quinone Reductase Type 2, a Metalloflavoprotein. *Biochemistry* **1999**, 38 (31), 9881-9886.

CHAPTER 5

CONCLUSIONS AND OUTLOOK

5.1 Summary

The ultimate goal of this research was the development of an enzyme-responsive liposome system composed of a fusogenic lipid, DOPE, capped with a quinone headgroup that is potentially capable of selectively delivering its contents at a desired tumor site. In this system, the stimulus was the human reductive enzyme NAD(P)H:quinone oxidoreductase type-1 (hNQO1) that is over-expressed in certain tumor tissues.¹⁻⁴ The hypothesized mechanism involves the interaction of hNQO1 with the liposomes via initial reduction of the quinone headgroup (quinone triggers), followed by cyclization of the corresponding hydroquinone moiety, subsequent bilayer destabilization, and contents release. Characterization of the quinone trigger groups was important to elucidate the electronic properties, kinetic profiles, and active site orientation of these triggers before attachment to the lipid that would be used to form liposomes.

An electrochemical technique named cyclic voltammetry was used to determine the reduction potential and cyclization rates of electrochemically-active quinones in aqueous media. It was found that naked quinones (no propionic acid handle) are electrochemically quasireversible systems because the difference in the anodic and cathodic peak potentials deviates from the ideal value of 30 mV. It was also observed that benzoquinone was the naked quinone easiest to be reduced (most positive reduction potential), whereas in the substituted benzoquinone series, addition of electron-withdrawing groups resulted in more positive reduction potentials, while addition of electron-donating groups resulted in more negative potentials. In the propionic acid quinone series, most of the systems were found to be electron-transfer irreversible with peak separations over 200 mV. As observed for the naked quinones, propionic acid quinones with electron-withdrawing groups displayed a less negative reduction

potential, while the inverse happened when electron-donating groups were present. It was also elucidated that the presence of a propionic acid handle on the quinone moiety made the reduction of the quinone more difficult (more negative reduction potential), and that difficulty increased as geminal methyls were added or when the whole trimethyl-lock unit was present. Interestingly, the nature of the propionic acid handle did not affect the electronic properties of the quinone derivatives based on the results obtained for Q_{Me} -COOH and Q_{Me} -ETA. In addition to the thermodynamic parameters of quinones, the cyclization rate for the disappearance of the corresponding hydroquinone after quinone reduction was determined. The higher cyclization rates corresponded to the quinones containing the trimethyl-lock moiety, in particular the ones with a methyl, an iodine or a bromine group at the 2-position of the quinone ring. Moreover, an enhancement in the cyclization rate was observed when buffer concentration was increased. Cyclic voltammetry studies on Q_{Me} -COOH at various salt concentrations revealed no change in the cyclization rate.

Solution-phase enzyme kinetics and molecular docking studies were applied to a variety of quinone propionic acid derivatives with the aim of establishing quinone-hNQO1 interactions. These quinone derivatives were divided in three groups: 1) trimethyl-lock quinones varying the functional group at the 2-position on the quinone, 2) quinones not possessing the trimethyl-lock unit vs. quinones with the trimethyl-lock unit, and 3) charged versus neutral quinones. In the first group, it was found that quinones with a hydrogen or halogen group presented higher affinity and faster turnover rates toward the enzyme, while quinones with an electron-donating group (methyl or methoxy) presented lower affinity and slower turnover rates. Docking studies in this group revealed that all quinones laid parallel to the isoalloxazine ring, with a slight variance in orientation and that the bromine analog was positioned deepest in the enzyme active site. In the second group, it was clear that quinones with no trimethyl-lock unit presented higher affinity and good turnover rates. Moreover, $Q_{nogenMe}$ -COOH, which is in this group, was the

best substrate for hNQO1 among all the quinone derivatives studied. It was found that Q_{nogemMe^-} -COOH was the one quinone located closest to the isoalloxazine ring in the enzyme active site. In the third group, no change in binding affinity was observed between quinones. However, the neutral quinone exhibited a higher turnover rate with respect to the charged quinone. Superimposed images of these two derivatives exposed that the neutral quinone is located deeper in the enzyme active site than the charged quinone. In addition, from all the quinone derivatives analyzed with docking, the preferable atom acceptor for hydride transfer appears to be the carbon atom (next to the carbonyl on the opposite side of the propionic acid handle) based on the distance measured from the N₅ atom of FAD and the closer atoms in the quinone ring. Docking studies also unveiled no strong correlation between the theoretical binding energies and the experimental binding affinities.

Finally, quinone triggers were characterized and ready to use in the design of enzyme-responsive liposomes. $Q_{\text{Me}}\text{-COOH}$ was the only quinone trigger group used to form a variety of liposome systems. Stability studies on five quinone-based liposome formulations and one DOPC liposome formulation in the presence of hNQO1 common assay components were accomplished. DLS, zeta potential and chemical release curves on the liposome formulations were also performed. The liposomal formulation containing only $Q_{\text{Me}}\text{-DOPE}$ was stable in the presence of NADH. None of the quinone-based liposomal formulations designed to date were stable under the individual presence of BSA or hNQO1. Conversely, liposomes composed of only DOPC were stable in the presence of BSA and hNQO1. Inclusion of DOPC lipids or cholesterol in the quinone-based liposome formulation resulted in alterations of their chemical release profiles compared with the chemical release profile for a 100% $Q_{\text{Me}}\text{-DOPE}$ liposome reported previously. All quinone-based liposomes had an average diameter between 110 and 124 nm and a zeta potential between -48 and -60 mV. The diameter of the DOPC liposomes was 126 nm, and its zeta potential was -7 mV.

5.2 Conclusions

The results of this research demonstrated that the electronic properties of quinone derivatives can successfully be tuned by addition of various functional groups, as well as by inclusion of structural changes such as a handle. Quinone triggers followed a qualitative trend where electron-donating groups retarded the turnover rate with respect to hNQO1 while the opposite happened with the inclusion of electron-withdrawing groups. Docking studies qualitatively predicted the position of the quinone triggers, and the trend was in agreement with the kinetic outcomes. The best substrate for hNQO1 corresponds to the quinone located closer to the isoalloxazine ring of FAD in the active site of hNQO1. All quinone-based liposomes were destabilized and leaky after addition of BSA or hNQO1. It is believed that the key factor for the leakage of liposomes is the quinone headgroup. Modifying quinone-based liposomes by inclusion of other lipid components can result in a formulation able to release its contents in a controllable manner.

5.3 Outlook

Carving through the last 20 years of literature, it is clear that a great deal of research is focused on prodrugs and carriers for triggerable drug release. Also there is extensive literature on the structure-activity relationships between antitumor quinones and NQO1 for the development of new prodrug systems. Nevertheless, few prodrugs are currently being marketed and no triggerable drug delivery liposomal system has made it to clinical use.⁵⁻⁹

The detailed information provided in this dissertation on simple quinone triggers could be useful in the design of new quinone-based prodrugs for fast or slow release as well as for the development of carriers where combination of both is also possible. However, further studies need to be performed in order to optimize the quinone-based liposome formulations described in this research document. The optimized formulation would lead to a system that is stable in the presence of BSA and hNQO1 (at low concentrations) but unstable at the concentrations were

hNQO1 is over expressed in the human body. This ideal situation has a key piece that is still unknown in the hNQO1 field and corresponds to the quantitative information on the concentration of hNQO1 in the body.^{2,10,11} In the absence of that information, it is important to investigate the behavior of quinone-based liposomes at various hNQO1 concentrations to obtain a correlation between calcein release rates and hNQO1 activity. Moreover, quinone-based liposome stability could be increased by: 1) addition of other lipids such of those with higher T_m values than DOPE (1,2-distearoyl-*sn*-glycero-3-phosphoethanolamine (DSPE $T_m = 74\text{ }^\circ\text{C}$)¹² or 1,2-dielaidoyl-*sn*-glycero-3-phosphoethanolamine (DEPE $T_m = 38\text{ }^\circ\text{C}$)¹² that could form more rigid bilayers, 2) reduction of the quinone-DOPE content in the liposomal formulation to investigate if dilution of the quinone prevent the liposomes from leaking, and 3) attach a positive charged quinone to decrease the negative surface charge of liposomes.

The optimized triggerable system will selectively release their contents at the desired site, thus maximizing efficacy and reducing unwanted release on healthy cells. The versatility of these systems allow them to be loaded with a variety of units such as drugs, probes, genes and virus for application in drug delivery, cell imaging or gene and virus therapy.

5.4 References

- (1) Cresteil, T.; Jaiswal, A. K., High-Levels of Expression of the Nad(P)H-Quinone Oxidoreductase (Nqo1) Gene in Tumor-Cells Compared to Normal-Cells of the Same Origin. *Biochem. Pharmacol.* **1991**, *42* (5), 1021-1027.
- (2) Siegel, D.; Franklin, W. A.; Ross, D., Immunohistochemical Detection of Nad(P)H : Quinone Oxidoreductase in Human Lung and Lung Tumors. *Clin. Cancer Res.* **1998**, *4* (9), 2065-2070.
- (3) Rooseboom, M.; Commandeur, J. N. M.; Vermeulen, N. P. E., Enzyme-Catalyzed Activation of Anticancer Prodrugs. *Pharmacol. Rev.* **2004**, *56* (1), 53-102.
- (4) Awadallah, N. S.; Dehn, D.; Shah, R. J.; Nash, S. R.; Chen, Y. K.; Ross, D.; Bentz, J. S.; Shroyer, K. R., Nqo1 Expression in Pancreatic Cancer and Its Potential Use as a Biomarker. *Appl. Immunohistochem. Mol. Morphol.* **2008**, *16* (1), 24-31.

- (5) Zhang, L.; Gu, F. X.; Chan, J. M.; Wang, A. Z.; Langer, R. S.; Farokhzad, O. C., Nanoparticles in Medicine: Therapeutic Applications and Developments. *Clin. Pharmacol. Ther.* **2008**, *83* (5), 761-769.
- (6) Kaasgaard, T.; Andresen, T. L., Liposomal Cancer Therapy: Exploiting Tumor Characteristics. *Expert Opin. Drug Deliv.* **2010**, *7* (2), 225-243.
- (7) Khan, D. R., The Use of Nanocarriers for Drug Delivery in Cancer Therapy. *J. Cancer Sci. Ther.* **2010**, *2* (3), 58-62.
- (8) Patterson, A. V.; Saunders, M. P.; Greco, O., Prodrugs in Genetic Chemoradiotherapy. *Curr. Pharm. Des.* **2003**, *9* (26), 2131-2154.
- (9) McKeown, S. R.; Cowent, R. L.; Williams, K. J., Bioreductive Drugs: From Concept to Clinic. *Clin. Oncol.* **2007**, *19* (6), 427-442.
- (10) Siegel, D.; Ross, D., Immunodetection of Nad(P)H : Quinone Oxidoreductase 1 (Nqo1) in Human Tissues. *Free Radical Biol. Med.* **2000**, *29* (3-4), 246-253.
- (11) Siegel, D.; Ryder, J.; Ross, D., Nad(P)H: Quinone Oxidoreductase 1 Expression in Human Bone Marrow Endothelial Cells. *Toxicol. Lett.* **2001**, *125* (1-3), 93-98.
- (12) Forsythe, J. Kinetics and Mechanisms of Release by Redox-Active Liposomes in Drug Delivery. Ph.D. Dissertation, Louisiana State University, Baton Rouge, LA, 2011.

APPENDIX A: SUPPLEMENTAL INFORMATION

Table A.1. Extinction coefficient values for NADH in a 96-well plate. Experiments performed at 22±2 °C in 0.007% BSA solution.

	Trial 1	Trial 2	Trial 3		
NADH (μM)	Abs. (a.u.)	Abs. (a.u.)	Abs. (a.u.)	Average (a.u)	St. Dev.
10	0.0304	0.0192	0.0112	0.0203	0.0096
30	0.1232	0.11105	0.1062	0.1135	0.0088
50	0.1866	0.2258	0.2128	0.2084	0.0200
80	0.3336	0.3412	0.3264	0.3337	0.0074
100	0.3873	0.4078	0.4058	0.4003	0.0113
120	0.4828	0.5258	0.5028	0.5038	0.0215
150	0.597	0.6348	0.598	0.6099	0.0215
200	0.84255	0.8534	0.8306	0.8422	0.0114
250	1.0858	1.10255	1.0726	1.0870	0.0150
300	1.3153	1.3058	1.276	1.2990	0.0205

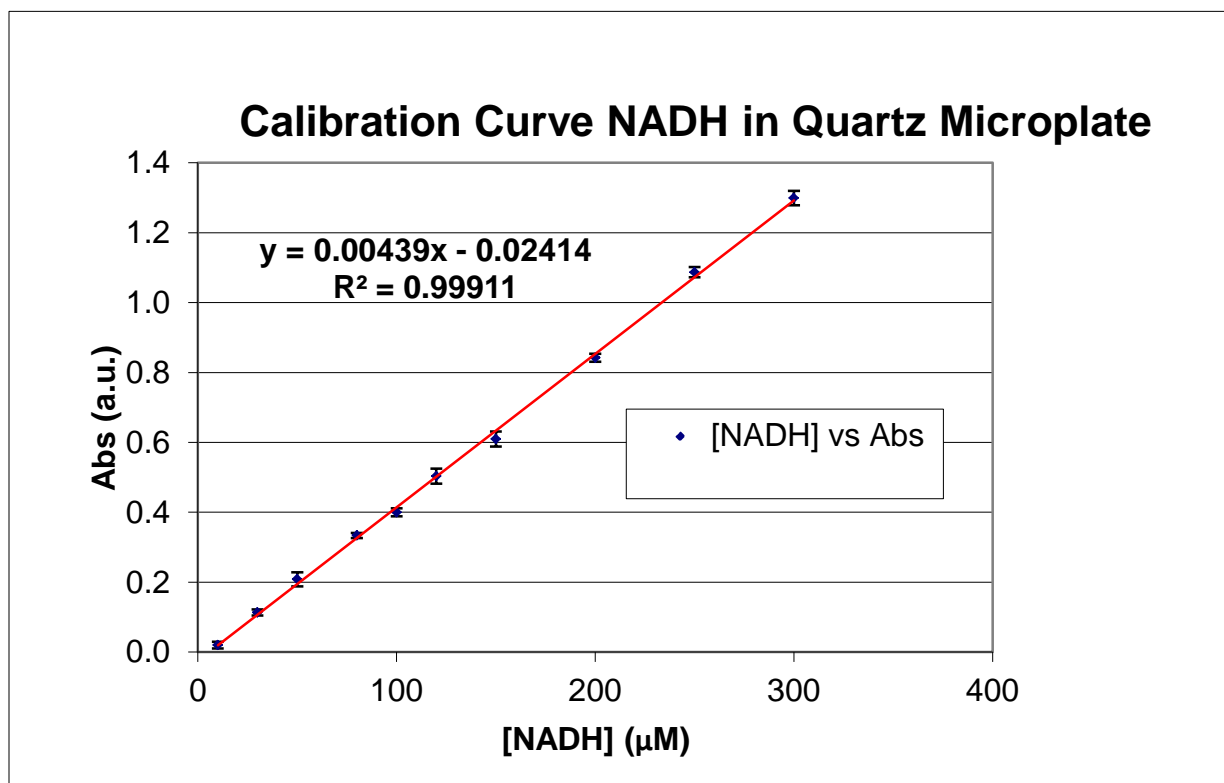


Figure A.1. Calibration curve for NADH in a 96-well plate. Experiments performed at 22±2 °C in 0.007% BSA solution.

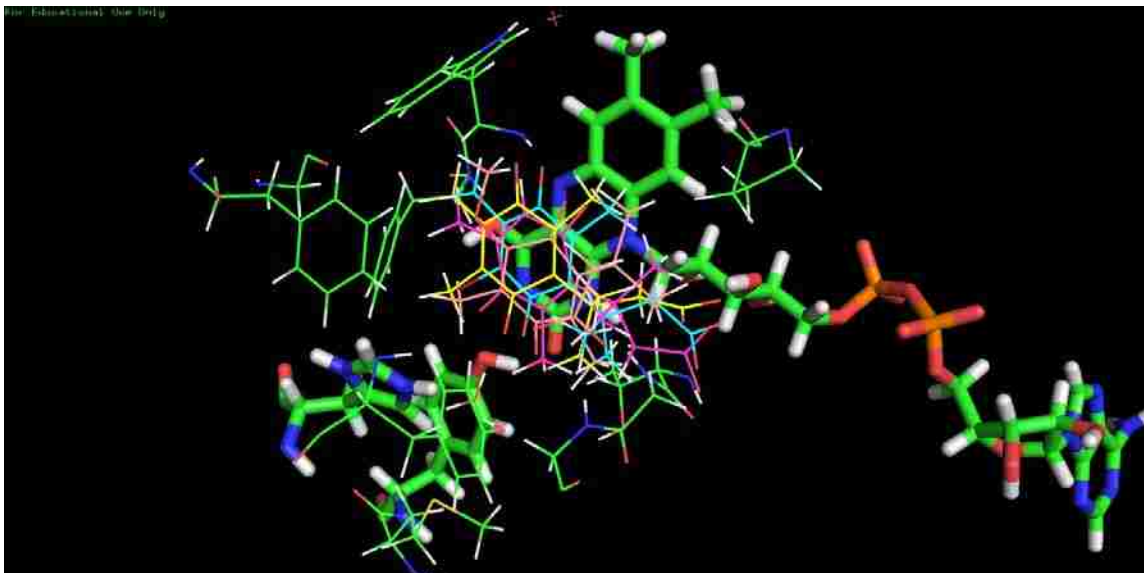


Figure A.2. Superposition of trimethyl-lock quinones in the active site of hNQO1. Representation of Q_{Br}-COOH (sky blue), Q_H-COOH (magenta), Q_{Me}-COOH (yellow), Q_{MeO}-COOH (light pink); amino acids (lines display; color by atom type, carbon atoms colored green); Tyr 155, His 161 and FAD (stick display; color by atom type, carbon atoms colored green). The figure was created using PyMOL.

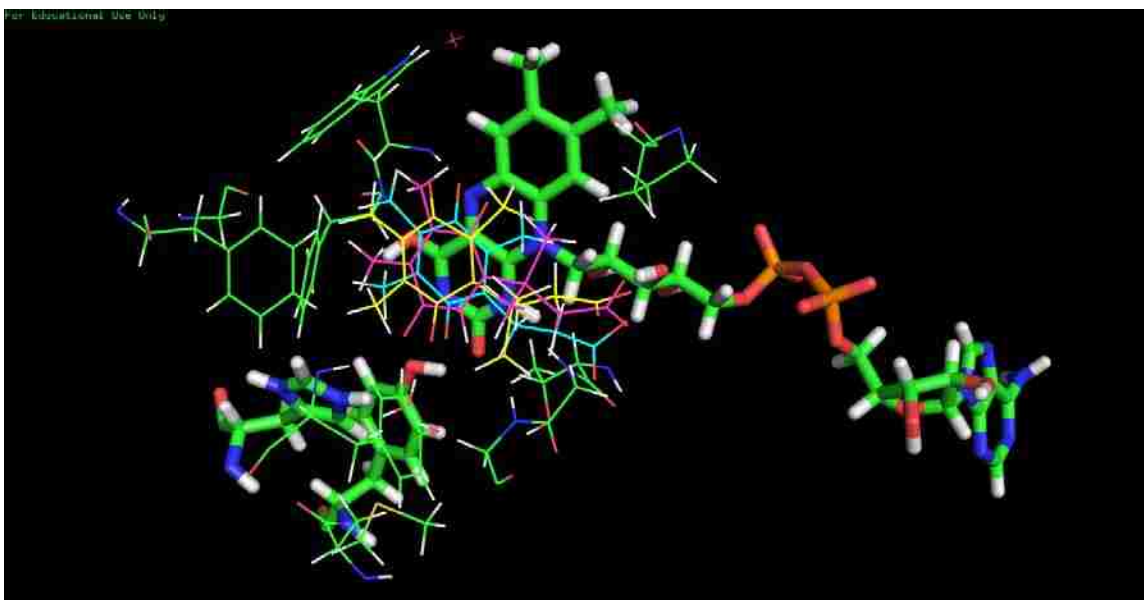


Figure A.3. Superposition of quinones with and without presence of trimethyl-lock in the active site of hNQO1. Representation of Q_{nogenMe}-COOH (sky blue), Q'-COOH (magenta), Q_{Me}-COOH (yellow); amino acids (lines display; color by atom type, carbon atoms colored green); Tyr 155, His 161 and FAD (stick display; color by atom type, carbon atoms colored green). The figure was created using PyMOL.

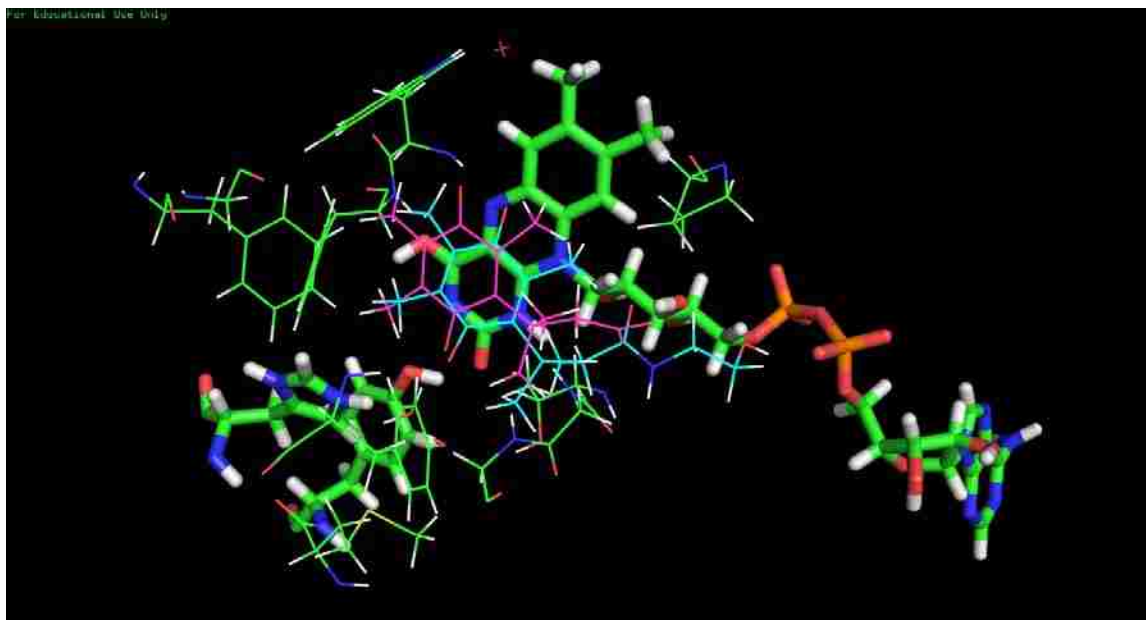
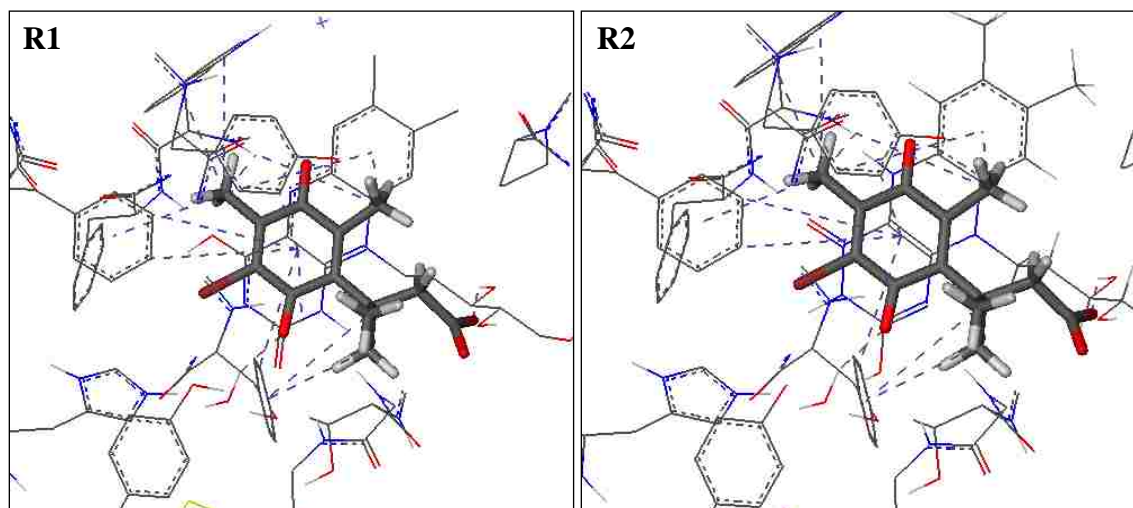


Figure A.4. Superposition of charged quinone versus neutral quinone in the active site of hNQO1. Representation of Q_{Me} -ETA (sky blue), Q_{Me} -COOH (magenta); amino acids (lines display; color by atom type, carbon atoms colored green); Tyr 155, His 161 and FAD (stick display; color by atom type, carbon atoms colored green). The figure was created using PyMOL.

Table A.2. Associated energies for Q_{Br} -COOH when docked in hNQO1 active site. Above is the lowest score energy for each receptor and the components of the Böhm scoring function.

Receptor	Score ($\text{kJ}\cdot\text{mol}^{-1}$)	Match	Lipo	Ambig	Clash	Rot
1	-25.2018	-19.7347	-12.0594	-6.8892	3.8815	4.2000
2	-24.7270	-19.0412	-11.8116	-7.0926	3.6185	4.2000
3	-24.1662	-18.5762	-12.2120	-6.9455	3.9675	4.2000
4	-23.6224	-17.8762	-11.8138	-7.4545	3.9220	4.2000
5	-24.1743	-19.7347	-11.2013	-6.7019	3.8636	4.2000
6	-23.6994	-19.0412	-10.9535	-6.9053	3.6006	4.2000



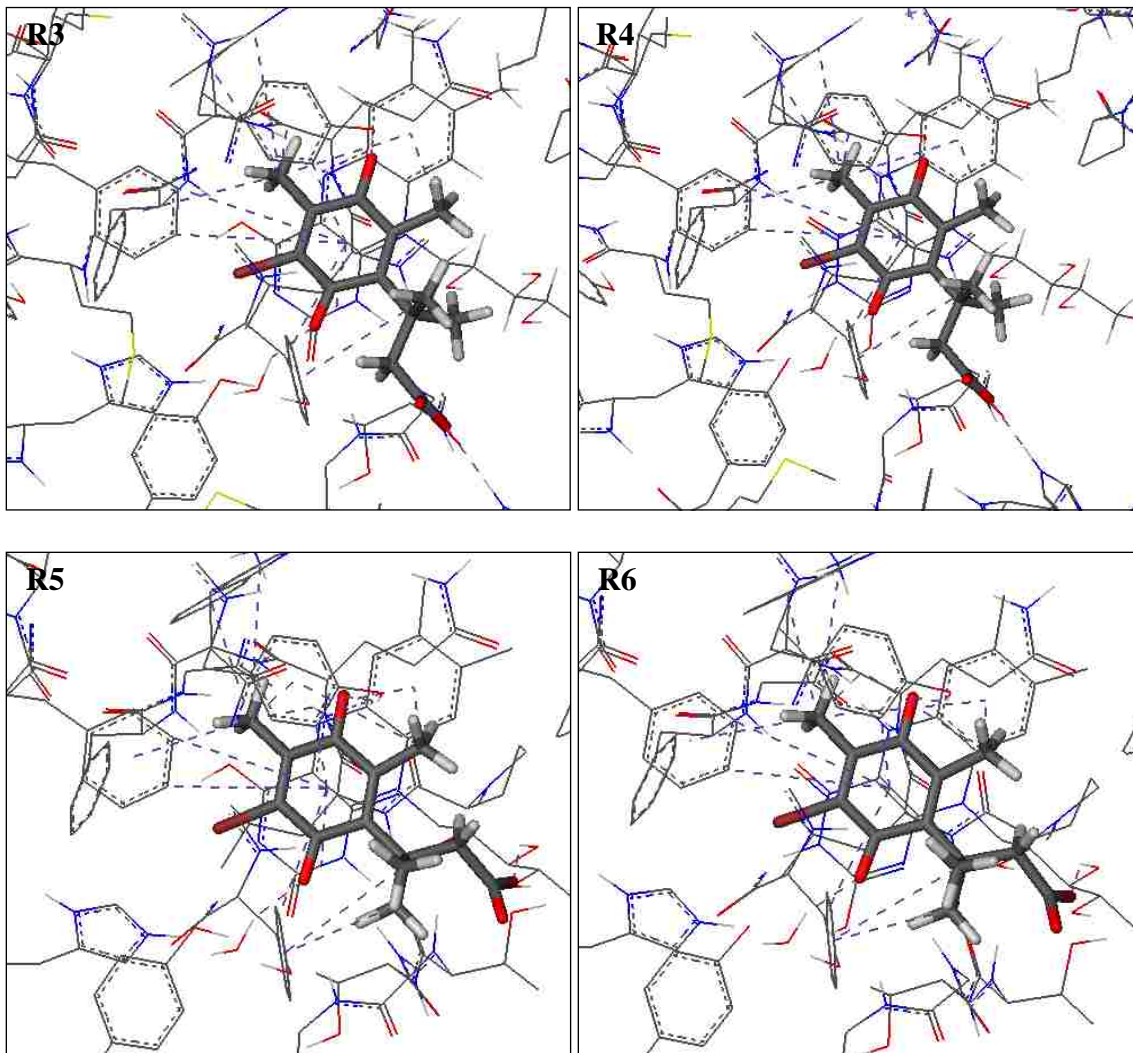
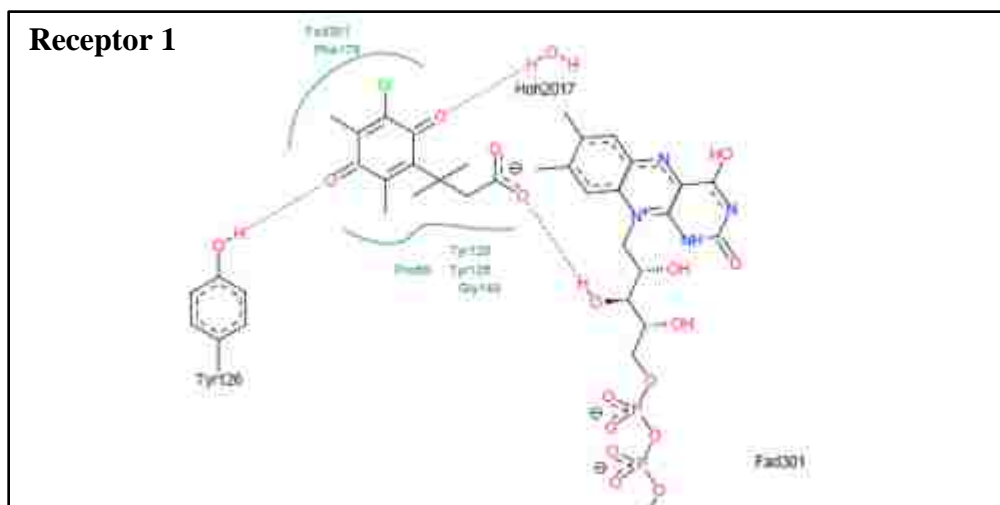
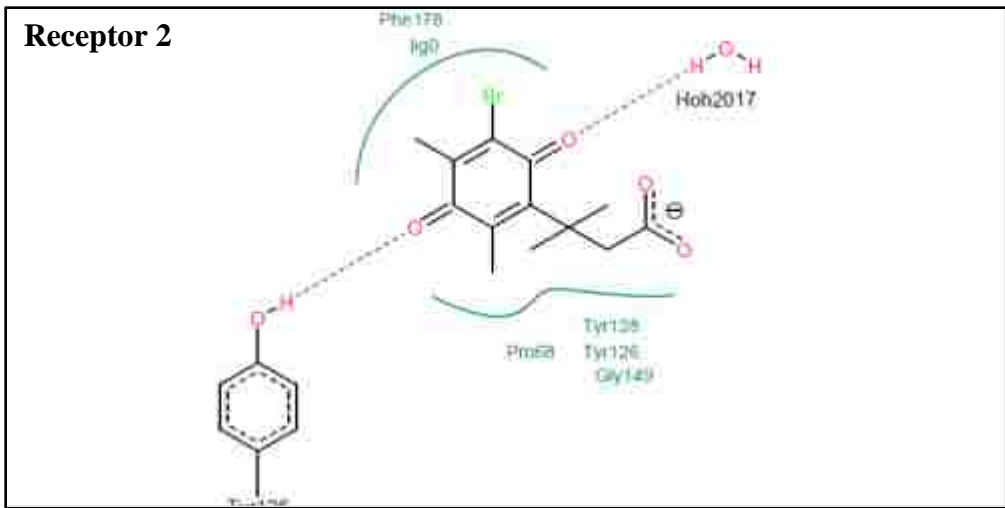


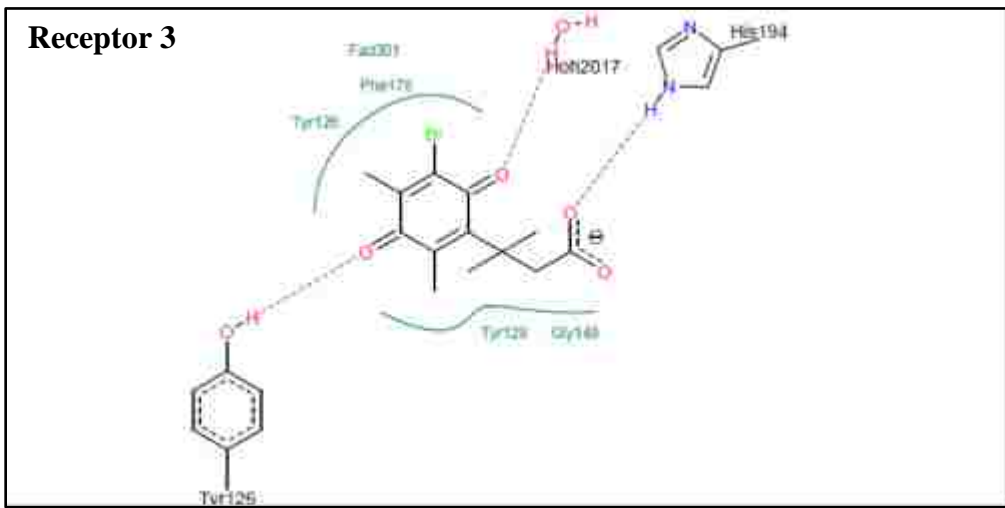
Figure A.5. Lowest score frames of $Q_{Br}-COOH$ in all the receptors. Representation of $Q_{Br}-COOH$ (stick display; color by atom type, carbon atoms colored grey); amino acids and FAD (lines display; color by atom type, carbon atoms colored grey). Dashed purple lines corresponded to hydrophobic interactions.



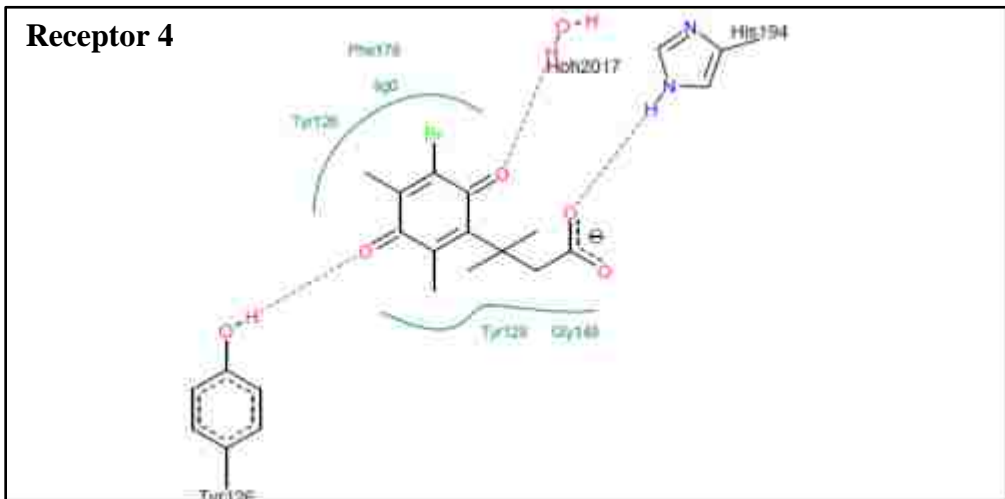
Receptor 2



Receptor 3



Receptor 4



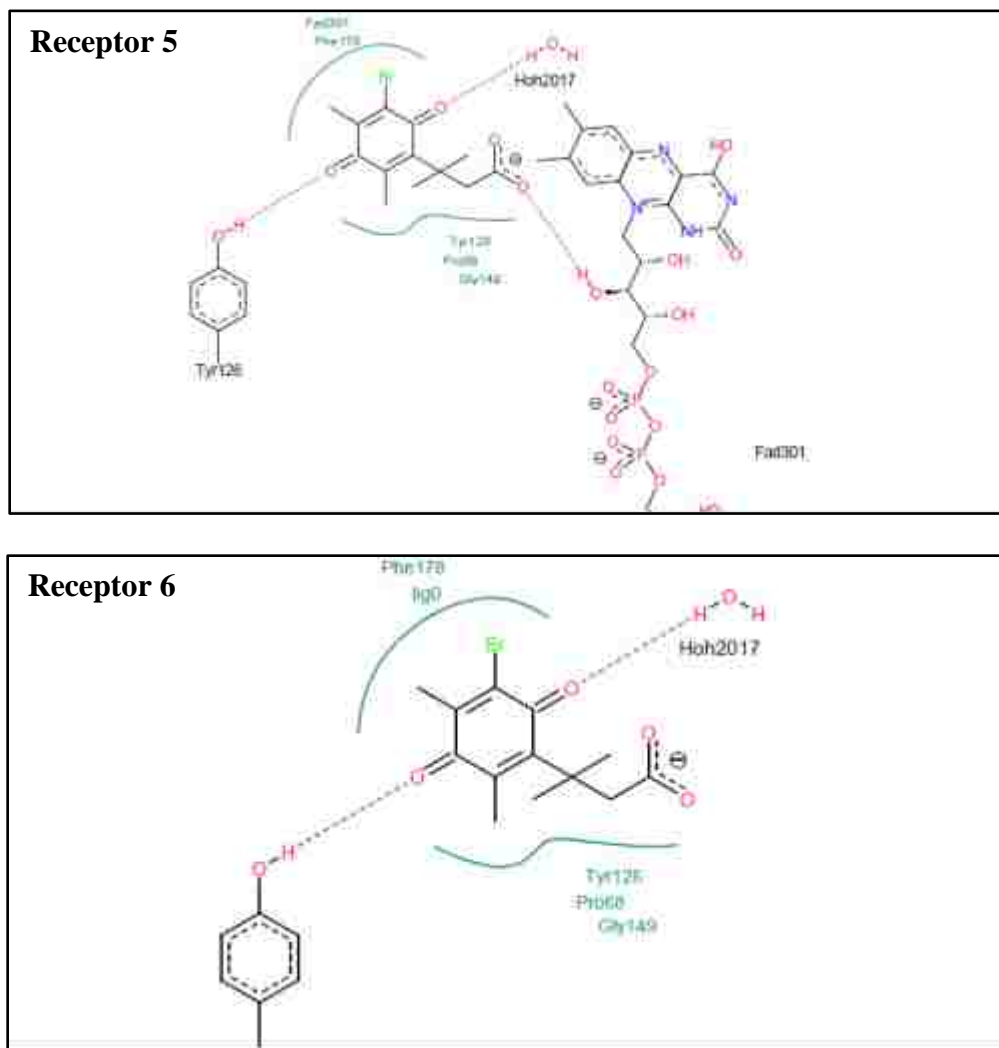


Figure A.6. Poseview frames of $Q_{Br}-COOH$ in all the receptors. Representation of a 2D view of the docked pose of $Q_{Br}-COOH$ (line display; color by atom type, carbon atoms colored black); amino acids and FAD label in green or structure line display; color by atom type, carbon atoms colored black. Hydrophobic interactions are displayed as green contact curves with only the names of the interacting residues attached to these lines. Dashed lines corresponded to hydrogen bond interactions.

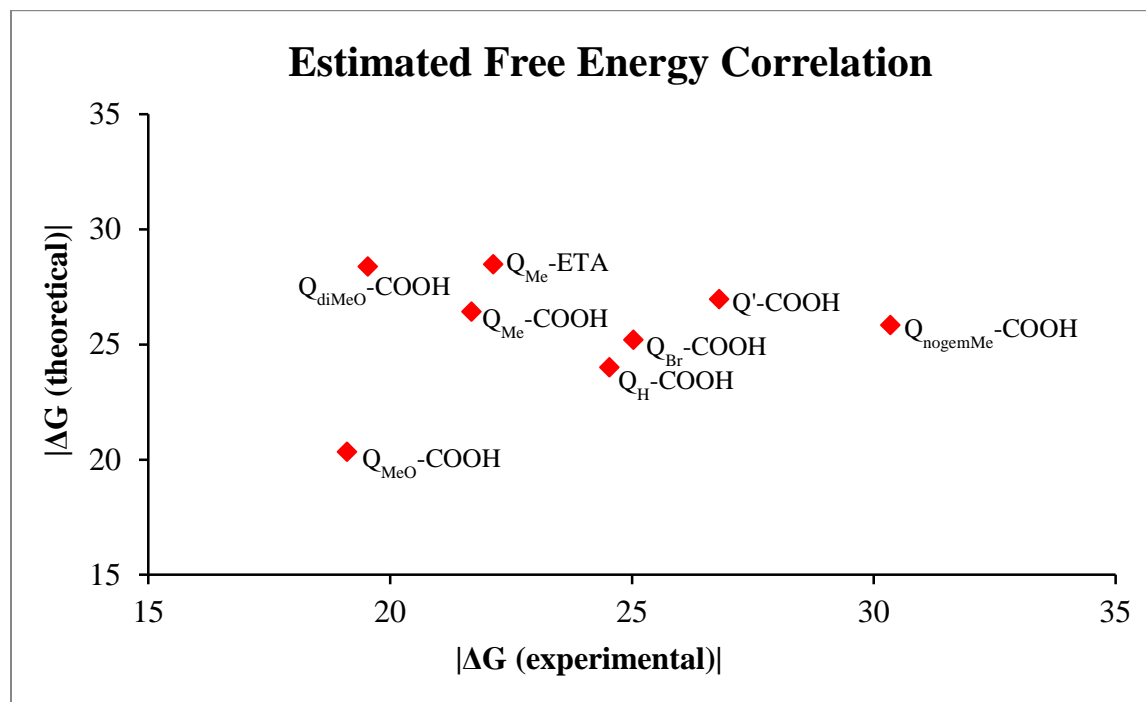


Figure A.7. Correlation of estimated theoretical and experimental free energies of binding.

Chemical Synthesis and Characterization of Q_{Me}-ETA.

Preparation of *N*-(2-hydroxyethyl)-3-methyl-3-(2,4,5-trimethyl-3,6-dioxocyclohexa-1,4-dien-1-yl)butanamide (Q_{Me}-ETA). The quinone amine derivative was prepared by adding Q_{Me}-NHS¹ (150 mg, 0.4328 mmol) into a 25 mL round bottom flask and letting the solid dry under high vacuum for 15 minutes. Then argon was purged through the flask to have it under inert atmosphere; the flow was stopped for two minutes to add 4.5 mL of dichloro methane. Continue argon flow and cooled the mixture to 0 °C. Then add dropwise triethylamine (310 μL, 2.2241 mmol) followed by ethanolamine (40 μL, 0.6647 mmol) using glass syringes. Stopped the argon flow and sealed the round bottom flask. Let the mixture stir for 4 hours. Reaction was followed by TLC (3:1:2 DCM/MeOH/Hex) until no Q_{Me}-NHS was present. After the reaction was completed, the mixture was diluted with 50 mL of dichloro methane and washed with 5 % of sodium bicarbonate (2 X 100 mL). Organic layer was dried over sodium sulfate, and evaporated to yield 87.8 mg of a yellow solid (75 %).

^1H NMR (400 MHz, CDCl_3): δ 1.44 (s, 6H), 1.95-1.97 (d, 6H), 2.14 (s, 3H), 2.85 (s, 2H), 3.32-3.33 (q, 2H), 3.65 (t, 2H), 5.82 (s, 1H).

^{13}C NMR (400 MHz, CDCl_3): δ 12.13, 12.68, 14.15, 28.98, 38.34, 42.20, 49.14, 62.48, 137.95, 138.09, 143.45, 153.12, 173.06, 187.54, 191.35.

HRMS (ESI+) m/z $[\text{M}+\text{H}]^+$, calcd = 294.1706 (calcd for $\text{C}_{16}\text{H}_{24}\text{NO}_4$), obsd = 294.1709, 0.9 ppm error.

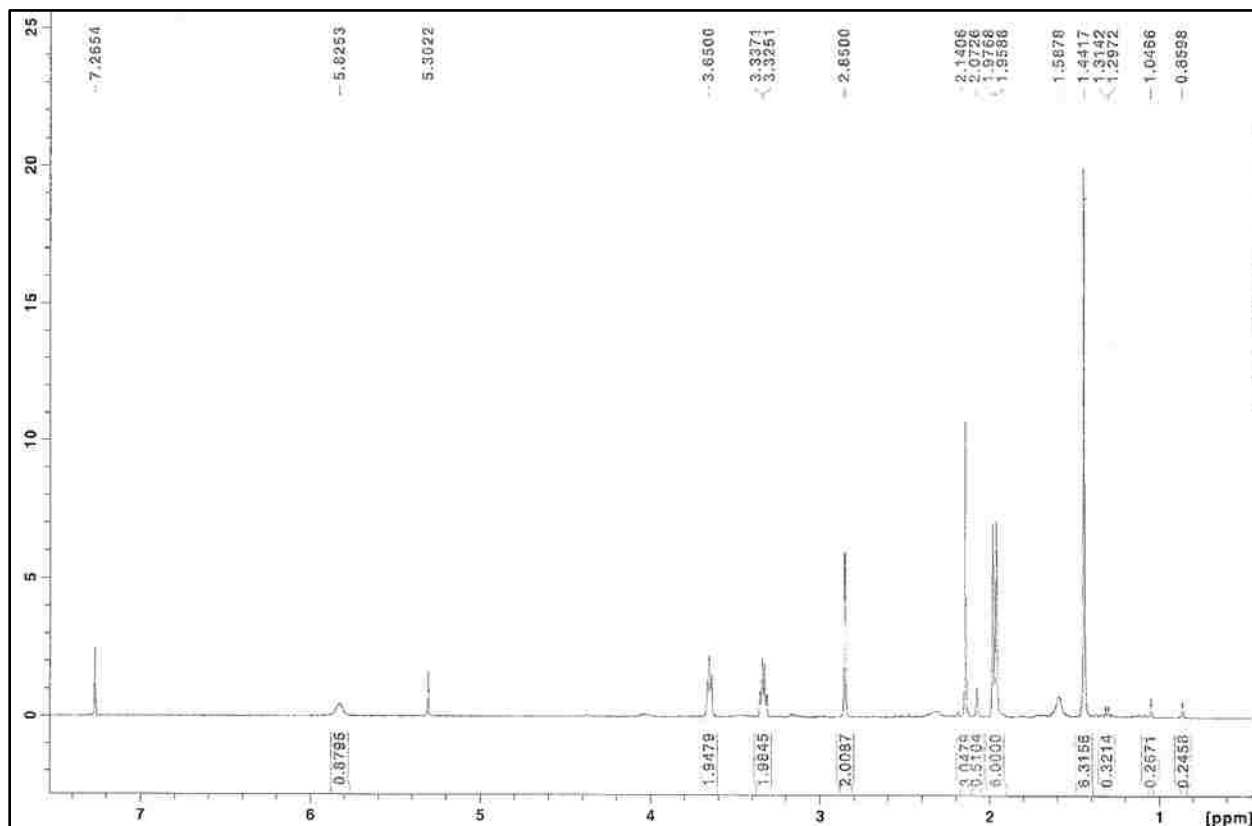


Figure A.8. ^1H NMR for $\text{Q}_{\text{Me}}\text{-ETA}$ (CDCl_3 , 400 MHz)

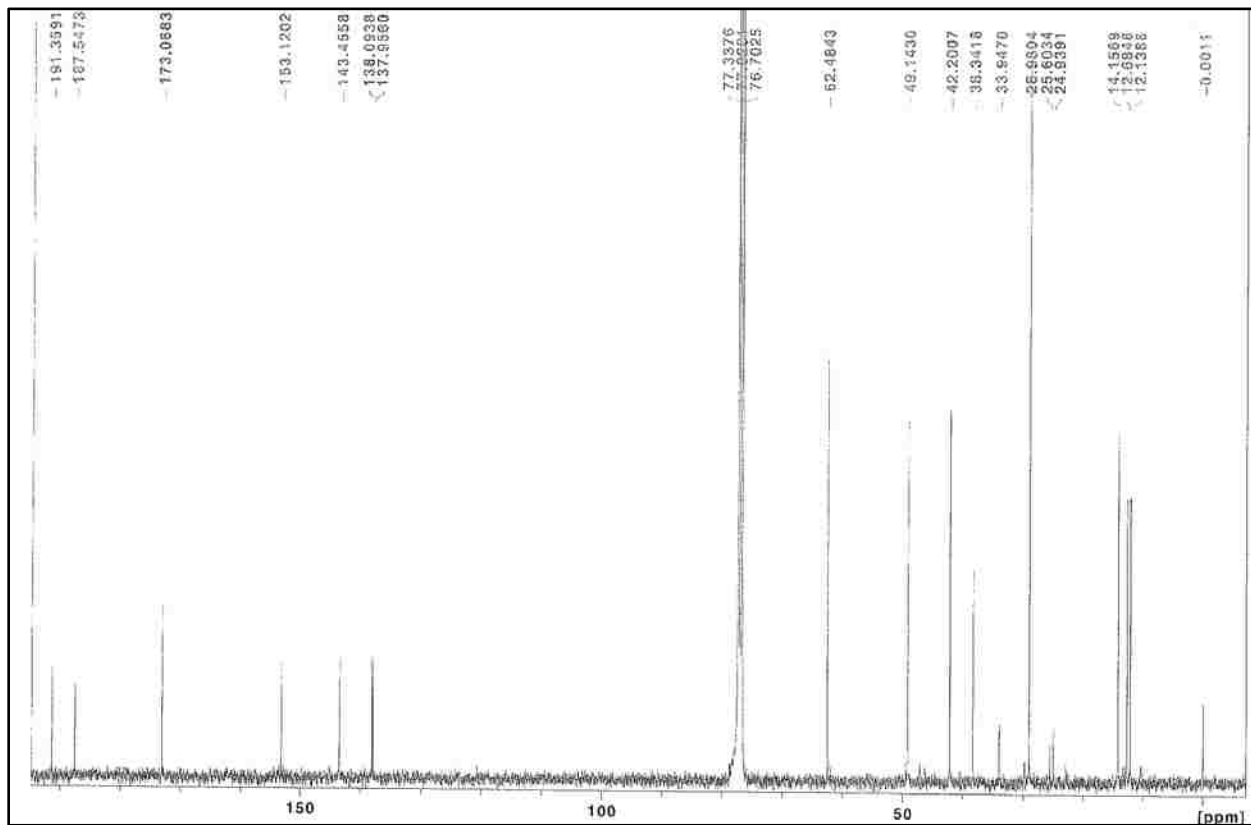


Figure A.9. ^{13}C NMR for $\text{Q}_{\text{Me}}\text{-ETA}$ (CDCl_3 , 400 MHz)

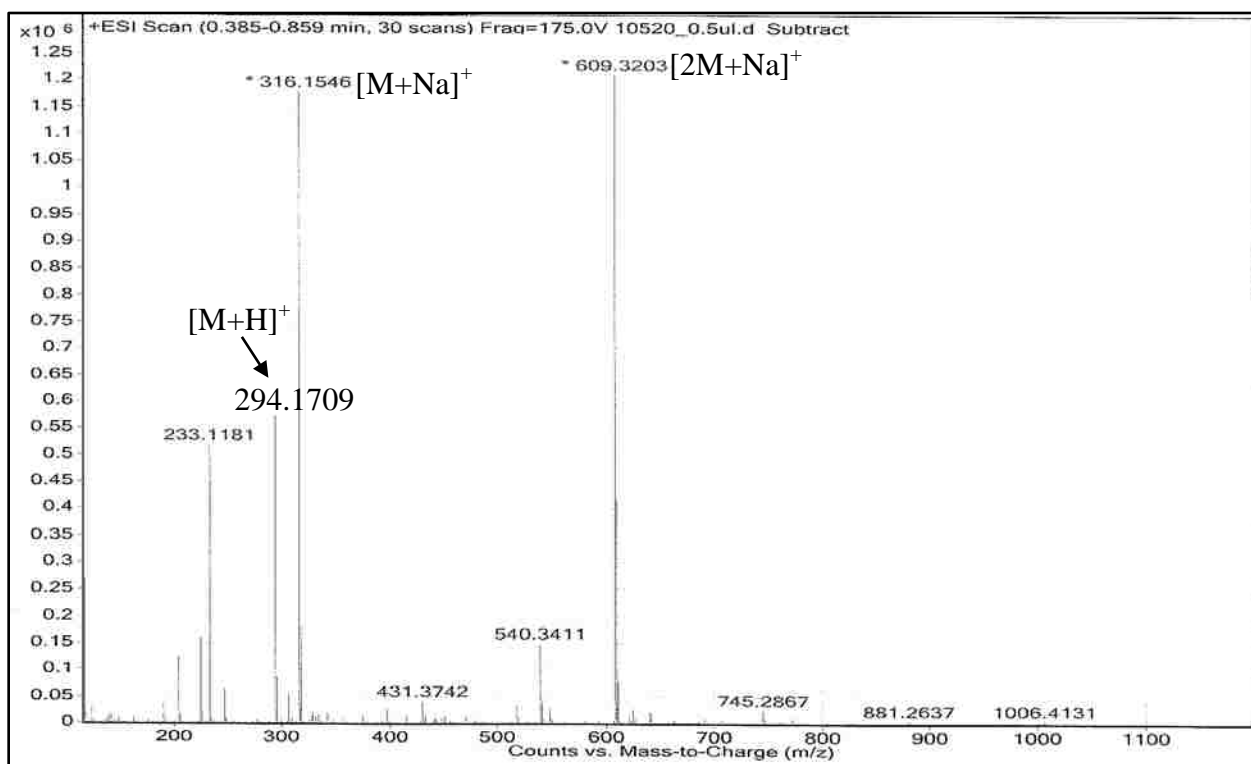


Figure A.10. High resolution mass spectrum (positive ion, electrospray ionization) for $\text{Q}_{\text{Me}}\text{-ETA}$.

References

- (1) Carrier, N. H. Redox-Active Liposome Delivery Agents with Highly Controllable Stimuli-Responsive Behavior. Ph.D. Dissertation, Louisiana State University, Baton Rouge, LA, 2011.

APPENDIX B: PERMISSIONS

SPRINGER LICENSE TERMS AND CONDITIONS

Feb 17, 2012

This is a License Agreement between Maria E. Mendoza ("You") and Springer ("Springer") provided by Copyright Clearance Center ("CCC"). The license consists of your order details, the terms and conditions provided by Springer, and the payment terms and conditions.

All payments must be made in full to CCC. For payment instructions, please see information listed at the bottom of this form.

License number	3851440502504
License date	Feb 17, 2012
Original content publisher	Springer
Licensed content category	Culture and Molecular Life Sciences
Licensed content title	Physiological functions of D-amino acid oxidases: from yeast to humans
Licensed content author	L. Pellegrini
Licensed content date	Jun 1, 2007
Volume number	64
Issue number	11
Type of use	Thesis/Dissertation
Portion	Figures
Author of this Springer article	No
Article reference number	
Title of your thesis / dissertation	Characterization of Triggerable Quinones for the Development of Enzyme-Responsive Liposomes
Expected completion date	May 2012
Estimated size (pages)	170
Total	0.00 USD

Terms and Conditions

If you would like to pay for this license now, please remit this license along with your payment made payable to "COPYRIGHT CLEARANCE CENTER" otherwise you will be invoiced within 48 hours of the license date. Payment should be in the form of a check or money order referencing your account number and this invoice number RLNK500721739.

Once you receive your invoice for this order, you may pay your invoice by credit card. Please follow instructions provided at that time.

Make Payment To:
Copyright Clearance Center
Dept 001
P.O. Box 843006
Boston, MA 02284-3006

JOHN WILEY AND SONS LICENSE
TERMS AND CONDITIONS

Feb 03, 2012

This is a License Agreement between Maria I. Mendoza ("You") and John Wiley and Sons ("John Wiley and Sons") provided by Copyright Clearance Center ("CCC"). The license consists of your order details, the terms and conditions provided by John Wiley and Sons, and the payment terms and conditions.

All payments must be made in full to CCC. For payment instructions, please see information listed at the bottom of this form.

Article Number	2841520892654
License date	Feb 03, 2012
Licensed content publisher	John Wiley and Sons
Licensed content publication	Medicinal Research Reviews
Licensed content title	Design of anticancer prodrugs for reductive activation
Licensed content author	Yu Chen, Longlin Hu
Licensed content date	Jan 1, 2009
Start page	29
End page	64
Type of use	Dissertation/Thesis
Institution type	University/Academic
Format	Print and electronic
Portion	Figure/table
Number of figures/tables	2
Number of extracts	
Original Wiley figure/table number(s)	Scheme 21 and Scheme 22
Will you be translating?	No
Order reference number	
Total	0.00 USD
Terms and Conditions	

TERMS AND CONDITIONS

This copyrighted material is owned by or exclusively licensed to John Wiley & Sons, Inc. or one of its group companies (each a "Wiley Company") or a society for whom a Wiley Company has exclusive publishing rights in relation to a particular journal (collectively "WILEY"). By clicking "accept" in connection with completing this licensing transaction, you agree that the following terms and conditions apply to this transaction (along with the billing and payment terms and conditions established by the Copyright Clearance Center Inc., ("CCC's Billing and Payment terms and conditions"), at the time that you opened your Rightslink account (these are available at any time at <http://www.wiley.com/go/rightslink>)).

Copyright Permission Policy

This journal's copy to the reuse of articles, figures, tables, and other material: *Journals of Biological Chemistry*, *Molecular & Cellular Biochemistry*, and *Journal of Lipid Research*.

For authors reusing their own material:

Each article's PDF contains the journal's obtain access to reuse their own material. They are made available through permission to copy the following:

- Reproduction of any part of the article of their own work
- Other reuse with any type of media
- Copy and article for teaching or classroom use
- Copying for internal use only in the author's agency. If the author is a government employee, it is not for use that author's agency may reuse the article for teaching purposes.
- Making a copy of a table or figure for personal or classroom use only
- Full copies of the journal's PDF that are generated via BioRxiv.org.

Each author who is listed on their papers, under the "Multiple Choice" option, is notified the final edited PDF is available by the publisher to their department or university. We advise:
All authors may link to the online version of their final PDF created by the publisher.

Please cite the authors' name(s) and the journal name. Also, when it is needed, the appearance of a DOI for material.

This is not an original article. Please include the name and address of the journal's publisher. For example, "The American Society for Biochemistry and Molecular Biology."

For other parties using material for noncommercial use:

Other parties are welcome to copy, distribute, or reuse any of the work, as long as existing with their permission to reuse the work. In any case, they attribute the work to the original author(s) and the journal(s).

Examples of noncommercial use include:

- Redistribution of work to colleagues or properties that use noncommercial work with attribution.
- Making a copy of a table or figure for personal or classroom use only.

For other parties using material for commercial use:

Navigate to the article's page and click the "Request" button. The article's page navigation bar also indicates if right of reuse is allowed through the site's article reuse permission page.

Examples of commercial use by parties that are not authors include:

- Reuse of any material of text under the terms of reference page of an article for a commercial journal or other publication.
- Reuse of any material of text under the terms of reference page of an article for a commercial journal or other publication.

© 2009 American Society for Biochemistry and Molecular Biology

Services

2009 American Society for Biochemistry and Molecular Biology
100 Brook Hill Drive
West Nyack, NY 10994-2133
Phone: 845.352.7000
Fax: 845.352.7001
Email: info@asbmb.org

Responses

100 Brook Hill Drive

Citing Articles

100 Brook Hill Drive

Pub Med

100 Brook Hill Drive

100 Brook Hill Drive

100 Brook Hill Drive

100 Brook Hill Drive

100 Brook Hill Drive

100 Brook Hill Drive

100 Brook Hill Drive

100 Brook Hill Drive

100 Brook Hill Drive

100 Brook Hill Drive

100 Brook Hill Drive

100 Brook Hill Drive

100 Brook Hill Drive

100 Brook Hill Drive

100 Brook Hill Drive

100 Brook Hill Drive

100 Brook Hill Drive

100 Brook Hill Drive

100 Brook Hill Drive

100 Brook Hill Drive

100 Brook Hill Drive

100 Brook Hill Drive

100 Brook Hill Drive

ELSEVIER LICENSE
TERMS AND CONDITIONS

Feb 03, 2012

This is a License Agreement between Maria F Mendoza ("You") and Elsevier ("Elsevier") provided by Copyright Clearance Center ("CCC"). The license consists of your order details, the terms and conditions provided by Elsevier, and the payment terms and conditions.

All payments must be made in full to CCC. For payment instructions, please see information listed at the bottom of this form.

Supplier:	Elsevier Limited The Boulevard Langford Lane Kidlington, Oxford, OX5 1GB, UK
Registered Company Number:	1982084
Customer name:	Maria F Mendoza
Customer address:	2000 Brightside Dr. Baton Rouge, LA 70820
License number:	2841550925622
License date:	Feb 03, 2012
Licensed content publisher:	Elsevier
Licensed content publisher:	Biochimica et Biophysica Acta (BBA) - Biomembranes
Licensed content title:	Triggerable liposomal fusion by enzyme cleavage of a novel peptide-lipid conjugate
Licensed content author:	Charles C Pak, Shaukat Ali, Andrew S Janoff, Paul Meers
Licensed content date:	24 June 1998
Licensed content volume number:	1372
Licensed content issue number:	1
Number of pages:	15
Start Page:	13
End Page:	27
Type of Use:	reuse in a thesis/dissertation
Section:	figures/tables/illustrations
Number of figures/tables/illustrations:	1
Format:	both print and electronic
Are you the author of this Elsevier article?	No
Will you be translating?	No

ELSEVIER LICENSE
TERMS AND CONDITIONS

Feb 03, 2012

This is a License Agreement between Maria F. Mendoza ("You") and Elsevier ("Elsevier") provided by Copyright Clearance Center ("CCC"). The license consists of your order details, the terms and conditions provided by Elsevier, and the payment terms and conditions.

All payments must be made in full to CCC. For payment instructions, please see information listed at the bottom of this form.

Supplier	Elsevier Limited The Boulevard, Langford Lane Kidlington, Oxford, OX5 1GB, UK
Registered Company Number	1982064
Customer name	Maria F. Mendoza
Customer address	2000 Brightside Dr. Baton Rouge, LA 70820
License number	2841550589600
License date	Feb 03, 2012
Licensed content publisher	Elsevier
Licensed content publication	Progress in Lipid Research
Licensed content title	Advanced strategies in liposomal cancer therapy: Problems and prospects of active and tumor specific drug release
Licensed content author	Thomas L. Andresen, Simon S. Jensen, Kent Jorgensen
Licensed content date	January 2005
Licensed content volume number	44
Licensed content issue number	1
Number of pages	30
Start Page	68
End Page	97
Type of Use	reuse in a thesis/dissertation
By text	figures/tables/illustrations
Number of figures/tables/illustrations	1
Format	both print and electronic
Are you the author of this Elsevier article?	No
Will you be translating?	No

Rights and Permissions

Copyright and License to Publish

Beginning with articles submitted in Volume 106 (2009), the author(s) retains copyright to individual articles, and the National Academy of Sciences of the United States of America retains an exclusive license to publish these articles and holds copyright to the collective work. Volumes 90–105 (1993–2008), copyright © by the National Academy of Sciences; Volumes 1–89 (1915–1992), the author(s) retains copyright to individual articles, and the National Academy of Sciences holds copyright to the collective work.

The PNAS listing on the SHERPA/ReMEO publisher copyright notices & self-archiving detail pages can be found [here](#).



Requests for Permission to Reprint

Requests for permission should be made in writing. For the fastest response time, please send your request via e-mail to PNASPA@nas.edu. If necessary, requests may be faxed to or mailed to:

PNAS Permissions Editor
130 11th Street, NW
Suite 450
Washington, DC 20001 USA
Phone

Anyone may, without requesting permission, use original figures or tables published in PNAS for noncommercial and educational use (i.e., in a review article, in a book that is not for sale) provided that the original source and the applicable copyright notice are cited.

For permission to reprint material in volumes 1–89 (1915–1992), requests should be addressed to the original author(s), who hold the copyright. The full journal reference must be cited.

For permission to reprint material in volumes 90–105 (1993–2008), requests must be sent via e-mail, fax, or mail and include the following information about the original material:

1. Your full name, affiliation, and title
2. Your complete mailing address, phone number, fax number, and e-mail address
3. PNAS volume number, issue number, and issue date
4. PNAS article title
5. PNAS author's name(s)

Rights and Permissions

- Author Rights and Permissions
FAQ
- Requests for Permission to Reprint
- Requests for Permission
to Photocopy

SPRINGER LICENSE
TERMS AND CONDITIONS

Feb 17, 2012

This is a License Agreement between Maria E. Mendoza ("You") and Springer ("Springer") provided by Copyright Clearance Center ("CCC"). The license consists of your order details, the terms and conditions provided by Springer, and the payment terms and conditions.

All payments must be made in full to CCC. For payment instructions, please see information listed at the bottom of this form.

License Number	285147117899
License date	Feb 17, 2012
Licensed content publisher	Springer
Licensed content publication	Springer eBook
Licensed content title	One- and Two-Electron-Mediated Reduction of Quinones: Enzymology and Toxicological Implications
Licensed content author	David Siegel
Licensed content date	Jan 1, 2009
Type of use	Thesis/Dissertation
Portion	Figures
Author of this Springer article	No
Order reference number	
Title of your thesis/dissertation	Characterization of Triggerable Quinones for the Development of Enzyme-Responsive Liposomes
Expected completion date	May 2012
Estimated size (pages)	170
Total	0.00 USD
Terms and Conditions	

If you would like to pay for this license now, please remit this license along with your payment made payable to "COPYRIGHT CLEARANCE CENTER" otherwise you will be invoiced within 48 hours of the license date. Payment should be in the form of a check or money order referencing your account number and this invoice number RLNK500721810.

Once you receive your invoice for this order, you may pay your invoice by credit card. Please follow instructions provided at that time.

Make Payment To:
Copyright Clearance Center
Dept 001
P.O. Box 843006
Boston, MA 02284-3006

For suggestions or comments regarding this order, contact RightsLink Customer Support: customer@copyright.com or +1-877-622-5543 (toll free in the US) or +1-

VITA

Maria Fabiana Mendoza Paris was born in Montevideo, Uruguay. She spent her elementary, middle and high school years at Escuela Parque Posadas, Liceo 18 and Liceo Miranda, respectively. She started her studies to be a pharmacist at the Facultad de Quimica in Montevideo. While she pursued her degree, she obtained a full soccer scholarship to continue her studies in the U.S.A. She received her Bachelor of Science degree in chemistry with a minor in biology from Missouri Baptist University in 2005 and graduated *cum laude*. She enrolled in the doctoral program in the Department of Chemistry at Louisiana State University in the fall of 2006. In the summer of 2007, she joined the research group of Prof. Robin L. McCarley. The degree of Doctor of Philosophy will be conferred at the Spring 2012 Commencement.